Novel Reductive Aminases for the Preparation of Chiral Amines

A thesis submitted to the University of Manchester for the degree of Doctor of Philosophy (PhD) in the Faculty of Science and Engineering

2021

Ryan B. Palmer

Department of Chemistry

Table of Contents

Word Count: 34006

List of Tables

Table of Figures

9

11

List of Abbreviations

APIs	Active Pharmaceutical Ingredients
PMP	*p*-methoxyphenyl
OMP	*o*-methoxyphenyl
MAO	Monoamine oxidase
FAD	Flavin adenine dinucleotide
AADH	Amino acid dehydrogenase
AmDH	Amine dehydrogenase
GDH	Glucose dehydrogenase
FDH	Flavin dehydrogenase
LeuDH	Leucine dehydrogenase
PheDH	Phenylalanine dehydrogenase
TA	Transaminase
IRED	Imine reductase
NADPH	Nicotinamide adenine dinucleotide phosphate
DHIQ	Dihydroisoquinoline
THIQ	Tetrahydroisoquinoline
RedAm	Reductive aminase
DoE	Design-of-experiment
INT	iodonitrotetrazolium
CAR	Carboxylic acid reductase
ADH	Alcohol dehydrogenase
ee	Enantiomeric excess
dr	Diastereomeric ratio
ToF	Turnover frequency

List of Amino Acids

Single Letter Code	Three Letter Name	Full Name
G	Gly	Glycine
A	Ala	Alanine
S	Ser	Serine
T	Thr	Threonine
C	Cys	Cysteine
V	Val	Valine
L	Leu	Leucine
I	Ile	Isoleucine
M	Met	Methionine
P	Pro	Proline
F	Phe	Phenylalanine
Y	Tyr	Tyrosine
W	Trp	Tryptophan
D	Asp	Aspartic acid
E	Glu	Glutamic acid
N	Asn	Asparagine
Q	Gln	Glutamine
H	His	Histidine
K	Lys	Lysine
R	Arg	Arginine

Abstract

Biocatalytic imine reductions and reductive aminations are an important tool to access high value primary, secondary, and tertiary chiral amines. Chiral amines are a prevalent functional group that is found in around 40% of pharmaceuticals and 20% of agrochemicals. Imine reductases, and the more recently discovered reductive aminases, are two valuable classes of biocatalysts that have emerged in recent years. They both possess a wide substrate scope of ketones and amines, therefore making them suitable candidates for reductive aminations, as well as a wide scope of imines for imine reductions.

Despite the promise that these two enzymes show over other relevant biocatalysts for accessing chiral amines such as transaminases and monoamine oxidases, IREDs and RedAms have their limitations. The activity and stereoselectivity of these enzymes have been shown to be very substrate dependent. Even small changes in substituents, e.g. in steric demands or electronic properties, can result in drastically reduced, or improved, activity, as well as invert the enantiopreference.

This report looks at exploring the activity and stereoselectivity of a reductive aminase from *Ajellomyces dermatitidis* (*Ad*RedAm) towards previously untested carbonyl acceptors that showed interest as pharmaceutical building block precursors. Of the 7 carbonyl acceptors chosen for investigation, only one showed conversion to the desired amine product which was 1-methylpiperidine-2,3-dione. This achieved conversions of up to 80% and 78.6% with allylamine and trifluoroethylamine as the amine donors respectively. A secondary peak in GC traces was observed with this reactions which corresponding to the intermediate enamine compound that formed through tautomerization after the *in situ* formation of the imine intermediate. Through enzyme and no enzyme control reactions it was observed that this *in situ* imine formation and enamine tautomerization was not enzyme catalysed and reach 100% conversion to the enamine after 1 hour.

The poor feasibility of the chosen substrates as carbonyl acceptors for reductive amination lead to a rational engineering investigation into a selection of active site residues. A total of six residues (N93, Y177, W208, H215, M237, and Q238) were

selected in *Ad*RedAm based on crystallographic data previously obtained from the reductive aminase from *Aspergillus oryzae* (*Asp*RedAm)[90] and screed against 2-phenylpyrroline and other cyclic imines with an aromatic substituent in the 2-position. Of the seven variants generated, W208A and M237G stood out as the best performing due to showing either an improvement in activity or stereoselectivity, or an inversion in stereoselectivity. *Ad*WT showed a conversion of 19% for 2-phenylpyrroline and was 92% (S)-selective whereas W208A and M237G showed conversions of 100% and 54% with *ee* values of >99% (S) and 88% (R) respectively. Addition of a para-chloro group onto the aromatic resulted in a change of stereoselectivity of *Ad*WT, N94A, Y177F, and H215A to the (R)-enantiomer. This substrate was more accepted by *Ad*WT with conversion of 39% to the amine after 3 hours. W208A and M237G showed conversions of 99% and 25% with *ee* values of 74% (S) and 88% (R) respectively. A para-methoxy substituent on the aromatic ring resulted in <5% conversion for all variants other than W208A which showed >99% conversion and was >99% (S)-selective. Upon changing the ring size to a 6-membered ring, W208A and M237G both showed 100% conversion and *ee* >99% (R) compared to the *Ad*WT with a conversion of 30% and 72% (R)-selective. This shows that the stereoselectivity of this reductive aminase is also substrate dependent as well as the shape and chemical nature of the active site.

An in-silico docking was carried out of 2-phenylpyrroline into *Asp*WT as well as the corresponding mutations of W208A and M237G from *Ad*RedAm (W210A and M239G). It was seen in both variants, a domain shift around positions 238 and 239 had occurred which appears to push the substrate closer to the cofactor, resulting in a faster turnover of the substrate. It can also be seen in both variants that the phenyl group is oriented in the same direction however, a different face of the imine is adjacent to the transferred hydride from the cofactor in each model explaining the inversion in stereoselectivity.

W208A was chosen for testing for the reductive amination between different carbonyls with aniline and substituted anilines due to its excellent conversions the imine reduction of different cyclic imines. *Ad*WT showed reductive amination activity between cyclohexanone and aniline at a 1:1 ratio, however 56% of the amine product

was see when W208A was used instead. This value dropped for different carbonyl ring sizes with aniline with cyclopentanone and cycloheptanone showing conversions of 16% and 3.2% respectively. Open chain carbonyls were less accepted than cyclic carbonyls with conversions seen of 16%, 8%, and 4% for the reductive amination between aniline and 2-heptanone, 2-hexanone, and 2-pentanone respectively. Benzaldehyde was a far better carbonyl acceptor for aniline with conversion to the secondary amine product >99%.

When looking at different substituents on aniline, cyclohexanone was chosen as the carbonyl acceptor. Steric crowding around the reaction centre (near the nitrogen of aniline) was unflavoured with para-methyl, meta-methyl, and ortho-methyl giving conversion of 19%, 9.7%, and 0% respectively. Electron donating substituents were more favoured than electron withdrawing with para-methoxy and para-chloro giving the amine in 42.4% and 22% and para-fluorine and a para-nitro group having conversions of 5.3% and 0%.

We have shown that through single point mutations of a reductive aminase, activity towards both imine reduction and reductive amination can be drastically improved on as well as a level of control over stereoselectivity for some substrates.

Declaration

That no portion of the work referred to in the thesis has been submitted in support of an application for another degree or qualification of this or any other university or other institute of learning.

Copyright Statement

The following four notes on copyright and the ownership of intellectual property rights must be included as written below:

i. The author of this thesis (including any appendices and/or schedules to this thesis) owns certain copyright or related rights in it (the "Copyright") and s/he has given the University of Manchester certain rights to use such Copyright, including for administrative purposes.

ii. ii. Copies of this thesis, either in full or in extracts and whether in hard or electronic copy, may be made only in accordance with the Copyright, Designs and Patents Act 1988 (as amended) and regulations issued under it or, where appropriate, in accordance with licensing agreements which the University has from time to time. This page must form part of any such copies made.

iii. The ownership of certain Copyright, patents, designs, trademarks and other intellectual property (the "Intellectual Property") and any reproductions of copyright works in the thesis, for example graphs and tables ("Reproductions"), which may be described in this thesis, may not be owned by the author and may be owned by third parties. Such Intellectual Property and Reproductions cannot and must not be made available for use without the prior written permission of the owner(s) of the relevant Intellectual Property and/or Reproductions.

iv. Further information on the conditions under which disclosure, publication and commercialisation of this thesis, the Copyright and any Intellectual Property and/or Reproductions described in it may take place is available in the University IP Policy (see http://documents.manchester.ac.uk/DocuInfo.aspx?DocID=2442 0), in any relevant Thesis restriction declarations deposited in the University Library, the University Library's regulations (see http://www.library.manchester.ac.uk/about/regulations/) and in the University's policy on Presentation of Theses.

I dedicate this thesis to myself as proof, that with perseverance and self-belief, it is possible to weather and triumph over any hardships and challenges that may appear.

Acknowledgements

I would firstly like to give thanks to my supervisor Professor Nicholas J. Turner and my co-supervisor Professor Sabine L. Flitsch for giving me the opportunity to work as part of their group, as well as for all the guidance provided throughout the PhD. I would also like to thank the European Research Council for funding for the project.

I would like to thank Dr. Juan Mangas-Sanchez for initial training in the field, constant support and guidance in the lab, and for being a great mentor during his time in the group. I would like to thank Dr. Rachel Heath alongside Dr. Juan Mangas-Sanchez for the support and aide given upon the termination of the initial project-funding source, helping me pick my feet up, and focusing on a new branch of the project. I would also like to thank Dr. Rachel Heath, as well as Dr. Christian Schnepel, for offering to proof read and to provide advice on this thesis.

I would like to thank all members of the Turner-Flitsch group who have been wonderful friends and colleagues throughout my PhD and who have created a pleasurable and fun environment to work in. I would also like to thank all the friends that I made during my time in Manchester that have made this experience as fun and unforgettable as it has been, and for providing moral support when it was necessary.

Last, but certainly not least, I would like to thank my parents who have constantly supported me and encouraged me throughout my life and pushed me to be the person I am today.

Chapter 1: Introduction

When looking at approaches to accessing enantiomerically rich compounds, the use of biocatalysis is a relatively new technique when compared to traditional chemical synthetic procedures. Applications of biocatalysis were relatively slow to move away from the starting line. Initially, a limited understanding and knowledge of enzymes limited progress in the application of biocatalysis. It was in 1833 when the first enzyme was discovered, a diastase, which other enzymes quickly followed.[113] Breakthroughs in molecular biology such as understanding of DNA structures, cloning techniques, and recombinant expression of enzymes allowed for harvesting of enzymes from their original sources to be circumvented.[1] In combination with these advances, the first enzyme structures were elucidated in the 1960's allowing for biochemical characterization.[2] In the early stages of biocatalysis, the work was very limited. Enzymes are catalysts that have evolved to work on a limited set of substrates for a single specific reaction. This reaction specificity and substrate scope limitations is usually accompanied with narrow ranges of operating conditions such as temperatures and reaction pH.[3]

Although standard chemical synthetic techniques have improved over decades regarding their efficiency, robustness and improved stereo- and chemoselectivity, conventional syntheses come along with notable disadvantages: high pressures and temperatures are often necessary to obtain satisfactory yields, posing both environmental and safety risks.[2] Moreover, the use of transition metal catalysts that is inevitable in some cases, may lead to residual traces of metals in the final product. Trace residues can pose serious health risks further down the line, especially in the synthesis of pharmaceuticals (although not exclusively) and so additional steps are required to ensure proper removal of contaminants.[2,4]

It is mentioned in a report by Gao-Wei Zheng in 2011 that only 150 biocatalytic processes were used in industrial applications.[5] This has increased over the last decade with several hundred process in 2019[112] encompassing several different types of reactions (e.g. reductive aminations, alcohol oxidations, amide formation etc.) in multiple different sectors (such as the food industry, pharmaceuticals, agrochemicals, and detergents to name a few).[6,7] Over recent years, it has become

easier to incorporate biocatalysis into traditional synthetic routes due to improved techniques for DNA sequencing, recombinant gene expression, protein characterisation, and the vast increase of sequence space in public databases. There are several companies now that provide enzyme libraries to be used to screen substrates to look for desired chemical activity and stereoselectivity (eg. Prozomix, Codexis, Almac). Screening allows for identifying of activity towards a transformation of interest with desired selectivity. Even if the enzyme shows low activity and does not fulfil certain process criteria, engineering allows further optimisation to end up with a viable catalyst. Directed evolution (see section 5.2) of enzymes through protein engineering is a powerful tool, allowing for the controlled changing of amino acid residues within protein chains.[8–10] This can result in modification and tuning of several enzyme properties such a substrate scope, stability, solvent tolerance, stereo-, regio-, and chemoselectivity, and turnove.[2,5,11] This has advantages over the design of new metal catalysts as it does not require the synthesis of complex ligands.

1.1 Chiral amines

Chiral amines are a key and important functional moiety that exists in a wide range of applications. They are commonly found as components in the pharmaceutical, agrochemical, and dye industries as well as find use as synthetic tools in organocatalysis. In fact, around 40% of all active pharmaceuticals (APIs) and 20% of agrochemicals contain a chiral amine centre.[12,13] The 40% of APIs that contain a chiral amine moiety also show diversity across a range of treatment areas. They can be found in drug candidates for oncology, in the treatment of hormonal, and neurological disorders, for cardiovascular, and infectious diseases and have even found use in the treatment of diabetes, renal disorders, and sexual health, (see Figure 1).[14]

Due to their prevalence in APIs, and the need for these compounds to exist in high enantiopurity, it is crucial that highly efficient and selective synthetic routes are developed. Traditional chemical synthetic techniques have improved over the years regarding their efficiency, robustness, and improved stereo-, and chemo-selectivity, however they still have some disadvantages. High pressures and temperatures are typically employed in combination with expensive and toxic metal catalysts which

can be difficult to remove. Combined with multiple protection and deprotection steps, the overall atom economy of these reactions can be poor. [2,4]

Biocatalysis has shown promise over recent years as an alternative route to accessing chiral amines. Enzymes possess the natural ability to carry out synthetic reactions with in high regio-, chemo-, and excellent enantioselectivity. They are also capable of working at milder conditions than traditional synthetic methods. For instance, enzymes typically operate at standard atmospheric pressure as well as physiological temperatures and pH in aqueous media. Enzymes are also inherently biodegradable, thereby eliminating the need for the removal of toxic metal catalysts.[2–4,12]
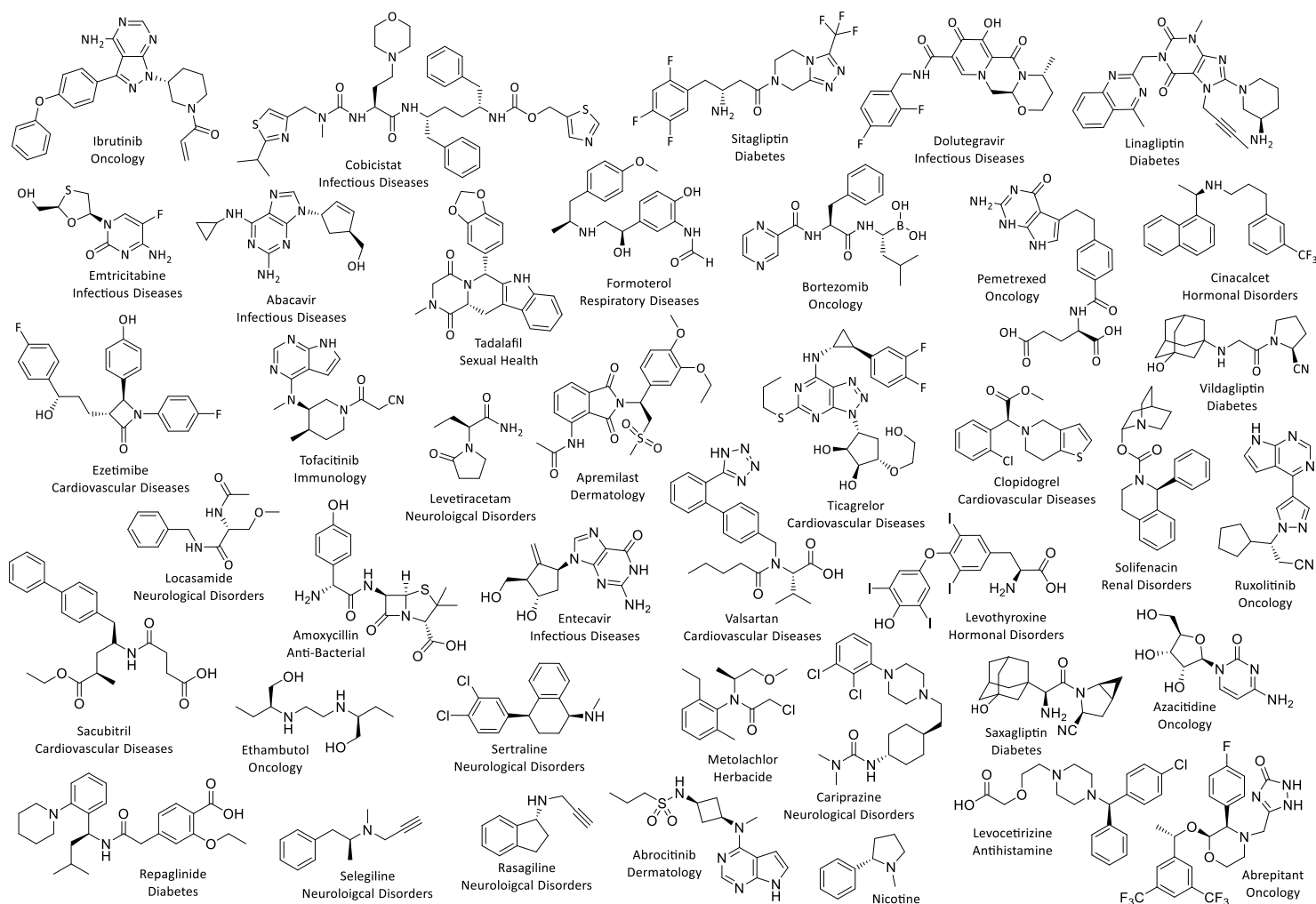
Figure 1: Compounds of interest (mostly APIs) that can be accessed via, or contain, a chiral amine centre[112]

1.2 Chemical Synthesis of Chiral Amines

Several different routes can be chosen in order to chemically synthesis chiral amines, Figure 2. In order to create a stereogenic centre and control which enantiomer is generated, chiral auxiliaries and chiral ligands can be utilised in different reactions such as reductive aminations, C-H insertions, and *N*-alkylations. If accessible and isolable, reactions can start from the prochiral imine precursor that can be reduced into the chiral amine. It is also possible to start from a racemic mixture of the desired amine product and end up with an enantiomerically pure sample using kinetic resolution. [12]
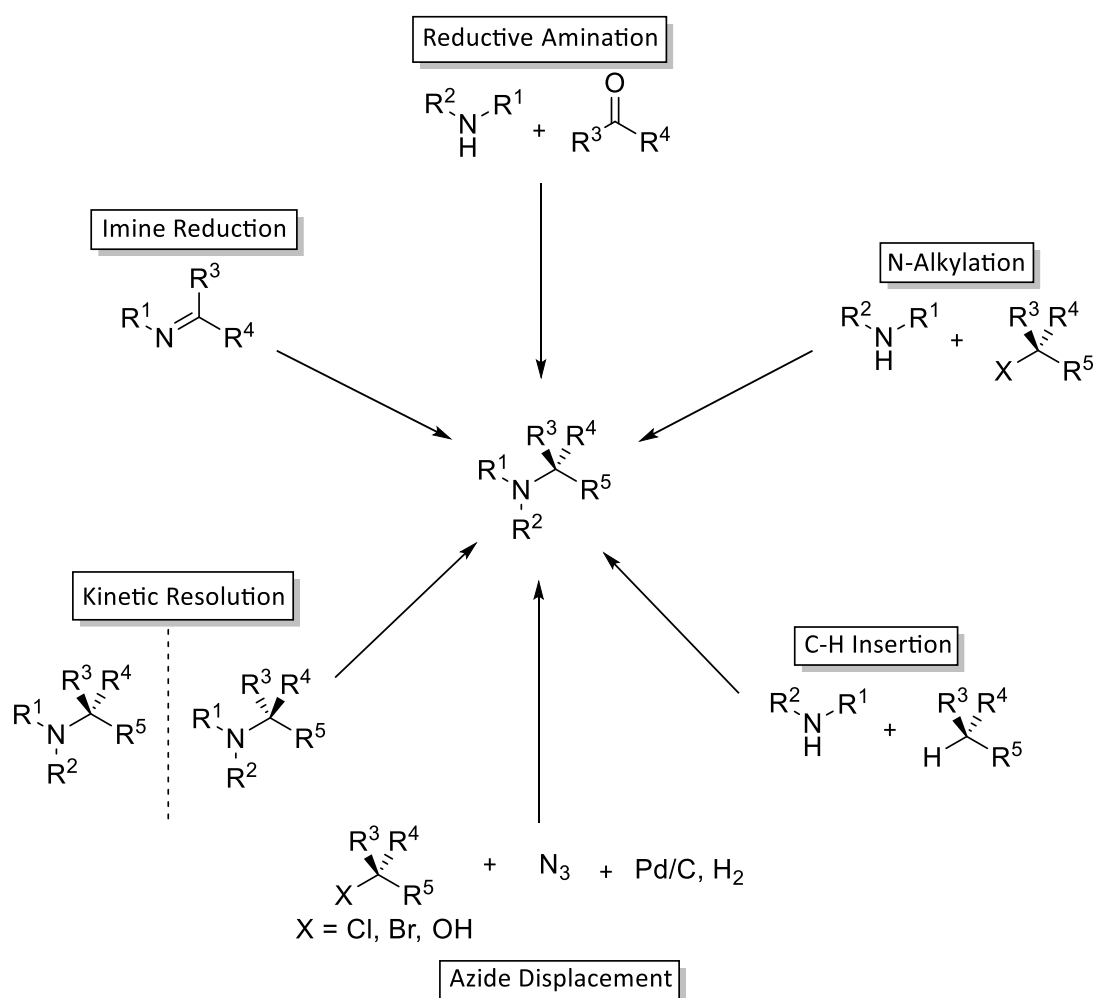
Figure 2: Common synthetic routes for the formation of chiral amines

1.3 Metal Catalysis

The asymmetric metal catalysed formation of chiral amines has literature references dating as far back as 1992. Christopher Willoughby and Stephen Buchwald at MIT reported the first early transition metal based catalyst utilised in the asymmetric hydrogenation of imines. They utilised a titanocene complex co-ordinated to 1,1'-binaphth-2,2'-diolate (Figure 3) to carry out the reduction of a range of cyclic and acylic imines in moderate to excellent *ee*.[15,16] In the 30 years since this work has been carried out, several alternative chiral ligands have been developed and employed to access chiral amines.
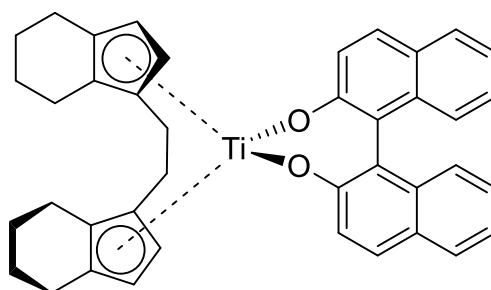
Figure 3: First early transition metal catalyst used for the asymmetric hydrogenation of imines[17]

A review in 2005 by Vassylyev *et al.* summarised major contributions on the development of these titanocene complexes that had been carried out since 1992. They discuss how the chirality of these titanium-ligand complexes can be introduced in various ways and how this chirality can influence the enantioselectivity of hydrogenations. The titanocene compounds can express ligand-derived chirality, such as in the case in Figure 3. This can be generated from ligands that possess chirality before binding, or this can come from prochiral ligands that don't possess their own chirality, but upon binding to the titanium centre generates a chiral compound. There also exists metal-centred chirality in which four different ligands can be coordinate to a tetravalent titanium atom.[17]

1.3.1 Diphosphine ligands

One of the most common ligand types that has seen development and implementation for the asymmetric synthesis of chiral amines are diphosphine ligands. Their structures can vary significantly, or only through small substituent changes. These ligands can be chiral through being single enantiomers, combinations of diastereomers, or they can exist as atropisomers (molecules that do not possess a chiral centre but chirality is induced through the hindered rotation of a bond).

An early review from 1999 by Shu Kobayashi and Haruro Ishitani discusses the enantioselective reduction of imines carried out by several groups in the mid to late 1980s and early 1990s. Most of these reduction reactions utilised either ruthenium, rhodium, or iridium as the metal catalyst used in combination with several different chiral diphosphine ligands (see Figure 4).[18]
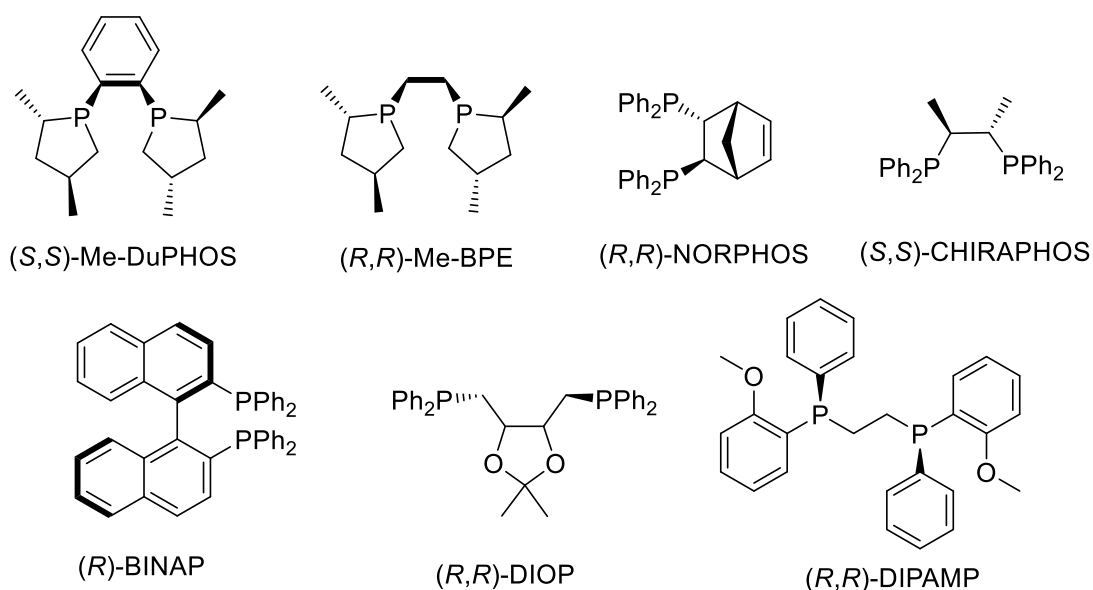
Figure 4: Early diphosphine ligands used for the enantioselective reduction of imines

The hydrogenation of enamides is one route to access chiral amines using diphosphine ligands. Two phosphine ligands, Me-DuPhos and Me-BPE, were found to be highly effective towards the selective hydrogenation on a selection of α-arylenamides.[19] Following this work, the diphosphine ligands of DIPAMP and BINAP were developed further, also in the hopes of carrying out efficient selective hydrogenation of α-arylenamides. These new ligands had advantages over the Me-

DuPHOS and Me-BPE ligands as they were more easily accessible, resulting in an overall more efficient synthetic procedure.[20]

Not only was this Me-DuPHOS ligand capable on selective hydrogenations of alkenes adjacent to amines, but it was also utilised for the selective alkylation of imines. Through mono-oxidation of one of the phosphorous groups, the new ligand BozPHOS was generated (Figure 5). When combined with a copper triflate complex, the successful reduction of a range of substituted *N*-phosphinoylimines was performed in excellent yields and improved enantioselectivities when compared to the starting ligand Me-DuPHOS.[21]
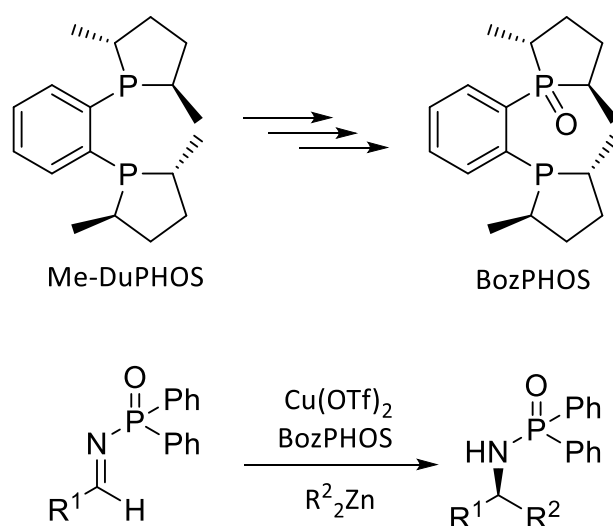
Figure 5: BozPHOS catalysed asymmetric alkylation of N-phosphinoylimines

Several other ligands have been utilised for the reduction of imines without activating phosphinoyl groups. Cyclic amines are a structurally important group and Zhang *et al.* showed the possibility of accessing these through the reduction of 3,4-dihydro-2H-pyrrole with varying substituents in the 2-position. Through screening of several diphosphine ligands, they chose the ferrocene containing ligand (*R,R*)-f-spiroPhos (Figure 6). When screened against a selection of substituted cyclic imines that had also been tested against Me-DuPHOS, only a slight improvement was observed in *ee*s.[22]
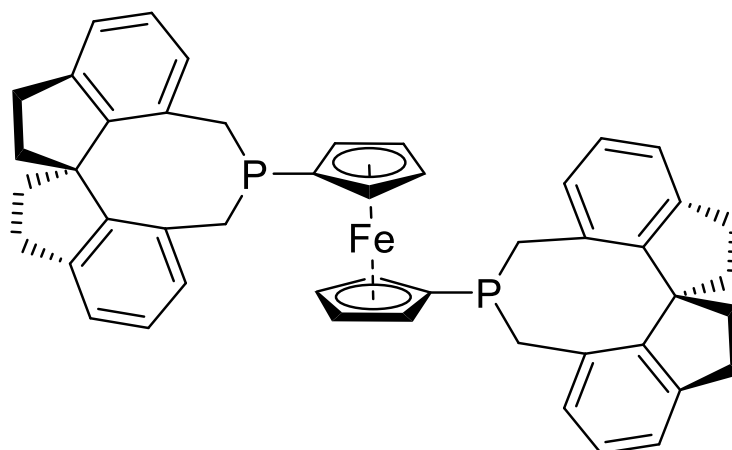
Figure 6: Chiral phosphine ligand used for the asymmetric reduction of cyclic imines

1.3.2 Monophosphine ligands

Ligands containing only one phosphine group have also been used to successfully access chiral amines. In 2005 Zhang *et al.* screened a panel of phosphoramadite ligands for the *N*-alkylation of different amines using iodobenzene. Around ten different ligands were investigated, containing different aryl groups and different *N*-substituents (Figure 7). A binapthol based phosphoramidite ligand with a dibenzyl substituted nitrogen, used in tandem with CuBr, was determined to be the best performing ligand resulting in amine products in high yields.[23]

Another successfully utilised monophosphine ligand was TRIP (Figure 8). When combined with iridium supported on polystyrene, this ligand aided in the asymmetric reduction, and direct asymmetric reductive amination, of protected imines and amines (with either *p*-methoxyphenol (PMP), *o*-methoxyphenol (OMP), or dimethoxybenzene). The reaction was shown to be selective towards the reduction of a small panel of aromatic imines, and for the reductive amination of a small selection of aliphatic ketones. One of the reductive amination products, once deprotected, was a suitable precursor for the alpha-blocker Tamsulosin, which was isolated in 74% yield and a 91% *ee*.[24]

Figure 7: Phosporamidite ligands screened for the N-alkylation of amines using iodobenzene
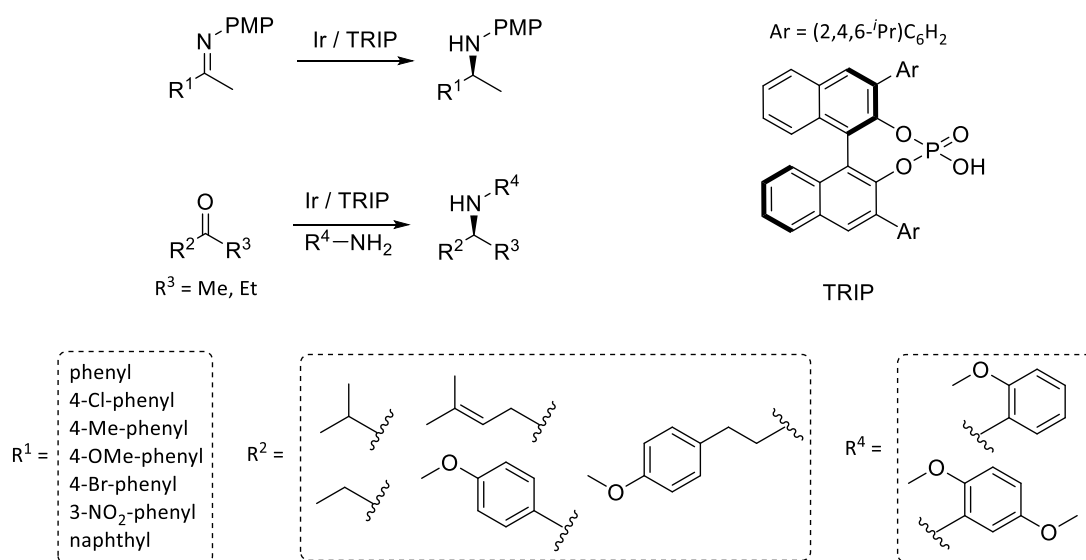
Figure 8: TRIP directed synthesis of chiral amines via imine reduction and reductive amination

Although over the years many efforts concentrated on improving its efficiency, metal-catalyzed asymmetric synthesis still comes along with severe drawbacks. For example, synthesis of BozPHOS from Me-DuPHOS requires three reaction steps, yet in comparison to Me-DuPHOS *ee*s catalyzed reactions, *ee*s of imine alklylations were only improved by a mere 10%. All of the reactions mentioned so far require the use of toxic metals such as titanium, iron, rhodium, iridium, ruthenium, and copper, which typically result in purification issues. Recent advances in graphene oxide nanoparticles have shown to be effective ways at removing heavy metals.

In the cases of the TRIP catalysed imine reductions and titanocene hydrogenations, molecular hydrogen was used at almost 20 atms. These high-pressure systems are not only dangerous but require specialised equipment that can be expensive to manufacture and operate. These reactions also require hazardous organic solvents, typically toluene, as well as the requirement for protecting groups.

On the contrary, biocatalysis has emerged as a viable alternative to traditional chemical routes in recent years. The biodegradable nature of enzymes, as well as the ability to carry out reactions at ambient temperatures and pressures make enzymes attractive to achieve greener processing routes. Over the years, many different approaches have been used to synthesis chiral amines biocatalytically. Many different enzyme classes have been employed depending on substrate and product demand, stereoselectivity and the type of amine required (e.g. primary, secondary or tertiary). Monoamine oxidases, amine dehydrogenases, transaminases and the more recently developed imine reductases and reductive aminases are all types of enzymes that have been used.[11]

1.4 Enzymes for Amine Synthesis

1.4.1 Monoamine Oxidases

Monoamine Oxidases (MAOs) are homo dimer enzymes that catalyse the irreversible conversion of amines to imines with the aid of a flavin cofactor.[25] The irreversible nature of this process allows for the control of the position of equilibrium. Stereoselective MAOs are used in tandem with non-selective reducing agents (such as sodium borohydride) for the kinetic resolution of racemic amines to give products

with excellent yields and enantioselective excesses. The monamine oxidase from *Aspergillus niger* (MAO-N) has been well developed over the years. MAO-N and the related cyclohexylamine oxidases (CHAOs) are both largely *S*-selective whereas the oxidase from *Anthrobacter nicotinovorans* 6-hydroxy-nicotine oxidase (HDNO) is typically *R*-selective.[26] Levocetirizine and solefenacin are example drug molecules that are obtained through kinetic resolutions. They both contain benzylhydroamine moiety, making them complicated molecules for use with MAOs as the wild type enzymes possess a limited substrate scope.[27]

The structure of the MAO from *Aspergillus niger* was first elucidated in 2008 and this allowed for rational design directed evolution to improve the activity. Two variants that were established from this work were MAO-D3 (which possesses three point mutations) and MAO-D5 (which possesses five point mutations). MAO-D3 showed improved activity towards chiral secondary amines compared to the wild type and MAO-D5 showed activity towards chiral tertiary amines (see Figure 10).[28]
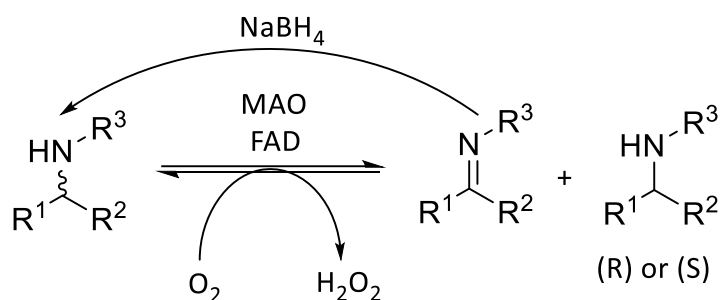
Figure 9: General reaction scheme for the kinetic resolution of racemic amines using monoamine oxidases

MAO-D5, is very commonly applied in kinetic resolution reactions and was chosen for rational design in order to carry out kinetic resolutions of more complex, bulky amines. It was hypothesised by Ghislieri *et al.* that the substrate scope can be expanded by increasing the cavity size of the active site. Modelling of MAO-D5 with the simpler homologue amine α-methylbenzene identified two potential residues for site-directed mutagenesis and the W450G mutant showed activity towards aminodiphenyl methane (unlike other MAO variants) and this variant was labelled MAO-D10 which possessed an active site ~1.4 times larger than D5. A further four

mutations were carried out on MAO-D10 within the entrance channel to the active site (F210L, L213T, M242Q, I246T) to generate a variant labelled MAO-D11 increasing the active site cavity size to a value ~3 times larger than D5.[27]
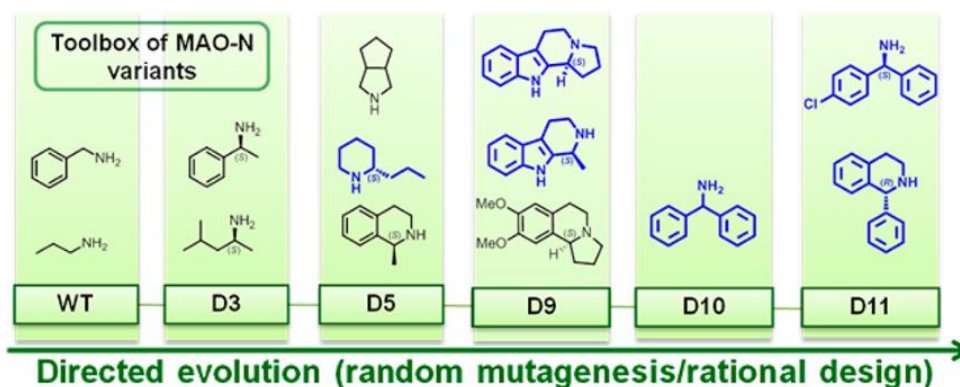
Reprinted with permission from D. Ghislieri, A. P. Green, M. Pontini, S. C. Willies, I. Rowles, A. Frank, G. Grogan and N. J. Turner, J. Am. Chem. Soc., 2013, 135, 10863–10869. Copyright 2013 American Chemical Society.

Figure 10: Variants of MAO-N created through directed evolution and the substrate scope associated to each variant

Other complex molecules that show interest for the kinetic resolution with MAOs are tetrahydro-β-carbolines (THBCs), an important structural motif found in many bioactive alkaloid natural products. Surprisingly the D9 and D11 variants displayed an inversion of stereoselectivity. Both variants are (*S*)-selective, however the measured enantiomeric excesses for both variants were <50%. The D10 variant which differed from D9 and D11 through four point mutations in the entrance channel (L210F, T213L, Q242M, and T246M) gave the (*R*)-enantiomer with 97% ee, and this was down to the substrate being positioned ~0.3Å closer to the FAD cofactor than with the D11C variant.[29]

The scope of MAOs has been well investigated with D5, D9 and D11 variants having been screened with 132 racemic chiral amines covering a wide range of functionalities ((α-substituted methylbenzylamines, benzhydrylamines, 1,2,3,4-tetrahydronaphthylamines (THNs), indanylamines, allylic and homoallylic amines, propargyl amines). Of the three variants, D11 has been labelled as the high end MAO

33

due to its ability to successfully oxidise sterically hindered primary, secondary and tertiary amines. However of the three, MAO-N-D9 variant was show to been the most active of the three enzymes towards most of the amines tested providing excellent enantioselectivites.[30]

1.4.2 Amine Dehydrogenases

Enzyme catalysed reductive amination reactions between ammonia and prochiral ketones are very limited. Substrates have been limited to α-keto acids for the preparation of amino acids using amino acid dehydrogenases (AADH).[31] Amine dehydrogenases (AmDH), a class of enzymes very closely related to AADHs, pose an ideal route to the synthesis of chiral amines. When paired with a recycling system for the regeneration of the nicotinamide cofactor (e.g. glucose dehydrogenate (GDH) or formate dehydrogenase (FDH)), reactions can be carried out only using up cheap consumables such as glucose/formate and free ammonia.[32] The first identified amine dehydrogenase was in 2000 by Itoh *et al.*, which showed a broad substrate scope. [33] It would however be at least a decade until this enzyme class was pursued further due to limited genetic information and insufficient enantioselectivity. [34]
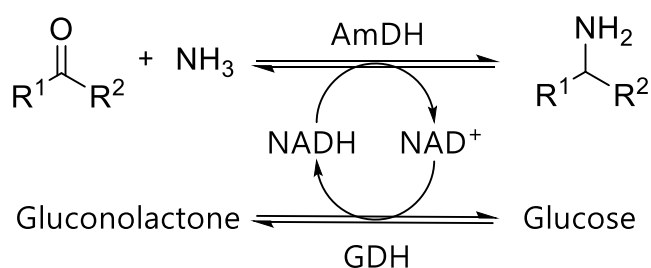
Figure 11: General reaction scheme for the synthesis of a chiral primary amine using an amine dehydrogenase. $R^1 \neq R^2$.

Bommarius and coworkers reported one of the first cases of engineering of an amino acid dehydrogenase, a leucine dehydrogenase (LeuDH), to create an amine dehydrogenase. The LeuDH is capable of producing leucine from the corresponding keto-acid. After 11 rounds of mutations, a final four point mutant variant was developed which showed little activity towards the natural substrate, L-Leucine, and showed high activity towards the corresponding compound with no carboxyl group. This four point mutant (K68S/E114V/N261L/V291C) was highly active towards non-

keto acids and led to enhanced amination of all ketones investigated with the exception of methyl acetoacetate.[32]

A second amine dehydrogenase was generated from another AADH which possessed 48% sequence match and 66% similarly with LeuDH. Phenylalanine dehydrogenase (PheDH) was chosen as it was theorised that the resulting amine dehydrogenase, PheDH-AmDH, would have a higher specific activity and an increased substrate scope compared to LeuDH-AmDH. The influential mutations from the LeuDH-AmDH (K67M, E113V, N261V) were investigated both individually and as a combination on the PheDH scaffold. The corresponding residues were identified in PheDH and the double variant K77M/N276V was shown to be possess activity towards methyl isobutyl ketone (MIBK) and even higher activity towards 4-fluorophenylacetone with excellent (R)-stereoselectivity. This double variant mutation was explored further and found that K77S/N276L mutation provided higher reductive amination activity.[35]

The development of these two amine dehydrogenases engineered from amino acid dehydrogenases led to the creation of more AmDHs. Unfortunately, despite the advances that have been made AmDHs have found limited applicability in industrial processes due to their limited scalability.[34] Conversions are affected due to factors such as enzymes stability under process conditions, inhibition of the enzyme from products/substrates, unfavourable equilibria, and catalytic parameters. In fact, the best performing AmDH, PheDH-AmDh, with the best performing ketone, 4-fluorophenylacetone, shows turnover numbers ~14 times less than for wild-type AADHs with no reports so far of reactions exceeding a substrate concentration greater than 80 mM.[36] Many step have been taken to improve on these Figures, especially in the use of biphasic aqueous-organic solvent systems using water immiscible organic solvents. This allows for effective reactions of hydrophobic ketones and easier separation of products without the destabilising effect on enzymes that some organic solvents can pose.[36,37]

Engineering of amino acid dehydrogenases to create amine dehydrogenases has been necessary as it was believed that AmDHs were not ubiquitous to nature. However this has been proved to be incorrect recently. Mayol et al. screened the sequence space starting from a 2,4-diaminopentanoate dehydrogenase. 169 proteins

with at least 30% identity match were collected and screened for activity for the reductive amination of ketones without and α or β carboxylic acid group. These enzymes were screened using 4-oxopentanoic acid, a γ-keto acid, and found 6 with activity, with the amine dehydrogenase from *Petrotoga mobilis*, AmDH4, showing the best activity. This was the first native enzyme to show reductive amination towards ketones without an α- or β-carboxylic acid group and was labelled as an ω-amine dehydrogenase.[31]

Since the discovery of these ω-amine dehydrogenases, more native amine dehydrogenases have been identified. AmDH4 was used as a starting point to explore the sequence space even further than was done initially. Several enzymes were identified that had been previously labelled as dihydropicolinate reductases. One of these enzymes, the AmDH from *Mycobacterium smegmatis*, *Msme*AmDH, as well as an uncharacterized protein from *Cystobacter fuscus*, *Cfus*AmDH, were both active towards a range of ketones and aldehydes with ammonia and methylamine.[38]

1.4.3 Ammonia Lyases

Ammonia lyases are a class of enzymes that catalyze the reversible deamination of C-N bonds, typically of α-amino acids and several different classes of ammonia lyases exist. Phenylalanine ammonia lyases (PALs), histidine ammonia lyases (HALs), and tyrosine ammonia lyases (TALs), are all examples of aromatic amino acids ammonia lyases that catalyze the deamination of the corresponding amino acids. These are just a few of the identified ammonia lyases and other ammonia lyases exist that work on other canonical α-amino acids.

Ammonia lyases are a restricted class of enzymes. They lack diversity across the panel of identified enzymes with the substrate scope is limited to α-amino acids, with some engineered ammonia lyases accepting β-amino acids.[39–41]

1.4.4 Transaminases

Transaminases (TAs) are enzymes that transfer an amine group from an amino donor to a carbonyl amine acceptor producing a new amine and a ketone coproduct of which there are two classes of transaminases: α-TAs and ω-TAs. α-TAs require either the amino donor or amino acceptor to possess an alpha-carboxyl acid group which

limits the enzymes to the synthesis of α-amino acids only. ω-TAs do not require the presence of a carboxylic acid group and so allow access to substrates that are ketones, aldehydes and keto-acids. The structure of TAs is a dimeric system with two cavities within the binding site: one large and one small.[42] ω-TAs can be utilised for both the asymmetric synthesis of chiral amines and for the kinetic resolution of racemic amines.
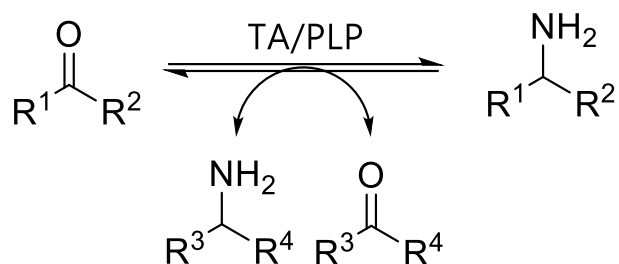
Figure 12: General reaction scheme for transaminases

The main challenge that comes with transaminases is that the yields of reactions rely on the equilibrium between the prochiral ketone substrate and the chiral amine product. One way in which this can be encouraged is through the removal of the ketone co-product that is produced. Many techniques have been employed to remove the ketone co-product and to drive the equilibrium in the direction of the products. In cases where the amino donor used is alanine, a lactate dehydrogenase can remove the pyruvate produced as the ketone co-product.[43] If isopropylamine is used instead of alanine (as is quite common) then the acetone that is formed, if removed in situ, or increasing the concentration of the amino donor can also be used to drive the equilibrium.[44]

One less commonly employed technique is to use an amino donor such as 3-aminocyclohexa-1,5-dienecarboxylic acid. Although this compound is less readily available and more expensive that alanine and isopropylamine, the corresponding ketone is unstable and undergoes tautomerization to the more stable 3-hydroxybenzoic acid which prevents the reverse reaction.[45]

Transaminases suffer from a limited substrate scope due to the two parts of the active site cavity, one large and one small, only ketones where one of the alpha

substituents is relatively small are accepted. Sitagliptin is an API of desire, used in the treatment of diabetes, and contains a chiral amine moiety surrounded by bulky substituents. Through a combination of in-silico design and directed evolution, and (R)-selective ω-TA (ATA-117) was engineered towards activity for the amination of the prositagliptin ketone. The final mutation that showed a good level of activity with high enantioselectivity possessed 27 mutations in and around the active site.[44]
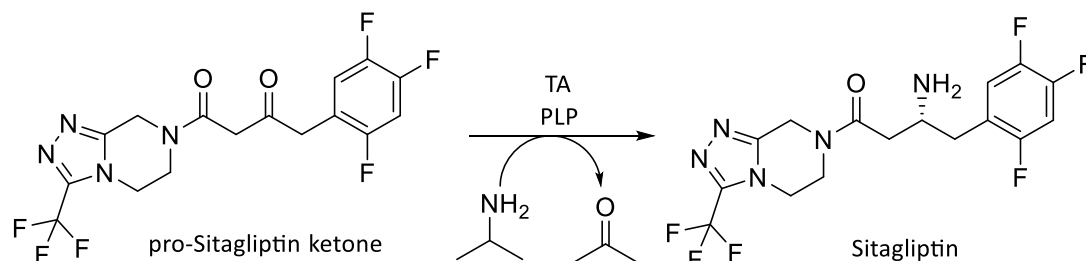
Figure 13: Transamination of the prositagliptin ketone to Sitagliptin

The use of 'smart' amino donors has seen a rise in use. These are compounds that carry out a secondary role other than just the amination of the ketone. O-xylylenediamine is one such smart donor that is also used as a high-throughput screening. Upon amination of a ketone, the co-product 2-(aminomethyl)benzaldehyde is formed which undergoes spontaneous polymerisation to product a black substance to identify the success of the reaction (Figure 14).[45]
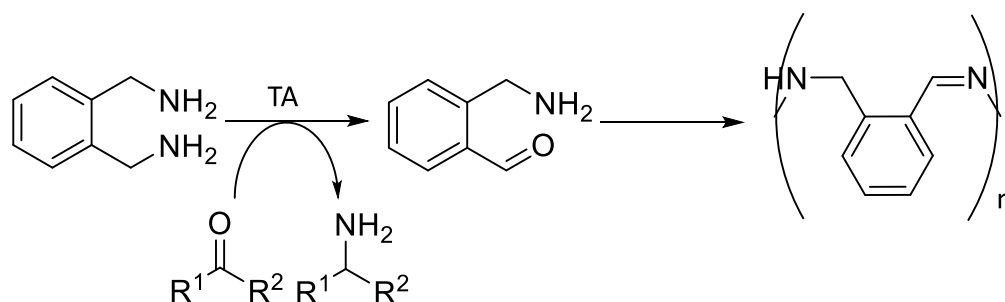
Figure 14: Spontaneous polymerization of 2-aminomethylbenzaldehyde when O-xylylenediamine is used as an amine donor

Transaminases have also been used with diamino and diketone substrates. Monoamination of 1,4- and 1,5-diketones leads to the spontaneous cyclisation to

form 5- or 6-membered cyclic imines which can then be reduced to give the cyclic amine. Vicinal diamines have shown good applications to the synthesis of aromatic pyrazines when used as an amino donor. The alpha-amino ketone co-product undergoes spontaneous dimerization with a second alpha-amino ketone after which spontaneous oxidative aromatisation occurs to generate the pyrazine.[46] The cyclic imine intermediates that are formed in this reaction are the target compounds for another class of enzymes called imine reductases (see Chapter 2).

Chapter 2: Imine Reductases

2.1 Initial discovery

Imine reductases (IREDs) are an NADPH-dependent class of oxidoreductase enzymes. As the name suggest, they catalyse the asymmetric reduction of prochiral imines to their asymmetric amine counterparts. Mitsukura et al. at Gifu University, Japan discovered the first IREDs in 2010. They were interested in finding an imine-reducing enzyme towards the reduction of 2-methyl-1-pyrroline (2-MPN), a cyclic imine that was shown to be highly stable in aqueous solutions. They initially expected to find an active enzyme from several yeasts, however of the 226 different yeast strains they found no activity. The search was then expanded to look at 261 strains of bacteria, 117 strains of actinomycetes, and 84 strains of fungi. Despite a wide range of species being tested, only five successful hits were identified, all from bacteria of the *Streptomyces* sp. family. Of these five bacterial enzymes, two stood out to be of novel activity. The enzymes from *Streptomyces* sp. GF3587 and GF3546 showed high conversion of 2-MPN to the (*R*)- and (*S*)-2-methylpyrroline, respectively. [47]

These two IREDs were purified and characterised further. The (*R*)-IRED from *Streptomyces* sp. GF3587 was found to not only catalyse the reduction of 2-MPN but also the oxidation of the amine to the imine when under basic conditions. It was however reported that this enzyme was only active towards 2-MPN.[48] Mitsukura *et al.* then explored the (*S*)-IRED from GF3546 further and found that this was active towards a couple of other cyclic imines. When the methyl group of 2-MPN was replaced with a carboxylic acid group, the conversion dropped from 100% to 34%. A couple of bicyclic compounds were also tested, however these were shown to be even poorer substrates. 1-methyl-3,4-dihydroisoquinoline, and the bulkier 6,7-dimethoxy-1-methyl-3,4-dihydroisoquinoline were screened and displayed conversion values of 23% and 2%, respectively (Figure 15).[49]

2-methyl-1-pyrroline
(100%)

1-pyrroline-2-carboxylic acid
(34%)

1-methyl-3,4
-dihydroisoquinoline
(23%)

6,7-dimethoxy-1-methyl
-3,4-dihydroisoquinoline
(2%)
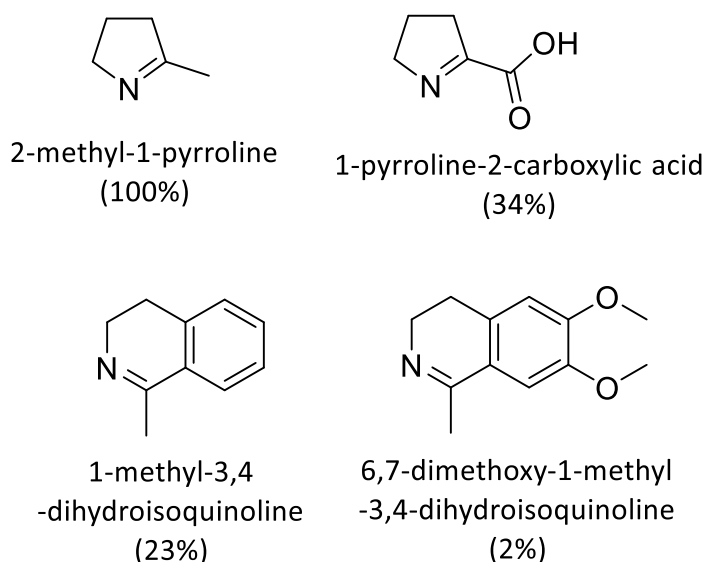
Figure 15: Initial substrate scope of (S)-IRED from Streptomyces sp. GF3546

Both the (*S*)-IRED and (*R*)-IRED were investigated further by the Turner group at the University of Manchester. They initially investigated the (*S*)-IRED since it had been shown by Mitsukura to be active on more than just the initial 2-methyl-1-pyrroline substrate. The IRED expressed in *E. coli* and whole cell biocatalysis was carried out on a range of cyclic imines of different ring sizes, as well 3,4-dihydroisoquinolines (DHIQs), and dihydro-β-carbolines (Figure 16).

The dihydroisoquinolines **14**, **15**, and **16** were all readily accepted by both IREDs yielding the corresponding amine products in high yields and high *ee* values with retention of stereochemistry. When comparing ring sizes of cyclic imines, we can see that for the (*S*)-IRED from GF3546, the larger six- and seven-membered rings are more readily accepted than 2-methyl-1-pyrroline. It can also be seen that the type of substituent in the 2-position of these rings can have an affect in conversion values. Typically larger substituents result in a decrease in activity providing the corresponding amine products in lower conversions. We can also see for the (*R*)-IRED from GF3587 that the substituents also play a role in the relative *ee* values, with the size, shape, and electronic properties playing a role, with small changes resulting in large differences (see substrates **2**, **3**, **4**, and **5**). It was also shown that even larger ring systems such as dihydro-β-carbolines are readily accepted with conversions ranging from 50% to > 98% (compounds **17-21**).[50–52]

12, R = Me (>98%, >98% (S) : >98%, >98% (R))
13, R = p-MeOPh (n.r., n.r. : 50%, >98% (S))

22, R = H (>90%, n.a. : 97%, n.a.)
23, R = Me (n.r., n.r. : 24%, 74% (R))

6, R = Me (>98%, >98% (S) : >98%, >98% (R))
7, R = n-propyl (n.r., n.r. : >98%, 66% (S))
8, R = isopropenyl (n.r., n.r. : >98%, 96% (S))
9, R = 1-napthyl (n.r., n.r. : 4%, 27% (n.d.))
10, R = Ph (n.r., n.r. : >98%, 37% (S))
11, R = p-MeOPh (n.r., n.r. : >98%, >98% (S))

17, R^1 = H, R^2 = Me (>98%, >98% (S) : n.r., n.r.)
18, R^1 = H, R^2 = Et (>98%, >98% (S) : n.r., n.r.)
19, R^1 = H, R^2 = iPr (69%, 98% (S) : n.r., n.r.)
20, R^1 = H, R^2 = cyclohexyl (97%, >98% (S) : n.r., n.r.)
21, R^1 = OMe, R^2 = Me (50%, >98% (S) : n.r., n.r.)

1, R = Me (55%, >95% (S) : >98%, >98% (R))
2, R = Ph (36%, 87% (R) : >98%, 8% (S))
3, R = p-MeOPh (17%, >98% (R) : 20%, >98%(S))
4, R = p-FPh (42%, 98% (R) : 86%, 26% (S))
5, R = cyclohexyl (n.r., n.r. : >98%, 66% (S))

14, R^1 = R^2 = R^3 = H (>98%, n.a. : >98%, n.a.)
15, R^1 = R^2 = H, R^3 = Me (>98%, 98% (S) : >98%, 71%(R))
16, R^1 = R^2 = OMe, R^3 = Me (92%, >98% (S) : n.r., n.r.)

Conversion and enantioselectivity data for GF3546-IRED[50] and GF3587-IRED[51] given in blue and red respectively
Change in absolute configuration is reflective of a change in Cahn-Ingold-Prelog assignment for 2-substituted imines with larger
substituents.[52] n.r. = not recorded; n.d. = not determined; n.a. = not applicable.
Figure recreated using data from references [4], [5], and [6].

Figure 16: A selection of cyclic imines from the expanded substrate scope for the (S)- and (R)-IREDs from Streptomyces sp.

Reductive aminations (discussed more in section 2.6) are other important routes to accessing chiral amines, and unlike imine reductions, allow for the addition of certain groups attached to either the carbonyl carbon or to the amine donor. A small panel of carbonyls and amines was additionally tested with (*S*)-IRED, as well as another IRED from *Streptomyces aurantiacus*. Unfortunately, the best result from this was the reductive amination between 4-phenylbutan-2-one and methylamine. [53]

The success shown from these initial IREDs from *Streptomyces* sp. resulted in a lot of interest from several different groups to explore the sequence space for other IREDs. This search for new IRED sequences was mainly driven by the desire to increase the substrate scope and to expand these enzymes into carrying out reductive amination reactions.

In 2013, an NADPH-dependent oxidoreductase Q1EQE0 was discovered from *Streptomyces kanemyceticus* (*Sk*-IRED). It was found to be active towards the asymmetric reduction of 2-methyl-1-pyrroline (the substrate initialled screened by Mitsukura) in high *ee*. This IRED also became the first crystal structure to be elucidated, given insight into its structural characteristics and potential active site residues (Figure 17). It was through this structure elucidation that the IREDs were identified to exist as a dimer protein which each monomer consisting of an N-terminal Rossman-fold domain and a C-terminal helix and that these two areas of each subunit formed and interface generating the active site.[54]
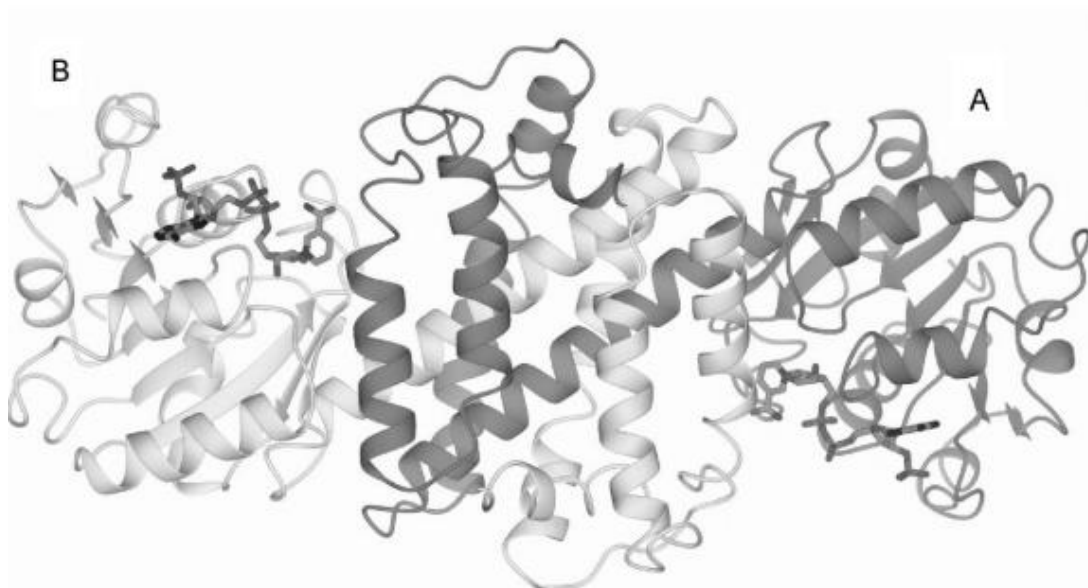
Figure 17: First IRED crystal structure of the IRED from Streptomyces kanemyceticus[54] *– Permissions granted by Wiley*

The resolution of the crystal structure of the *Sk*-IRED aided in the discovery of other putative IREDs. Work from the groups of Bettina Nestl and Bernard Hauer used the *Imine Reductase Engineering Database* developed at Stuttgart[55] to look for other sequences with similarity to that of *Sk*-IRED. They identified two novel (*R*)-type and one (*S*)-type IRED from the database and screened against the reduction of 2-methyl-1-pyrroline in high stereoselectivity, and showed the potential of identifying new IREDs. [55]

The group of Matthias Höhne also looked for sequences of similarity to *Sk*-IRED and identified three novel IREDs from *Paenibacillus elgii* (SIR-Pel), *Streptomyces ipomoeae* (RIR-Sip), and *Pseudomonas putida* (RIR-Ppu). With these three newly characterised IREDs, they managed to not only access endocyclic amines, but also acyclic amines with varying degrees of activity. This was one of the first examples showing access to acyclic amines, highlighting the potential substrate scope with IREDS. RIR-Sip was shown to be able to access these acyclic amines with higher activity when compared to the previously tested cyclic amines. [56]

2.2 Expanding the substrate scope

Over the decade since the discovery of the IRED, a lot of work has been carried out in increasing the available substrate scope that these enzymes can work on. Reduction of more complex imines, such as bulkier compounds or ones containing heteroatoms, as well as reductive amination reactions have all be desirable.

After the first initial substrate screen of pyrrolines, dihydroisoquinolines, and β-carbolines, Hao Li *et al.* wanted to explore the capability for IREDs to reduce 3*H*-indoles to 3*H*-indolines (Figure 18). They screened 50 putative IREDs and found that the imine reductase from *Paenibacillus lactis* (*Pl*SIR) showed high activity towards the reduction of compound **24**. The enzyme was then screened against a panel of different indoles and was found to particularly effective still when substituents were attached to the benzene ring. Compounds **24** to **32** were all reduced to the (*S*)-indoline in very good yields ranging from 68% (**31**) up to 86% (**28**). When a larger substituent was introduced to the 2-position or a spirocycle created at the 3-position, all activity was lost. The IRED was also capable of reducing iminium salts (**35 – 40**, yields ranged from 71% to 87% in >94% *ee*), with the *N*-Me- and *N*-Et-substituted iminiums being reduced faster than their non-*N*-substituted indoles counterparts. [57] Hao Li *et al*. also wanted to be able to access the (*R*)-enantiomer products of these 3*H*-indoles, and found an IRED also from *Paenibacillus lactis* (*Pl*RIR) that was capable of doing so in good to excellent yields (>71%) and with good to excellent *ee* (>66% (*R*)). It was observed, however, that although an improvement in activity was observed for the reduction of iminium salts, the (S)-enantiomer was still the preferred configuration.[58]

24
75%, >99% (S)
>99%, 96% (R)

25
74%, >99% (S)
99%, 90% (R)

26
82%, >99% (S)
99%, 96% (R)

27
80%, >99% (S)
98%, 98% (R)

28
86%, 97% (S)
96%, 83% (R)

29
83%, 89% (S)
71%, 91% (R)

30
79%, >99% (S)
97%, 96% (R)

31
68%, 89% (S)
65%, 87% (R)

32
82%, 99% (S)
82%, 66% (R)

33
n.d.
n.d.

34
n.d.
n.d.

35
71%, >99% (S)
>99%, 84% (S)

36
71%, >99% (S)
>99%, 92% (S)

37
74%, 96% (S)
>99%, 98% (S)

38
83%, >99% (S)
>99%, 89% (S)

39
87%, >99% (S)
>99%, 90% (S)

40
76%, 94% (S)
>99%, 82%
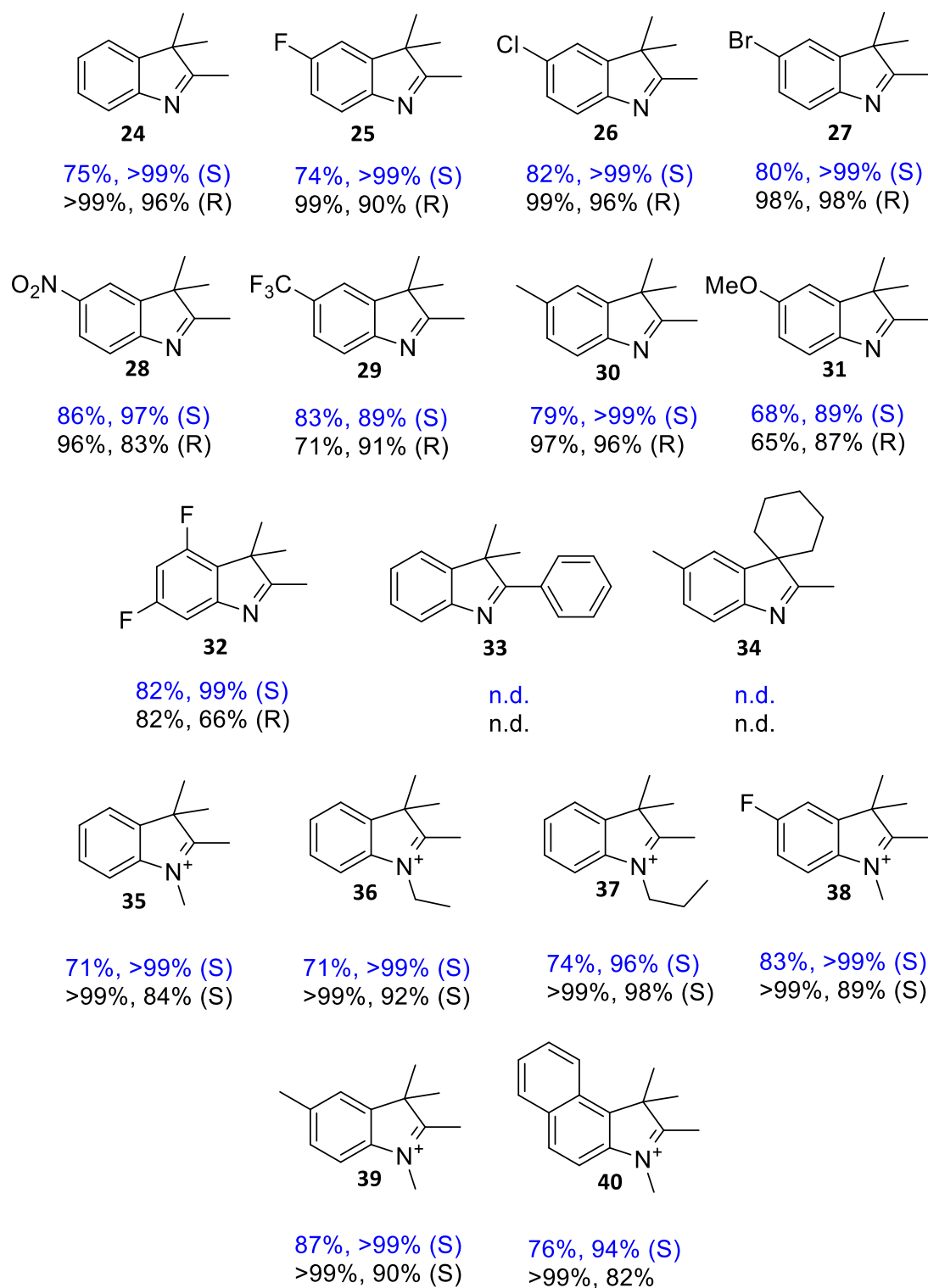
Figure 18: Panel of 3H-indoles and 3H-indole based iminium salts for imine reduction by IREDs from Paenibaccilus lactis to access 3H-indolines. Data for PlSIR in blue and PlRIR in black.

It has previously been shown that dihydroisoquinolines are readily accepted substrates for IREDs.[50,51] This scope has been expanded on by Li *et al*. who identified an IRED from *Stackebrandtia nassauensis* that was capable of accepting DHIQs with different sized alkyl groups (methyl, ethyl, propyl, and isopropyl) in the 1-position.[59] Derivatives of isoquinolines, such as benzylated octahydroisoquinolines (OHIQs), are important building blocks towards the morphinan skeleton. A panel of 48 different IREDs were screened towards the reduction of 1-(4-methoxylbenzyl)-3,4,5,6,7,8-hexahydroisoquinole (HHIQ), **41**, and the best (*S*)-selective (IR30-GDH) and best (*R*)-selective IRED (IR40-GDH) were chosen to then test a panel of different 1-benzyl-HHIQs. A range of different substituents on the benzyl motif was readily accepted with conversions ranging from 47% to 95% and *ee* values >94% (Figure 19). [60]

41
IR40-GDH - 80%, >99% (*R*)
IR30-GDH - 74%, 98% (*S*)

42
IR40-GDH - 78%, >99% (*R*)

43
IR40-GDH - 90%, 99% (*R*)

44
IR40-GDH - 73%, 98% (*R*)

45
IR40-GDH - 95%, 99% (*R*)

46
IR40-GDH - 85%, 99% (*R*)

47
IR40-GDH - 87%, 99% (*R*)

48
IR40-GDH - 47%, 97% (*R*)
IR30-GDH - 70%, 94% (*S*)
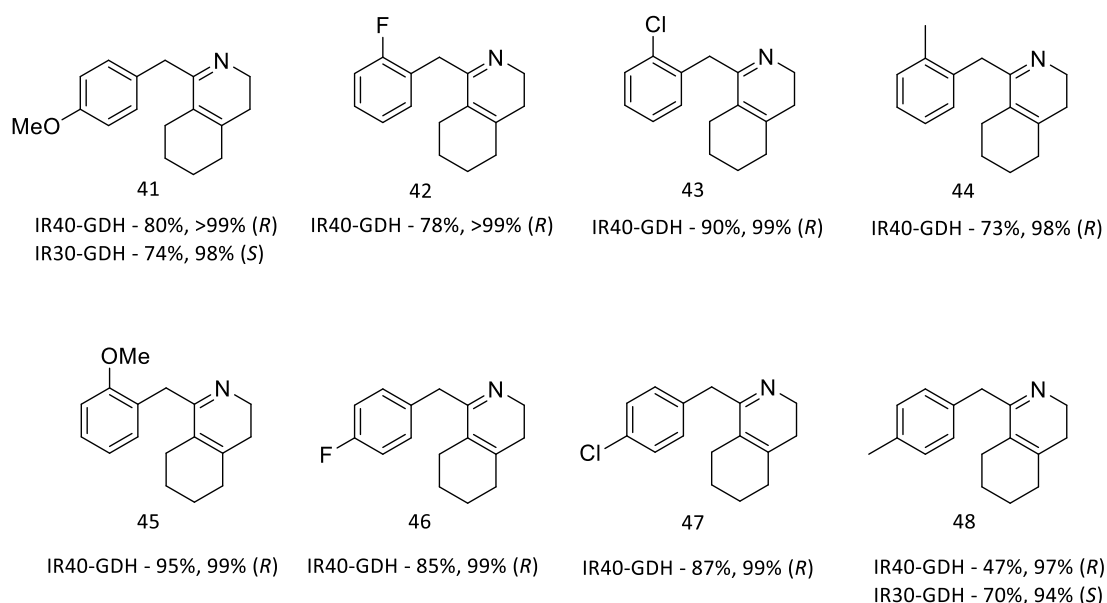
Figure 19: Substituted 1-benzyl-HHIQs scope screened to access precursors for the morphinan skeleton

We have also seen in recent years, the expansion of 2-phenyl-1-pyrroline based compounds suitable for imine reduction. An (*R*)-selective and an (*S*)-selective IRED from *Streptomyces clavuligerus* (*Sc*IRED) and *Streptomyces viridochromogenes* (*Sv*IRED) respectively. They were shown to both accept 2-phenyl-1-pyrroline compounds with a fluorine, chlorine, or methyl group in either the ortho- meta-, or

para-position of the benzene ring. The corresponding pyrrolidines were all produced in good yields (60% to 80%) with *ee* values > 99%.[61]

Pharmaceutically relevant amines have also been accessed through IRED catalysed reductive aminations. Matzel *et al.* looked investigated a panel of IREDs, both from in house and provided from Roche, in order to find an enzyme capable of accessing APIs such as Rasagaline, Selegiline and Pramipexole. A small selection of precursor carbonyls and amines were initially chosen and screened using the amine donors in a 50-fold excess (Figure 20). Of the four carbonyls tested, cyclohexanone, **41**, was the most readily accepted across all enzymes, and was most successful when combined with amines **a**, **b** and **c**. The other three carbonyls performed less successfully, with **44** not being accepted by any enzyme tested for the reductive amination with methylamine **d**. The synthesis of **41b** with Roche IRED IR_14 and IR-Sip showed the first example of a secondary amine donor being successfully used for reductive aminations with IREDs. These two IREDs were also successful in accessing both (*R*)-rasagaline and (*S*)-rasagaline on a preparative in 58% and 81% yield and *ee* values of 90% and 72% respectively using a 50-fold amine loading.[62]
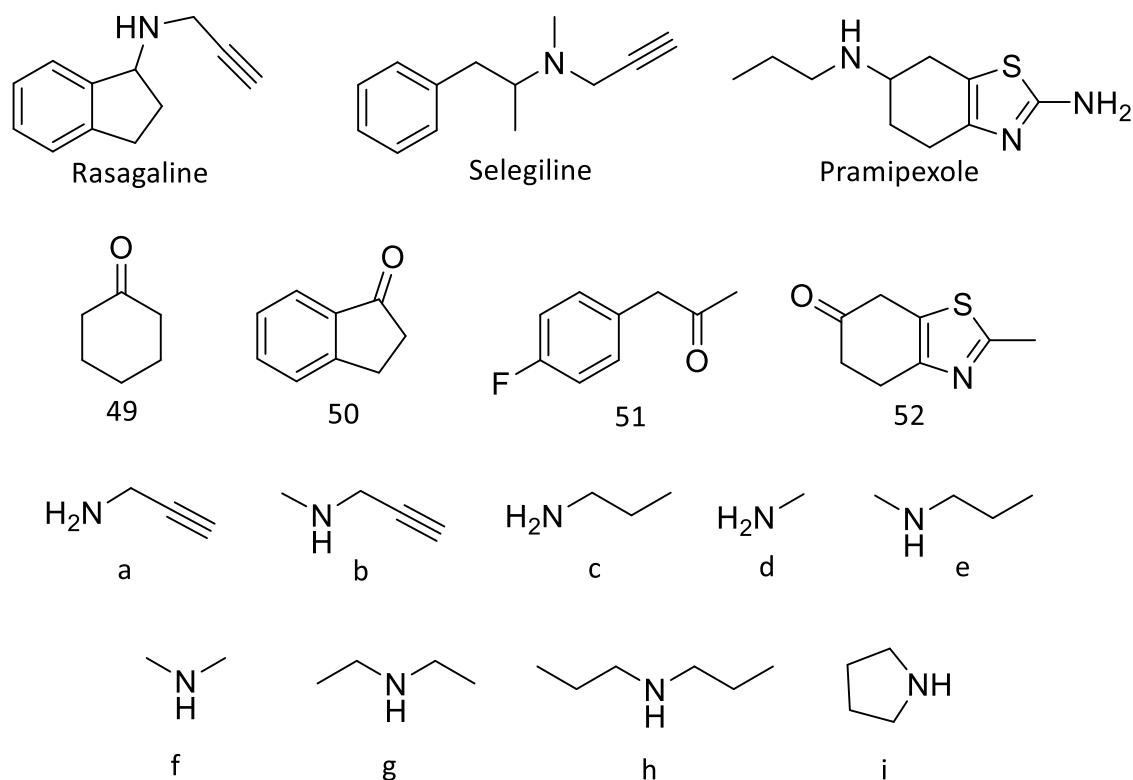
Rasagaline

Selegiline

Pramipexole

49

50

51

52

a

b

c

d

e

f

g

h

i

48

In recent years, the Gröger group have shown a lot of interest in cyclic imines containing endocyclic heteroatoms. They initially focused on identifying an IRED capable of reducing the imine bond in 2-monosubstituted-3-thiazolines (**53** and **54**). They identified an IRED from *Mycobacterium smegmatis* that was capable of reducing the imines in 77% and 21% conversion respectively. Impressively, this IRED had no stereopreferance for each of the compounds and both reductions had an ee of 0%.[63] The group then wanted to see if they could carry out a one-pot chemoenzymatic reaction making the thiazoline ring **55** via an Asinger synthesis, then using the IRED from *Mycobacterium smegmatis* in whole cell form for the imine reduction. They successfully managed to carry out this overall reaction in 100 mM pH 7 potassium phosphate buffer, producing the reduction product of **55** in 28% isolated yield and 99% *ee* towards the (*S*)-enantiomer. [64]

The Gröger group then looked at expanding the substrate scope of these reactions (Figure 21C) to a larger panel of sulfur containing cyclic imines (both 5- and 6-membered rings). They investigated 31 IREDs using a colourmetric assay to determine activity. Of the 31 IREDs screened, six gave conversions to compounds **56** to **64**, all in excellent *ee*s. [65] The 31 IREDs were then also screened against benzoxazines **65**, **66**, and **67**. Each compound was active with four different IREDs, with the best hits producing the corresponding amine products in 99%, 82%, and 84% conversion. Benzozaxine **65** was scaled up to a 40 mL reaction at an imine concentration of 50 mM and resulting in the (*S*)-amine in 71% yield and 99% *ee*. [66]
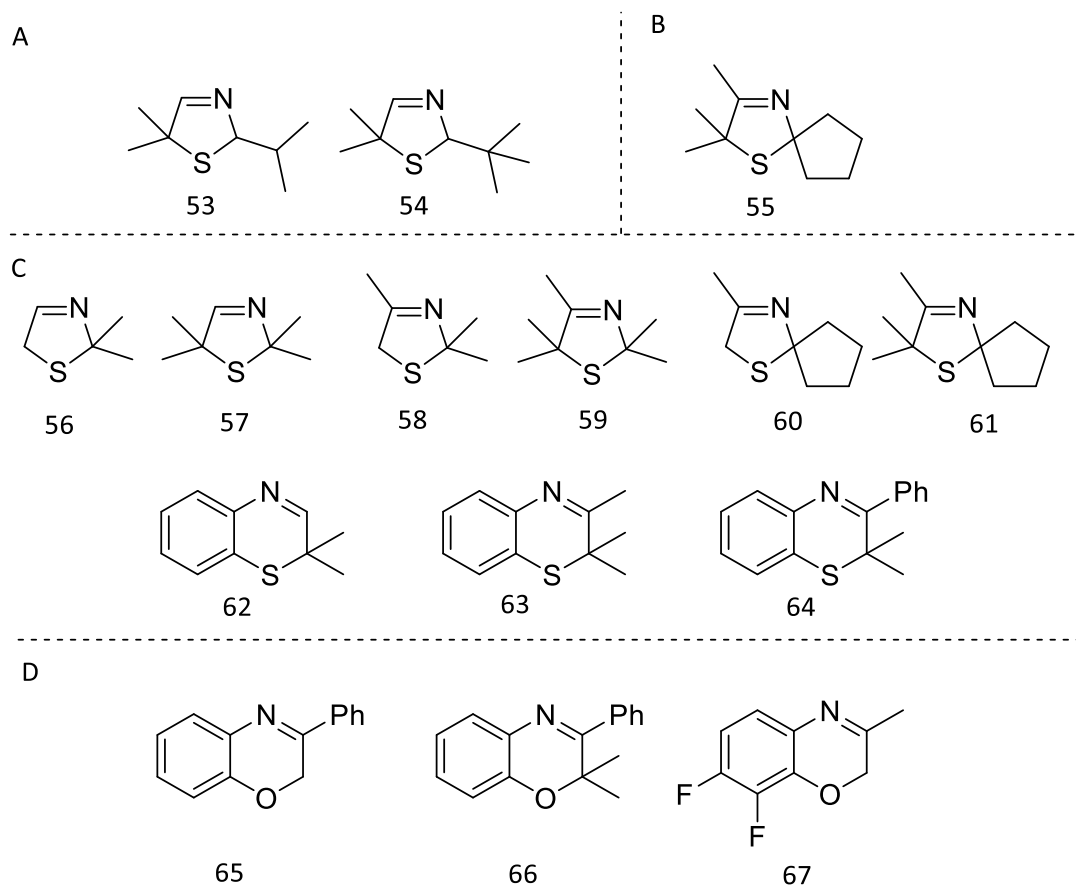
Figure 21: Scope of cyclic imines containing endocyclic heteroatoms

Several different groups have looked at accessing reductive amination reactions with IREDs with multiple chiral amine products in mind. One of the first successful accounts for IRED catalysed reductive aminations was in 2015 by the group of Bettina Nestl. They used the IRED they discovered from *Streptosporangium roseum Sr*-IRED[55] for the reductive amination benzaldehyde, acetophenone, and cyclohexyl methyl ketone with ammonia, methylamine, and aniline. In the case of benzaldehyde, the amine product with all three amines, however in order to observe these reactions in high yields, higher excess of amine is required (up to 50-fold). For the reductive aminations between acetophenone and cyclohexyl methyl ketone, 50 amine equivalents of ammonia and methylamine were required. In these cases, yields of up to 53% were observed, but only when the reaction was carried out at pH 9.[67] The excess of amine and the higher pH of the reactions aids in the reaction as it drives the equilibrium of imine formation to the right, resulting in a higher in situ concentration of imine.

50

Nitrogen-containing heterocycles such as piperazine and homopiperazine have been highlighted as important building blocks towards pharmaceutical compounds.[68,69] One route that has been utilised to access piperazines is through the double reductive amination of dicarbonyls and diamines. Borlinghaus *et al.* showed that a range of chiral piperazines could be achieved with aryl- and alkyl-substituents in good enantioselectivities. [68] Homepiperazines (or 1,4 diazepanes) have also been achieved through intramolecular reductive amination reactions in high *ee* values and excellent conversions. [69] This shows that we can access a wide range of important structural motifs through multiple routes highlight the structural diversity that IREDs are capable of working on.

2.3 Structure of IREDs

As mentioned in section 2.1, the IRED from *Streptomyces kanemyceticus* was the first IRED crystal structure to be resolved (Figure 17). The cofactor was identified to bind in the N-Rossman domain. They exist as dimeric proteins, where each monomer unit contains an N-terminal Rossmann domain, which binds the cofactor, and a C-terminal connected via an alpha helix. The active site is formed between the N-terminus of one monomer and the C-terminus of the second. A search for protic amino acid residues within a 9 Å distance from NADPH. Three total residues were identified, Thr254, Ser111, and Asp187 (Figure 22). When compared to the structure of an NAD(P)H-dependent ketoreductase, it was revealed that the Asp187 lined up with the proton transfer residue played by a lysine. A mutation of this residue to both alanine and asparagine resulted in an inactive enzyme proving that Asp187 is crucial for proton transfer in the reduction of imines. [54]
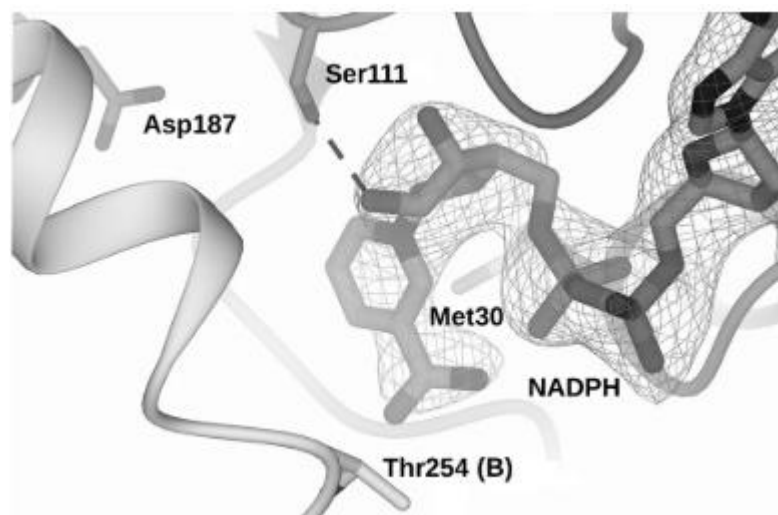
Figure 22: Active site of the IRED from Streptomyces kanemyceticus highlighting the proton transfer residue Asp187 [54] – Permissions granted by Wiley

The Grogan group at the University of York in collaboration with the Turner group at the University of Manchester obtained crystal structures of two other IREDs from *Bacillus cereus* (*Bc*IRED) and *Nocardiopsis halophila* (*Nh*IRED). The structures for GF3546-IRED, *Bc*IRED, and *Nh*IRED were all overlayed with the structure from *Sk*IRED. Where it was shown for *Sk*IRED that the aspartate residue was crucial for proton transfer, this was not the case for the other three IREDs. All three showed a tyrosine residue superimposed on top of the aspartate residue. Tyrosine has played a role in proton transfer in other NADPH-dependent enzymes such as pteridine reductase,[70] so it is possible this is the role in the other three IREDs. The tyrosine in GF3546-IRED was mutated to a phenylalanine, and just like the mutations to alanine in *Sk*IRED, this removed all activity in the enzymes. It was also noted that in the reduction of 2-methyl-1-pyrroline, these tyrosine containing IREDs all resulted in the (*S*)-amine whereas the aspartate containing *Sk*IRED produced the (*R*)-amine.[71]

The difference in these tyrosine containing and aspartate containing IREDs was further explore by Velikogne *et al*. An *in-silico* sequence based approach was carried out to discover and identify putative IREDs. The two IREDs from *Streptomyces* sp. (GF3587 and GF3546) as well as *Sk*IRED and the IRED from *Streptomyces roseum* were used as starting points for this approach. Using three paramaters (i. E-Value less than

or equal to 10^{-50}; ii. A Rossman domain for cofactor binding; iii. An acidic residue in position 187 (*Sk*IRED numbering), 182 different hits were identified. These were grouped together in a phylogenetic tree containing two main branches. These branches were determined based on the protic residue that existed in the active site. Of the 182 hits identified, 116 contained an aspartate residue (the 'D-type') and the rest contained a tyrosine (the 'Y-type') (Figure 23).
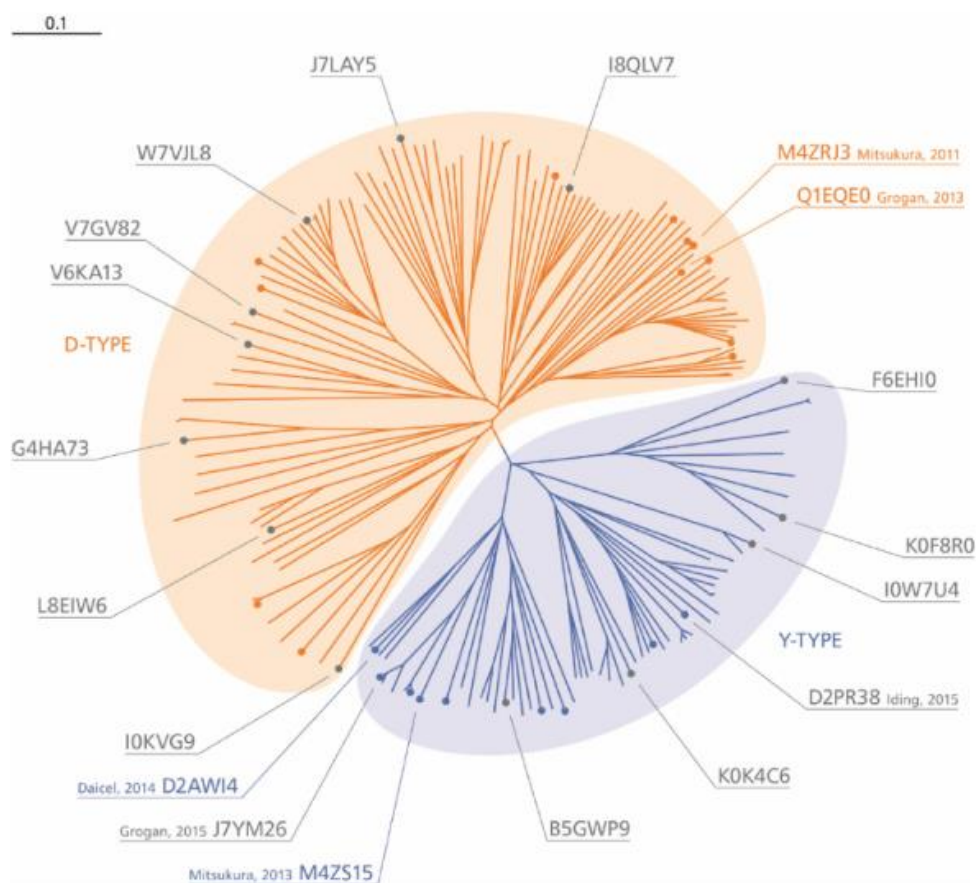
Figure 23: Phylogenetic tree of 182 IREDs group into those containing an aspartate ('D-type') or a tyrosine ('Y-type') as the proton transfer residue[72]

A selection of these IREDs were the screen against a small selection of imines (compounds **1**, **2**, **6**, **12**, **15**, **16**, **17**, **21**, and **24**). For most of the substrates the D-type resulted in the (*R*)-amine and the Y-type produced the (*S*)-amine products, as we seen previously. The enantiomers produced were opposite for 2-phenyl-1-pyrroline, **2**,

with most of the IREDs screened in imine reduction, showing there is still some substrate dependency on the stereoselectivity of these enzymes.[72]

Aleku *et al*. at the University of Manchester carried out further structural studies using an IRED from *Amycolatopsis orientalis* (*Ao*IRED). *Ao*IRED was capable of carrying out the reduction of a range of monocyclic imines, as well as dihydroisoquinolines, in good to excellent yields and *ee* values. Three different crystal structures were obtained for *Ao*IRED: an *apo*-structure with no cofactor or substrate bound, an IRED-NADPH complex, and a complex with both cofactor and the (*R*)-amine product of substrate **15** bound. When the *apo*-structure was superimposed with the NADPH-IRED complex, they noticed a domain shift. This domain shift is initiated by the binding of the cofactor resulting in a loop reorganisation and repositioning NADPH closer to the active site (Figure 24).

From the ternary complex of amine-IRED-NADPH, several residues in the active site were identified for mutagenesis (Figure 25). A tyrosine and two different asparagine residues were chosen and mutated to either phenylalanine, alanine, or to an aspartate. The asparagine at position 241 was thought to play a role in binding of the imine. Mutation to an alanine resulted in an increase in K_M for smaller monocyclic imines, however resulted in a slight improvement in the reduction of larger bi- and tricyclic imines. Asn171 in *Ao*IRED was equivalent to aspartate and tyrosine residues identified in other IREDs for proton transfer. Although asparagine can not play a role in proton transfer, it was theorised to play a role in early substrate recognition. This also highlights the potential of some non-protic IREDs to exist that are still capable to perform imine reduction. [73]

Figure 24: Superposition of the apo AoIRED (green) with the AoIRED-NADPH complex (gold)
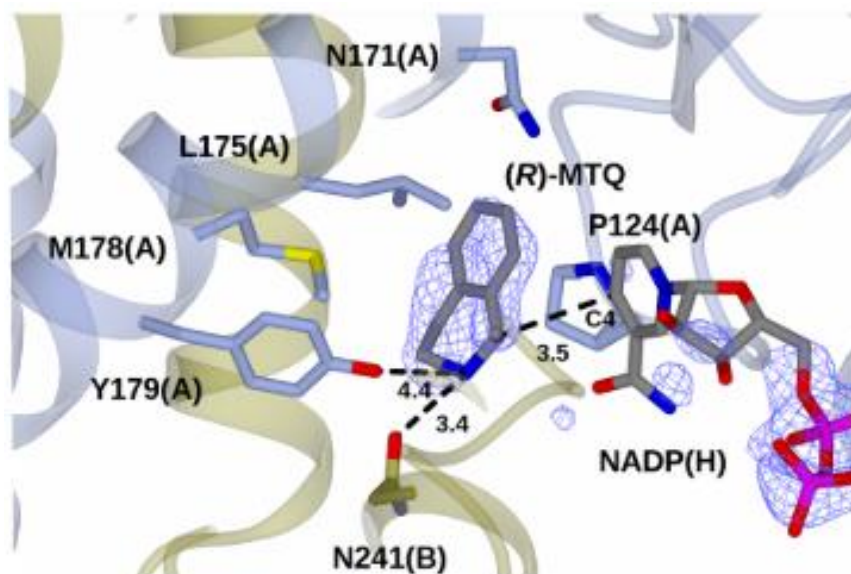
Figure 25: Ternary complex of AoIRED-NADPH-MTQ showing the active site and residues of interest for mutagenesis studies

2.4 Industrial efforts

Industry have played a huge role in expanding the number of IREDs and in pushing the substrate scope and chemistry that can be done with these enzymes as well as aiding in the understanding of how they work. One of the first industrial companies that had a concentrated effort was Roche, based in Basel, Switzerland. They created a Hidden Markov model (which allows for the constructing of complex models for sequence analysis[74]) based on the hypothesis that the N-terminal Rossman fold is a conserved domain amongst IREDs. From this, they identified 20 novel imine reductases that they then tested against a panel of cyclic imines (Figure 26).
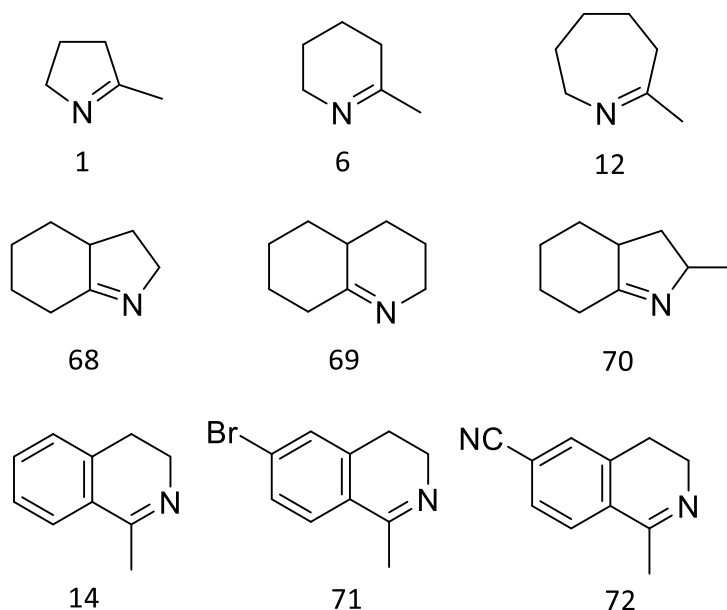
Figure 26: Substrates screened for the novel IRED candidates by Roche.

2-methyl-1-pyrroline, **1**, has been the standard screening substrate for IREDs, and this was readily accepted in 15 of the 20 novel IREDs with all but one of those 15 showing high stereoselectivity. The majority of the IREDs identified had good activity towards most of the imines tested (>90%) in good to excellent enantioselectivities. IREDs IR_2, IR_3 and IR_6 (Roche numbering) showed a very limited substrate scope compared to the rest, only working on less than half the substrates and in low conversions. Although most of these new IREDs were highly stereoselective across the panel of substrates, producing the same enantiomer throughout, some showed a substrate dependency on stereoselectivity. IR_14 showed this the most where compounds **1**, **6**, **12**, and **14** were reduced to the corresponding (*R*)-imine, where **71** and **72**, which showed only small substituent additions on **14**, were both reduced to the (*S*)-enantiomer. This inverted stereoselectivity observed for substrates **71** and **72** was also seen for other IREDs IR_20 and IR_22. [75]

The group at Roche also looked at using these novel IREDs reported here, as well as others they discovered, for the reductive amination between some simple ketones and small amines. They screened a total of 26 in house IREDs (and 28 in total) for the substrates shown in Figure 27. In order to aid in these reductive amination reactions, the amines were used at high equivalencies (250 mM amine compared to 20 mM of

ketone) with methylamine being the more accepted amine donor of the three. They were able to achieve each of the amine products **49a**, **73a – 76a**, **49b**, **73b – 76b**, and **49c**, **73c – 75c** with at least one of 28 IREDs tested, however conversion values ranged drastically from < 10% (in the cases of **73a** and **73c**) all the way up to 94% with **75b**.[76]
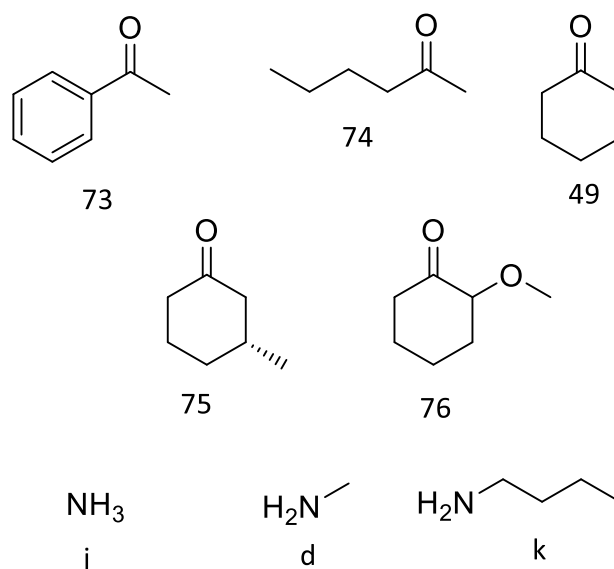
Figure 27: Panel of simple ketones and amines tested for the reductive amination of IREDs

GSK carried out a similar approach by looking at sequences that were available from public databases and compared these to the sequences of already identified IREDs. By setting a sequence similarity limit of at least 60%, they identified 42 putative IREDs that were the screened in combination with 37 other known IREDs against a selection of ketones and amines for reductive amination. The amine scope looked at consisted of a few previously tested small amines as well as some aromatic and heteroaromatic amines. Of the enzymes, 69 showed activity with all carbonyl and amine combinations at near-stoichiometric ratios which had not previously been reported with IREDs. This approach was taken due to the near-stoichiometric reductive aminations that could be carried out with the reductive aminase (RedAm) class of enzymes (see section 2.6). Successful reductive aminations were carried out with aniline, and heteroaromatic amines, with conversions up to 99% conversion between cyclohexanone and aniline. This was one of the first reports of aniline being used as

a successful amine donor with previous reports stating that it was incompatible with bioreductive aminations. [77]

The IRED library was further expanded with 27 novel enzymes through a collaboration with Pfizer and the Turner group. These novel IREDs were identified through using the Basic Local Alignment Search Tool (BLAST) against three different IRED sequences. These 27 IREDs were then screened, along with 18 previously described IREDs, against a small panel of ketones and amines for the bioreductive amination reactions (Figure 28). These new IREDs aided in the expansion of the substrate scope of amines and carbonyls tested, especially towards the N-protected pyrrolidinones, **79** and **80**. In order to understand the variable substrate scope, comparison of active site residues of the best performing IREDs. Other than the aspartate residue involved in proton transfer being regularly conserved, several of the other residues varied throughout. This shows the potential for engineering and mutation of active site residues towards different substrate scopes and activities of these IREDs. [78]
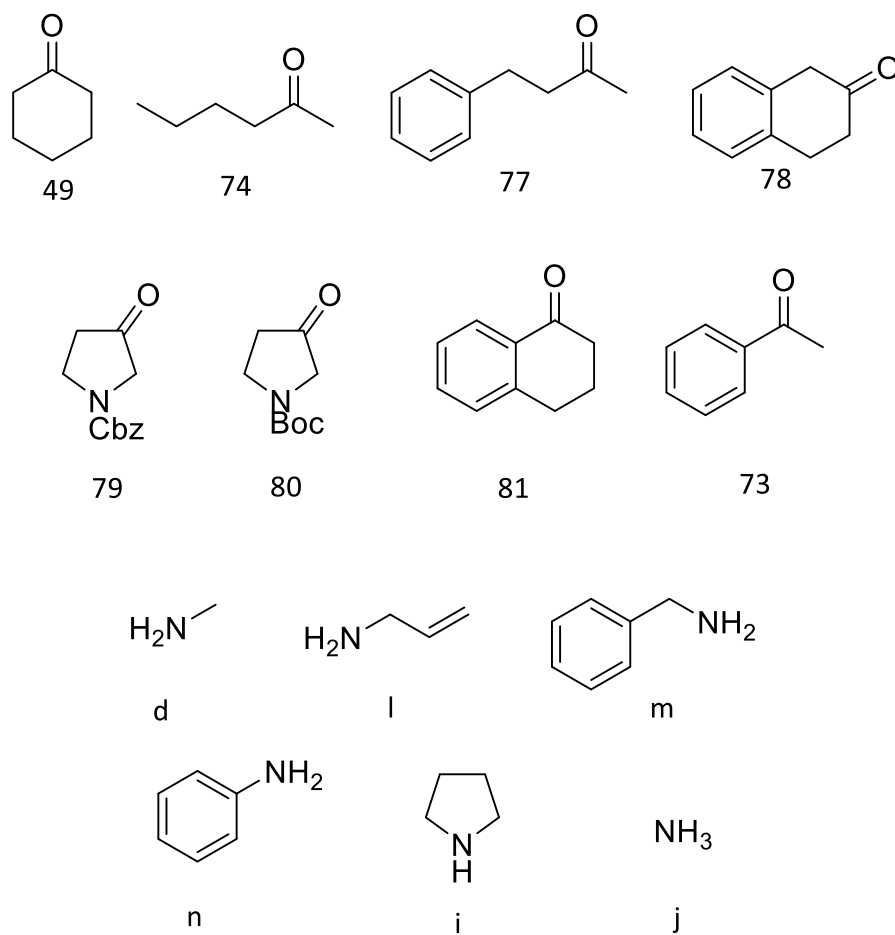
Figure 28: Panel of ketones and amines tested by Pfizer to test the reductive amination capability of novel imine reductases

IREDs have been shown to not only be good enzymes for both the reduction of imines and for bioreductive aminations at analytically, and small preparative scales, but have also been utilised for large scale up. A 2019 paper from Johnson Matthey discussed some of the considerations that needed to be looked at for the large scale up of reductive aminations using IREDs. A phylogenetic tree was produced which features around 1400 sequences from the IRED database of which only a fraction have been characterised and also highlights those IREDs identified by individual pharmaceutical companies. Johnson Matthey showed that through a combination of kinetic studies and design-of-experiment (DoE) they could efficiently scale up reactions with IREDs using stable and active candidates with suitable parameters.[79]

Not all enzymes however are going to be as easily scaled up like the IREDs reported by Johnson Matthey, and in these cases, engineering can be a valuable tool. GSK recently reported the evolution of an imine reductase to carry out a reductive amination step in the synthesis of an LSD1 inhibitor GSK2879552 (Figure 29). The overall objective was to improve reaction conditions and reaction outcomes in 6 different areas to give a synthetic route more efficient and practical that the current chemical synthesis route. An IRED that showed initial activity towards the reductive amination was chosen and taken through three rounds of evolution to achieve a variant that showed a >38,000 fold improvement. This involved engineering the IRED to operate at more acidic reaction conditions (pH 4.6 compared to 6.3), at a high substrate loading, and a lower biocatalysts loading (1.2 %w/w compared to the wild-type enzyme at 453.7 %w/w). This biocatalytic step also circumvented one synthetic step in the chemical reaction, the removal of boron-containing waste, and half the number of organic solvents.[80]
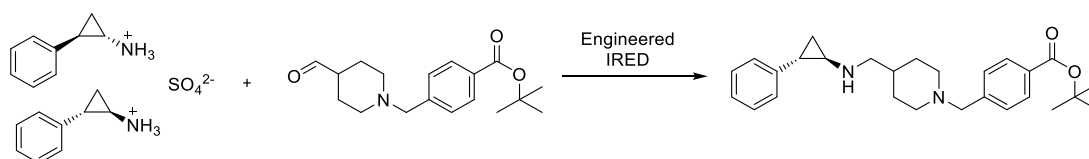
Figure 29: IRED catalyzed reductive amination to the GSK2879552 precursor

Work carried out by Montgomery *et al*. focused on not only trying to expand the number of IREDs but to also gain some insight into the structure-activity relationships of these enzymes. A panel of 95 enzymes, which contained 80 putative IRED sequences, was screened for reductive amination activity. Of the ketones and amines tested, at least one IRED gave conversion to the desired products, however no one enzyme stood out across all reactions. It was observed that enzymes showing similar activity towards certain substrate combinations and some showing similar enantioselectivities possessed high sequence identity. Six of these enzymes were further studied using a SmartScaffold approach and put through a tool called "Structure and Ligand-based and Active site Predictions (SLAP)" and four positions in each IRED were identified of interest. Homology models of two of the IREDs were created using the crystal structure of *Asp*RedAm (see section 2.6) and cyclohexanone

and aniline were both docked into the active sites. A total of 23 IREDs were identified as possibly coming into contact with one, or both, of the substrates and highlighted as potential positions of interest for engineering. Despite this, it was observed that the structure-activity relationship of IREDs are still very highly substrate dependant.[81]

One of the biggest efforts applied to expanding the IRED library was a recent approach from Prozomix in collaboration with the Turner group. Rather than searching the sequence space for putative IREDs, they developed a large panel of metagenomic IREDs from around the United Kingdom. A total of 677 full-length sequences were obtained, and through removal of redundant sequences, a total panel of 302 putative IREDs was left, with no two sequences having a >95% sequence identity. A further 90 genomic IREDs were added to the list in order to increase the sequence diversity. From this panel of now 392 IREDs, a 384-well plate colorimetric assay was developed for the high-throughput screening of activity and scope of the enzymes. The colorimetric assay relied on screening reductive aminations in the oxidative reaction. On formation of the prochiral imine and NADPH, a coenzyme diaphorase reduces iodonitrotetrazolium (INT, colourless) to INT-formazan (red). The more intense the red colour produced, the more active that specific enzyme is towards the formation of the amine tested. The versatility of the enzymes in this panel has been tested showing a wide substrate scope for the reduction of cyclic imines and for reductive aminations of a wide range of ketones and amines. This was also shown through the identification of IREDs in the panel capable of synthesising N-substituted β-amine acids, which had previously not been reported.[82]

2.5 IRED cascades

There is great appeal in being able to combine IREDs into cascade reactions with other enzyme classes as it allows access to chiral amines from a more diverse panel of starting substrates. Although not exactly a cascade, one of the first examples of IREDs being used in tandem with other enzymes was the deracemization of cyclic amines by Heath *et al*. This work utilised an amine oxidase (AO), capable of selectively oxidising one enantiomer of a racemic to the imine, which would then be selectively reduced to the opposite enantiomer using an imine reductase in a one-pot reaction. This had previously been carried out using an AO and sodium borohydride which

would non-selectively reduce the imine to either enantiomer, however the development of IREDs allowed for more control. The selectivity of each enzyme in the reaction could be changed dependent on the desired enantiomer of choice and this was shown to be effective towards a large panel of piperidines and pyrrolidines.[83]

Cyclic amines can be accessed by several routes, and high enantiopurity can be introduced along the reaction pathway without the need for deracemization reactions. Work by the Turner group look at obtaining a range of mono- and disubstituted pyrrolidines and piperidines. By utilising a carboxylic acid reductase (CAR), a transaminase (TA), and an IRED, they were able to synthesise these cyclic amines from the corresponding keto acids (Figure 30). It was shown that this cascade could tolerate several different substituent groups adjacent to the carbonyl group, as well as a methyl group in all positions along the keto acid chain. High enantioselectivities towards the (R)- and (S)-amines were achievable as well as retention of stereochemistry of the methyl groups along the chain. [84]
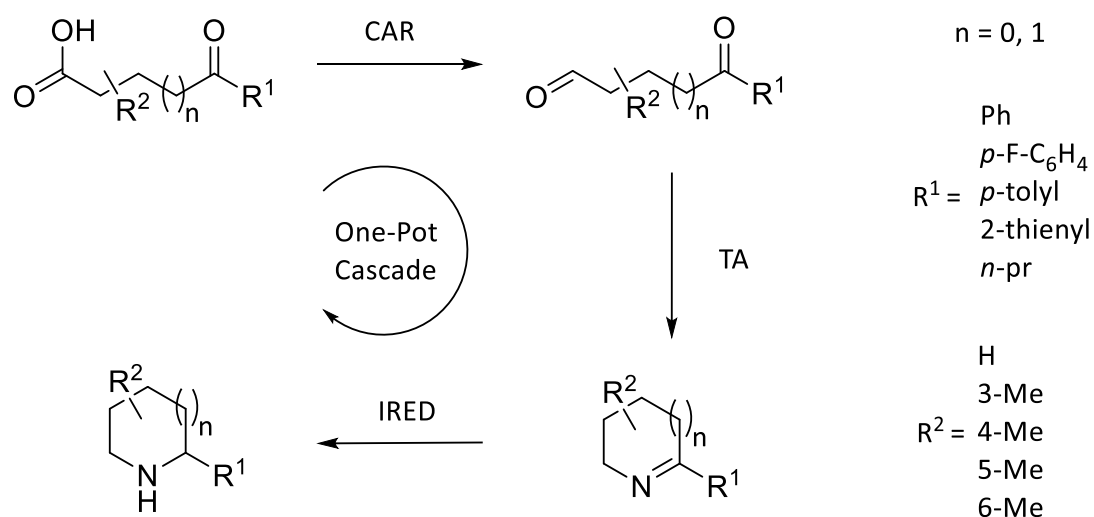
Figure 30: Three-enzyme, one-pot biocatalytic cascade to access pyrrolidines and piperidines from corresponding keto acids. Numbering of R[2] groups base on position in cyclic amine ring.

The Nestl group, amongst others, also showed an interest in accessing substituted pyrrolidines and piperidines, but via an alternative synthetic route. Rather than

starting from keto acids and introducing an amine group to allow the spontaneous cyclisation to the prochiral imines, they looked at using diamines as their starting point. They utilised a putrescine oxidase, which was engineered towards a greater substrate scope of diamines, for the selective monooxidation of an amine to an aldehyde, followed by an IRED to reduce the *in situ* formed imine. Although they successfully increase the substrate scope of the putrescine oxidase, only a small selection of non-substituted and methyl substituted pyrrolidines and piperazines were accessed. This substrate scope, although smaller than shown in the three enzyme one-pot cascade from keto acids, it shows that there are multiple routes to accessing chiral amines from multiple different starting points. [85,86] Piperidines and azepanes with amino substituents can be also accessed via IRED cascades. By using amino alcohols containing a *N*-protected amine group in the chain, a galactose oxidase is used to access the amino-aldehyde. This spontaneously cyclises and the imine is then selectively reduced. [87]

Work done by the Turner group also looked at combining ene-reductases with IREDs for the selective double reduction of α,β-unsaturated cyclic imines. Although work had been done previously on the selective imine reduction of this chemical scaffold, the selective double reduction had not been previously reported. 5-, 6-, and 7-membered imine rings were all accepted as well as both methyl and ethyl groups on the alkene. [88]
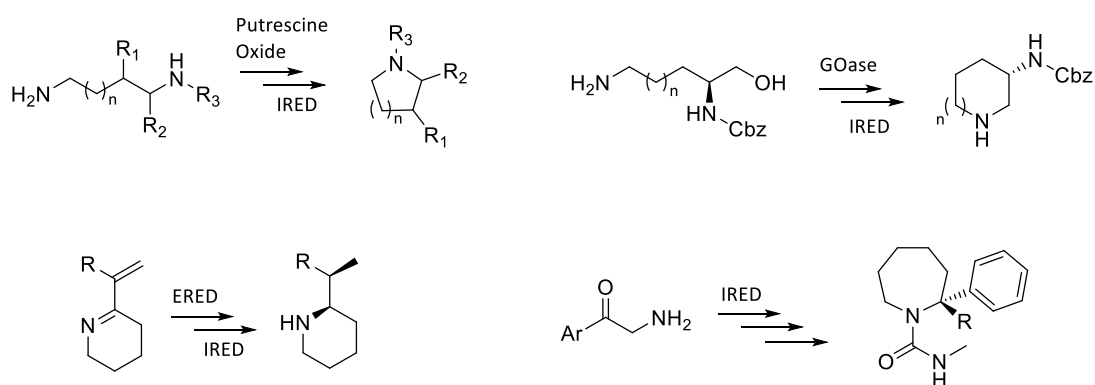
Figure 31: Summary of enzymatic cascades involving an IRED

64

IREDs have also shown utility within chemoenzymatic cascades for the synthesis of substituted azepanes. A small panel of 2-aryl substituted azepanes were synthesised from their corresponding imines using either and (*R*)- or (*S*)-selective IRED in excellent *ee* and good yield. The (*R*)-2-phenyl azepane was then developed further using organolithium catalysed α-functionalization reactions to develop a range of 2,2-diaryl azepanes in excellent yields with retention of stereochemistry observed across the scope. [89]

2.6 Reductive aminases

Alongside the identification of new IRED sequences, a sequence of similarity to known IREDs was identified in the fungi *Aspergillus oryzae*. This IRED was found to have a broad substrate scope for imine reduction of cyclic and preformed (*in situ*) imines. It was also found to be highly effective in the oxidative dehydrogenation of amines to produce imines. When tested for the kinetic resolution of a racemic mixture of rasagiline, it was observed that the enzyme produced indanone, and was playing a role in the deamination reaction. In order to exploit this further, this IRED from *Aspergillus oryzae* was screened against a large panel of carbonyls and amines for reductive amination reactions (Figure 34) with the amines in various degrees of excess (stoichiometric to 50-fold).

In order for these imine-reducing enzymes to be capable of reductive amination reactions, more basic reaction conditions are typically required. However when this new IRED was run in reactions at both pH 7.0 and pH 9.0, very little change in the reaction rate was observed. This meant that this enzyme did not require the preformation of an imine between the carbonyl and amine in order to carry out reductive amination. With the capability of this new IRED to carry out reductive amination reactions at near stoichiometric ratios of carbonyl and amine (as opposed to previously shown need for an amine excess as shown in section 2.2) without the need for imine preformation prompted Aleku *et al*. to coin this enzyme a Reductive Aminase (RedAm) and is believed to be a subclass of IREDs. These reductive aminations catalyzed by RedAms differ to those mentioned in sections 2.1 to 2.5 carried out with IREDs due to not requiring the preformation of the intermediate imine *in situ*.

2.6.1 Structure

Kinetic studies were carried out to understand the mode of operation of the *Asp*RedAm using cyclohexanone and methylamine as the testing substrates. By varying the concentration of each substrate, as well as the cofactor, in turn, a Ter Bi mechanism was observed. A sequential binding of NADPH cofactor, ketone, and then amine was determined, followed by product and cofactor release. In addition to this, a crystal structure was obtained of the "closed" form with rasagiline and NADP(H) in complex (Figure 32). [90]
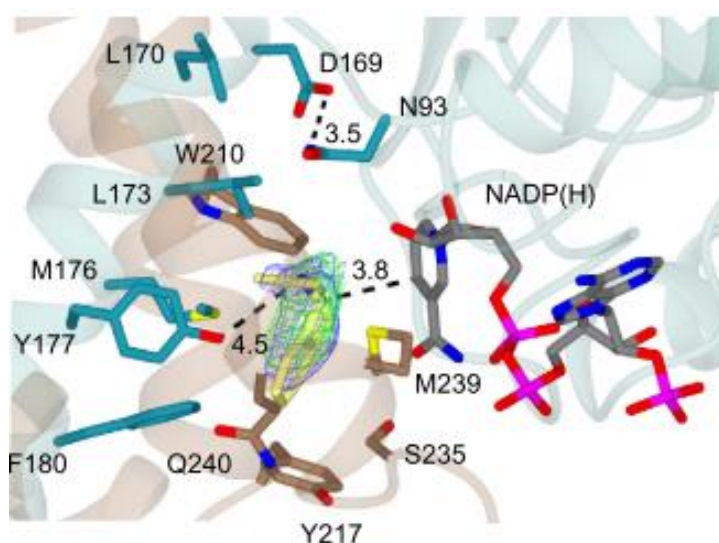
Figure 32: Active site of the ternary complex of AspRedAm-NADP(H)-Rasagaline – Permissions Granted by Nature
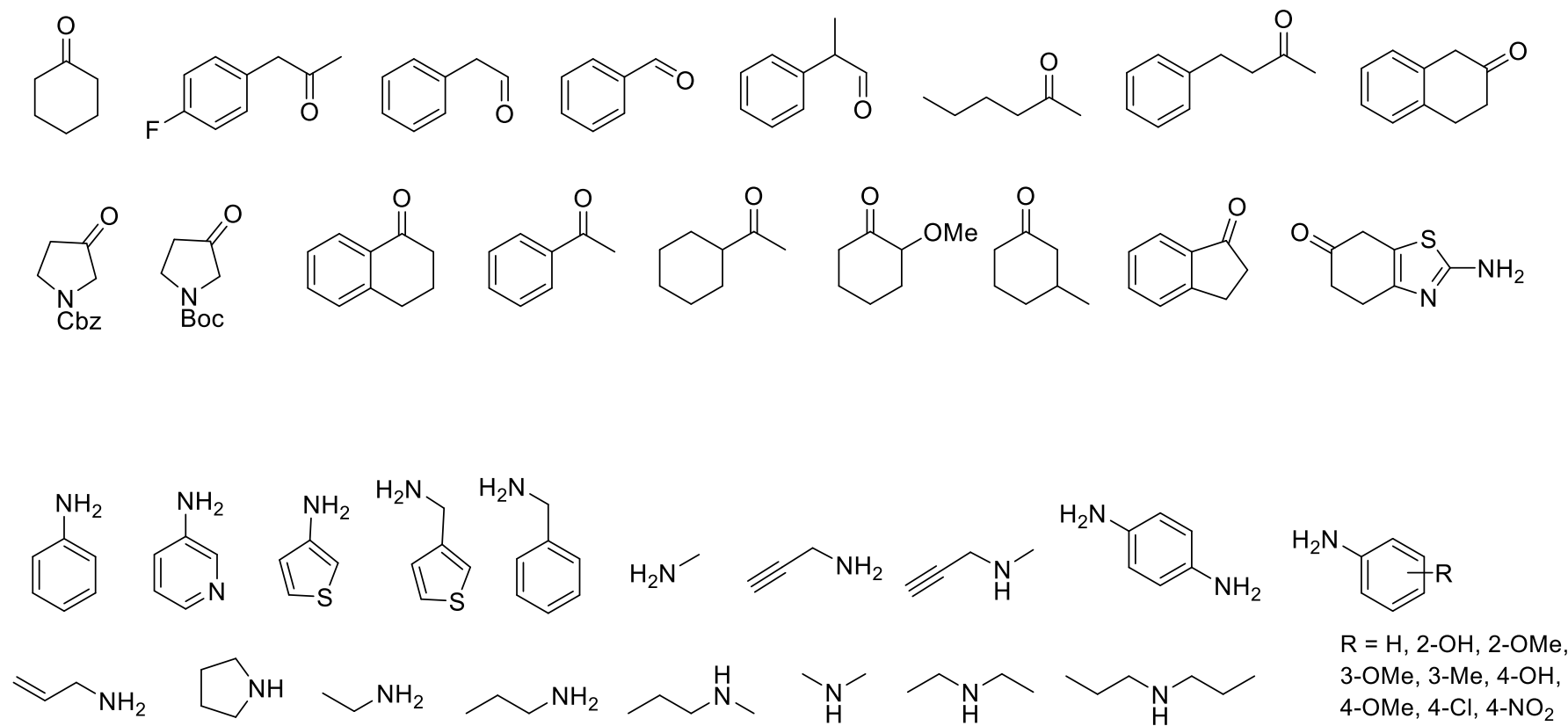
Figure 33: Scope of carbonyls and amines used for reductive amination reactions with IREDs

Figure 34: Scope of carbonyls and amines used for reductive amination reactions with the reductive aminase from Aspergillus oryzae

2.6.2 Mechanism

Collaboration between the Grogan group at the University of York and the Turner lab at the University of Manchester was carried out in order to determine the mechanism of this reductive aminase. The active site determination of *Asp*RedAm afforded the first insight into active site residues and interactions with both product and cofactor. In order to understand the mechanism further, Sharma *et al.* looked at two further characterised RedAms from *Aspergillus terreus* (*At*RedAm) and *Ajellomyces dermatitidis* (*Ad*RedAm). A combination of structural understanding of *At*RedAm and kinetic studies from *Ad*RedAm provided insight into the mechanism.[91]

Kinetic rates for the two RedAms to catalyse reductive aminations were compare to those of the IRED from *Streptomyces* sp. GF3546 as well as against the chemical reducing agent NaBH$_3$CN. It was seen that the rate of conversion was much greater for the reductive amination between cyclohexanone and allylamine for the two RedAms (73% and 45% after 3h for *At*RedAm and *Ad*RedAm respectively) than it was for the IRED and NaBH$_3$CN (both < 10%). In order to identify key residues in the active site, a ternary complex was generated of *At*RedAm in complex with cyclohexanone, allylamine, and NADPH$_4$ (the inactive form of the cofactor). The omit map of this complex revealed coordination of the cyclohexanone to the tyrosine residue at position 183. The amine was observed to be in proximity to both the aspartate residue at position 175, which was shown in previous IRED studies to be crucial in proton transfer, as well as an asparagine residue at position 98.[91]

Mutagenesis studies of each of these residues was then carried out to further explore this. In both *Ad*RedAm and *At*RedAm, mutation of the aspartate residues resulted in inactive enzymes. Mutation of the tyrosine to phenylalanine in both RedAms resulted in an increase in K$_M$ for cyclohexanone. Kinetic studies carried out for investigation of the K$_M$ of allylamine by mutation of the asparagine residue to alanine resulted in data too low to be reliable which was suggestive of this residue crucial in amine binding. Investigation of these three residues, along with the knowledge provided by Aleku *et al.* of the sequential binding order of substrates, the mechanism shown in Figure 35 was determined.[91]
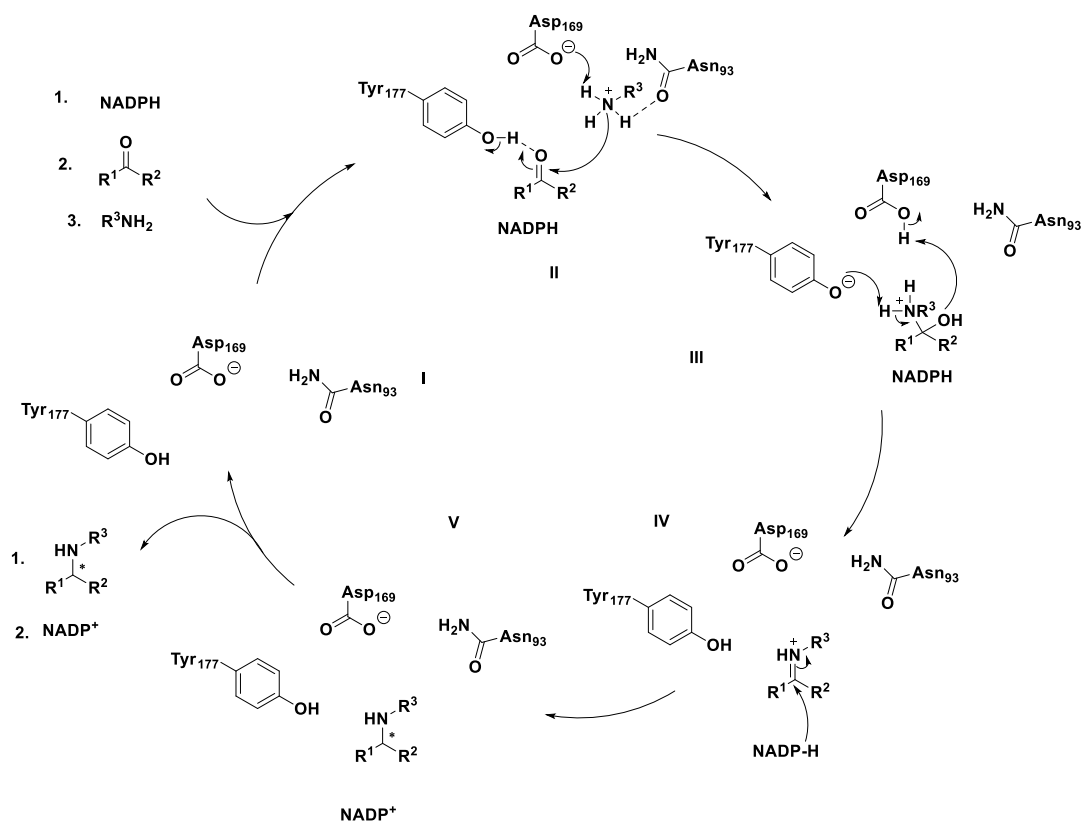
Figure 35: Mechanism for reductive amination determined for reductive aminases showing the sequential binding and release of substrates and products

2.6.3 Substrate Scope

These reductive aminases have shown applicability to a wide range of different applications. Not long after their discovery, the *Asp*RedAm was used as part of a hydrogen-borrowing cascade with an alcohol dehydrogenase (ADH) (Figure 36). This worked through the dehydrogenation of an alcohol using NADP+, producing the corresponding ketone or aldehyde and NADPH. This reduced cofactor could then be used for hydrogenation of the imine formed between the carbonyl product from the ADH and different amines. These were shown to be effective towards a range of small aliphatic amines with a panel of primary alcohols such as cyclohexanol.[92] This work was then extended to the amination of unfunctionalised alkanes by using a cytochrome P450 to synthesise the alcohols for the hydrogen-borrowing step.[93]
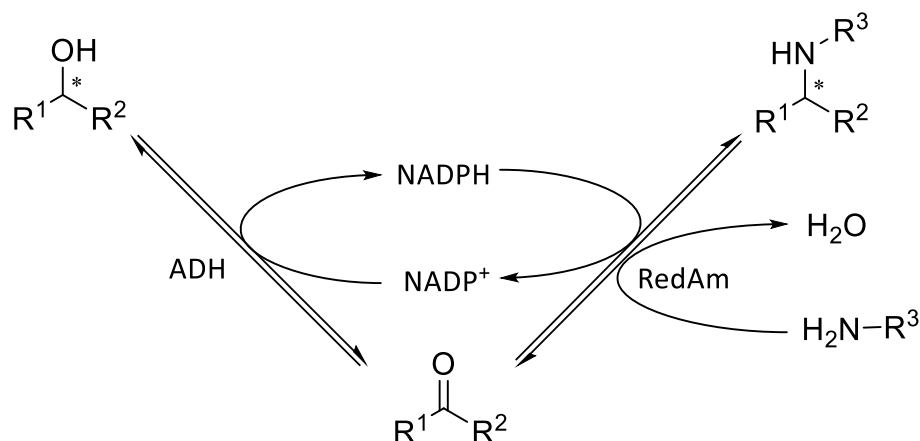
Figure 36: Hydrogen borrowing cascade between an alcohol dehydrogenase and a reductive aminase for the synthesis of chiral amines from alcohols

The stereoselectivity of the *Asp*RedAm was also tested. It was shown to be highly effective for not only the kinetic resolution of amines, but also for deracemization of amines. This was initially tested by looking at the oxidative deamination of racemic amines, both cyclic and acyclic. These kinetic resolutions carried out with *Asp*RedAm resulted in the accumulation of (*S*)-amines in excellent *ee* values, showing the selectivity of the enzyme towards the (*R*)-amine. They also tested to RedAm variants, one which showed an improved selectivity towards the (*R*)-amines than the wild-type and one that showed the inverted selectivity. This allowed Aleku *et al.* to access both enantiomers of these amines, however only up to 50% conversion due to the nature of kinetic resolutions. To improve on this, a deracemization was carried out on a small selection of the amines by using ammonia borane as a non-selective reducing agent for the imine formed by the enzyme. Of the amines tested they were able to achieve conversions > 97% in all cases except one which had conversion of 74%, all in excellent *ee* values.[94]

The scope of the RedAms have been very well studied since their discovery in 2017 past the initial carbonyl and amine scope that was shown. Along with a panel of IREDs, the reductive aminases *Asp*RedAm, *At*Redam, and *Ad*RedAm were tested for the reduction of imines as precursors to dibenz[*c,e*]azepines. *Asp*RedAm and *Ad*RedAm performed just as well as the best performing IREDs for two of the four compounds selected, with one showing negligible conversion across the panel of

enzymes, and one compound showing conversions of 5% and 41% conversion respectively. Although this subset of IREDs have been termed as reductive aminases for their reductive amination capability, they still show good activity towards the reduction of cyclic imines.[95]

It has been highlighted several times so far that cyclic amine structures such as pyrrolidines are important functional motifs in compounds such as alkaloids. Most approaches to these compounds has been through the reduction of the prochiral imines. Costa *et al.* looked synthesis 2,5-disubstituted pyrrolidines from the corresponding 1,4-diketones. A transaminase was used to selectively aminate one of the carbonyls in the diketones. This aminoketone compound would then undergo spontaneous cyclization to the cyclic imine that can then undergo reduction by the reductive aminase. Several different length aliphatic chains were accepted by both transaminase and reductive aminase to access multiple substituents in the 2-position of pyrrolidine, however phenyl was not as accepted.[96]

As was shown with the hydrogen-borrowing cascade, we can access carbonyl acceptors from alcohols using an alcohol dehydrogenase. Another cascade work by Ramsden *et al.* looked at accessing chiral amines from aldehydes which had been made through either the oxidation of primary alcohols using an engineered choline oxidase, or from carboxylic acids using a CAR. These two novel cascade approaches to the synthesis of chiral amines afforded several compounds in good to excellent yields. [97]
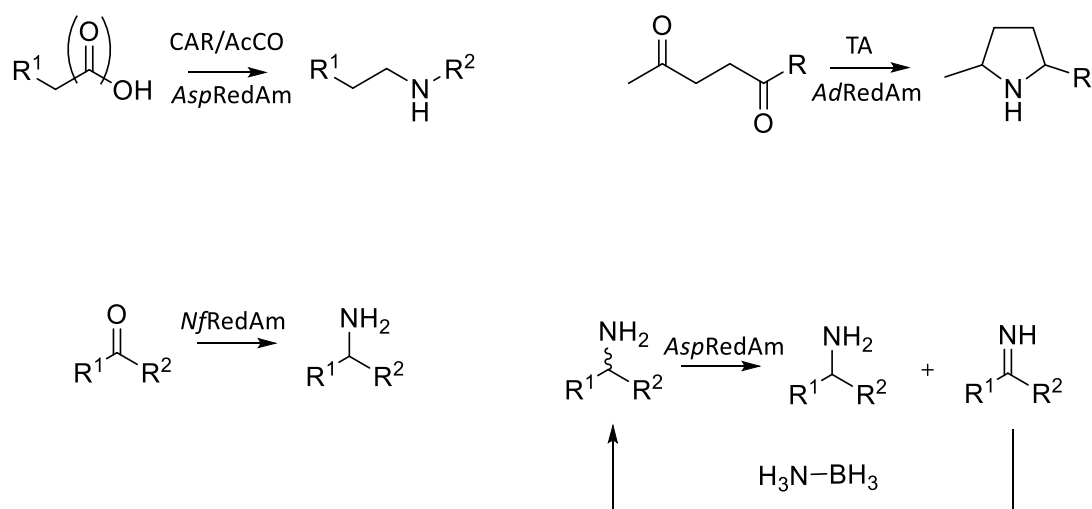
Figure 37: Summary of scope of reactions carried out using reductive aminases

The large scope of carbonyls and amines shown to be effective as substrates for reductive aminase catalysed reductive aminations led to further investigation of ammonia as an amine donor. Synthesis of primary amines using ammonia with IREDs has been shown in the past albeit with low conversions and although transaminases can catalyse the synthesis of primary amines successfully, they require removal of by-products to achieve high yields.

Initial work carried out by González-Martínez *et al.* looked at using two RedAms from *Neosartorya fumigatus* (*Nf*RedAm) and *Neosartorya fischeri* (*Nfis*RedAm) for reductive amination on fluorinated acetophenones. These fluorinated acetophenones are difficult carbonyl acceptors due to the conjugate of the ketone. The more fluorine groups adjacent to the carbonyl also add a problem, with trifluoroacetophenone being prone to ketone reduction over reduction amination. [98] The reductive amination between acetophenone and ammonia was shown to be successful with 10% conversion achieved with an the amine in 25-fold excess.[99] Mangas-Sanchez *et al.* then extended this work by testing different ketones with ammonia. All ketones tested were carried out using ammonia in a 100-fold excess with all corresponding products obtained in at least 4% conversion or more. Three of the ketones (cyclohexanone, 2-hexanone, and 4-phenylbutan-2-one) were also tested with ammonia at stoichiometric ratios. *Nf*RedAm provided the corresponding amines in 90%, 72%, and 10% conversion respectively. [100]

2.6.4 Industrial Use

Recently, Pfizer looked at using the RedAm technology for a scale up synthesis to access abrocitinib, a JAK1 inhibitor (Figure 38). They screened a panel of in house enzymes and identified a reductive aminase from *Streptomyces roseum* (*Sr*RedAm), the first RedAm from a bacterial source. Through six rounds of engineering, the TON value was increased from 288 to 36538 with a 19-fold increase in k_{cat} and a 11-fold increase in specific activity. They showed the scalability of this enzyme variant by carrying out a 230 Kg batch size reaction with a 73% yield in >99% purity and >99.5% dr.[101]
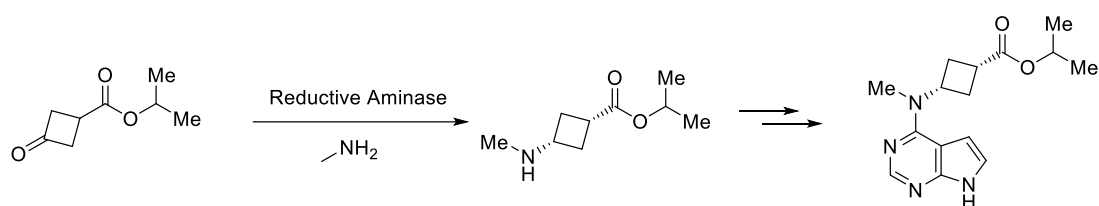
Figure 38: Reductive aminase step to access a precursor of abrocitinib

2.7 Outlooks and conclusions

IREDs and RedAms have both been shown as valuable tools for accessing chiral amines, either via the reduction of prochiral imines or the reductive amination between carbonyl acceptors and amine donors. They have both been shown to have a wide substrate scope allowing for the access of cyclic amines such as pyrrolidines, piperidines and azepanes, and several aliphatic and aromatic primary, secondary, and tertiary amines.

Despite this, several reductive aminations catalyzed by these enzymes require the use of an excess of amine, which is not desirable for industrial applications. A clearly extensive effort has been put in to identifying more and more IREDs from the sequence space to improve on this and find enzymes more suitable for industry. An understanding of the mechanistic properties has been carried out on several different IREDs and a couple of the RedAms however outside of identifying the crucial proton transfer residues of aspartate and tyrosine, as well as the amine and ketone binding residues, the rest of the active site is not so understood.

This leaves a lot of space for these enzymes to be further characterized and modified to carry out their chemistry at closer to true reductive amination conditions (stoichiometric ratios of ketone and amine) and for their application into larger scale syntheses which has only been seen in a couple of examples.

Chapter 3: Aims

The prevalence of chiral amines as a functional moiety shows how important it is that they can be synthesised in the most efficient and greenest way possible. Biocatalysis provides an appealing alternative to traditional chemical synthetic routes. Imine reductases and reductive aminases have been worked on extensively to show a wide substrate scope to access a wide range of chiral amines. Several efforts have been made to identify new putative IREDs however very little work has been done to understand the roles of active site residues outside of understanding the mechanism of reaction. If we can gain an understanding of the active site residues further we can aim to engineer reductive aminases to carry out reactions closer to stoichiometric ratios and potentially access more complicated substrates such as aniline. As part of this PhD project I aimed to:

- Investigate the substrate scope of reductive aminases further to access a wider range of chiral amines either through reductive amination reactions between carbonyl acceptors and amine donors or through reduction of cyclic imines.
    - Dihydroisoquinolines and 2-phenylpyrroline are substrates that have been well explored in the past for imine reduction reactions and provide suitable starting substrates to explore the activity of reductive aminases.
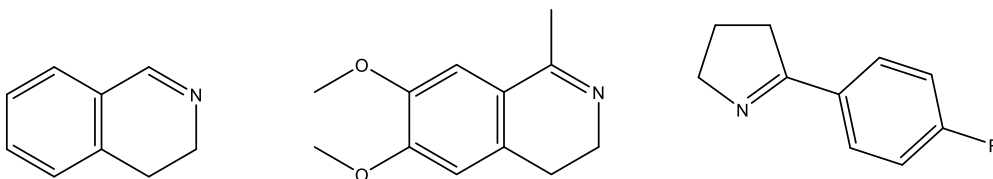
- Investigate amino acid residues in the active site to gain an understanding of their role in substrate scope, activity, and stereoselectivity. Directed evolution of a select panel of residues based on their catalytic role or position within the active site will be done in an effort to improve and control on enzyme activity and stereoselectivity.

- Positions of interest will be identified either through previous crystallographic data obtained on *Asp*RedAm (which shares 52% sequence identity) or from new crystallographic data of the reductive aminase in question in this project, *Ad*RedAm.
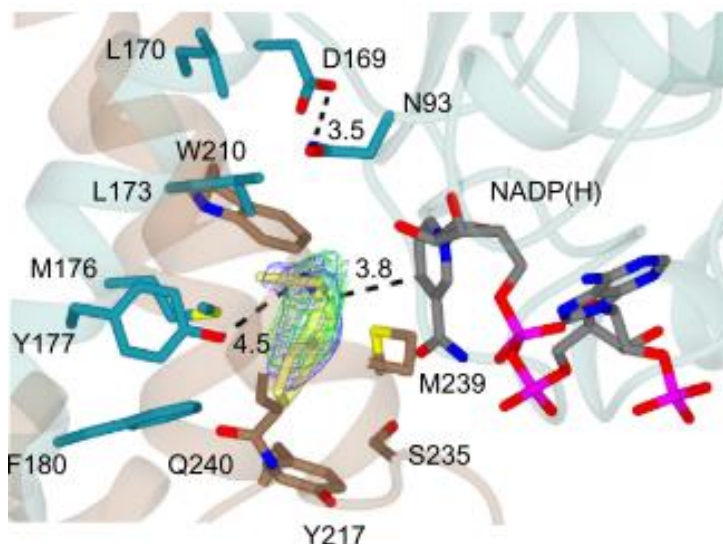
- Carry out reductive amination reactions with challenging substrates such as aniline and substituted anilines will be tested with the best performing variants generated in order to gain access to previously difficult to synthesise amines.
  - Due to the poor nucleophilic nature of aniline, high stoichiometries are typically required resulting in low yields and is a common precursor to compounds of interest such as Metolachlor.

Metolachlor
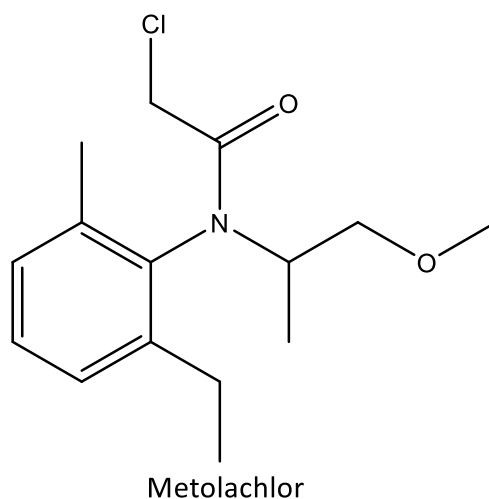
Chapter 4: Initial Screening of Reductive Aminases

4.1 Foreword

The work in this chapter focuses on a collaboration effort where the funding ended before the results could be finalised and supply of some compounds came to halt. All work that was carried out as part of the funding effort are reported as follows.

Compound numbering for this chapter correspond to compounds in this chapter only.

4.2 Initial Work

To further explore the substrate scope of reductive aminases, a small panel of ketones and amines that are of interest as building blocks for pharmaceutical ingredients were collated and screened against two RedAms as lyophilized lysate: *Ad*RedAm from *Ajellomyces dermatitidis* and *Nf*RedAm from *Neosartoria fumigata*.
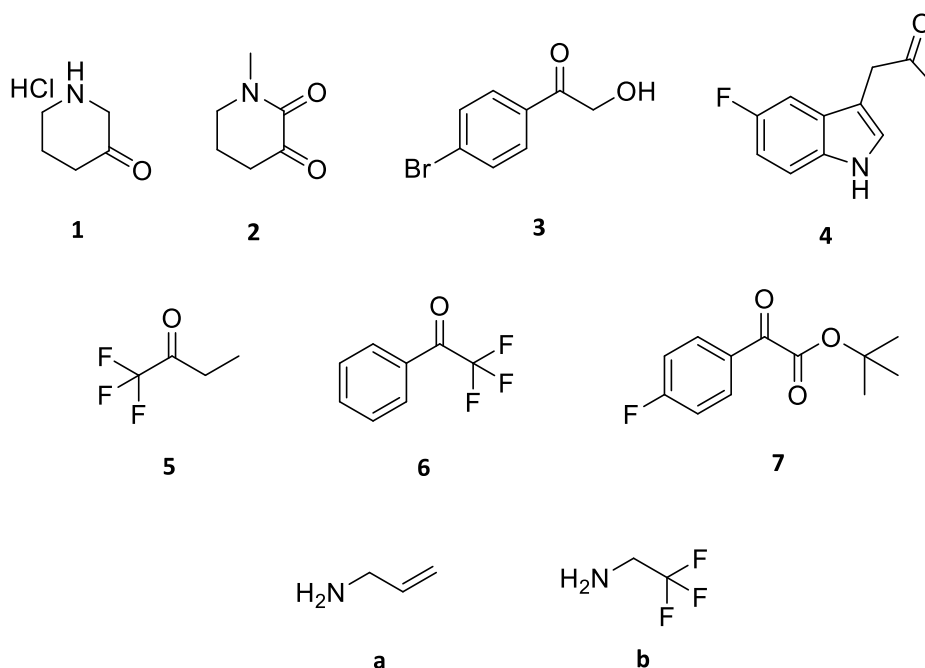

Figure 39: Panel of amines and ketones to be tested with the reductive aminases from Ajellomyces dermatitidis and Neosartoria fumigata

Before screening was carried out with the substrates in Figure 39, two simpler ketone homologues (acetophenone and 4-fluorophenylacetone) that had previously been

shown to work with reductive aminases[1] were tested to gain an idea of initial activity. The two ketones were tested with allylamine, **a**, in a molar excess of 5, 10, and 20-fold. 4-fluorophenylacetone was the better substrate of the two achieving conversions between 18% and 43% whereas acetophenone showed conversion < 4% (Figure 40).
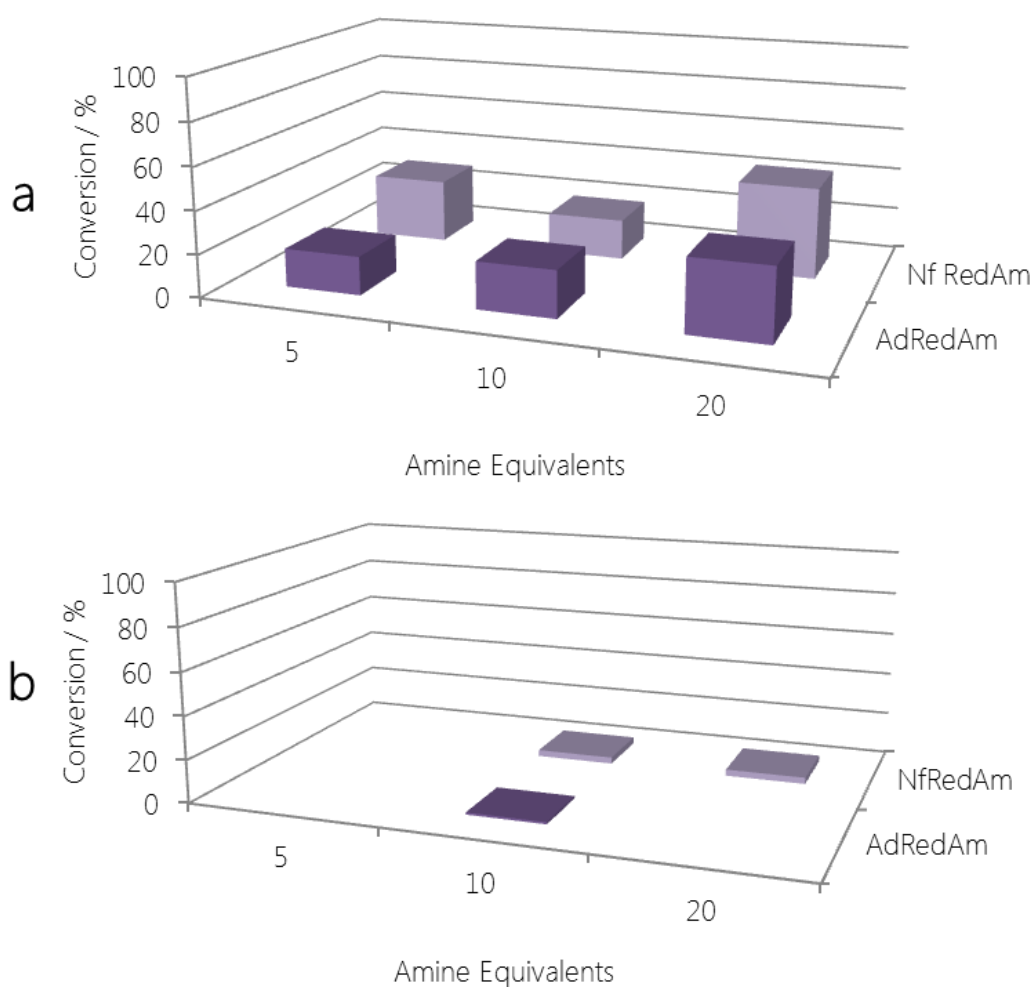
Figure 40: a) Conversions achieved in biotransformations with 4-fluorophenylacetone and allylamine. b) Conversions achieved with biotransformations of acetophenone and allylamine. Reaction conditions: 5 mM carbonyl, 25 mM amine donor, 10 mg mL^{-1} lyophilised RedAm, 0.5 mM NADP$^+$, 20 mM glucose, 0.1 mg mL^{-1} GDH (Codexis, CDX GDH-901 in 100 mM pH 7 phosphate buffer with 10% v/v DMSO.

Despite the limited success observed with acetophenone, all ketones from the initial panel were still screened with *Ad*RedAm and *Nf*RedAm with allylamine and trifluoroethylamine at varying amine concentrations (see Section 4.3).

---

[1] Personal communication from Dr. J. Mangas-Sanchez March 2018

Unfortunately, both the products and starting materials of reactions involving ketones **1** and **5** were not successfully extracted from the aqueous phase of the reaction. Therefore, no results were obtained and thus are not discussed from this point on.

4.3 Varying Enzyme Concentration

Both allylamine, **a**, and trifluoroethylamine, **b**, were tested at stoichiometric ratios with the panel of ketones (used at 5 mM), as well as in a 5-, 10-, and 20-fold excess in order to investigate the effect of amine concentration in aiding in the reductive amination capabilities of each enzyme. The first substrates from the panel tested with *Ad*RedAm and *Nf*RedAm were the bulkier ketones 1-(4-bromophenyl)-2-hydroxyethan-1-one, **3**, and 1-(5-fluoro-1H-indol-3-yl)propan-2-one, **4**. Both ketones proved to be unsuccessful candidates for reductive amination with either amine or either enzyme. Even by pushing the reaction conditions with a high excess of amine proved to have no effect.

Substrate **3** being an unsuitable ketone was not unsurprising. At the time this work was carried out, no data had been published on successful IRED or RedAm catalyzed reductive aminations involving hydroxyketones. The polar hydroxyl group in the alpha position must play a role in the reduced activity of these substrates. Either this could potentially be down to the hydroxyl group interrupting the catalytic capabilities of these enzymes, or the increased polarity of the compound can result in a substrate that is not readily accepted in the hydrophobic pocket of the active site. Mass screening of IREDs have been done since their discovery in 2010 (as mentioned in chapter 2) with no success towards hydroxyketones as suitable substrates, which leads to the belief that IREDs with more hydrophilic active sites is rare. Engineering of the active site introducing more hydrophilic amino acid residues could be one possible solution to this. In fact, Pfizer have very recently published work where they have taken an IRED from their internal library, which showed 5% activity for the reductive amination of a hydroxyketone and benzylamine, and increased the conversion to 43% through several rounds of engineering.[102]
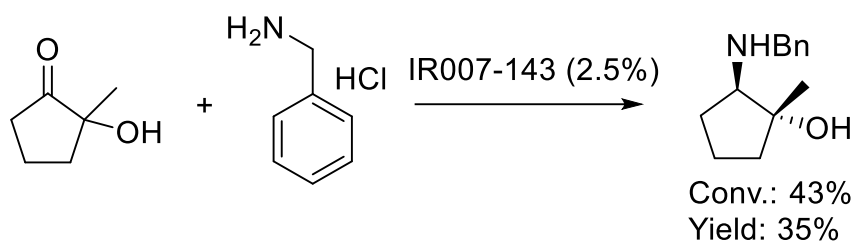
Figure 41: Biocatalytic reductive amination carried out by Pfizer between benzylamine and a hydroxyketone.

Indol, **4**, also failed to be successful as an acceptor for reductive amination. It had been reported by Aleku *et al.*[90] that other bicyclic ketones (**8**, **9**, and **10**, see Figure 41) were relatively poor acceptors requiring 50 equivalents of amine to achieve good yields. These ketones however were in conjugation with the aromatic ring on the compound which results in a poorer electrophile. When the carbonyl group was moved out of conjugation as is seen in compounds **11** and **12**, the activity improved. Although the carbonyl in indanol **5** is not in conjugation as it is in the poor bicyclic electrophiles, it is part of a propanone attached on to the ring adding steric bulk and requires fitting of both the propanone chain and the bicyclic into the active site.
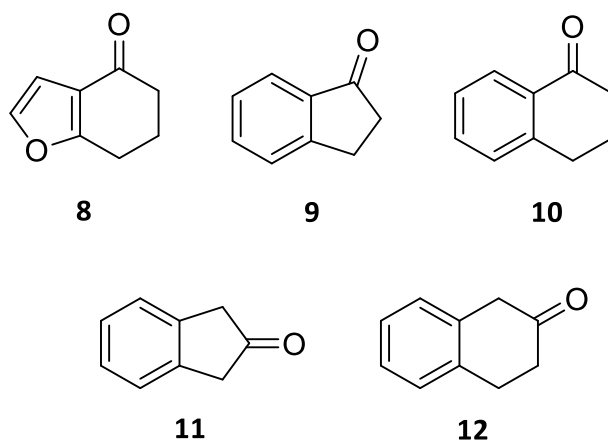

Figure 42: Examples of good and poor bicyclic carbonyls previously tested for RedAm catalyzed reductive aminations.[103]

Trifluoroacetophenone was tested for reductive amination reactions with both allylamine and trifluoroethylamine however, it was decided to remove the carbonyl from testing. This is due to work that was published from by Lenz *et al*. around the time that the work reported here was started. Lenz reported that

trifluoroacetophenone was prone to ketone reduction instead of reductive amination. By looking at the calculated activation energy of the carbonyl, they noticed that the three fluorine atoms caused the energy barrier to drop from 112.6 kJ mol^{-1} to 66.4 kJ mol^{-1}. This puts that activation energy of the carbonyl in the same level as for iminium ions and so will undergo similar reactions i.e. reduction to alcohol, over other reactions with a higher activation energy.[98] The reduction of trifluoroacetophenone was then shown further by González-Martínez *et al.*[99]

Biotransformations carried out with **7** appeared to be successful from initial experiments. The carbonyl starting material standard gave a retention time of 17.2 min, which corresponds to compound 2 in table 2. The other peak present across all biotransformations when detected occurred at around 16.9 min. It can safely be assumed that this peak does not correspond to the reductive amination products for two reasons: firstly, it is expected that the reductive amination products would appear later on the chromatogram and secondly, the retention time is the same whether allylamine or trifluoroethylamine was used. A selection of the biotransformations were taken for analysis via GC-MS and the peak at 16.9 min from the GC-FID trace corresponded to *p*-fluoromandelic acid according to the mass spec data. It was not determined however, whether this reduction was a result of the aqueous solution or the enzyme and was not explored further.
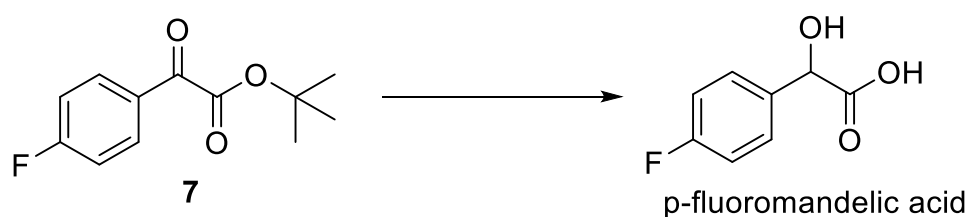

*Figure 43: Reaction scheme for the formation of p-fluoromandelic acid from **7***

Table 1: Biotransformation data for the reductive amination with carbonyl 7

Amine	Enzyme	Amine Eq.	p-fluoromandelic acid RT / min	p-fluoromandelic acid Area / %	Compound 2 RT / min	Compound 2 Area / %
Allylamine	AdRedAm	20	-	-	-	-
Allylamine	AdRedAm	10	-	-	-	-
Allylamine	AdRedAm	5	16.9	66.4	17.2	33.6
Allylamine	AdRedAm	1	16.9	100	-	-
Allylamine	NfRedAm	20	-	-	-	-
Allylamine	NfRedAm	10	-	-	-	-
Allylamine	NfRedAm	5	16.9	65.3	17.2	34.7
Allylamine	NfRedAm	1	16.9	100	-	-
Trifluoroethylamine	AdRedAm	20	16.9	100	-	-
Trifluoroethylamine	AdRedAm	10	16.9	53.6	17.2	46.4
Trifluoroethylamine	AdRedAm	5	16.9	58.6	17.2	41.4
Trifluoroethylamine	AdRedAm	1	16.9	89.8	17.2	10.2
Trifluoroethylamine	NfRedAm	20	16.9	100	-	-
Trifluoroethylamine	NfRedAm	10	16.9	65.7	17.2	34.3
Trifluoroethylamine	NfRedAm	5	16.9	59.6	17.2	40.4
Trifluoroethylamine	NfRedAm	1	16.9	97.0	17.2	2.80

1-methylpiperidine-2,3-dione, **2**, proved to be the most, and only, successful carbonyl tested from this panel. When either allylamine or trifluoroethylamine were used at stoichiometric ratios, no reaction was observed. Upon increasing the equivalency of amine to 5-, 10-, and 20-fold, full consumption of the dione was observed. Using allylamine at a concentration five times that of 1-methylpiperidine-2,3-dione resulted in two peaks on the GC trace at 17.57 min and around 17.9 min. When the concentration of allylamine was increased to 10 and 20 times that of the dione, the peak at around 17.57 min was no longer observed and only the peak at around 17.9 min was observed. The product, **2a**, was chemically synthesised and ran on GC-FID and was found to correspond to the peak at 17.5 min. Therefore, by using 5 amine equivalents with either *Ad*RedAm and *Nf*RedAm, 20% conversion to the product was being achieved, however 80% corresponded to this second peak (see table 3).

It was theorised that this second peak could be the intermediate imine compound, which due to the high excess of amine, would be formed *in situ*. In order to investigate this, the biotransformation extract was concentrated down and dissolved in deuterated chloroform for NMR analysis. From analysis of the 1H NMR spectrum, this compound was identified to be the enamine compound (Figure 45).

The same was observed when trifluoroethylamine was used and the amine donor. No reaction was observed at stoichiometric ratios, however upon increasing the amount of amine, full consumption of the starting material was observed and two peaks were formed. Again, the product standard, **2b**, was chemically synthesised and this corresponded to the peak around 15.7 min. Since no biotransformation showed full conversion to just one product, the reaction with the highest area of the peak not corresponding to the amine product was sent for NMR analysis. 1H NMR showed the presence of the enamine proton at carbon-4, the same as was observed for allylamine (Figure 46).
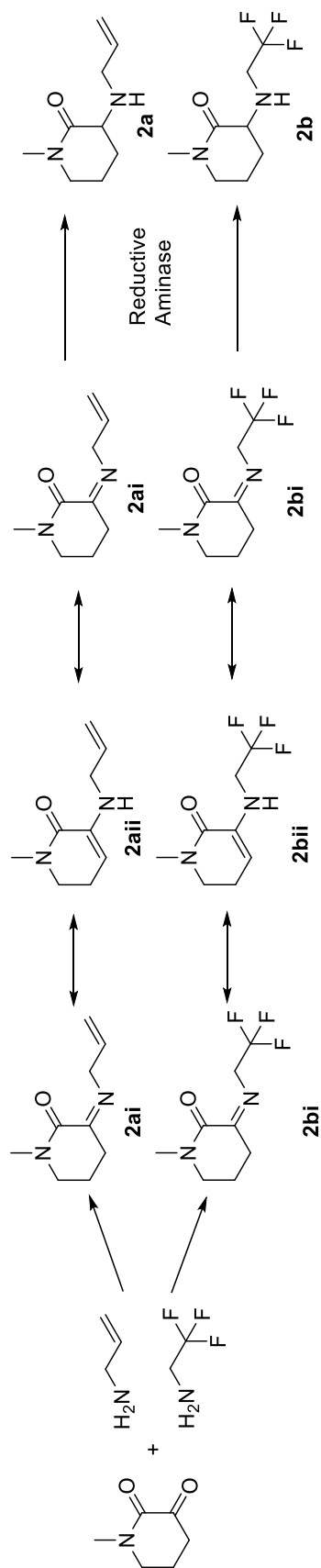
Figure 44: Formation of the imine intermediates 2ai and 2bi and tautomerization to the corresponding enamines 2aii and 2bii.

Table 2: Biotransformation data for the reductive amination with carbonyl 2

Amine	Enzyme	Amine Eq.	2a/2b RT / min	2a/2b Area / %	2aii/2bii RT / min	2aii/2bii Area / %
Allylamine	AdRedAm	20	-	-	17.9	100
Allylamine	AdRedAm	10	-	-	17.9	100
Allylamine	AdRedAm	5	17.6	79.7	17.9	20.3
Allylamine	AdRedAm	1	-	-	-	-
Allylamine	NfRedAm	20	-	-	17.9	100
Allylamine	NfRedAm	10	-	-	17.9	100
Allylamine	NfRedAm	5	17.6	80.0	17.9	20.0
Allylamine	NfRedAm	1	-	-	-	-
Trifluoroethylamine	AdRedAm	20	15.8	57.8	15.8	42.2
Trifluoroethylamine	AdRedAm	10	15.8	78.6	15.8	21.4
Trifluoroethylamine	AdRedAm	5	15.8	66.7	15.8	33.3
Trifluoroethylamine	AdRedAm	1	-	-	-	-
Trifluoroethylamine	NfRedAm	20	15.8	54.7	15.8	45.3
Trifluoroethylamine	NfRedAm	10	15.8	45.3	15.8	54.7
Trifluoroethylamine	NfRedAm	5	15.8	35.3	15.8	64.7
Trifluoroethylamine	NfRedAm	1	-	-	-	-
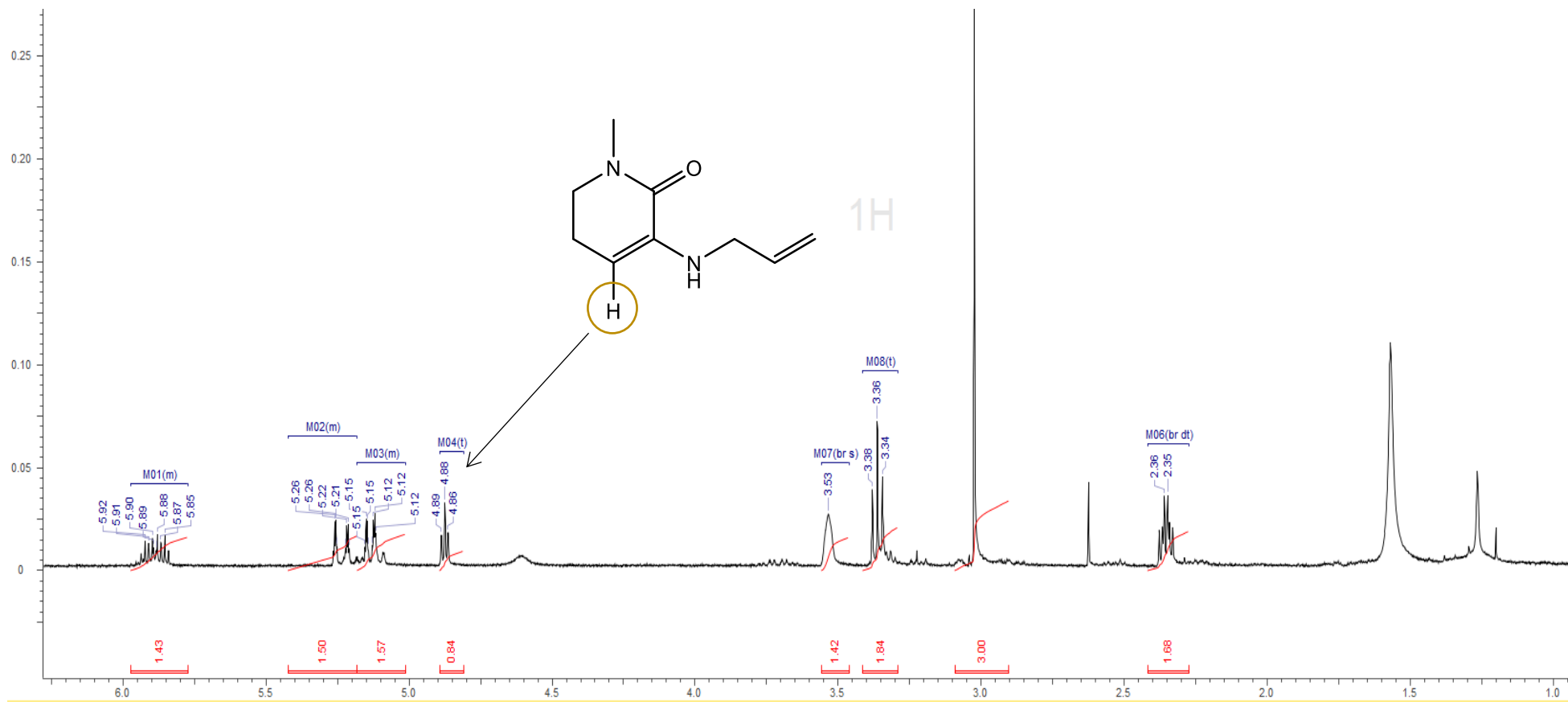
Figure 45: NMR identification of enamine by-products in the reductive amination between 2 and allylamine
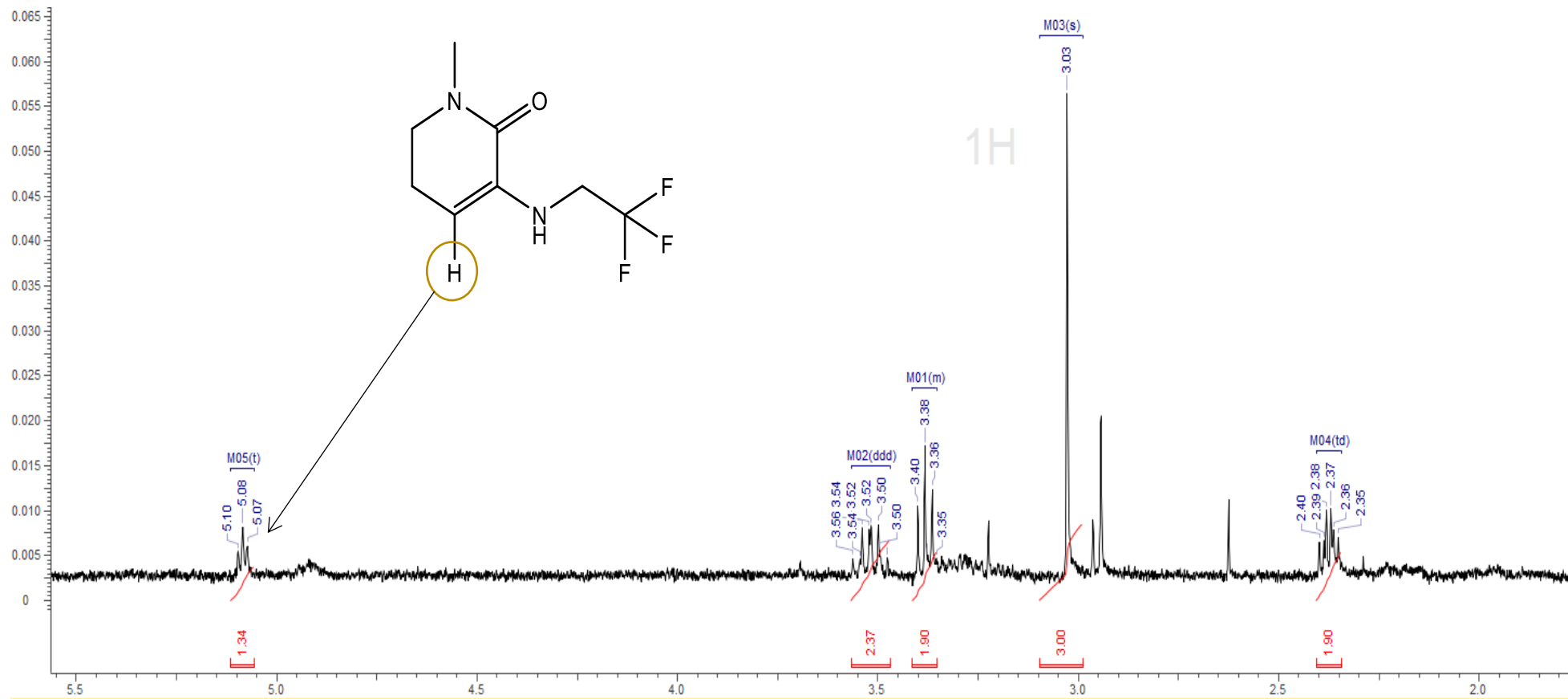
Figure 46: NMR identification of enamine by-products in the reductive amination between 2 and trifluorethylamine

In order to investigate formation of the enamine intermediate as well as formation of the amine, a time course investigation was carried out using *Nf*RedAm and cyanoborohydride, as well as a no reducing agent control to monitor the reaction between 1-methylpiperidin-2,3-dione and allylamine in a 5-fold excess.

4.4 Investigation into Enamine Formation

As mentioned above, a time course investigation was carried out using allylamine as the reductive amination partner (Figure 47). This was chosen over trifluoroethylamine due to the single peak observed at high amine ratios with a greater separation between amine and enamine. A reductive amination using cyanoborohydride was carried out in tandem to explore the role of the enzyme on any reduction of the enamine to the amine, and a no reducing agent control was carried out to see if enamine formation was enzyme catalyzed or not.

From the no enzyme/no cyanoborohydride control, it can be seen that within an hour 100% of the enamine is present with no starting ketone remaining and no amine product. This shows that enamine formation is not enzyme catalysed but is formed *in situ*. This can also be seen in the *Nf*RedAm reaction where the enamine has been fully formed after an hour and then gradually reduced to the amine over 10 hours. Reduction of the enamine to the amine can occur via two different routes. It could proceed either through direct reduction of the carbon-carbon double bond of the enamine, or via tautomerization of the enamine to the imine, which then undergoes reduction. Although the exact route was not determined, it is theorized that tautomerization to the imine followed by reduction is the most feasible route, instead of the reductive aminase being able to reduce the alkene (recent advances with IREDs however have shown that this in fact possible with some cyclic enimines).[88]
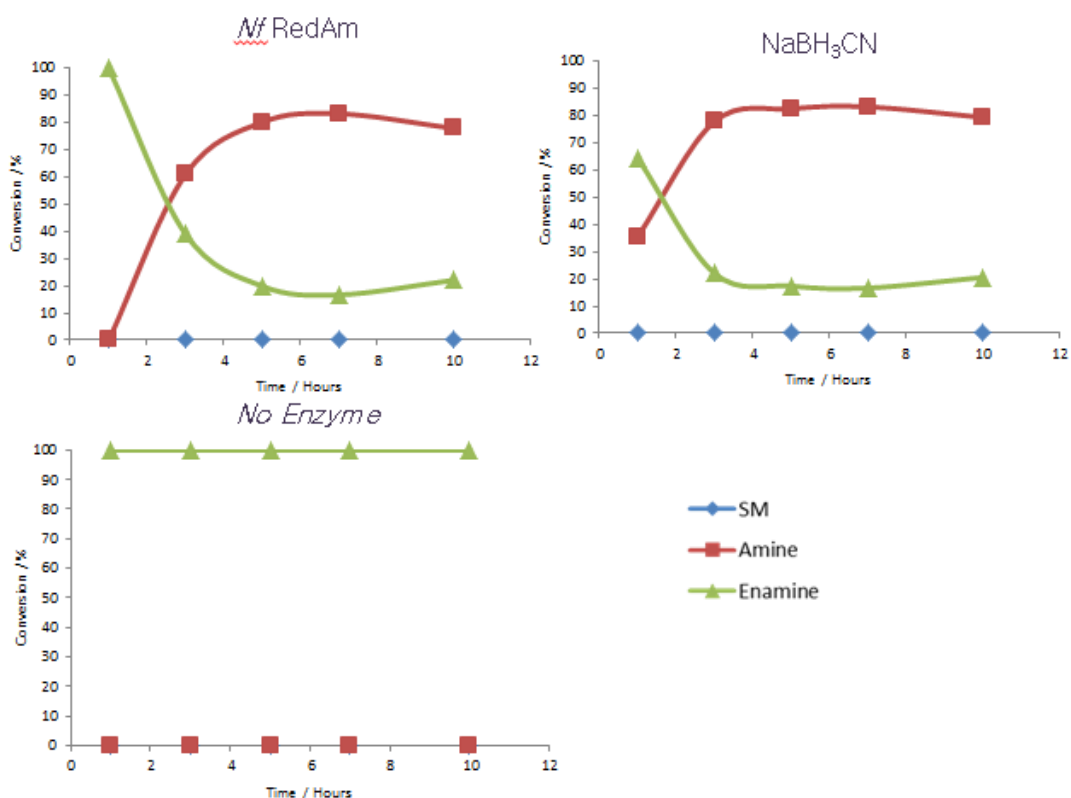
*Figure 47: Time course experiments performed to investigate the formation of enamine and reductive amination product in biotransformations of ketone **2** and allylamine. Reaction conditions: 5 mM carbonyl, 25 mM amine donor, 10 mg mL^{-1} lyophilised RedAm, 0.5 mM NADP$^+$, 20 mM glucose, 0.1 mg mL^{-1} GDH (Codexis, CDX GDH-901 in 100 mM pH 7 phosphate buffer with 10% v/v DMSO.*

4.5 Conclusions and Outlooks

An initial screening effort to expand the substrate scope of carbonyls to bulkier and with more functional group diversity (for example hydroxyketone and alpha keto ester) compared to those by reported by Aleku *et al.*[103] has been carried out. Not much success was observed with the panel of ketones, with some showing extraction issues (ketones   **1** and **5**) and some being unsuitable carbonyls for the reductive aminases tested (ketones **3**, **4**, and **6**).

It has been shown that the alpha keto ester **7** was an unstable substrate for reductive amination reactions undergoing ester hydrolysis to produce *p*-fluoromandelic acid. The cyclic dione was the most successful ketone tested in this panel. At amine excess higher than 5 equivalents resulted in the *in situ* formation of the corresponding enamine. This shift in equilibrium to the intermediate imine (and through

tautomerization the enamine)   creates a higher *in situ* concentration for reduction to the amine.

Enzyme engineering of active site residues in one route that can be carried out in order to improve the capabilities of the reductive aminases towards these poor carbonyl substrates. By looking at amino acid residues within the active site, it might be possible to gain an understanding into their role on substrate scope, as well as the stereoselectivity of these enzymes.

4.6 Experimental and Methods

4.6.1 Chemical Standards

All chemical compounds were provided for as part of the funding collaboration by the collaborators.

4.6.2 Synthesis of Product Standards

To a solution of ketone (70 mM) in dry THF (5 mL) containing molecular sieves under nitrogen were added amine (1.5 equivalents, 105 mM) and NaB(OAc)3H (1.5 equivalents, 105 mM1 111 mg). The reaction was stirred overnight at room temperature under N2 and quenched with NaOH (5 M, 10 mL) and extracted twice with EtOAc (15 mL). The aqueous layers were collected, washed with HCl (3 M, 10 mL) and extracted twice with EtOAc (15 mL), collected and dried over MgSO4. The solvent was removed under reduced pressure to afford the relevant amine products.
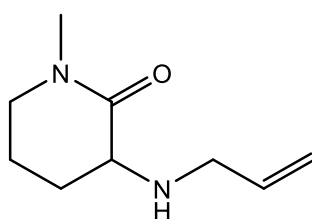
2a: 1H NMR (400 MHz, CDCl$_3$) δ: 5.95-5.85 (m, 1H), 5.23-5.09 (m, 2H), 3.36-3.19 (m, 5H), 2.93 (s, 3H), 1.86-1.76 (m, 1H), 1.70-1.57 (m, 1H), 1.28-1.23 (m, 2H)
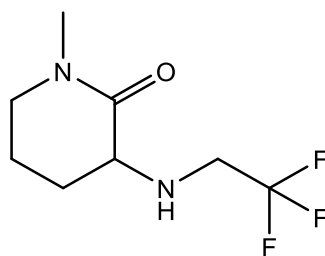
2b: 1H NMR (400 MHz, CDCl$_3$) δ: 3.38-3.13 (m, 5H), 2.94 (s, 3H), 1.74-1.59 (m, 4H)

4.6.3 Expression and Purification

The plasmids containing the genes for target enzymes were used to transform *E. coli* BL21(DE3) competent cells for gene expression. Pre-cultures were grown in TB-medium (15 mL) containing 10 µg mL^{-1} kanamycin for 18h at 37°C with shaking at 200 r.p.m. 400 mL volume cultures were inoculated with the pre-culture (15 mL) and incubated at 37°C, with shaking at 200 r.p.m. until an OD$_{600}$ of 0.6 – 0.8 was reached. Gene expression was induced by addition of IPTG 0.1 mM and shaking was continued overnight at 25°C with shaking at 200 r.p.m. The cells were then harvested by centrifugation at 4000 r.p.m. for 25 min and resuspended in 100 mM phosphate buffer pH 7. Cells were disrupted by ultrasonification for 15 min, 30 sec On, 30 sec Off cycles, and the suspension was centrifuged at 18,000 r.p.m. to yield a clear lysate. The N-Terminal His$_6$-tagged proteins were purified using immobilised-metal affinity chromatography (IMAC) using Ni_NTA column. In each case, the lysate was loaded onto a pre-equilibrated Ni_NTA columne, followed by washing with a load buffer (100 mM phosphate, 30 mM NaCl, 30 mM imidazole, pH 7). The bound protein was eluted using 100 mM phosphate buffer with 300 mM NaCl and 300 mM imidazole. The RedAm fractions were pooled, concentrated to 10 mg mL^{-1} and used for biotransformation reactions.

4.6.4 Biotransformation Procedure

A 500 µL reaction contained 20 mM D-glucose, 0.1 mg mL^{-1} GDH (Codexis, CDX GDH-901), 0.5 mM NADP$^+$, 10 mg mL^{-1} lyophilized lysate RedAm, 5 mM ketone and 10% v/v DMSO in 100 mM phosphate buffer pH 7. Amine concentrations were dependent on the ketone to amine ratio. Reactions used either 5 mM, 25mM, 50 mM, or 100 mM amine for 1, 5, 10, and 20 times amine concentration respectively. Time course biotransformations used 10 mM 1-methylpiperidine-2,3-dione and 10 mM allylamine
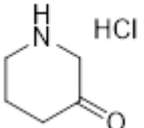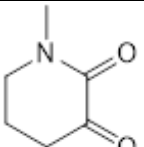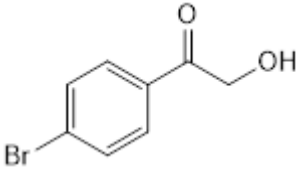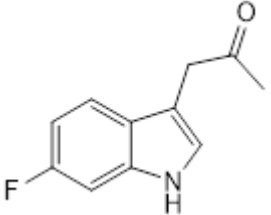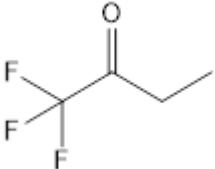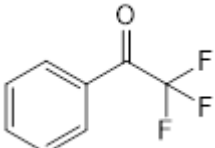
Reactions were incubated at 30 °C with 250 r.p.m. shaking for 18 h to 24 h, after which they were quenched by the addition of 100 μL 5M NaOH and extracted twice with 500 μL diethyl ether. The organic fractions where combined, dried over MgSO4 and analysed by GC-FID.
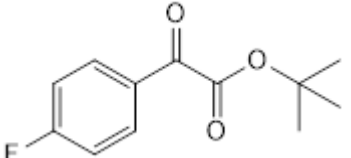
4.6.5 GC-FID Conditions

Samples were analysed using a HP-1 column, injector temperature of 200°C, a helium flow rate of 1.3 mL min^{-1}, oven temperature 40 °C – 320 °C with a ramp of 10 °C min^{-1}, and a detector temperature of 250 °C.
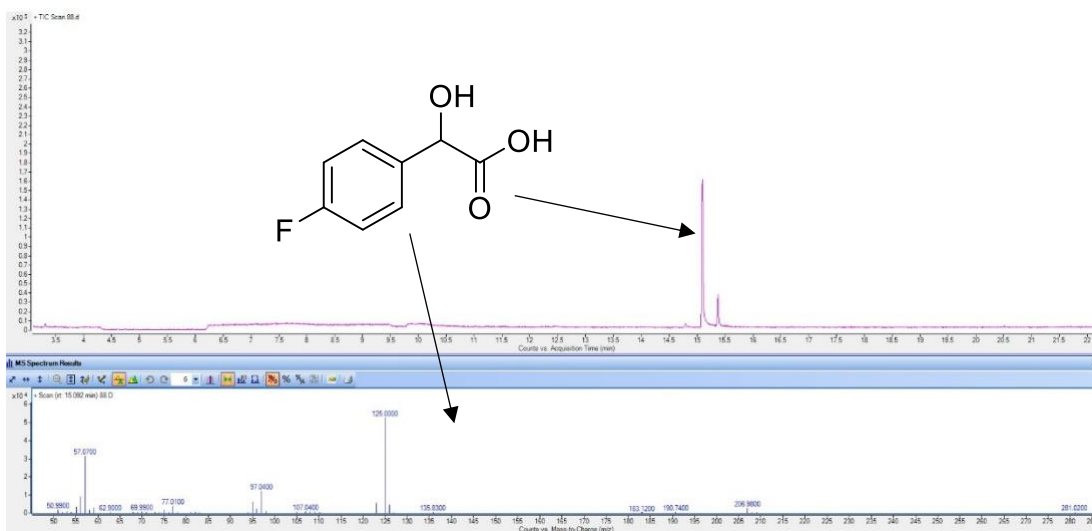
4.6.6 Substrate GC Retention Times

Table 3: Retention time of carbonyl substrates tested for reductive amination

Ketone	Structure	Retention Time
1		-
2		13.687 min
3		18.197 min
4		21.39 min
5		-
6		8.712 min

7		17.229 min

4.6.7 GC-MS trace for the reduction of carbonyl 7

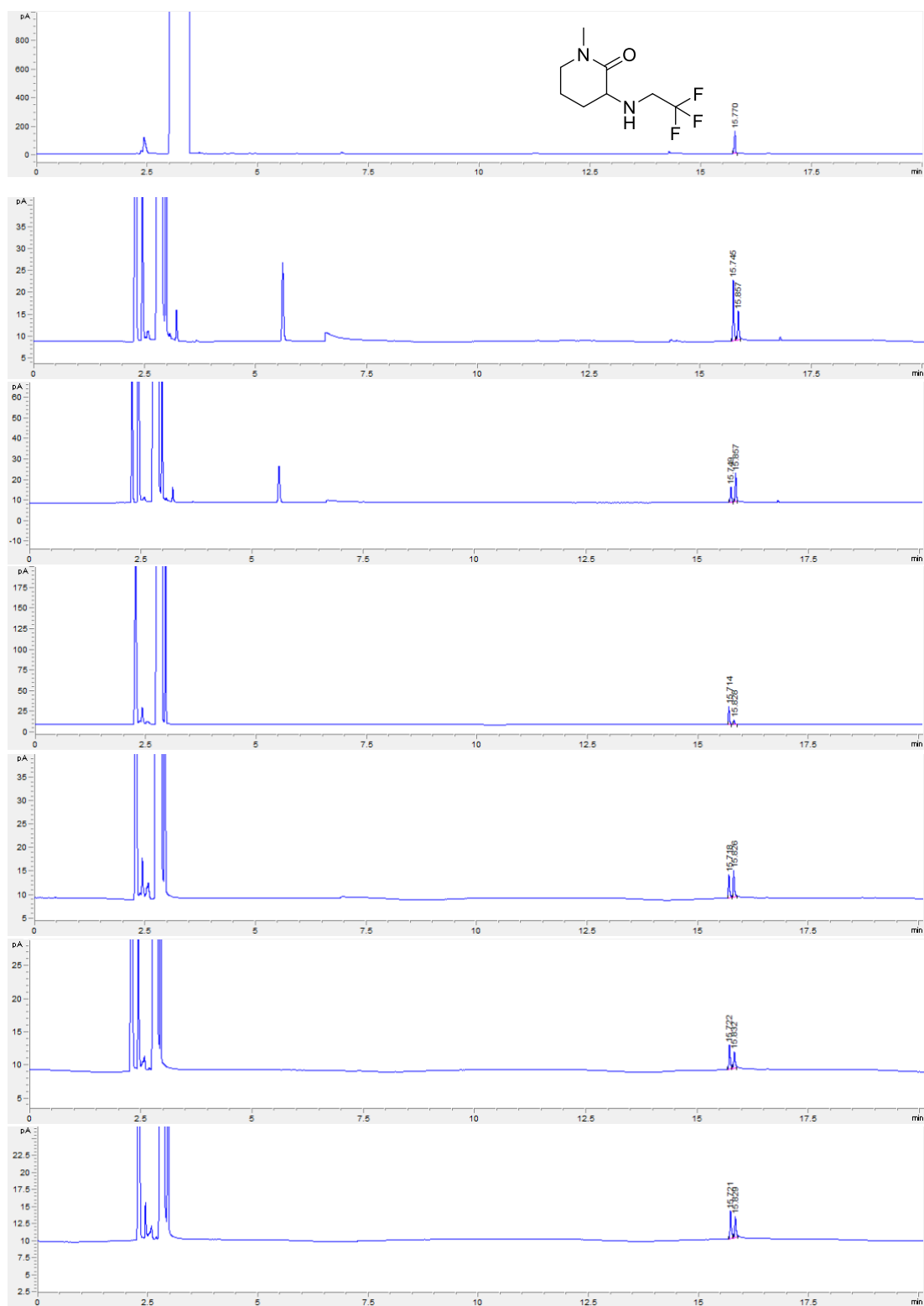## 4.6.8 GC-FID traces for the biotransformations of carbonyl 7

94
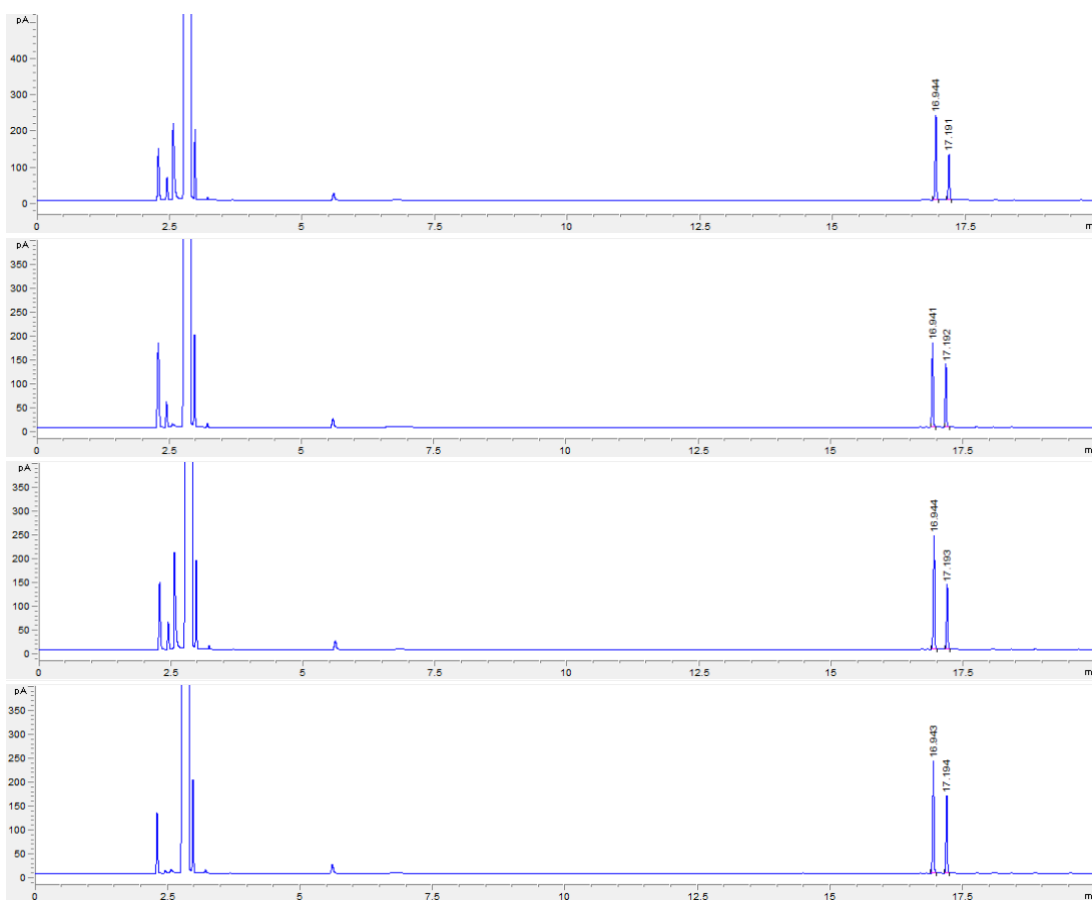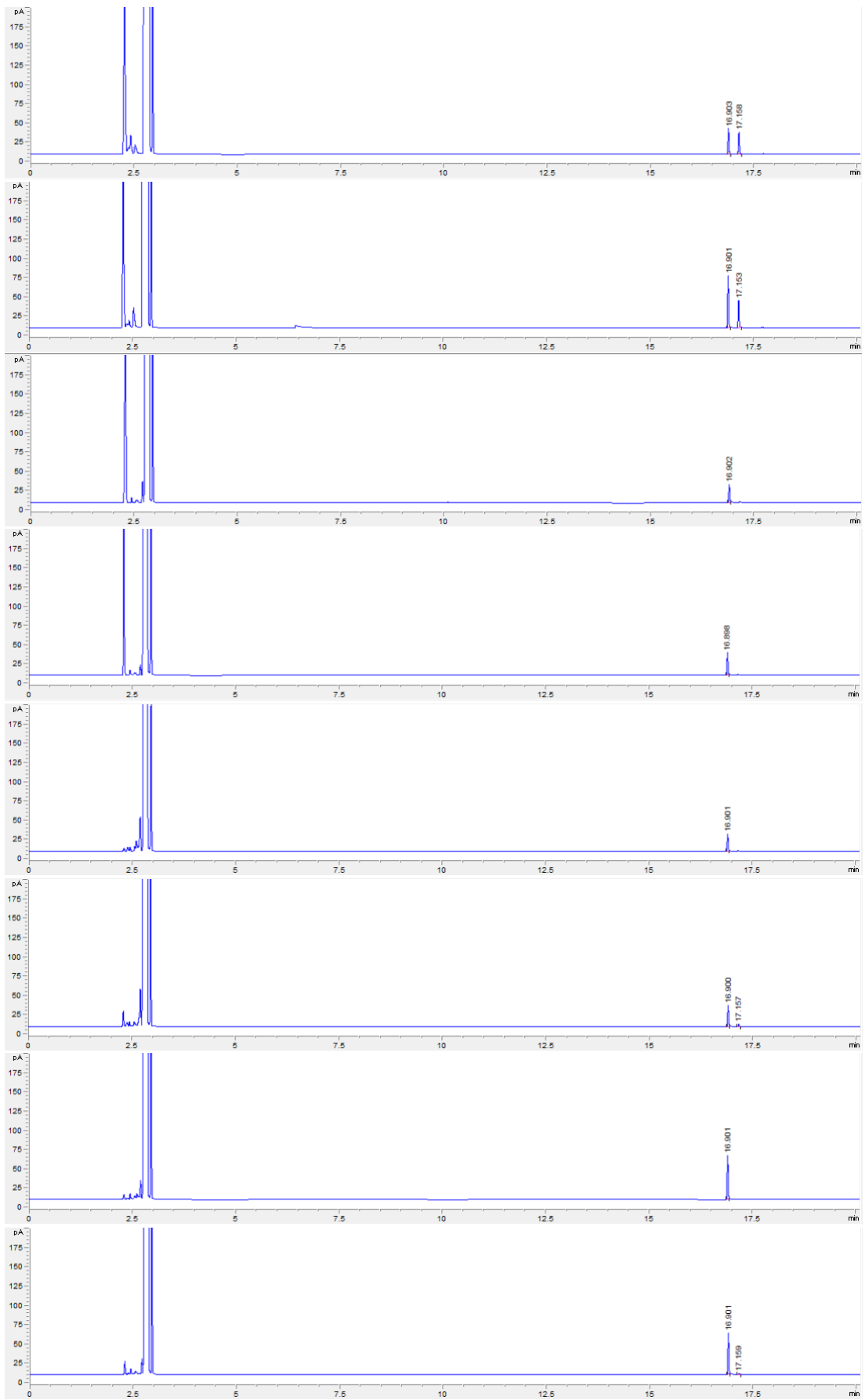
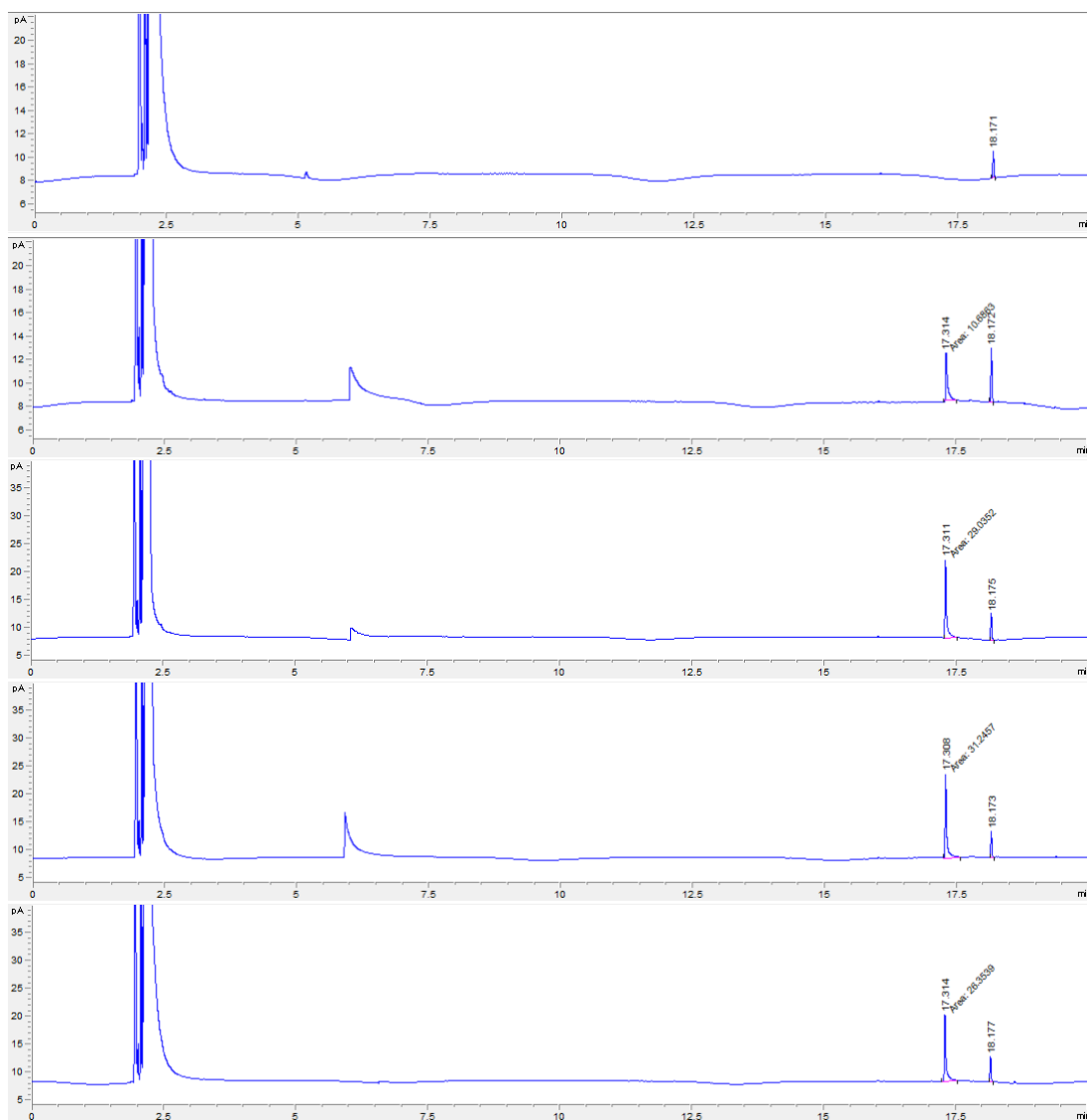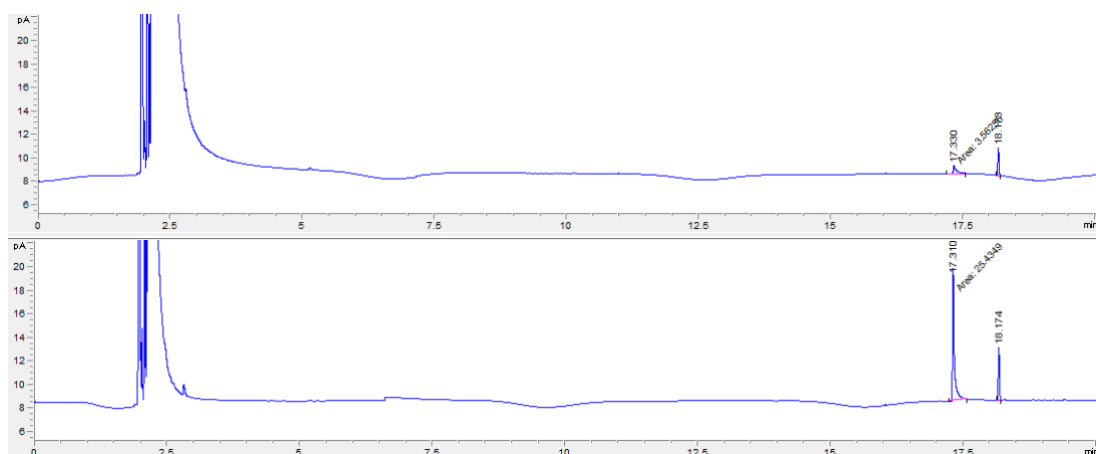## 4.6.9 GC-FID Traces for biotransformations of carbonyl 2 with allylamine
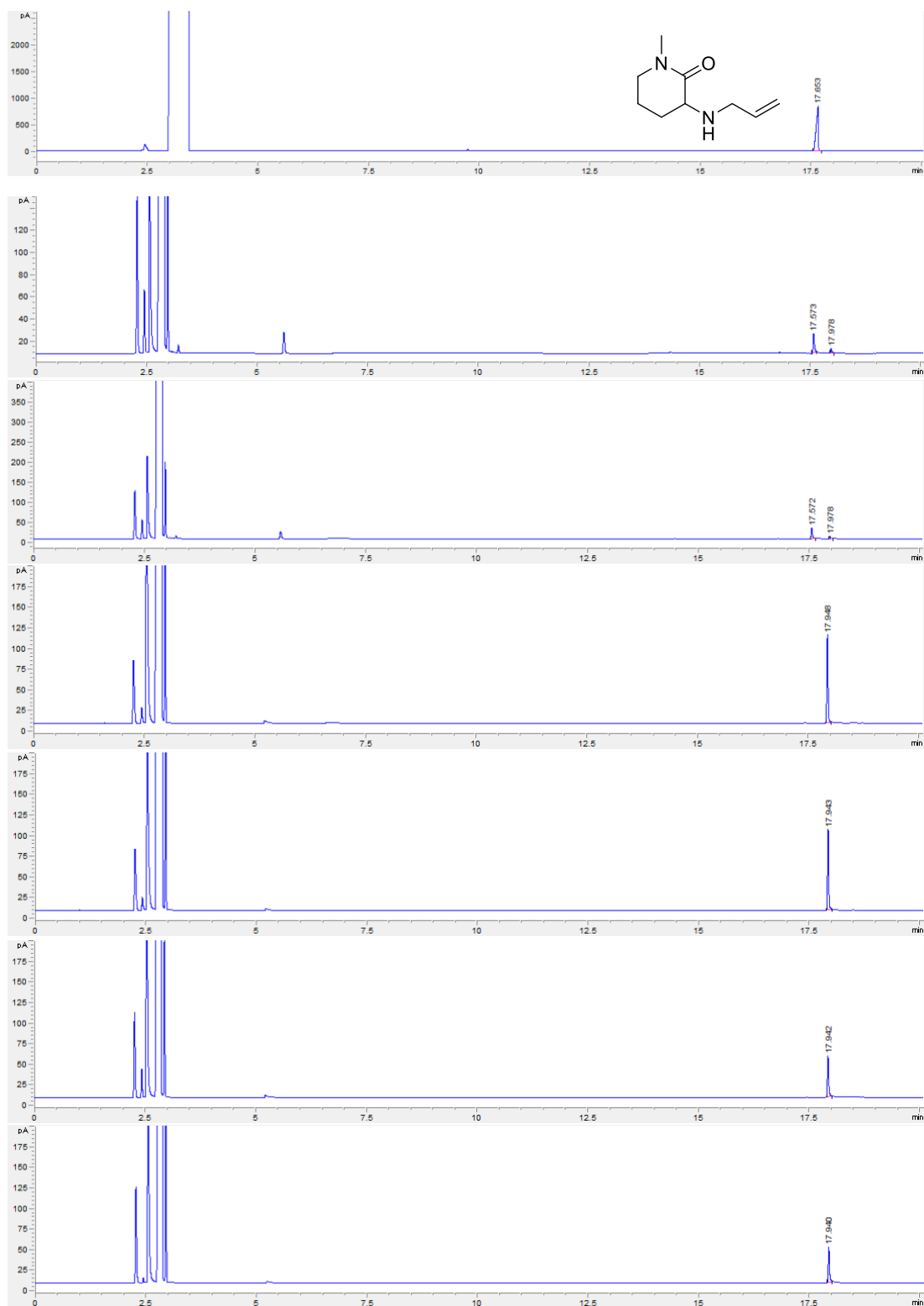
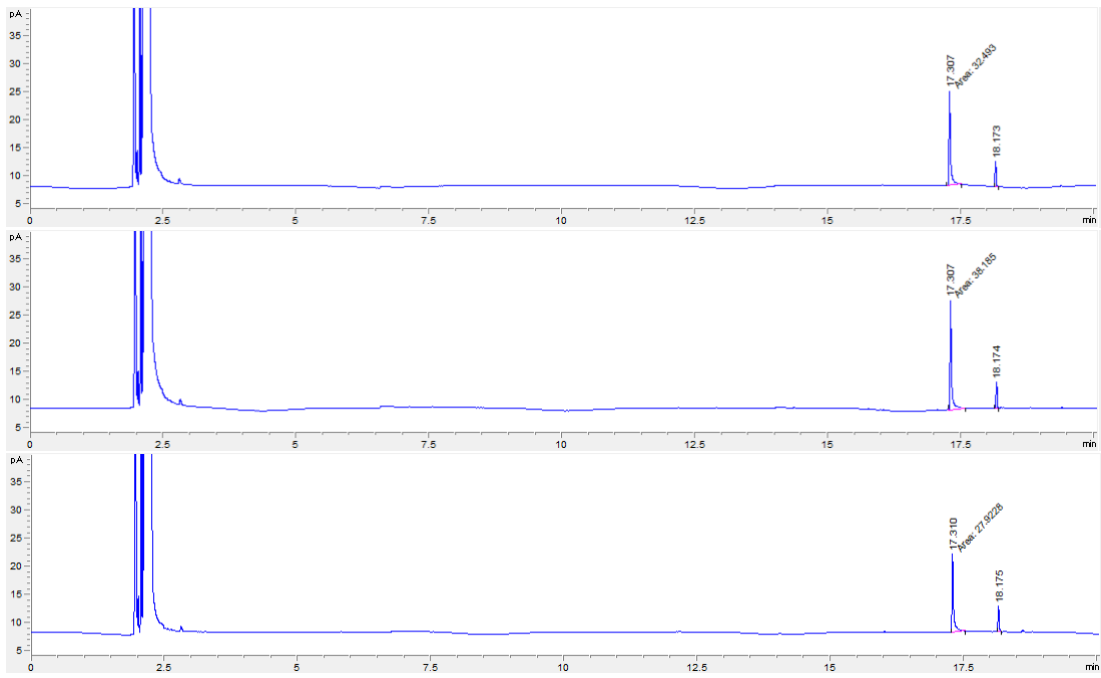## 4.6.10 GC-FID Traces for Biotransformations of Carbonyl 2 with Trifluoroethylamine

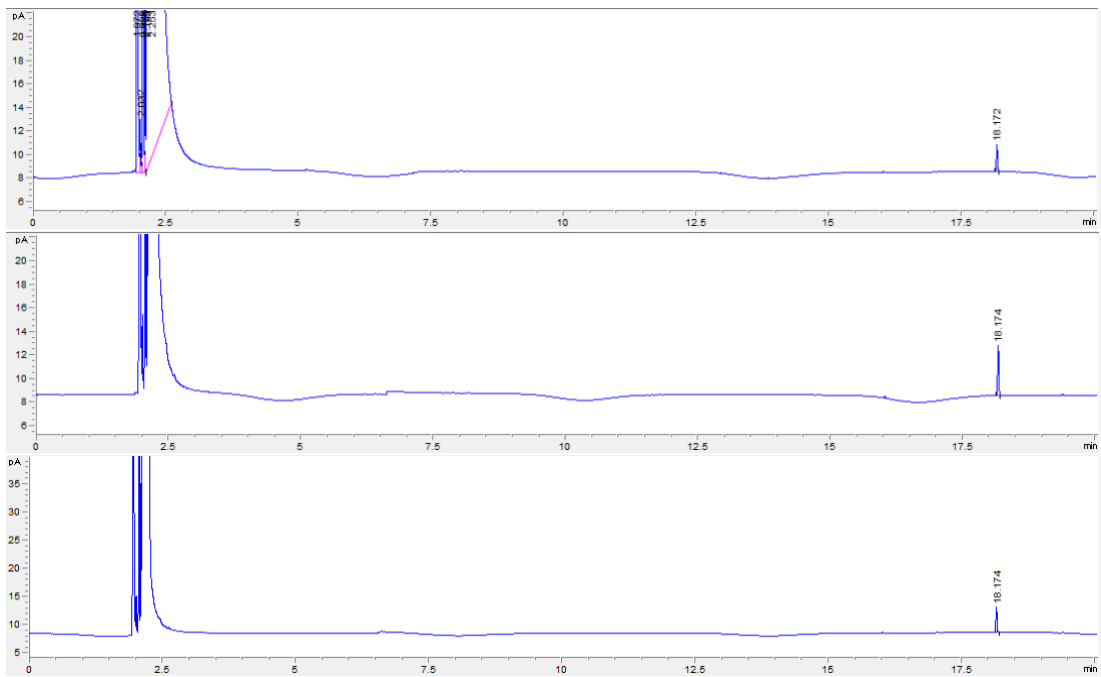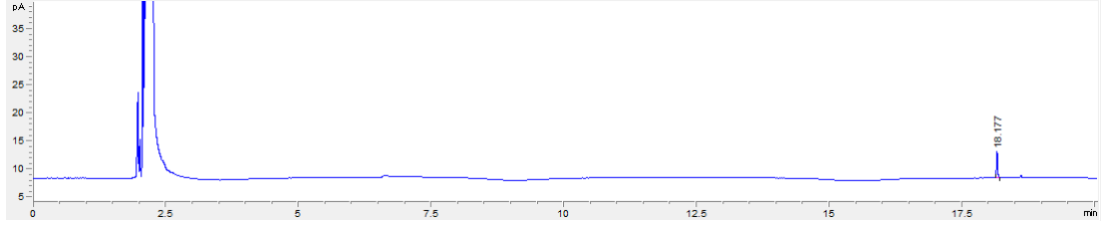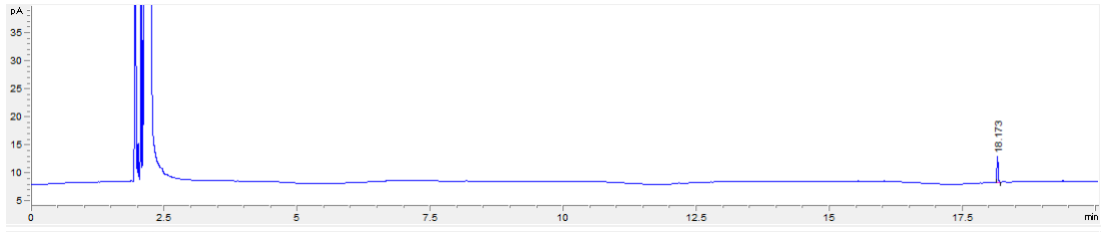*4.6.11 GC-FID Traces for the Time Course Biotransformations with Carbonyl 2, Allylamine and NfRedAm*

4.6.12 GC-FID Traces for the Time Course Biotransformations with Carbonyl 2, Allylamine, and Cyanoborohydride

4.6.13 GC-FID Traces for the Time Course Biotransformations of Carbonyl 2, Allylamine and No Reducing Agent

Chapter 5: Engineering of the Reductive Aminase from *Ajellomyces dermatitidis*

5.1 Foreword

Compound numbering for this chapter correspond to compounds in this chapter only.

5.2 Introduction

Imine reductases, and the related reductive aminases, have been well studied since their discoveries in 2010[48,49] and 2017[90] respectively. The substrate scope of these enzymes has been shown to accept a wide range of cyclic imines as well as several different amines and carbonyls for reductive amination. For IREDs, this has been achieved through a concentrated effort to identify new IREDs from either searching the sequence space or through metagenomics searches.

Compared to the large number of currently available IREDs, the panel of available RedAms is much smaller. Although they show an impressive substrate scope, we are limited to how efficient all reactions can be. For example, there exists certain carbonyl and amine combinations that still require an excess of amine in order to achieve sufficient yields. One way in which this can be improved is through the directed evolution of reductive aminases and gaining an insight into the role of amino acid residues within the active site.

Directed evolution is a technique that allows for the random or controlled mutagenesis of amino acid residues within enzyme architects in the aim of not only fine tuning the substrate scope but can also be used to control the reactivity and selectivity of the enzymes. Multiple different residues can be coded for in one position at the same time. Mutations can be made within the expression gene using degenerate codons that code for a number of different amino acids to create site-saturation libraries.[8,10,105] Random point mutations can also be created in the enzymes through the use of error prone PCR (which can then be identified through sequencing). Once this new gene has been cloned, transformed into competent cells, and expressed, individual colonies can be picked where each can be screened for activity. This can be a very time consuming approach as it can take time to find the

colony with the best mutation especially, again, if no established high-through put screen is available.[105] Site-directed evolution is a logical, less time-consuming method for developing enzyme variants; however it requires the three-dimensional structure of the enzyme, the amino acid residues within the active site, and the catalytically important residues to be known. By generating a combination of crystal structures of the apo-form, a complex with cofactor, and a ternary complex with cofactor and substrate/product, the amino acid residues in and around the active site as well as those of catalytic importance can be identified.[106] Certain mutations of these residues can then be made depending on what is to be investigated by imputing a codon that codes for specific amino acids rather than multiple ones. Once the mutant has been cloned and expressed, a quick sequencing check will reveal whether the variant has been successfully generated for investigative reactions to be carried out. [8,10,104–106]

5.3 Initial Screening

The initial identification of residues of interest was done using the ternary crystal complex of *Asp*RedAm-NADP(H)-Rasagaline that was determined by Aleku *et al.* (Figure 48). A total of seven positions within the active site were identified as interesting residues to be studied (due to being within 10Å of the crystallised substrate in Figure 48): N93, D169, Y177, W210, Y217, M239, and Q240. Previous studies have shown that removal of the protic aspartate residue to other amino acids such as alanine resulted in a completely inactive enzyme and so this residue was not carried forward for engineering.[91]
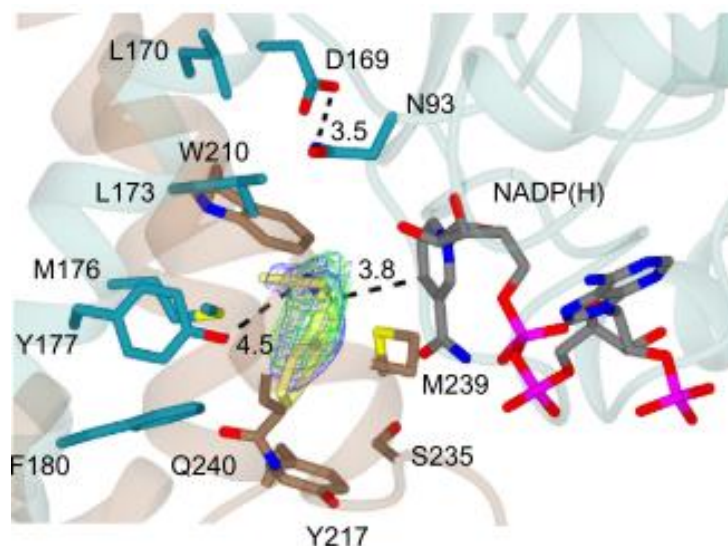
Figure 48: Active site of the ternary complex of AspRedAm-NADP(H)-Rasagaline – Permissions Granted by Nature

It was decided to carry out the engineering studies on the reductive aminase from *Ajellomyces dermatitidis* (*Ad*RedAm) due to an observed improvement in stability and expression levels from previous in lab studies[2] (not described here) over *Asp*RedAm. When compared to the sequence of *Ad*RedAm it was found that all residues were conserved within in at least two positions, except for the tyrosine at position 217 in *Asp*RedAm, which was a histidine at position 215 in *Ad*Redam. Single point mutations of all residues in *Ad*RedAm to alanine were generated (except for Y177 where phenylalanine was chosen), cloned, and expressed in *E. coli*.

---

[2] Personal communication from Dr. J. Mangas-Sanchez December 2019

```
AdRedAm      MANSPVSVFGLGAMGTALATQFLRKGHKTTVWNRTPAKAQPLIAIGASHAPTIDSAAAAS      60
AspRedAm     -MSKHIGIFGLGAMGTALAAKYLEHGYKTSVWNRTTAKAIPLVEQGAKLASTISEGVNAN      59
               .. :.:***********::.*..*:*.:***** *** **:  **. * **.... *.

AdRedAm      SLLIICQLDKASVMQTLQQAPTAWAAKTIVDLTNGTPAHARETADWALAHGARYIHGGIM     120
AspRedAm     DLIIICLLNNQVVEDALRDALQTLPSKTIVNLTNGTPNQARKLADFVTSHGARYIHGGIM     119
              .*:*** *:: * ::*::* : :****:****** :**: **:. :***********

AdRedAm      AVPFMIGQPDAMILYSGP-AEVFEGVKDTLSVLGTNTYVGEDVGLASLHDLALLSGMYGL     179
AspRedAm     AVPTMIGSPHAVLLYSGESLELFQSIESHLSLLGMSKYLGTDAGSASLHDLALLSGMYGL     179
             *** ***.*.*:.****   *.*:.::. **.** ..*:* *.* **************

AdRedAm      FSGFTHAVALVQSANIPA--AGFVATQLIPWLTAMTQHLNLLATQVDEKDYGDGGSSLDM     237
AspRedAm     FSGFLHAVALIKSGQDTSTTATGLLPLLTPWLSAMTGYLSSIAKQIDDGDYATQGSNLGM     239
             **** *****::*.:  :   *  :  * ***:*** :*. :*.*:*: **.  **.*.*

AdRedAm      QAKAAPNILEASQAQGVSVELIQPIFKLIERRVEEGKGSEGLAALVGMIMKGGTKDSV      295
AspRedAm     QLAGVENIIRAGEEQRVSSQMILPIKALIEQAVGEGHGGEDLSALIEYFKVGKNVD--      295
             *  .. **:.*.: * ** ::* ** ***: * **.*.*.*:**:  :  * . *
```

Figure 49: Sequence alignment of the reductive aminases from Ajellomyces dermatitidis and Aspergillus oryzae

Table 4: Amino acid residues and their relative positions in AspRedAm and AdRedAm and the corresponding residues they were mutated to.

| Residue in *Asp*RedAm	Residue in *Ad*RedAm	Mutation generated
N93	N94	N94A
Y177	Y177	Y177F
W210	W208	W208A
Y217	H215	H215A
M239	M237	M237A
Q240	Q238	Q238A

Of the six residues chosen for mutagenesis, two are involved in the catalytic mechanism for amine and ketone binding (N93 and Y177 respectively). Mutating these two residues should help give an insight into whether the role of the enzyme can be tuned between imine reduction and reductive amination. The other four residues were chosen primarily for steric reasons. The four residues occupied different space of the active site (other than M237 and Q238). Mutation to the small residue of alanine allowed for increasing the size of the active site without drastically altering the chemistry of the active site by introducing hydrophobic, hydrophilic, or aromatic groups. The aim for this was to be able to improve on the activity for imine

reduction (and ultimately reductive amination) as well as to identify residues that may be involved in controlling the stereoselectivity of the enzyme.

An initial screen for the reduction of 3,4-dihydroisoquinoline, **9**, was carried out for each variant as well as the *Ad*RedAm wild type over a two hour time course reaction with measurements taken at 15, 30, 60, and 120 minutes (Figure 51). Most of the variants resulted in full (or almost full conversion) within 15 minutes which made it difficult to determine relative activities to each other. Variants M237A and Q238A however showed a decrease in activity compared to the wild type with conversion <40% in 2 hours. Repeating these reactions with lower levels of enzyme would have allowed us to gain more insight into their activity of the variants toward **9**. However due to how quick full conversion was achieved (less than 20 mins), this would have resulted in very low enzyme concentrations, and so focus was turned to an alternative substrate.

In order to see discrepancies between each variant for activity, the bulkier 1-methyl-6,7-dimethoxy-3,4-dihydroisoquinoline, **10**, was tested (Figure 52). N94A showed to have very similar activity compared to *Ad*RedAm wild type with mutation of the ketone binding residue Y177F showed an improved activity with 100% conversion being reached in 30 minutes. As was observed with **9**, variants M237A and Q238A, as well as W208A and H215A, all showed drastically reduced activity towards the reduction of **10**, with M237A, Q238A, and W208A, all showing < 5% conversion after 2 hours.
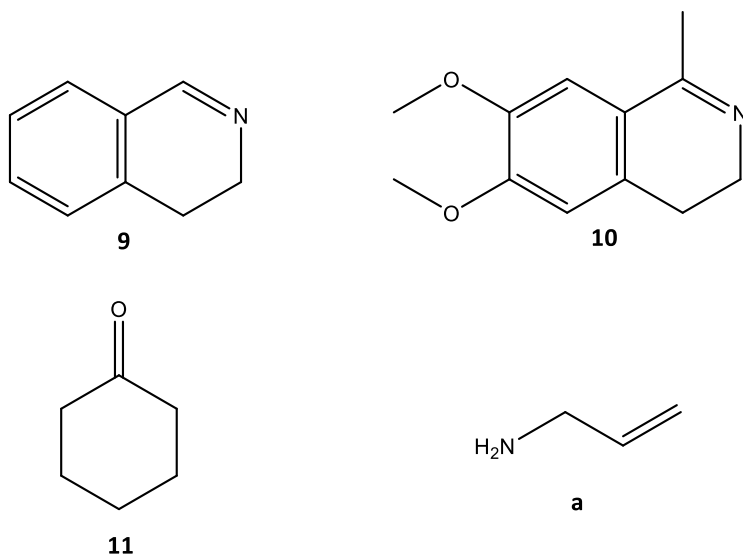
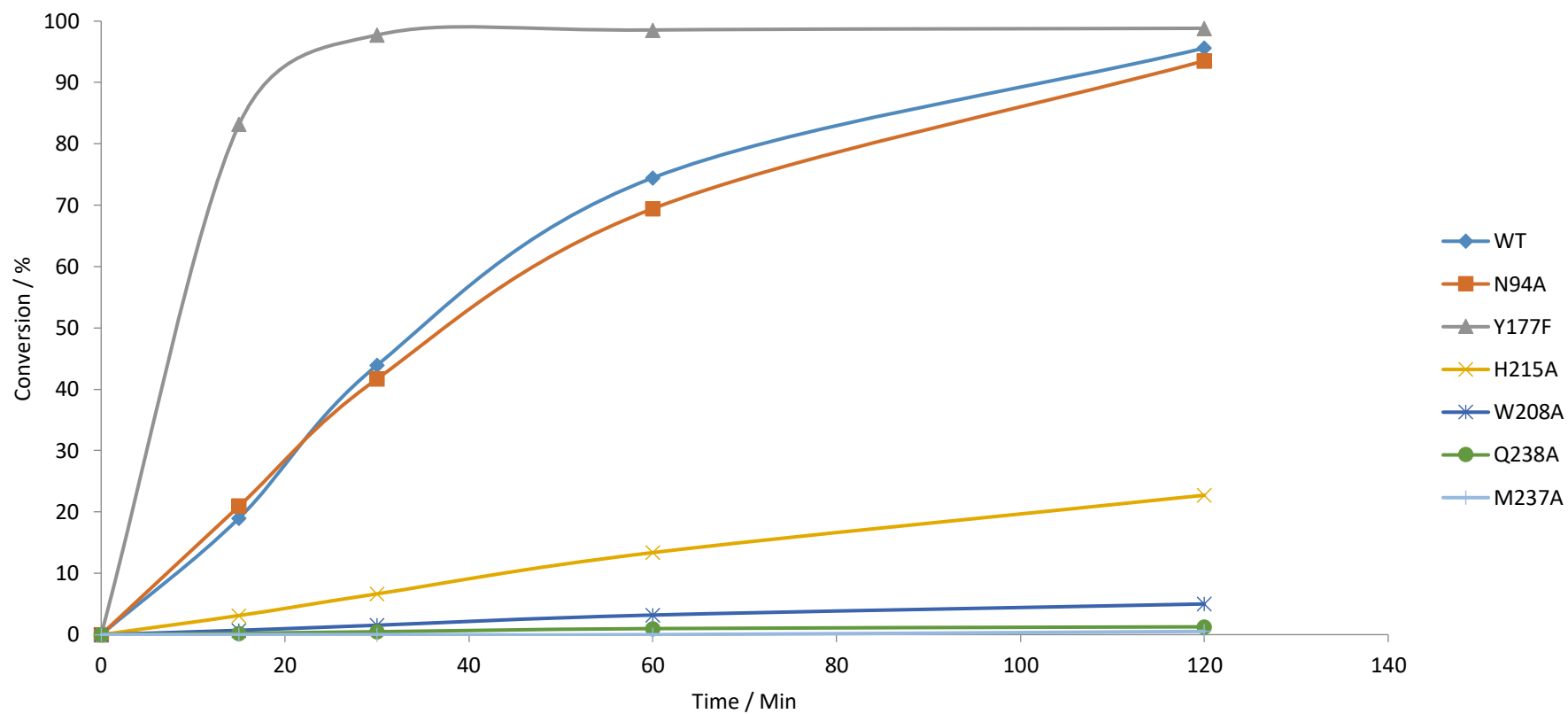*Figure 50: Substrates chosen for time course investigation of AdWT and Ad-variants*
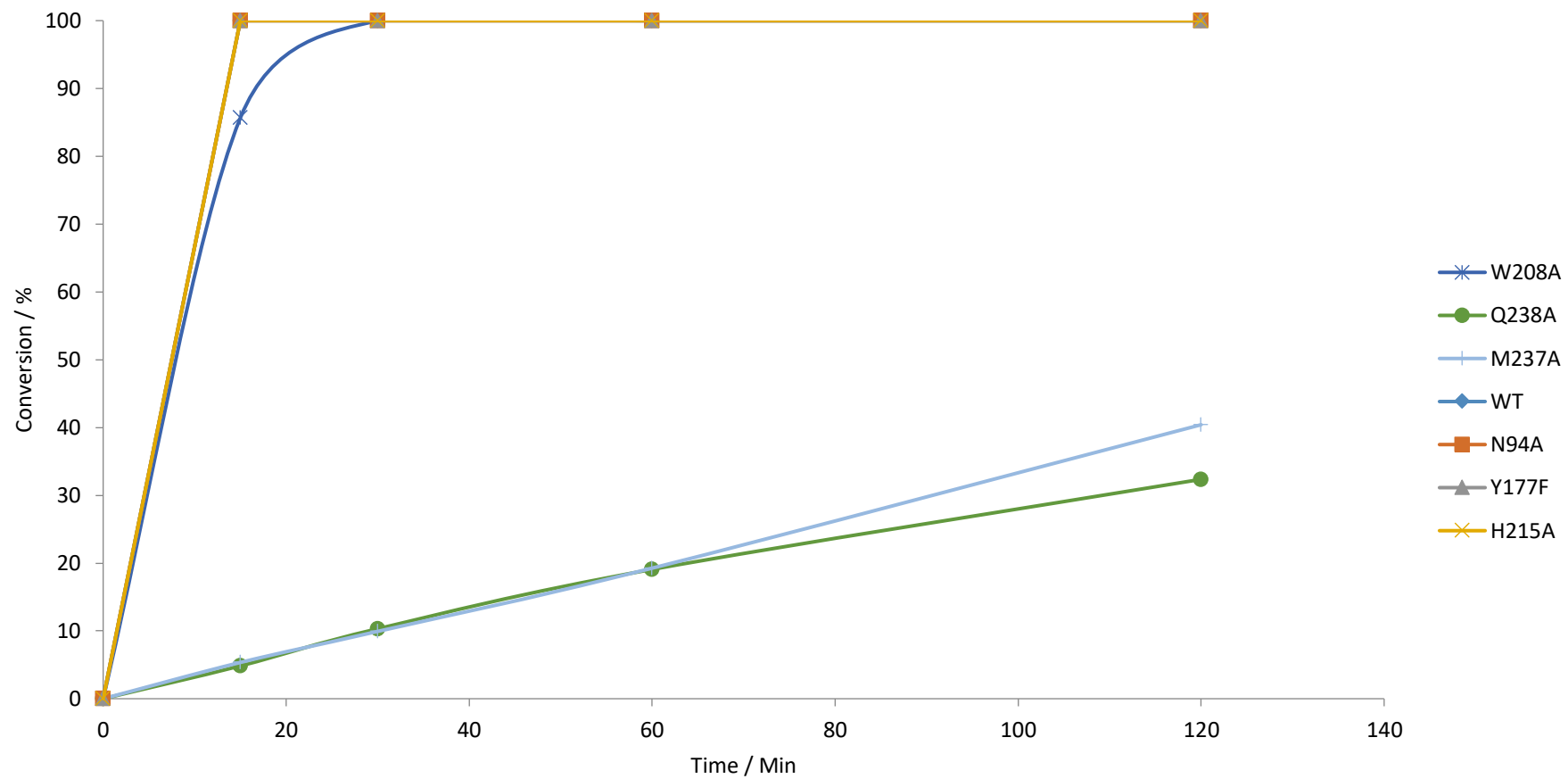
*Figure 51: Biotransformation time-course plot for the imine reduction of **9**. Reaction conditions: 10 mM imine, 0.5 mM NADP⁺, 1 mg mL⁻¹purifed RedAm, 20 mM glucose, 0.1 mg mL⁻¹ GDH (Codexis CDX GDH-901), 100 mM NaPi pH 7 buffer, 10% DMSO)*

*Figure 52: Biotransformation time-course plot for the imine reduction of **10**. Reaction conditions: 10 mM imine, 0.5 mM NADP+, 1 mg mL-1purifed RedAm, 20 mM glucose, 0.1 mg mL-1 GDH (Codexis CDX GDH-901), 100 mM NaPi pH 7 buffer, 10% DMSO)*

It has previously been shown by Aleku *et al.*[90] that cyclohexanone and allylamine are readily accepted substrates by *Asp*RedAm for reductive amination and so they were chosen to screen the reductive amination activity of the variants of *Ad*RedAm (Figure 53). N94A showed similar activity to the wild type enzyme just like it did for the reduction of **10**. As was determined for the mechanism of reductive amination for *Ad*RedAm, the amine is the last of the three substrates (NADPH, ketone, and amine) to bind. The similar activity of N94A to the wild type could potentially mean that the binding of the amine is also determined not just by the residue, but by the conformational changes that have already occurred upon cofactor and ketone binding respectively. Where the reduction of **9** and **10** occurred faster with Y177F, the reductive amination between **11** and **a** occurred at two-thirds the rate with only 37% conversion compared to 50% with the wild type after two hours. It can also be seen that variants H215A and W208A perform better towards this reductive amination than the imine reduction (45% conversion compared to 10% and 5% respectively), whereas both M237A and Q238A performed just as poorly with conversions <3%.

The variations seen between reductive amination and imine reduction highlight the substrate specificity towards the activity of *Ad*RedAm and the variants. In order to explore the activity of the enzymes, and their stereoselectivity, it was decided to take a different approach and focus on the reduction of cyclic imines, as these are substrates that have been well studied and documented.
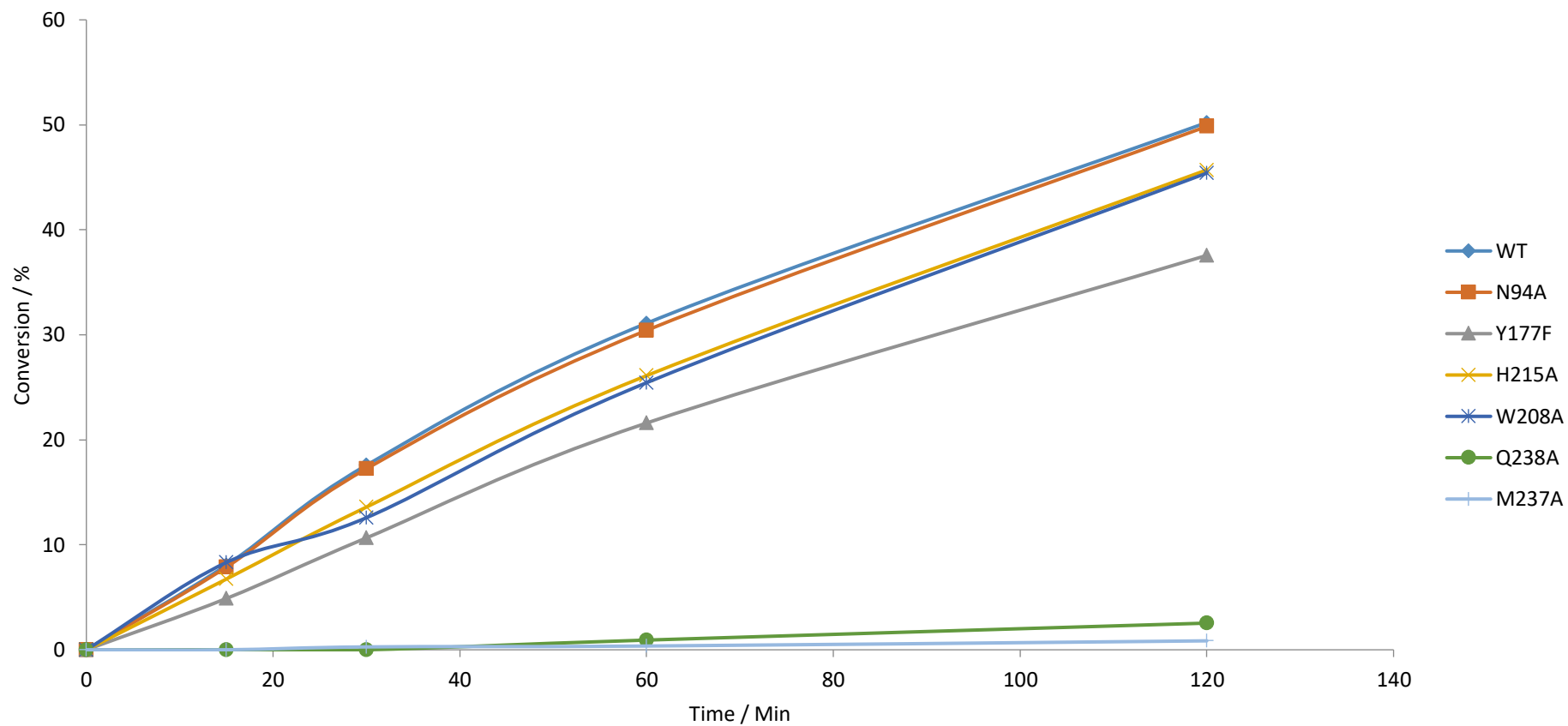
*Figure 53: Biotransformation time-course plot for the reductive amination of **11** and **a** (1 equivalent). Reaction conditions: 10 mM ketone, 10 mM amine, 0.5 mM NADP⁺, 1 mg mL⁻¹ purifed RedAm, 20 mM glucose, 0.1 mg mL⁻¹ GDH (Codexis CDX GDH-901), 100 mM NaPi pH 7 buffer, 10% DMSO)*

5.4 Reduction of Cyclic Imines

*Ad*RedAm has shown to be effective towards the reduction of 5-, 6-, and 7-membered cyclic imines with moderate to excellent conversions and this activity has been seen to fluctuate with varying ring sizes.[87,96] 2-Phenylpyrroline, **1**, (Figure 54) was chosen as the initial model substrate to investigate the activity and stereoselectivity of *Ad*RedAm and variants. Reaction using *Ad*RedAm wild type (1.0 mg mL^{-1} purified enzyme) gave an initial conversion value (after 3 hours) of 19% with an *ee* of 92% in favour of (*S*)-enantiomer. N94A performed just as well as the wild type with a similar conversion and the same stereoselectivity, however Y177F and H215A both showed a decrease in conversion and stereoselectivity. Variant W208A showed a remarkable improvement in activity with 100% conversion to the amine and improvement in wild type stereoselectivity at >99% (*S*)-enantiomer. Variants M237A and Q238A both showed an improvement in activity (from 19% conversion to amine to 46% and 40% respectively) and an inversion in stereoselectivity from the (*S*)- to the (*R*)-enantiomer, although in a lower *ee* value (77% and 78% respectively compared to 92% of the wild type, Table 5).

Table 5: Conversion and enantioselectivity data obtained for the reduction of cyclic imines catalysed by AdRedAm wild type and variants

Variant	Substrate 1		Substrate 3		Substrate 5		Substrate 7	
	Conv. / %	ee / %	Conv. / %	ee / %	Conv. / %	ee / %	Conv. / %	ee / %
WT	19	92 (S)	39	89 (R)	1	n.d.	30	72 (R)
N94A	18	92 (S)	38	88 (R)	1	n.d.	30	80 (R)
Y177F	6	87 (S)	17	96 (R)	<1	n.d.	12	69 (R)
W208A	100	>99 (S)	99	74 (S)	>99	>99 (S)	100	>99 (R)
H215A	18	89 (S)	27	97 (R)	1	n.d.	27	94 (R)
M237A	46	77 (R)	32	90 (R)	3	n.d.	100	>99 (R)
Q238A	40	78 (R)	33	95 (R)	3	n.d.	100	>99 (R)
M237G	54	88 (R)	25	99 (R)	5	n.d.	100	>99 (R)

Reaction conditions: *Ad*RedAm variant (1.0 mg mL^{-1}), imine (10 mM), NADP$^+$ (0.5 mM), CDX GDH-901 (0.1 mg mL^{-1}), D-glucose (20 mM), phosphate buffer (100 mM, pH 7), 30 °C, 250 rpm. Conversion data obtained via GC-FID after 3h, enantiomeric excess data obtained via HPLC after 18h.

The inversion of stereoselectivity from a single point mutation was remarkable (92 % (S) with AdWT and 77% (R) with AdM237A) and we wanted to see if we could improve on the level of stereoselectivity we obtained initially. The methionine at position 237 was chosen for further investigation and a site-saturation library was created using the degenerate NNK codon. A total of 94 colonies were picked and placed into a 96 well plate, with the final two wells being filled with AdWT and a negative control. An NADPH depletion assay was carried out and the best performing well compared to M237A was chosen and sent for sequencing (see section 5.8.7.1) . Sequencing results revealed the amino acid to replace methionine was glycine (M237G) and when used for a biotransformation for the reduction of **1**, gave an improved conversion and improved *ee* towards the (*R*)-enantiomer than M237A (Table 5).
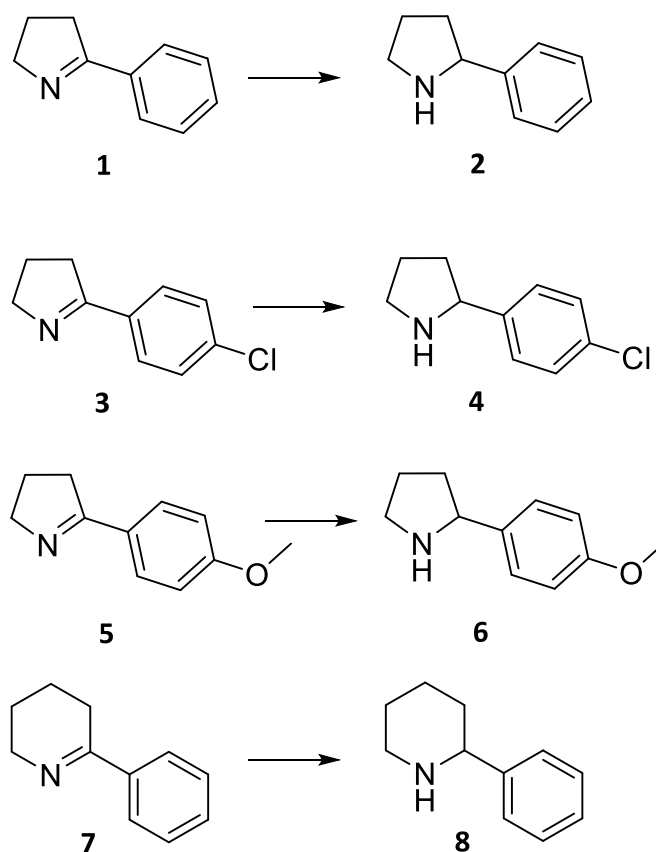
Figure 54: Cyclic imines screened to determine the role of residues in the active site of AdRedAm towards scope, activity, and selectivity

It was then decided to look at the effect of different substituents on the phenyl ring of 2-phenylpyrroline and the next substrate tested was 2-(4-chlorophenyl)pyrroline, **3** (Figure 54). This appeared to be a more ideal substrate for *Ad*RedAm wild type as well as N94A, Y177F, and H215A with higher conversions being achieved than for the reduction of **1**. It was observed though that the stereoselectivity of these four enzymes had inverted to give the (*R*)-amine product with an *ee* of 88% to 97%. The best performing variant for the reduction of **1**, W208A, retained both excellent activity (>99% conversion) and selectivity towards the (*S*)-enantiomer, although in reduced *ee* of 74%. M237A, Q238A, and M237G all showed a decrease in conversion compared to 2-phenylpyrroline however they all showed the same stereoselectivity with improved *ee* values of 90%, 95%, and 99% respectively. At this point, variants W208A and M237G are both acting as enantiocomplementary pairs producing the (*S*)- and (*R*)-enantiomers with excellent *ee* values respectively.

2-(4-Methoxyphenyl)pyrroline, **5**, (Figure 54) was the next substrate tested, changing the para-phenyl substituent from an electron withdrawing group to an electron donating group. This should, in theory, be a better substrate for imine reduction due to the increased electron density in the imine bond, making it more prone to reduction. This was not the case when biotransformations were ran with all the variants. All but W208A showed negligible reduction with the best performing of the rest of the variants being M237G at 5% conversion. W208A showed to be a much more active enzyme with >99% conversion being achieved after three hours. The (*S*)-selectivity was also retained producing (*S*)-**6** in an *ee* >99% but due to negligible conversion achieved for all other variants and the wild type, no *ee* data was obtained for these.

When expanding the ring size from a 5-membered cyclic imine to a 6-membered cyclic imines, the (*S*)-selectivity of half the variants (when **1** was the substrate) was lost with all variants producing the (*R*)-enantiomer and half of them reaching full conversion to **8**. One of these variants was W208A that had lost the (*S*)-selectivity observed with the pyrroline compounds. Although (*R*)-selectivity is maintained for M237A, Q238A, and M237G, it is hard to say whether this is due to the residue change or the substrate since all enzymes tested produce the (*R*)-enantiomer of **8**.

5.5 Investigation into Stereoselectivity

Crystallography was carried out in order to understand the inversion of stereoselectivity observed between *Ad*RedAm wild type and M237G with **1** as well as the improvement on the wild type stereoselectivity and activity seen with W208A. Each protein was purified as described in section 5.8.3.2 to a concentration of 10 mg/mL and sent for crystallisation to be carried out by Colin Levy from the Manchester Institute of Biotechnology. The protein crystals produced of *Ad*RedAm, W208A, and M237G were of insufficient quality to generate crystal structures so in-silico modelling of the structure of *Asp*RedAm was carried out instead. Using this crystal structure, the mutations of W210A and M239G (numbering based on *Asp*RedAm sequence) were introduced and generated using Yasara®. Once generated, compound **1** was docked into the active site of *Asp*RedAm, W210A and M239G and each variant docking structure overlaid that of the wild type.

It can be seen in both the variant models (cyan and fuchsia structures), Figure 55, that compound **1** appears to dock closer to the NADPH cofactor than it does in the wild type enzyme (green) (5.9 Å compared to 12.5 Å). This could explain the improved activity of each variant giving higher conversions than the wild type in three hours (19% for the wild type compared to 100% and 54% for W208A and M237G respectively). The orientation of 2-phenylpyrroline also differs between the two variant structures. In both cases, the phenyl group is oriented in the same direction (to the left). The side of the imine ring that faces the cofactor is opposite though, which explains why we see the inversion in stereoselectivity between W208A and M237G.

This change in stereoselectivity may not only just be down to the type of amino acid residue in the relative positions within the active site and their interactions with substrates. In both modelled variants, the same conformational change of the active site can be seen in the part of the enzyme containing residues 239 and 240. The shift of these two residues appears to create a smaller active site in the models and by doing so pushes the substrate closer to the cofactor for proton transfer.
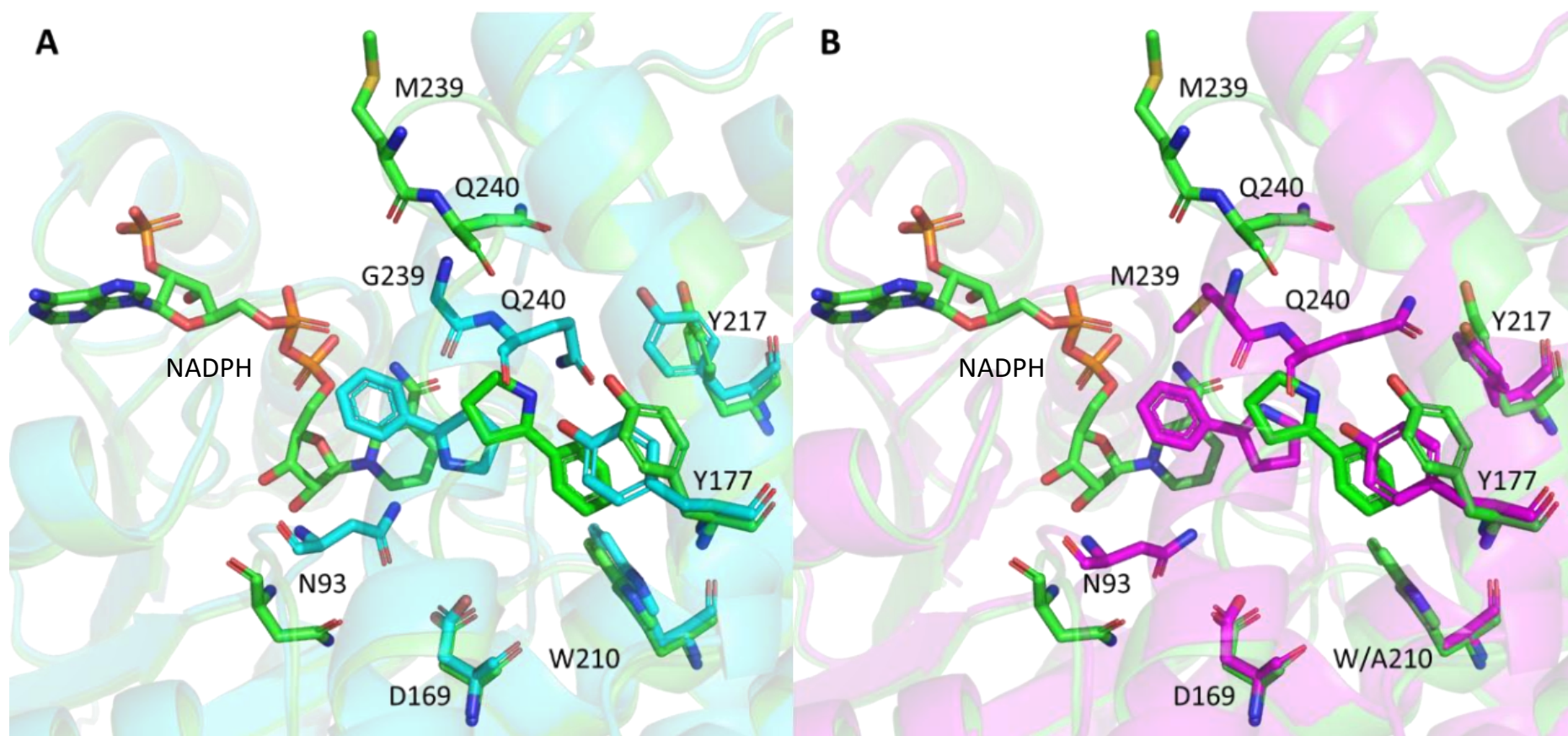
Figure 55: Active site of AspRedAm variant in-silico models superimposed on the crystal structure of AspRedAm wild type (green). (A) Superimposition with AspRedAmM239G (cyan). (B) Superimposition with AspRedAmW210A (fuchsia). Structures shown in complex with NADPH

5.6 Kinetic studies

Kinetic studies were carried out to further understand the effect of the role of the active site residues on substrate scope and activity. Work was carried out using compound **1**, 2-phenylpyrroline, for depletion assays in order to calculate catalytic rate and Michaelis-Menten concentrations of each variants and the *Ad*RedAm wild type. The K_M value was determined for *Ad*RedAm was determined to be 25.35 mM, Table 7. All variants except W208A and M237G showed an increase in K_M compared to the wild type with values ranging from 32 mM for M237A to 64 mM for Y177F. Interestingly, changing the alanine to glycine at position 237 resulted in a decrease in K_M to 23 mM and remarkably, W208A showed a drop in K_M to 3 mM (around 8-fold lower than for the wild type). The catalytic rate of the variants (k_{cat}) all increase compared to the wild type with Y177F having the fastest rate at 0.28 s^{-1} however the high K_M of this variants results in it being a less active variant. This can be seen by looking at the ratio between k_{cat} and K_M which when compared with respect to the wild type can be seen to be 0.64 for Y177F. The two variants that show an improvement in k_{cat}/K_M are W209A and M237G which were the two best performing variants from the biotransformations studies with a 12.1 and 1.5 fold improvement on *Ad*RedAm wild type respectively, Table 7.

To further explore the improvement observed with W208A variant, a ToF (turnover frequency) study was carried out and compared to *Ad*RedAm wild type for the reduction of **1** (Figure 56). Due to the increase in activity observed with W208A compared to *Ad*RedAm wild type, a fifth of the enzyme concentration was used. It can be seen at the reduced enzyme concentration that the W208A variant is still much more active than the wild type producing **2** in almost 90% conversion after just one hour compared to 5%. ToF values were calculated for the 60 min time point of *Ad*RedAm wild type and 20 min time point for W208A. The values were calculated to be 0.28 min^{-1} and 23.1 min^{-1} respectively, with the W208A variant having a ToF 82.5 fold higher than the wild type enzyme

Table 6: Michaelis-Menten kinetics for AdRedAm and its variants showing K_M concentrations and k_{cat} values

Enzyme	K_M / mM	V_{max} / μmol min^{-1}	k_{cat} / s^{-1}	k_{cat}/K_M / s^{-1} mM^{-1}	k_{cat}/K_M wrt WT
WT	25.4 ± 6.8	0.32 ± 0.04	0.17	0.0067	1.00
N94A	42.3 ± 8.8	0.43 ± 0.05	0.23	0.0055	0.81
Y177F	64.4 ± 21.7	0.53 ± 0.11	0.28	0.0044	0.64
W208A	3.1 ± 1.2	0.48 ± 0.05	0.26	0.0817	12.10
H215A	46.7 ± 9.3	0.52 ± 0.06	0.28	0.0059	0.87
M237A	31.9 ± 4.0	0.38 ± 0.02	0.20	0.0059	0.87
Q238A	41.2 ± 8.5	0.50 ± 0.06	0.27	0.0065	0.96
M237G	23.4 ± 3.7	0.46 ± 0.03	0.25	0.0105	1.55
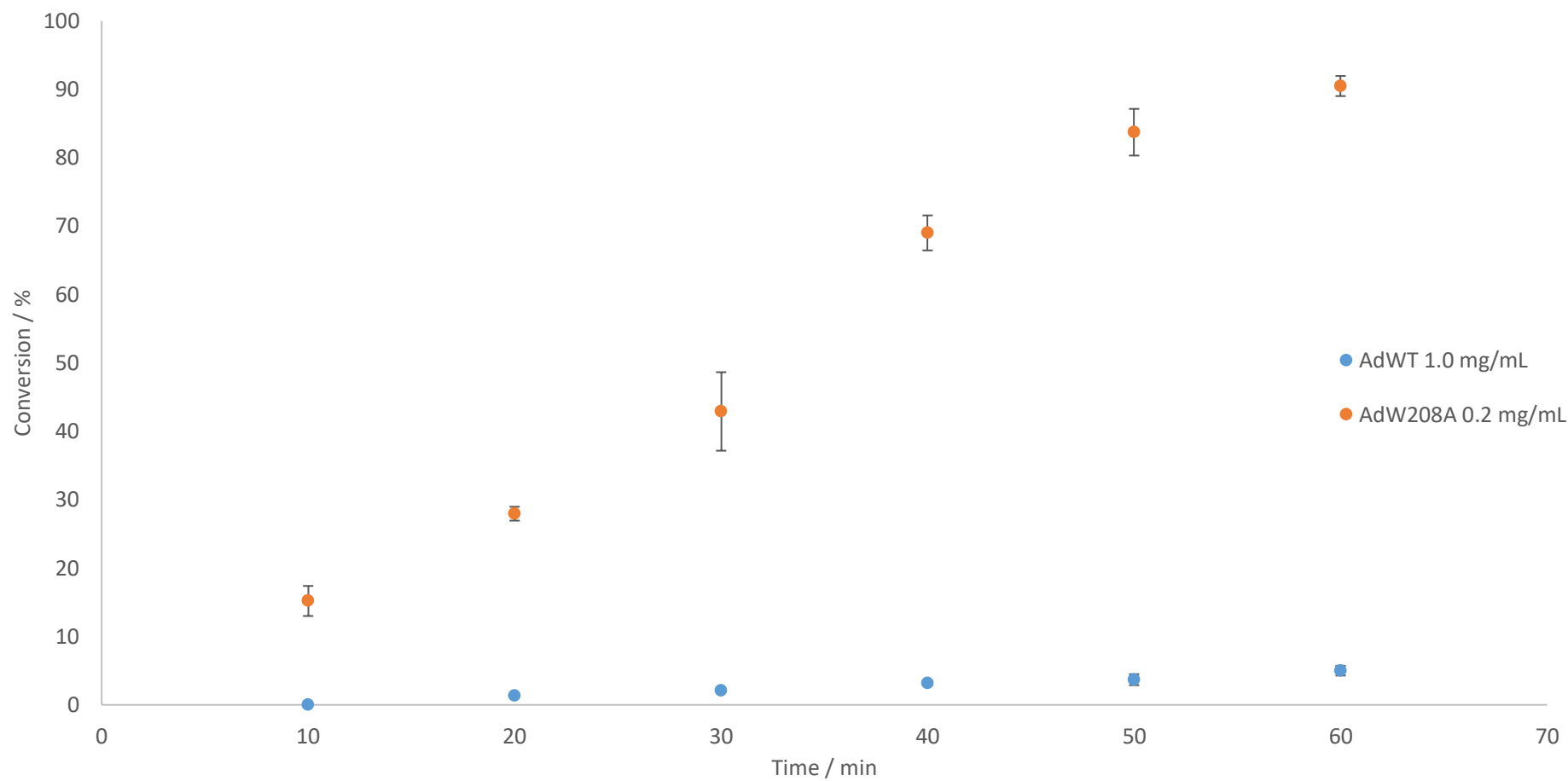
Figure 56: Time course reaction to calculate ToF values for AdRedAm wild type and W208A variant

5.7 Conclusions and Outlooks

It can be seen through mutagenesis of active site residues that the substrate scope, activity, and selectivity of the reductive aminase from *Ajellomyces dermatitidis* is very substrate dependent. This is shown through the reduction of different cyclic imines. The reduction of the bicyclic imines 3,4-dihydroisoquinoline and 1-methyl-5,6-dimethoxy-3,4-dihydroisoquinoline both show drastically reduced activity for variants W208A, M237A, and Q238A. However, for the reduction of 2-phenyl substituted 5- and 6-membered cyclic imines these variants prove to be more active than the *Ad*RedAm WT.

The stereoselectivity of these enzymes can be controlled to a certain degree. W208A has been shown to be an (*S*)-selective enzyme for the reduction of 5-membered cyclic imines **1**, **3**, and **5**, whereas the wild type enzyme showed opposite stereoselectivity (for **1** and **3**). The (*R*)-selectivity observed with M237G was also observed across the cyclic imines, although the reduction of **5** to **6** did not proceed with sufficient yield to determine stereoselectivity. This tuneable stereoselectivity is also substrate dependence as by expanding the cyclic imine size by just one carbon atom negated the observed (*S*)-selective of W208A.

As mentioned in section 5.5, this stereoselectivity change may not only be down to the actual residues and their interactions with the substrates. By changing the residue, the folding and conformational change upon binding of the substrates may occur differently. This can result in a different shape of the active site compared to the wild type enzyme inferring different stereoselectivity. Work previously carried out by Aleku *et al*. also looked at the mutations of W210A and Q240A in *Asp*RedAm (corresponds to W208A and Q238A in *Ad*RedAm) and tested for kinetic resolution of racemic amines. It was observed that these two variants were shown to be (*S*)- and (*R*)-selective respectively, corresponding the same as observed with the work presented here.

Kinetic studies were also carried out with the variants and it was shown that variants W208A and M237G were 12.1 and 1.5 fold more active than *Ad*RedAm wild type, with W208A have an 82.5 fold improvement in ToF.

The possibility to control the activity and stereoselectivity of reductive aminases has only just started to be explored in this work. The remarkable improvement on activity towards the reduction of cyclic imines observed through a single point mutation for the W208A variant shows the effect that engineering can have. However, this variant was not as successful as others when looking at bicyclic imines such as 3,4-dihydroisoquinoline. This substrate dependence makes it difficult to predict the best positions for mutations and the best residues to mutate to. Additionally, the change in stereoselectivity observed for variants such as N94A and Y177F between different substrates show that residue choices for mutation, although good for some substrates, may not be ideal for others.

5.8 Experimental and Methods

5.8.1 General

Solvents used were of HPLC grade and when necessary solvents were further dried over molecular sieves. Spectra from ^{1}H and ^{13}C NMR runs were recorded on a Bruker Avance 400 instrument (400 MHz for ^{1}H and 100 MHz for ^{13}C) in CDCl$_3$, (CD$_3$)$_2$SO, or CD$_3$OD using residual protic solvent as an internal standard. Reported chemical shifts (δ) (in parts per million (ppm)) are relative to the residual protic solvent signal (CHCl$_3$ in CDCl$_3$, ^{1}H = 7.26; ^{13}C = 77.0; (CHD$_2$)(CD$_3$)SO in (CD$_3$)$_2$SO, ^{1}H = 2.50; ^{13}C = 39.52; CHD$_2$OD in CD$_3$OD, ^{1}H = 3.31; ^{13}C = 49.0).

Chiral normal phase HPLC was performed on an Agilent system (Santa Clara, CA, USA) equipped with a G1379A degasser, G1312A binary pump, a G1367A well plate autosampler unit, a G1316A temperature controlled column compartment and a G1315C diode array detector.CHIRALPAK®IC Analytical (all Daicel (Osaka, Japan), 250 mm length, 4.6 mm diameter, 5 µm particle size) as well as CHIRALCEL®OD-H Analytical (Daicel (Osaka, Japan), 250 mm length, 4.6 mm diameter, 5 µm particle size) columns were used. The typical injection volume was 10 µl and chromatograms were monitored at 265 nm. All solvent mixtures are given in (v/v) ratios.

GC analysis was performed on an Agilent 6850 GC (Agilent, Santa Clara, CA, USA) with a flame ionization detector (FID) and autosampler using an HP-1 column with 0.32 mm inner diameter and 0.25 µm film thickness (Agilent, 6 Santa Clara, CA, USA).

5.8.2 Chemical Standards

5.8.2.1 Chemicals

All commercially available reagents were used without further purification and purchased from Fluorochem Ltd. (Hadfield, Derbyshire, UK). HPLC solvents were obtained from Sigma-Aldrich (Poole, Dorset, UK) or Honeywell (Seelze, Lower Saxony, Germany) and solvent additive diethylamine was obtained from Sigma-Aldrich (Poole, Dorset, UK). GC gases were obtained from BOC gases (Guildford, Surrey, UK). 2-phenylpyrroldine (2), (S)-2-phenylpyrroldine ((S)-2), 5-(4-chlorophenyl)-3,4-dihydro-2H-pyrrole (3), (S)-2-(4-chlorophenylpyrrolidine) hydrochloride ((S)-4), 5-(4-methoxyphenyl)-3,4-dihydro-2H-pyrrole (5), 1-((2R)pyrrolidin-2-yl)-4-methoxybenzene ((R)-5), 2-phenylpiperidine (8), and (R)-2-phenylpiperidine ((R)-8) were all purchased from Fluorochem Ltd. (Hadfield, Derbyshire, UK).

5.8.2.2 Synthetic Procedure for the Preparation of Imine 1
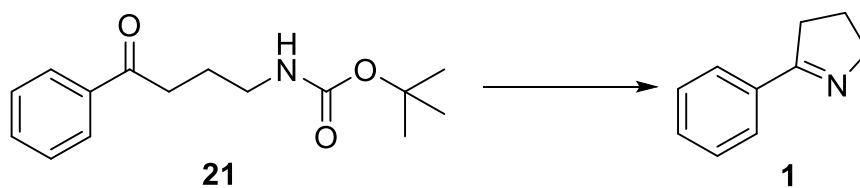
N-Boc-protected aminoketone **21** (790 mg, 3 mmol) was dissolved in TFA (2 mL) and stirred at room temperature for 4 h. The reaction mixture was then cooled to 0°C before addition of 10 M NaOH until pH 14. The aqueous phase was then extracted with CH_2Cl_2 (3 x 25 mL). The combined organic phases were dried over $MgSO_4$, filtered and concentrated under vacuum to yield the cyclic imine **1** (327.1 mg, 75% yield) as a yellow oil without need for further purification.

1
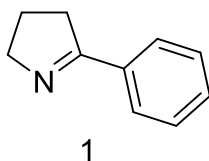
2-phenylpyrroline: ^{1}H NMR (400 MHz, DMSO) δ: 7.83 (dd, J = 6.8, 2.2 Hz, 2H), 7.48 – 7.39 (m, 3H), 3.94 (t, J = 7.2 Hz, 2H), 2.90 (tt, J = 8.7, 1.8 Hz, 2H), 1.93 (p, J = 7.8 Hz,

2H). ^{13}C NMR (101 MHz, DMSO) δ 172.19, 134.40, 130.19, 128.40, 127.43, 60.89, 34.47, 22.27.
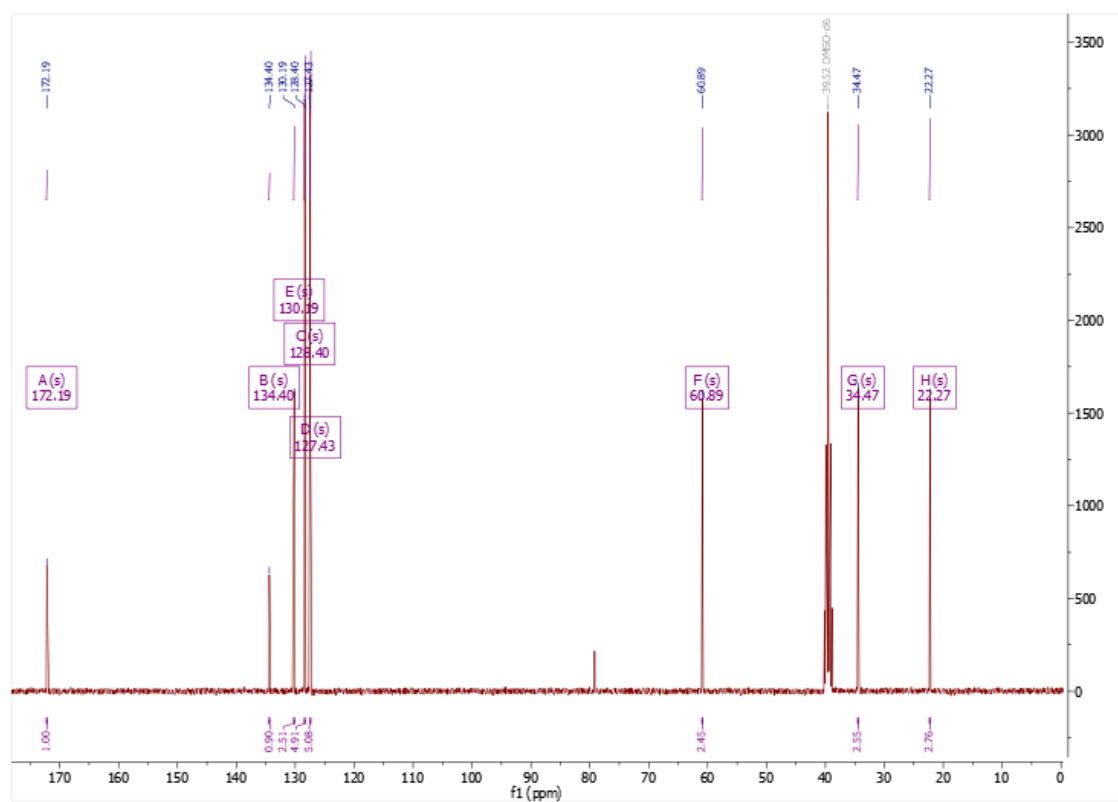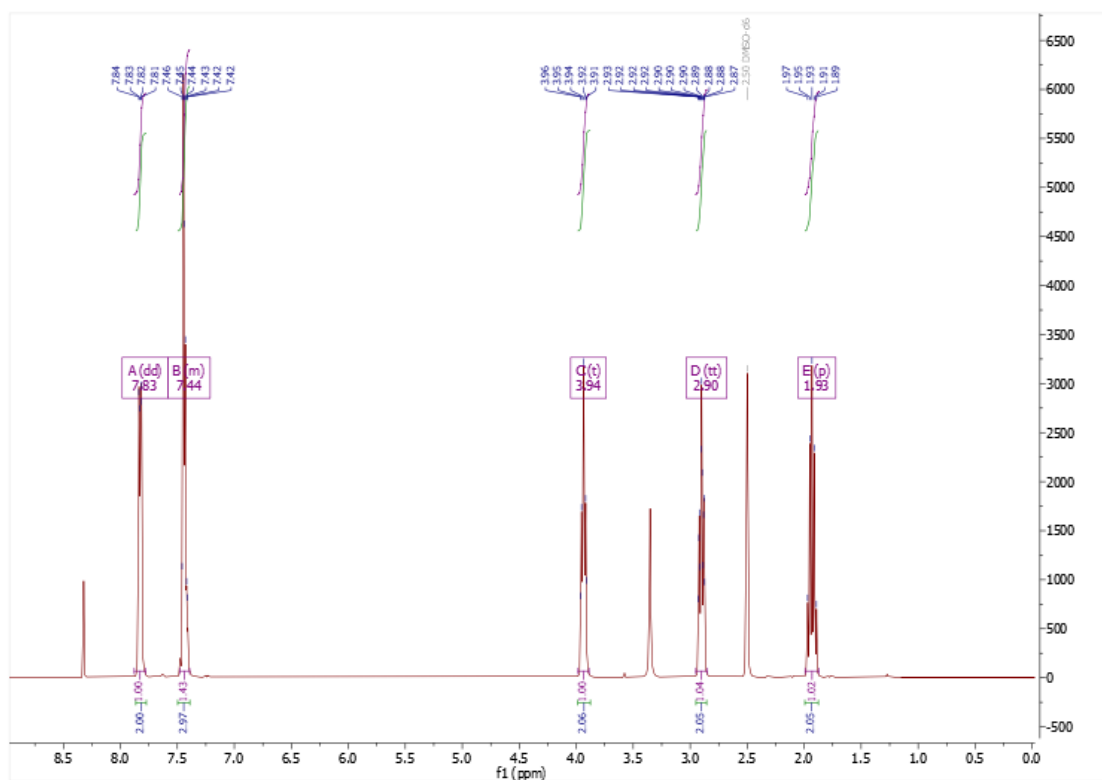
5.8.2.3   Synthetic Procedure for the Preparation of Imine 7

22
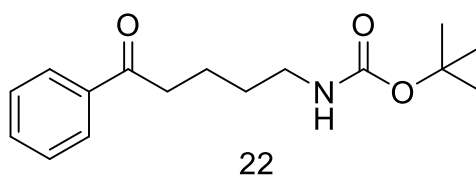
The cyclic imine was prepared in the same manner as reported in section 2.1 using N-Boc-protected aminoketone **22** (277.36 mg, 1 mmol).

After concentrating under vacuum, and without further purification, the imine free base was dissolved in dioxane and HCl (2 M in dioxane) was added. The resulting hydrochloride salt was washed with ethyl acetate and dried under vacuum to give the final product **7-HCl** (126.7 mg, 64% yield) as a white solid

7-HCl
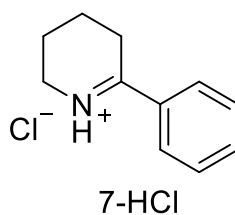
2-phenyl-1-piperideinium chloride: ^{1}H NMR (400 MHz, MeOD) δ 8.02 – 7.94 (m, 2H), 7.85 – 7.76 (m, 1H), 7.72 – 7.62 (m, 2H), 3.90 (tp, J = 4.3, 1.9 Hz, 2H), 3.41 – 3.32 (m, 2H), 2.13 – 2.00 (m, 4H). ^{13}C NMR (101 MHz, MeOD) δ 184.87, 136.06, 133.07, 130.64, 129.13, 46.45, 29.82, 20.31, 18.26, 18.21.

5.8.2.4   Synthetic Procedure for the Preparation of Amines 4 and 6

Sodium borohydride (1.5 eq) was added to a solution of cylic imine (**3** or **5**) and methanol (15 mL) and left to stir overnight at room temperature. The reaction was

quenched by addition of 3 M HCl until pH 1 and left to stir for 30 minutes, before adding 10 M NaOH until pH 14. The aqueous phase was extracted with CH$_2$Cl$_2$ (3 x 25 mL). The combined organic layers were then dried over MgSO$_4$, filtered and concentrated under vacuum to afford the freebase racemic cyclic amines.

4
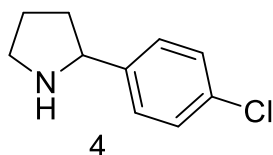
2-(4-chlorophenyl)pyrrolidine: **3** (179.65 mg, 1 mmol) was dissolved in methanol (15 mL) and was reduced by the addition of NaBH$_4$ (75.66 mg, 2 mmol). Amine **4** (149.56, 82% yield) was isolated as a light brown oil.

^{1}H NMR (400 MHz, DMSO) δ 7.43 – 7.29 (m, 4H), 4.02 (t, J = 7.6 Hz, 1H), 2.99 (ddd, J = 9.8, 7.4, 5.5 Hz, 1H), 2.88 (ddd, J = 9.9, 8.1, 6.7 Hz, 1H), 2.16 – 2.04 (m, 1H), 1.83 – 1.63 (m, 2H), 1.42 (ddt, J = 12.1, 9.1, 7.7 Hz, 1H). ^{13}C NMR (101 MHz, DMSO) δ 144.93, 130.59, 128.27, 127.86, 60.80, 46.35, 34.72, 25.19.
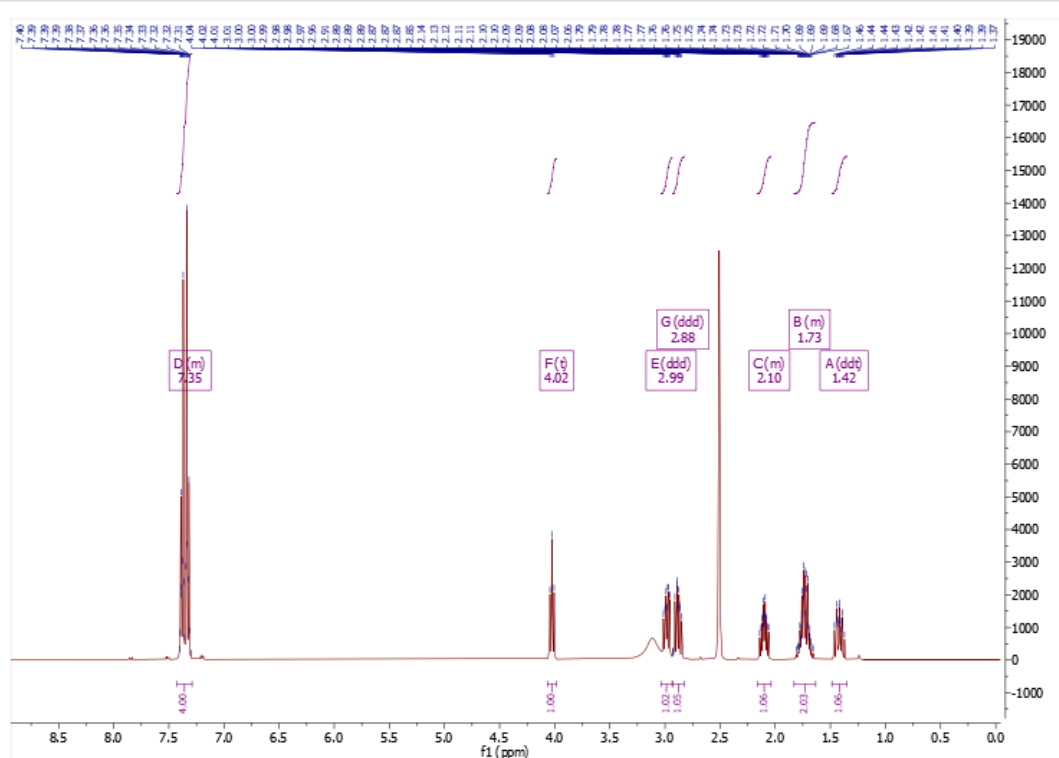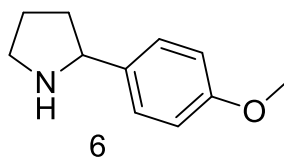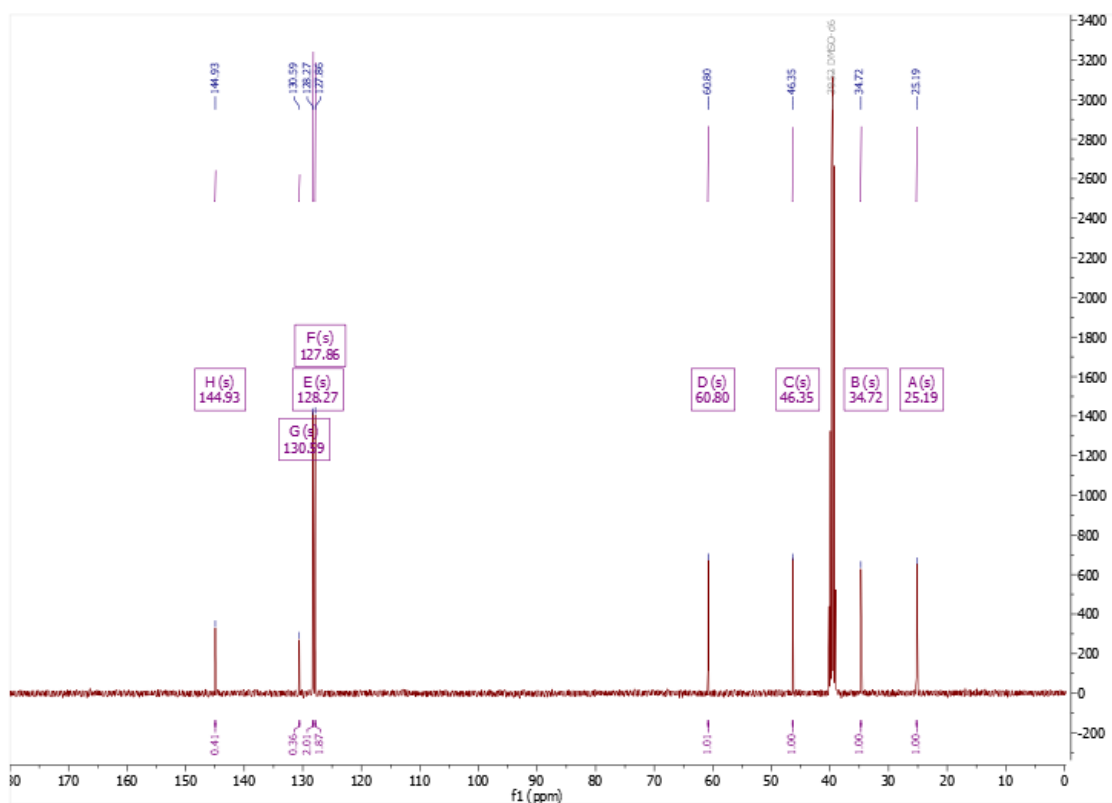
2-(4-methoxyphenyl)pyrrolidine: 5 (175.23 mg, 1 mmol) was dissolved in methanol (15 mL) and was reduced by the addition of NaBH$_4$ (75.66 mg, 2 mmol). Amine **6** (142.5 mg, 80% yield) was isolated as a light brown oil

^{1}H NMR (400 MHz, CDCl3) δ 7.33 – 7.24 (m, 2H), 6.95 – 6.81 (m, 2H), 4.05 (dd, J = 8.5, 7.0 Hz, 1H), 3.79 (s, 3H), 3.19 (ddd, J = 10.2, 7.8, 5.3 Hz, 1H), 2.98 (ddd, J = 10.2, 8.4, 6.7 Hz, 1H), 2.20 – 2.12 (m, 1H), 2.00 – 1.77 (m, 2H), 1.65 (dddd, J = 12.4, 9.4, 8.5, 7.5 Hz, 1H). ^{13}C NMR (101 MHz, CDCl3) δ 158.65, 136.68, 127.76, 113.87, 62.29, 55.41, 46.99, 34.34, 25.67.

5.8.3 Cloning, Expression, and Purification of AdRedAm

5.8.3.1 Cloning of AdRedAm

Cloning of *Ad*RedAm was carried out as previously reported by Sharma *et al.*[91]

5.8.3.2 Expression and Purification

The plasmids containing the genes for target enzymes were used to transform *E. coli* BL21(DE3) competent cells for gene expression. Pre-cultures were grown in TB-medium (15 mL) containing 10 μg mL^{-1} kanamycin for 18h at 37°C with shaking at 200 r.p.m. 400 mL volume cultures were inoculated with the pre-culture (15 mL) and incubated at 37°C, with shaking at 200 r.p.m. until an OD$_{600}$ of 0.6 – 0.8 was reached. Gene expression was induced by addition of IPTG 0.1 mM and shaking was continued overnight at 25°C with shaking at 200 r.p.m. The cells were then harvested by centrifugation at 4000 r.p.m. for 25 min and resuspended in 100 mM phosphate buffer pH 7. Cells were disrupted by ultrasonification for 15 min, 30 sec On, 30 sec Off cycles, and the suspension was centrifuged at 18,000 r.p.m. to yield a clear lysate. The N-Terminal His$_6$-tagged proteins were purified using immobilised-metal affinity chromatography (IMAC) using Ni_NTA column. In each case, the lysate was loaded onto a pre-equilibrated Ni_NTA columne, followed by washing with a load buffer (100 mM phosphate, 30 mM NaCl, 30 mM imidazole, pH 7). The bound protein was eluted using 100 mM phosphate buffer with 300 mM NaCl and 300 mM imidazole. The RedAm fractions were pooled, concentrated to 10 mg mL^{-1} and used for biotransformation reactions. Activity of enzymes were checked and validated with a reductive amination reaction between cyclohexanone and allylamine at 10 mM each at an enzyme loading of 1.0 mg/mL
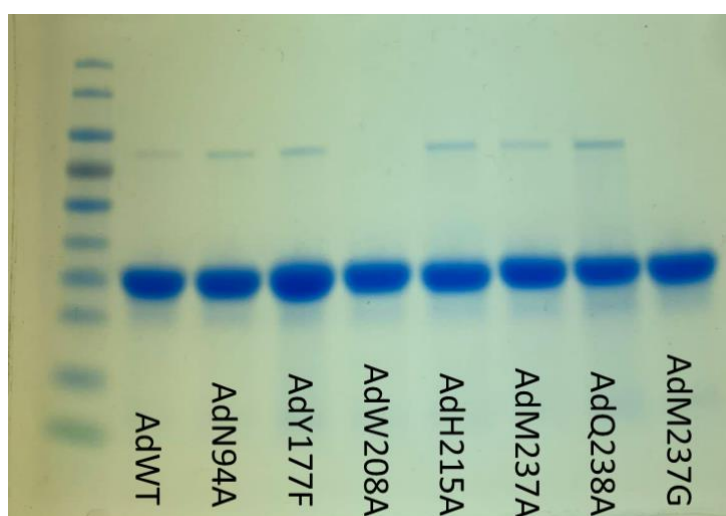
5.8.4 Site-Directed Mutagenesis of AdRedAm

All *Ad*RedAm active site mutants were generated using the procedure previously reported by Sharma *et al.*[91]

5.8.4.1   Primers used for the Construction of AdRedAm Variants

Variants N94A, Y177F, and H215A were constructed using the primers reported by Sharma *et al.*[91]

Table 7: Table of primers used for the mutagenesis of AdRedAm

Target Mutant	Mutagenesis Method	Primer ID	Base Sequence 5' to 3'
***Ad*RedAm W208A**	QuikChange	Fwd	CTGATTCCGGCGCTGACCGCAATGACC
		Rev	CTGGGTTGCAACAAAACCTGC
***Ad*RedAm M237A**	QuikChange	Fwd	GGTAGCAGCCTGGATGCGCAGGCAAAAGCC GCACC
		Rev	ACCATCACCATAATCTTTTTCATCAACCTGGG TGGC
***Ad*RedAm Q238A**	QuikChange	Fwd	AGCAGCCTGGATATGGCGGCAAAAGCCGCA CCG
		Rev	ACCACCATCACCATAATCTTTTTCATCAACCT G
***Ad*RedAm M237NNK**	QuikChange	Fwd	GGTAGCAGCCTGGATNNKCAGGCAAAAGCC GCACCGAATATTCTGG
		Rev	ACCATCACCATAATCTTTTTCATCAACCTGGG TGGC

5.8.5 Biotransformation Protocol

5.8.5.1   Typical Procedure for the RedAm-Catalyzed Imine Reduction

A 500 µL reaction contained 20 mM D-glucose, 0.1 mg mL-1 GDH (Codexis, CDX GDH-901), 0.5 mM NADP$^+$, 1 mg mL^{-1} purified RedAm, 10 mM imine, and 10% v/v DMSO in 100 mM phosphate buffer pH 7. Reactions were incubated at 30 °C with 250 r.p.m. shaking for 3 h (for GC analysis) or 18 h (for chiral-HPLC analysis), after which they

were quenched by the addition of 100 μL 5M NaOH and extracted twice with 500 μL diethyl ether. The organic fractions where combined, dried over MgSO$_4$ and analysed.

5.8.5.2 Typical Procedure for RedAm-Catalysed Reductive Amination

A 500 μL reaction contained 20 mM D-glucose, 0.1 mg mL-1 GDH (Codexis, CDX GDH-901), 0.5 mM NADP$^+$, 1 mg mL^{-1} purified RedAm, 10 mM ketone, 10 mM amine donor, and 10% v/v DMSO in 100 mM phosphate buffer pH 7. Reactions were incubated at 30 °C with 250 r.p.m. shaking for 18 h to 24 h, after which they were quenched by the addition of 100 μL 5M NaOH and extracted twice with 500 μL diethyl ether. The organic fractions where combined, dried over MgSO$_4$ and analysed by GC-FID.

5.8.6 Conditions used for GC-FID and Chiral HPLC Analysis of Reactions

5.8.6.1 GC-FID Analysis Conditions

Samples were analysed using a HP-1 column, injector temperature of 200°C, a helium flow rate of 1.3 mL min^{-1}, oven temperature 50 °C – 300 °C with a ramp of 25 °C min^{-1}, and a detector temperature of 250 °C.

5.8.6.2 GC-FID Chromatograms of Biotransformations and Chemical Standards for the Reduction of 1 to 2
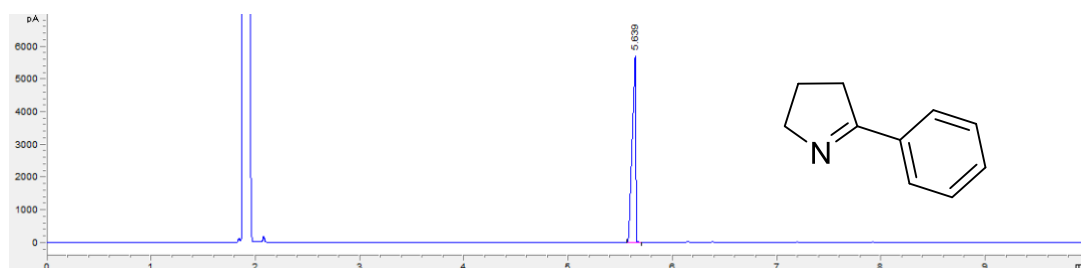
Figure 57: GC-FID chromatogram of chemical standard **1**
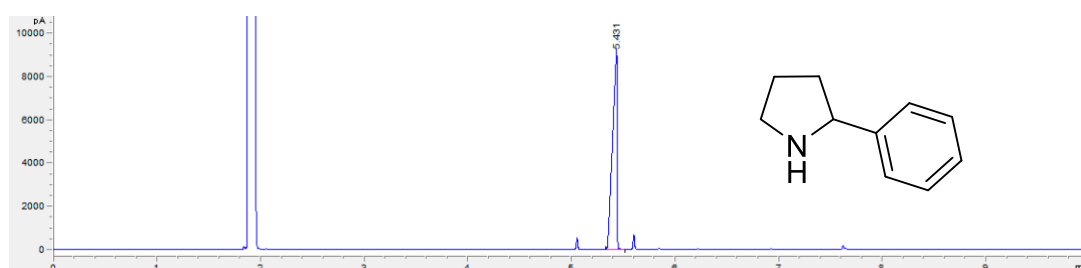
Figure 58: GC-FID chromatogram of chemical standard **2**
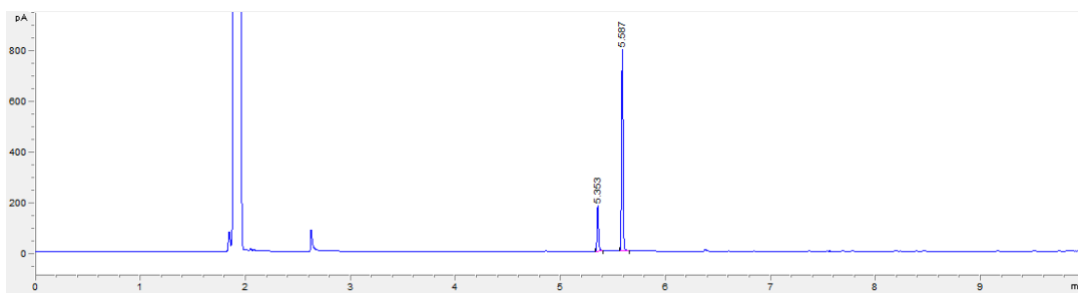
*Figure 59: GC-FID chromatogram of biotransformation of compound **1** with AdWT*
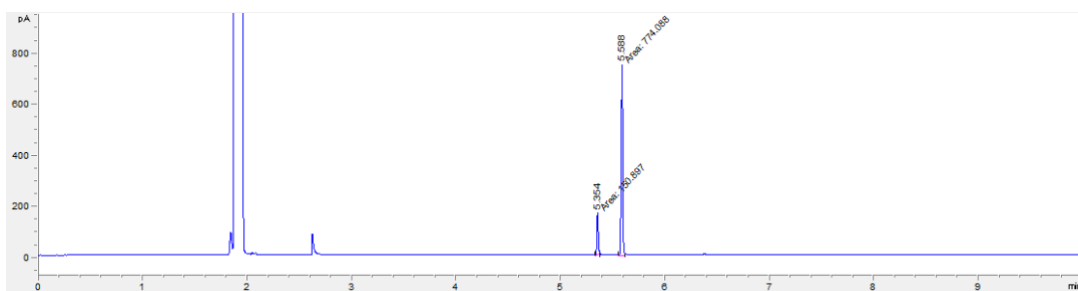
*Figure 60: GC-FID chromatogram of biotransformation of compound **1** with AdN94A*
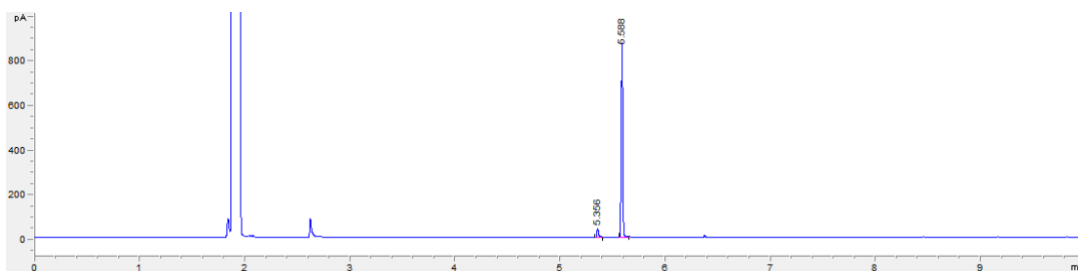
*Figure 61: GC-FID chromatogram of biotransformation of compound **1** with AdY177F*
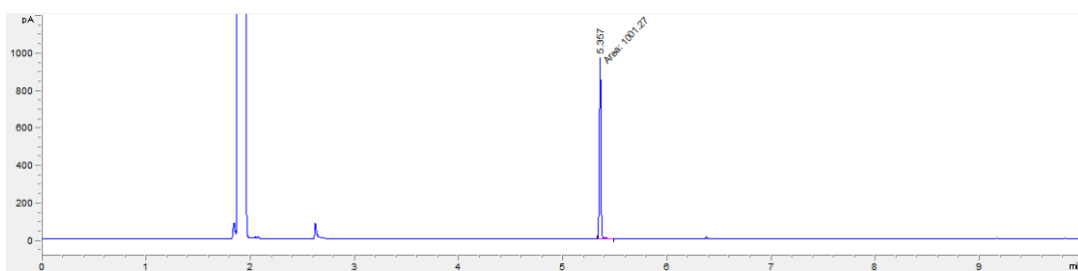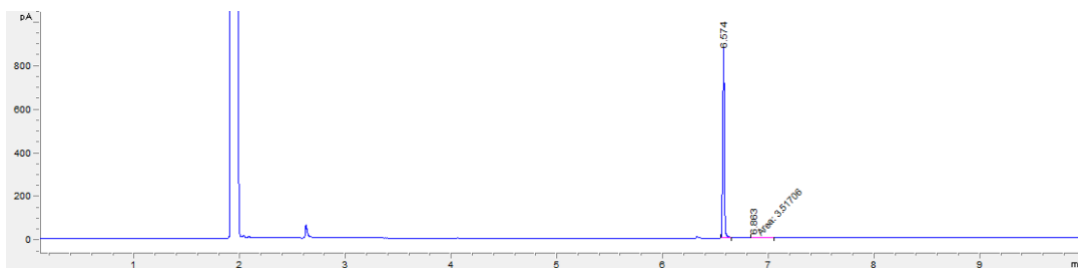

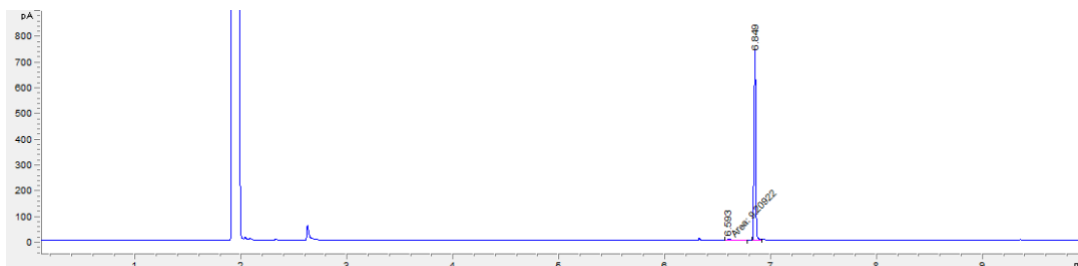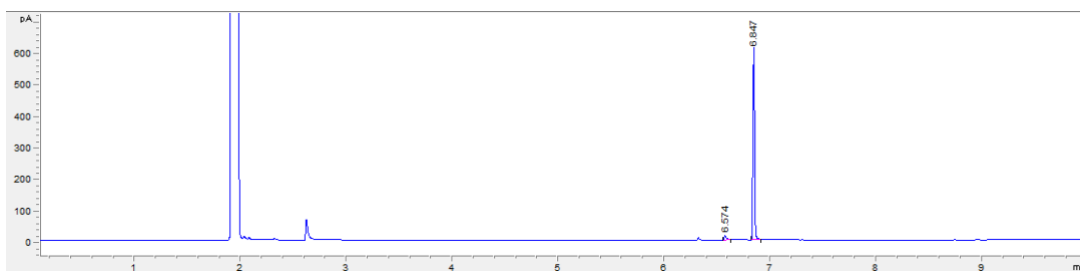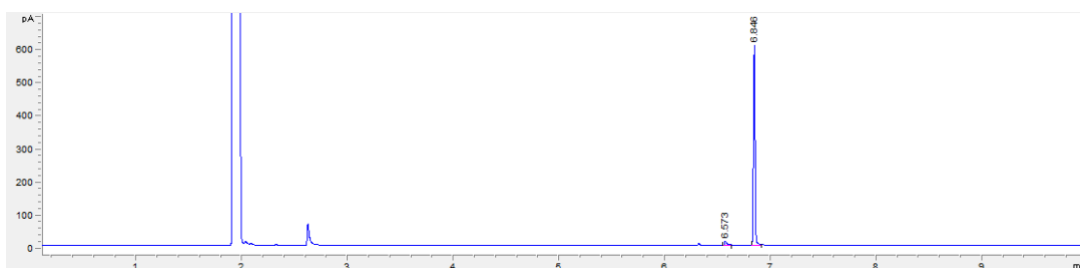*Figure 62: GC-FID chromatogram of biotransformation of compound **1** with AdW208A*
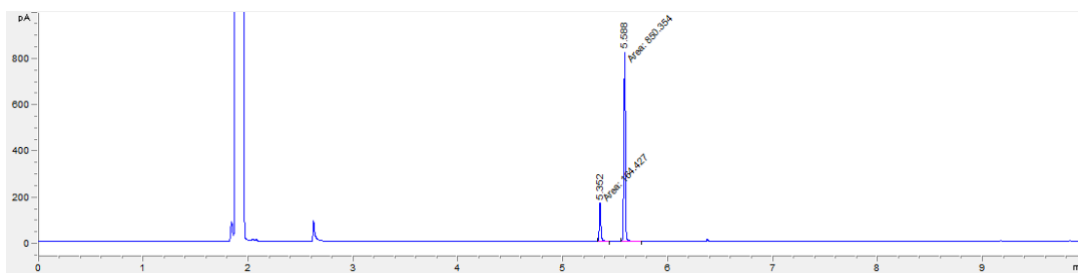
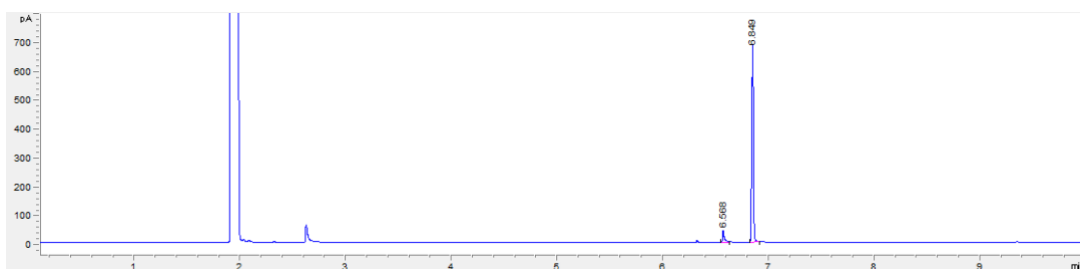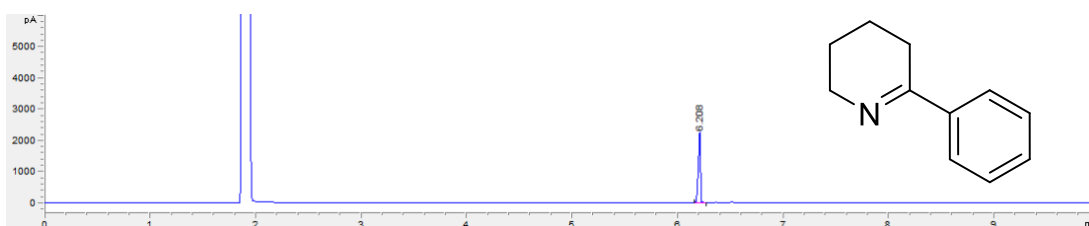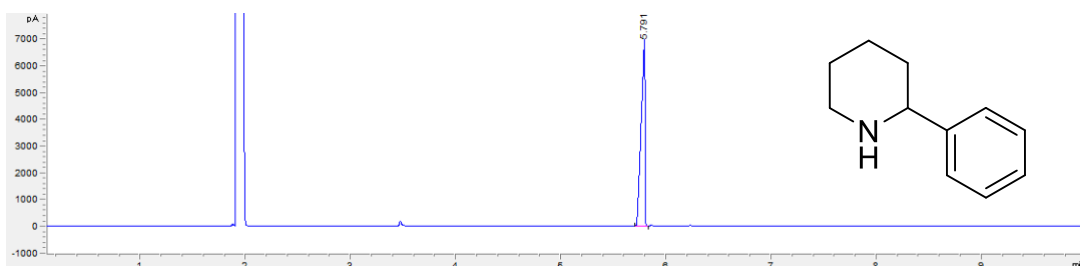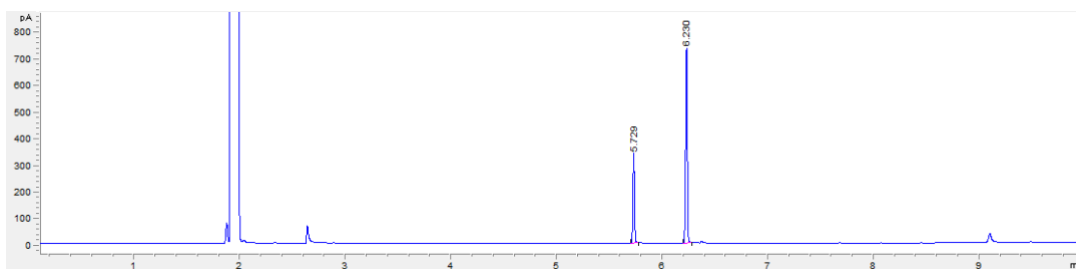*Figure 63: GC-FID chromatogram of biotransformation of compound **1** with AdH215A*
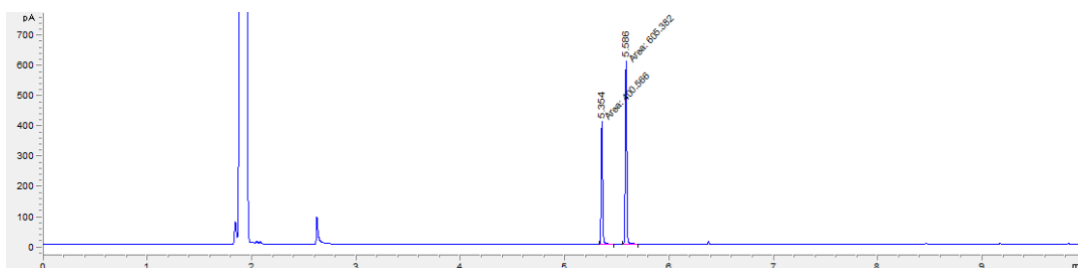
*Figure 64: GC-FID chromatogram of biotransformation of compound **1** with AdM237A*
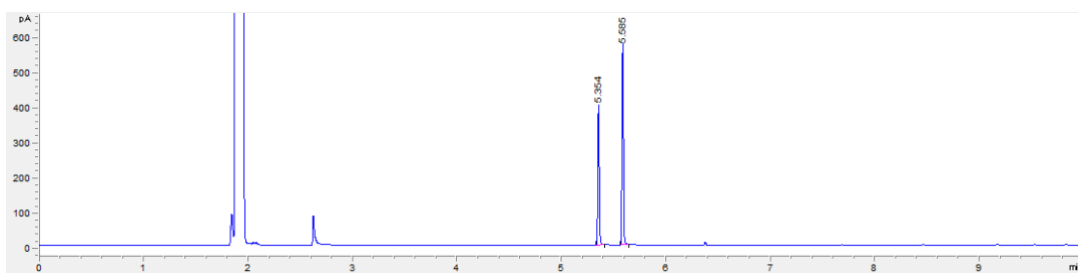
*Figure 65: GC-FID chromatogram of biotransformation of compound **1** with AdQ238A*
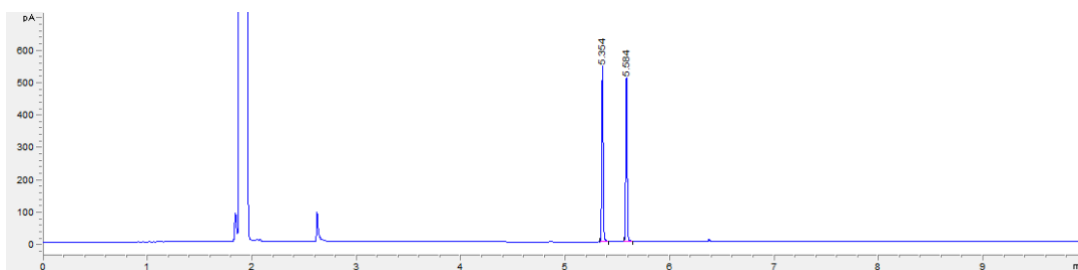
*Figure 66: GC-FID chromatogram of biotransformation of compound **1** with AdM237G*

5.8.6.3 GC-FID Chromatogram of Biotransformations and Chemical Standards for the Reduction of 3 to 4
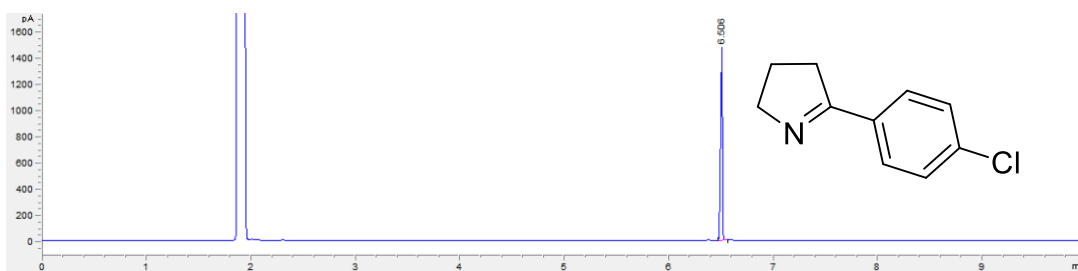
*Figure 67: GC-FID chromatogram of chemical standard **3***
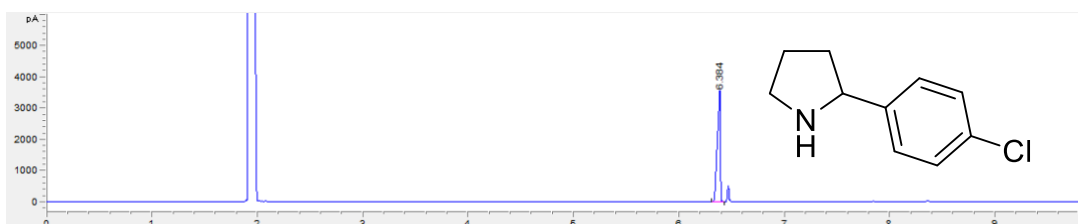
Figure 68: GC-FID chromatogram of chemical standard 4
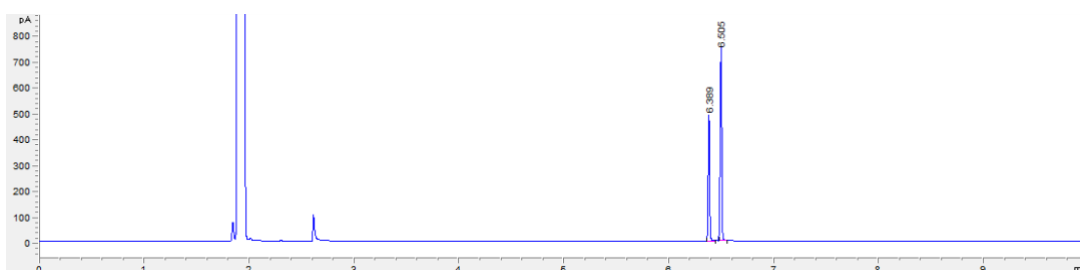
Figure 69: GC-FID chromatogram of biotransformation of compound 3 with AdWT
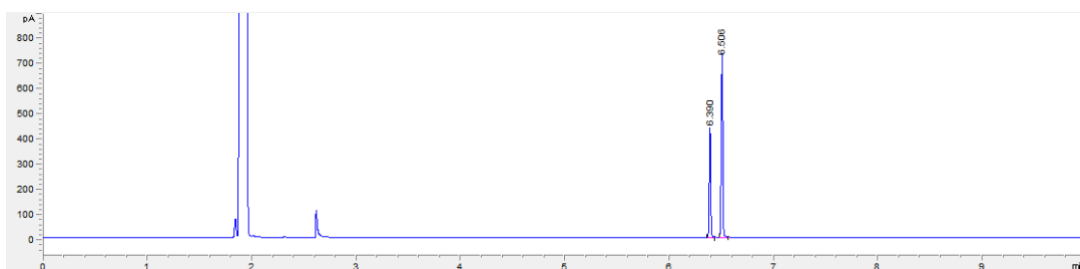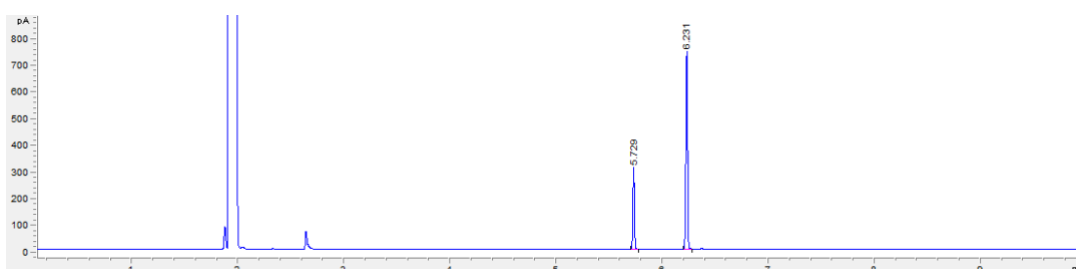

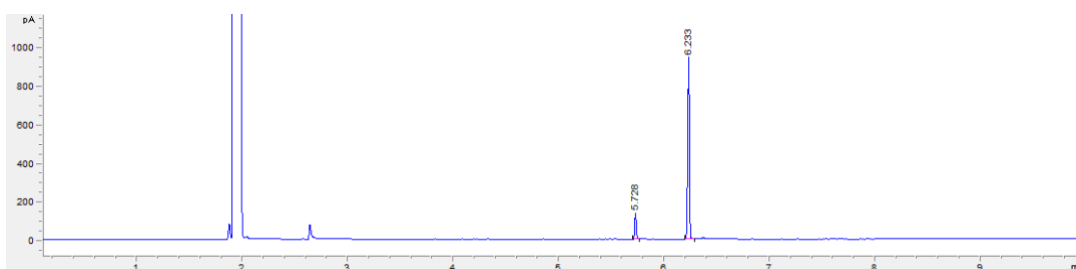*Figure 70: GC-FID chromatogram of biotransformation of compound 3 with AdN94A*
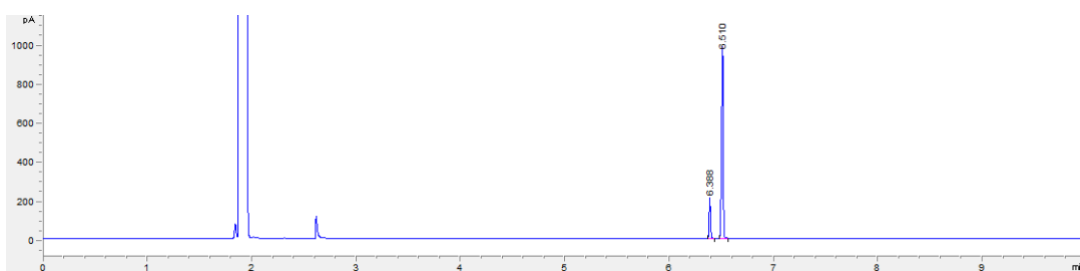
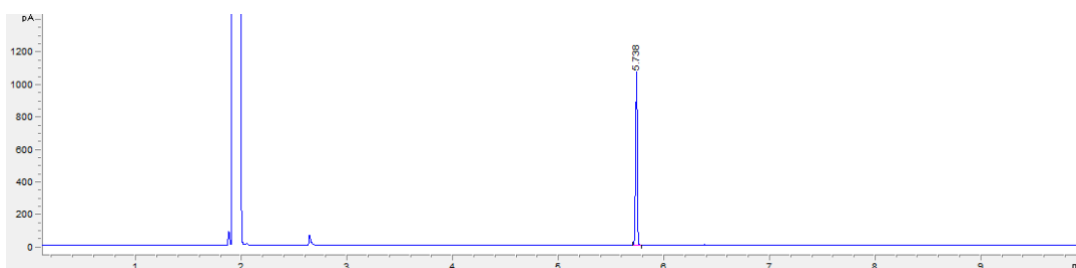*Figure 71: GC-FID chromatogram of biotransformation of compound 3 with AdY177F*
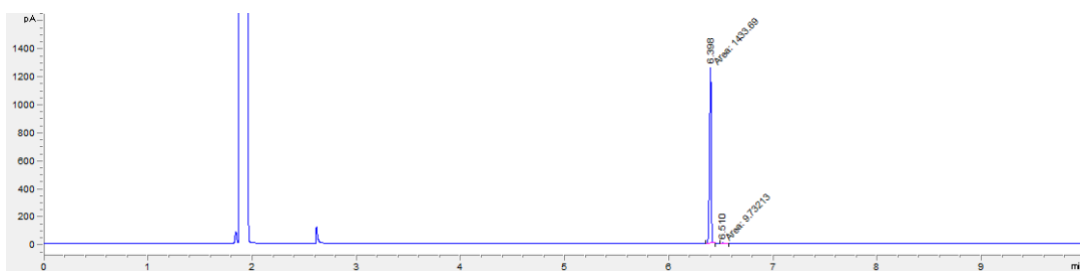
Figure 72: GC-FID chromatogram of biotransformation of compound 3 with AdW208A
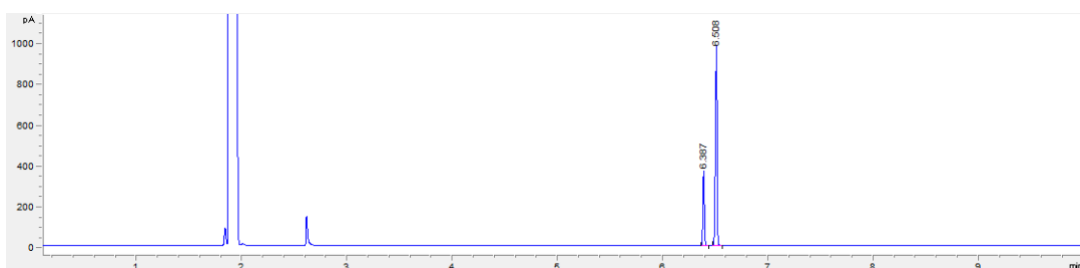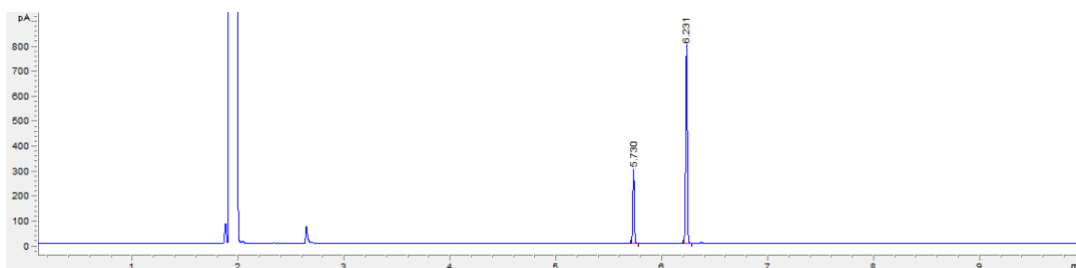

Figure 73: GC-FID chromatogram of biotransformation of compound 3 with AdH215A
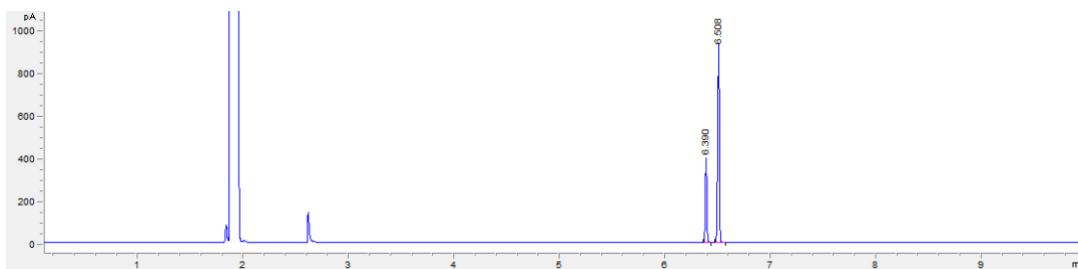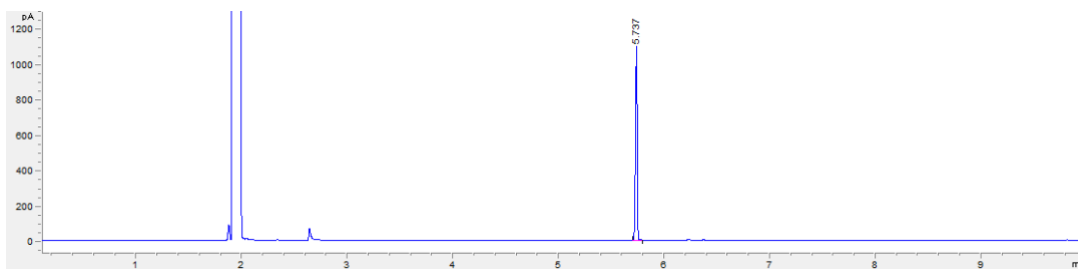
*Figure 74: GC-FID chromatogram of biotransformation of compound **3** with AdM237A*
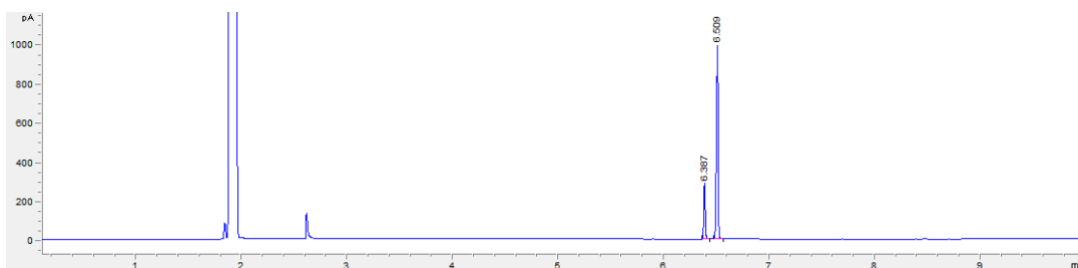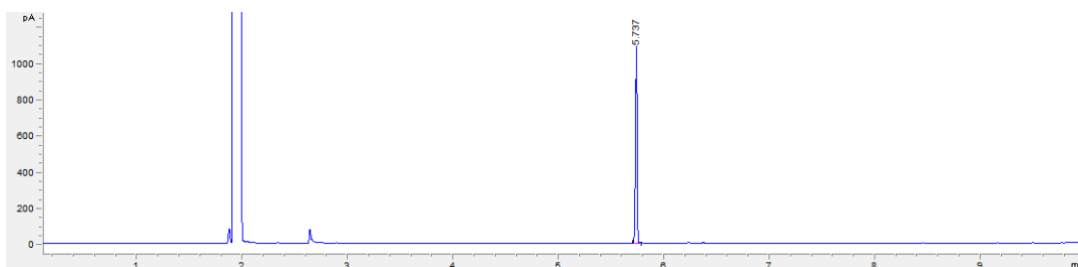

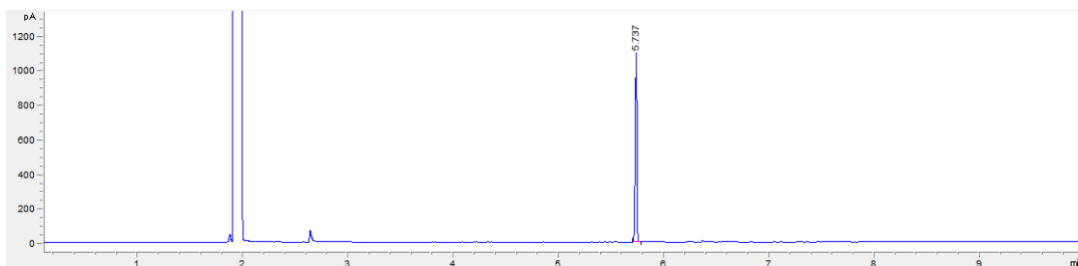*Figure 75: GC-FID chromatogram of biotransformation of compound **3** with AdQ238A*
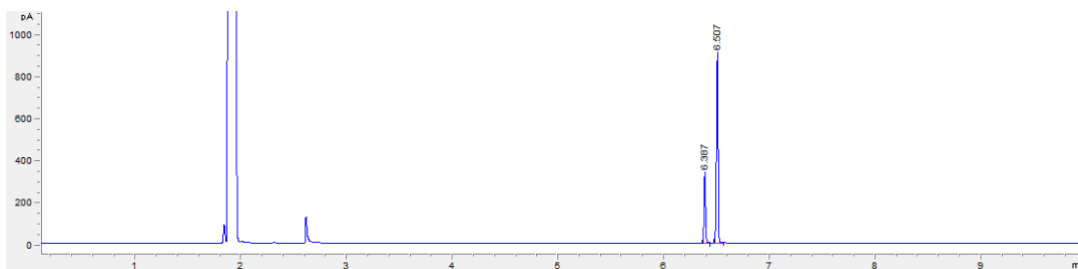
*Figure 76: GC-FID chromatogram of biotransformation of compound **3** with AdM237G*

5.8.6.4 GC-FID Chromatograms of Biotransformations and Chemical Standards for the Reduction of 5 to 6
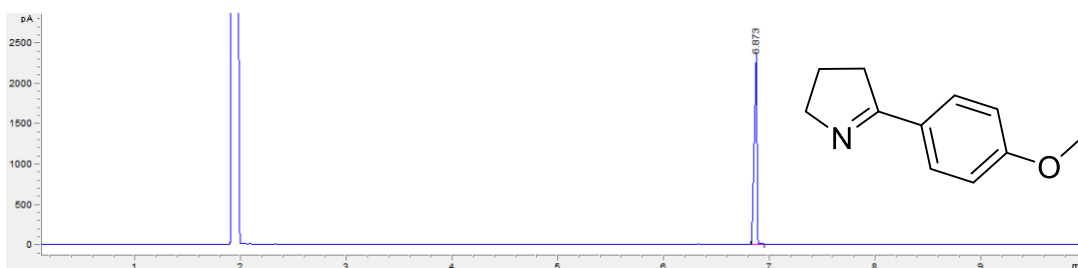
*Figure 77: GC-FID chromatogram of chemical standard **5***

*Figure 78: GC-FID chromatogram of chemical standard **6***
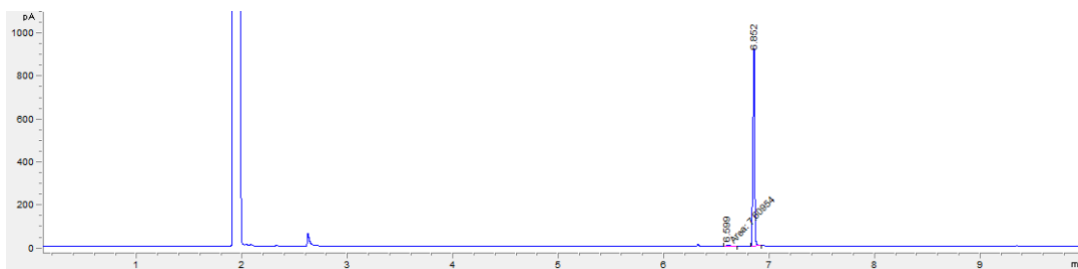
*Figure 79: GC-FID chromatogram of biotransformation of compound **5** with AdWT*
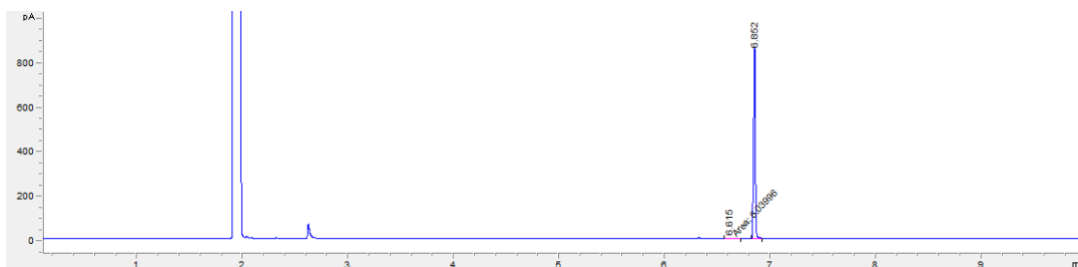
*Figure 80: GC-FID chromatogram of biotransformation of compound **5** with AdN94A*
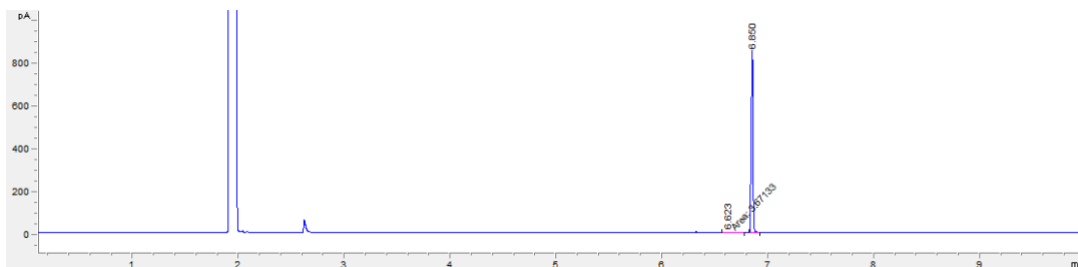
*Figure 81: GC-FID chromatogram of biotransformation of compound **5** with AdY177F*

*Figure 82: GC-FID chromatogram of biotransformation of compound **5** with AdW208A*

*Figure 83: GC-FID chromatogram of biotransformation of compound **5** with AdH215A*

*Figure 84: GC-FID chromatogram of biotransformation of compound **5** with AdM237A*

*Figure 85: GC-FID chromatogram of biotransformation of compound **5** with AdQ238A*

*Figure 86: GC-FID chromatogram of biotransformation of compound **5** with AdM237G*

5.8.6.5   GC-FID Chromatograms of Biotransformations and Chemical Standards for the Reduction of 7 to 8

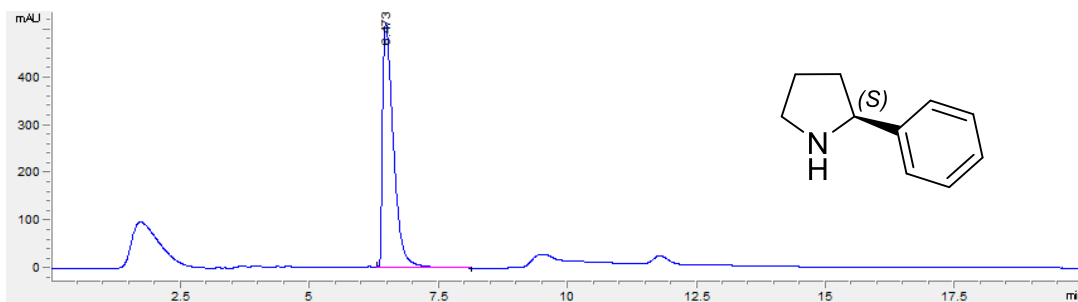
*Figure 87: GC-FID chromatogram of chemical standard **7***

*Figure 88: GC-FID chromatogram of chemical standard **8***

*Figure 89: GC-FID chromatogram of biotransformation of compound **7** with AdWT*

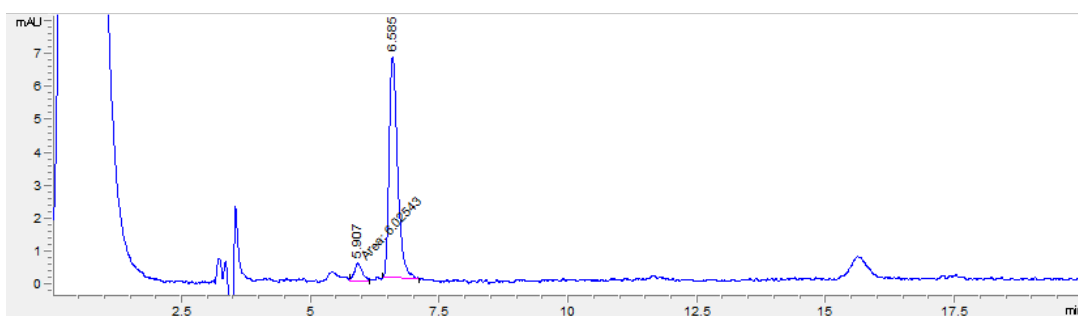*Figure 90: GC-FID chromatogram of biotransformation of compound **7** with AdN94A*

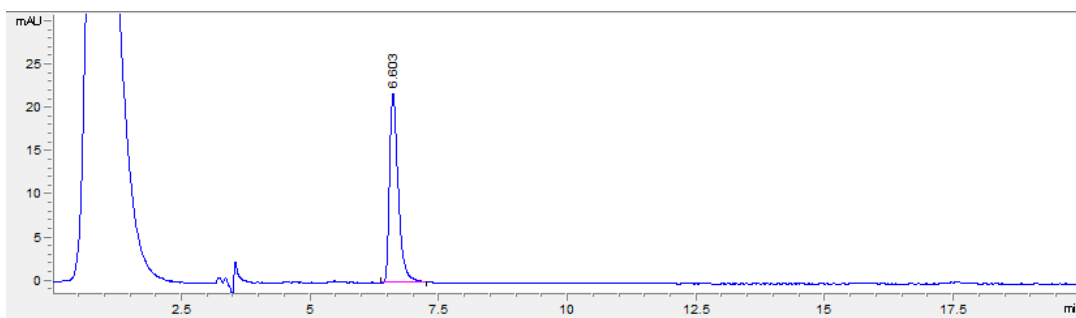*Figure 91: GC-FID chromatogram of biotransformation of compound **7** with AdY177F*

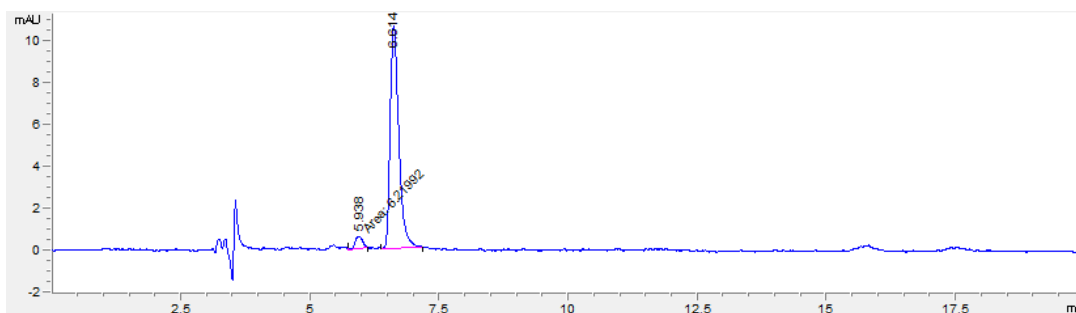*Figure 92: GC-FID chromatogram of biotransformation of compound **7** with AdW208A*

*Figure 93: GC-FID chromatogram of biotransformation of compound **7** with AdH215A*

*Figure 94: GC-FID chromatogram of biotransformation of compound **7** with AdM237A*

*Figure 95: GC-FID chromatogram of biotransformation of compound **7** with AdQ238A*

*Figure 96: GC-FID chromatogram of biotransformation of compound **7** with AdM237G*

5.8.6.6 HPLC Analysis Conditions

Samples were analysed using a normal phase CHIRALCEL®OD-H column

5.8.6.7 HPLC Chromatograms of Biotransformations and Chemical Standards for the Reduction of 1 to 2
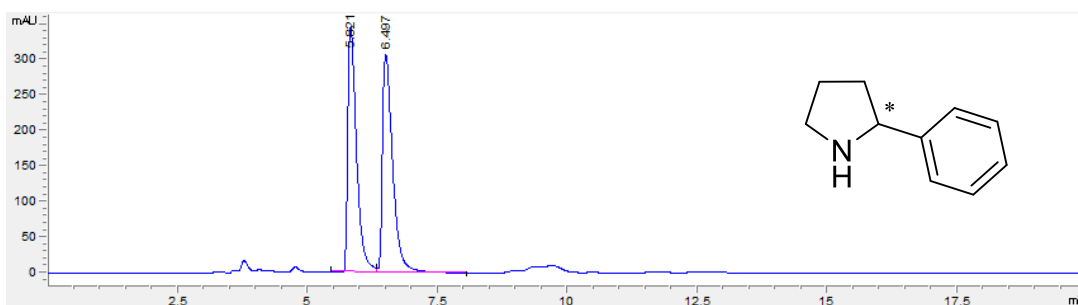
*Figure 97: HPLC chromatogram of chemical standard rac-**2***

*Figure 98: HPLC chromatogram of chemical standard (S)-**2***
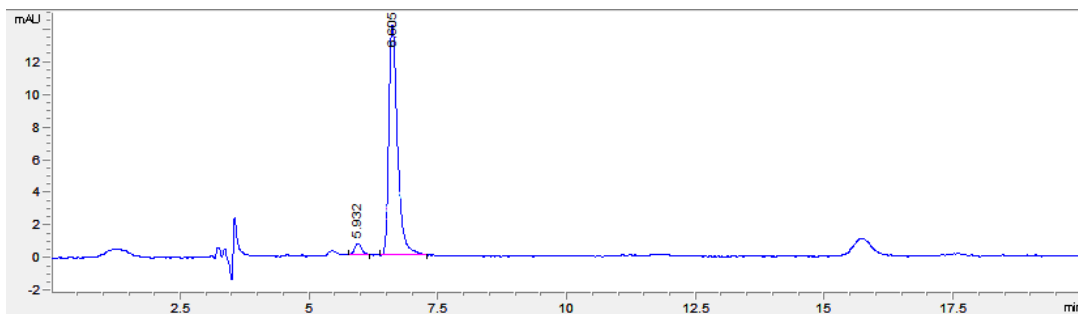
*Figure 99: HPLC chromatogram of biotransformation of compound **1** with AdWT*
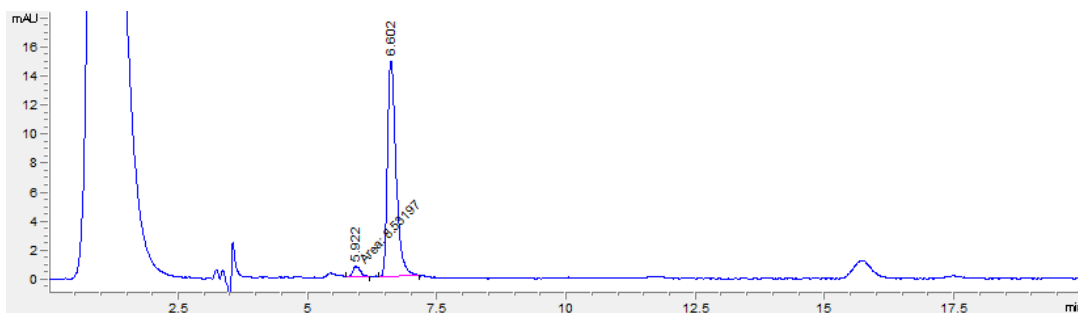
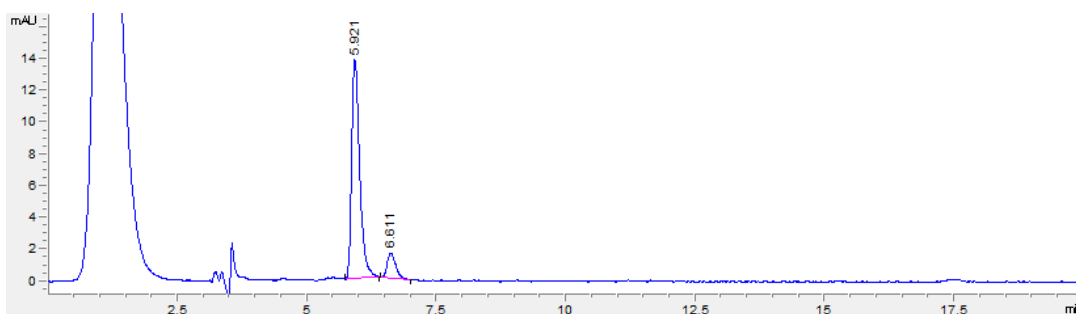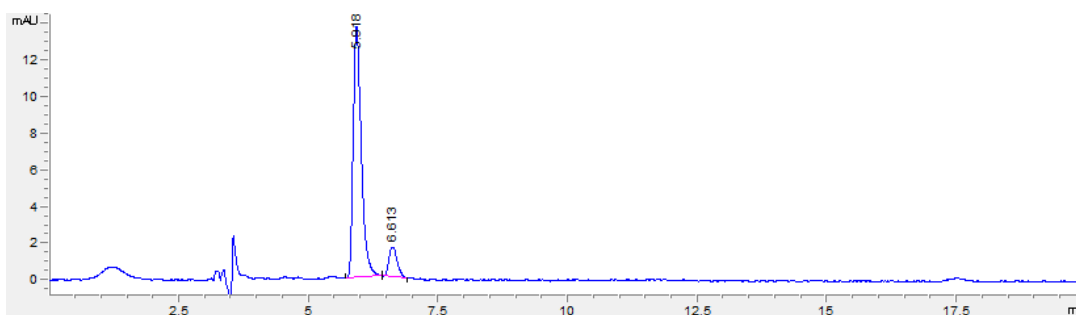*Figure 100: HPLC chromatogram of biotransformation of compound **1** with AdN94A*

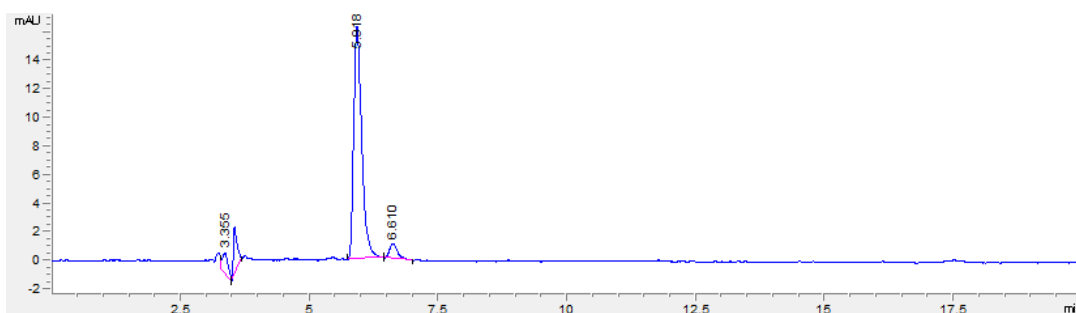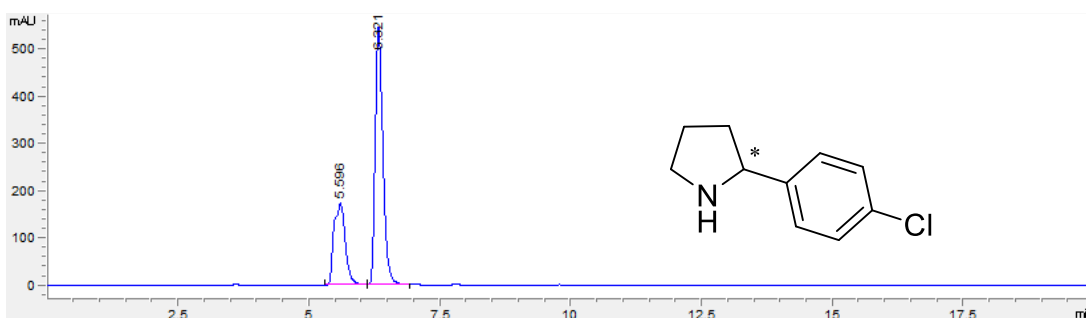*Figure 101: HPLC chromatogram of biotransformation of compound **1** with AdY177F*

*Figure 102: HPLC chromatogram of biotransformation of compound **1** with AdW208A*

*Figure 103: HPLC chromatogram of biotransformation of compound **1** with AdH215A*

*Figure 104: HPLC chromatogram of biotransformation of compound **1** with AdM237A*

*Figure 105: HPLC chromatogram of biotransformation of compound **1** with AdQ238A*

*Figure 106: HPLC chromatogram of biotransformation of compound **1** with AdM237G*

5.8.6.8 HPLC Chromatograms of Biotransformations and Chemical Standards for the Reduction of 3 to 4

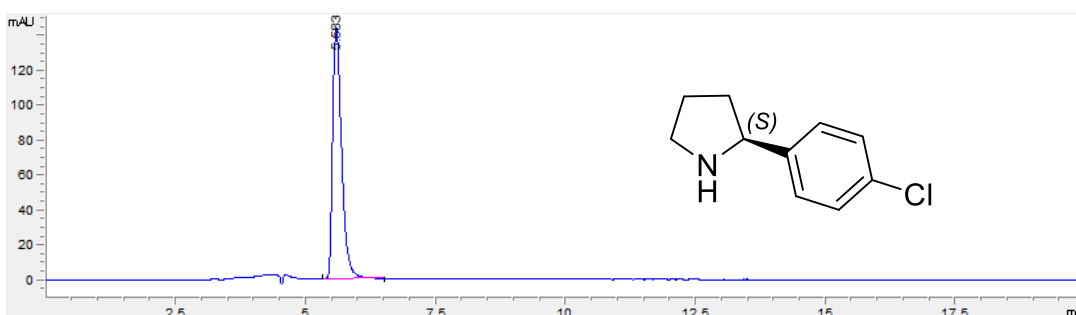*Figure 107: HPLC chromatogram of chemical standard rac-**4***

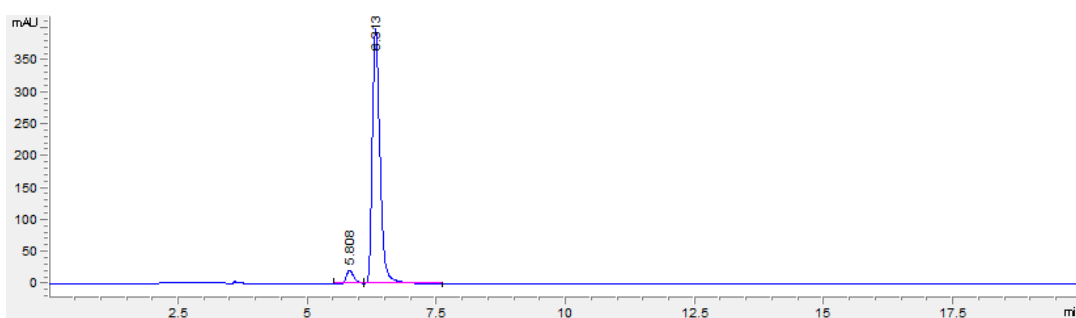*Figure 108: HPLC chromatogram of chemical standard (S)-**4***

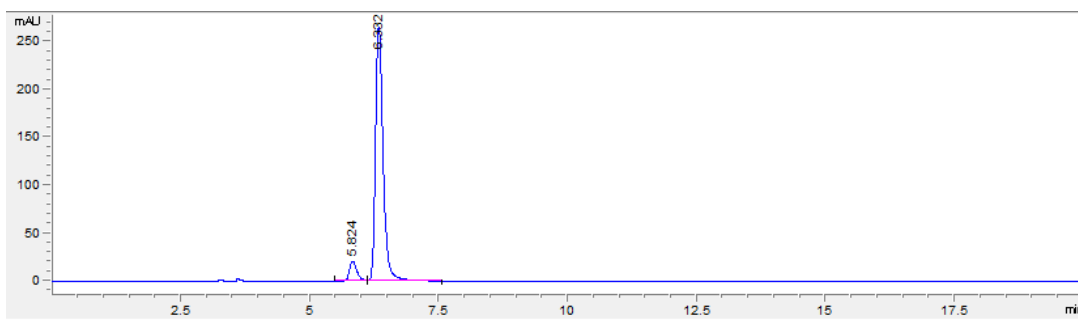*Figure 109: HPLC chromatogram of biotransformation of compound **3** with AdWT*

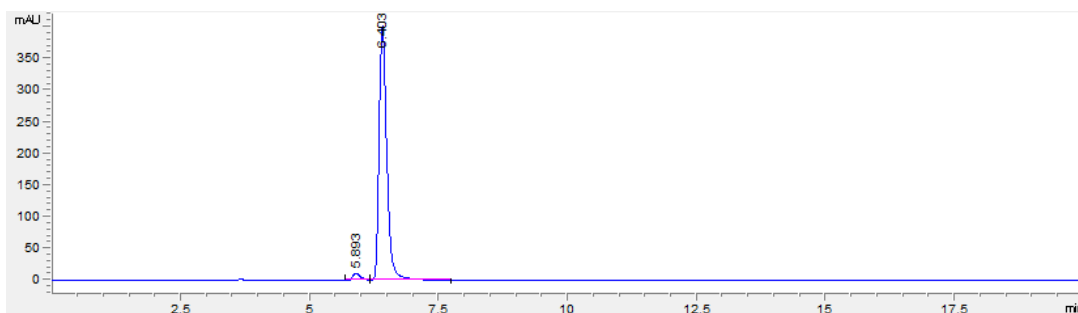*Figure 110: HPLC chromatogram of biotransformation of compound **3** with AdN94A*

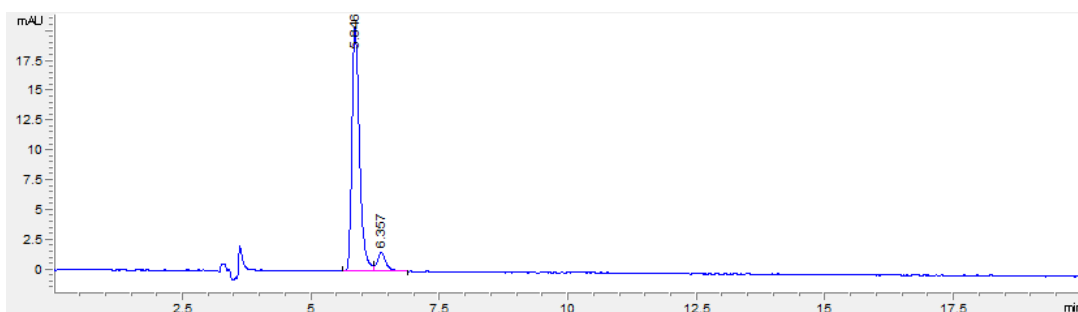*Figure 111: HPLC chromatogram of biotransformation of compound 3 with AdY177F*

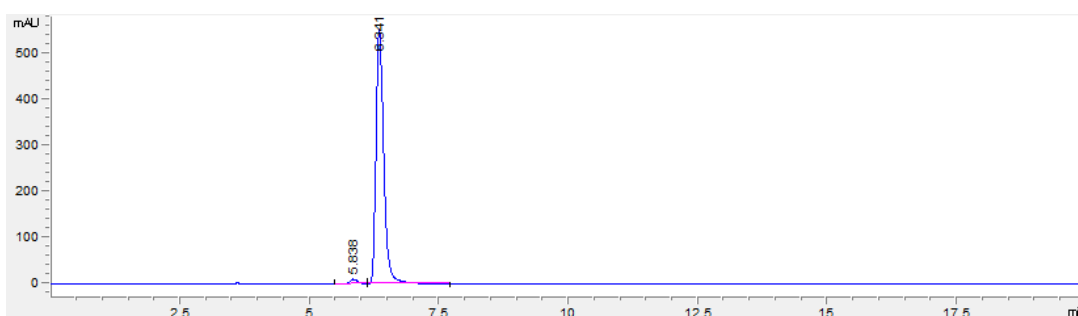*Figure 112: HPLC chromatogram of biotransformation of compound **3** with AdW208A*

*Figure 113: HPLC chromatogram of biotransformation of compound **3** with AdH215A*
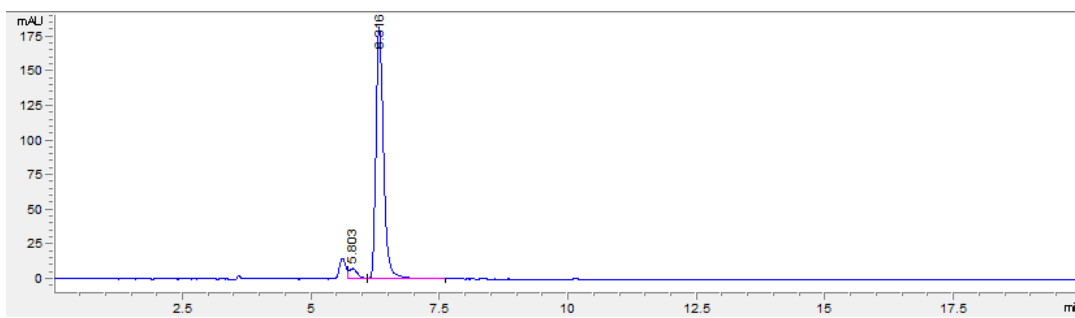
*Figure 114: HPLC chromatogram of biotransformation of compound **3** with AdM237A*
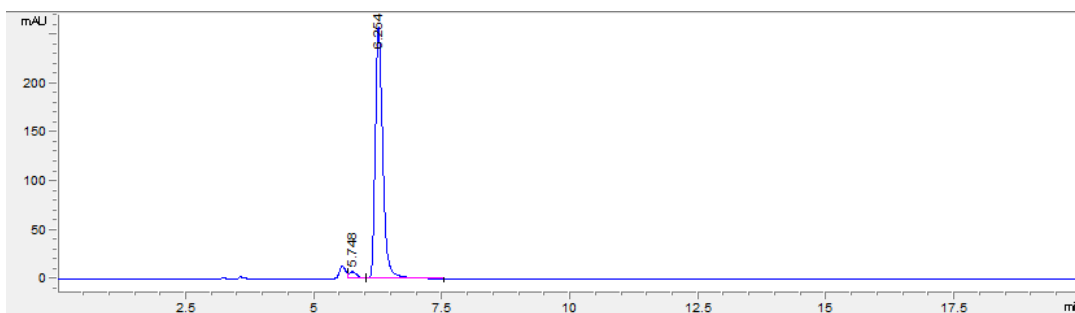

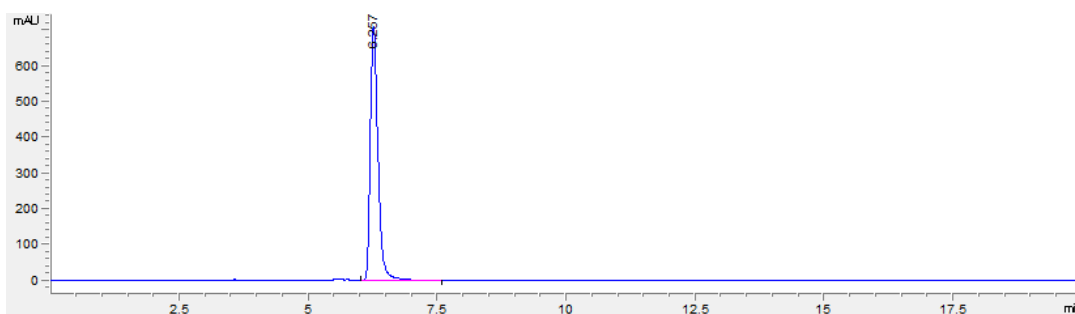*Figure 115: HPLC chromatogram of biotransformation of compound **3** with AdQ238A*

*Figure 116: HPLC chromatogram of biotransformation of compound **3** with AdM237G*

5.8.6.9 HPLC Chromatograms of Biotransformations and Chemical Standards for the Reduction of 5 to 6

*Figure 117: HPLC chromatogram of chemical standard rac-**6***

Figure 118: HPLC chromatogram of chemical standard (R)-6
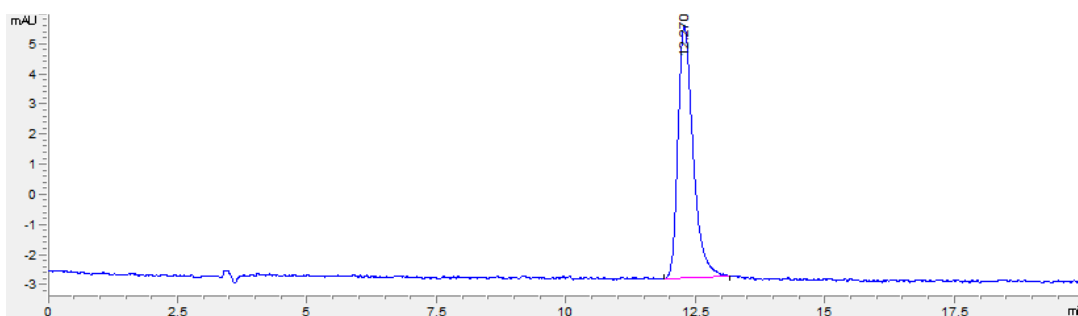
Figure 119: HPLC chromatogram of biotransformation of compound 5 with AdW208A

5.8.6.10 HPLC Chromatograms of Biotransformations and Chemical Standards for the Reduction of 7 to 8
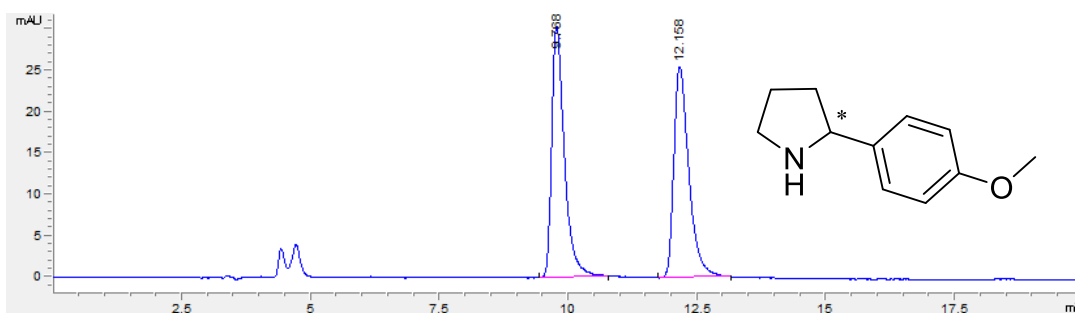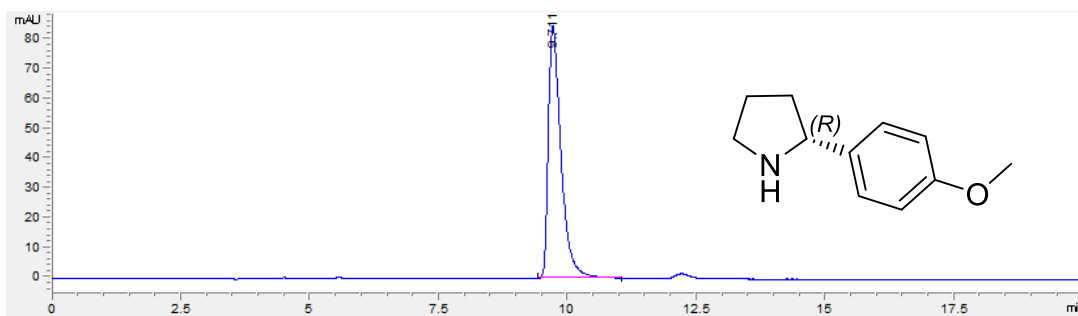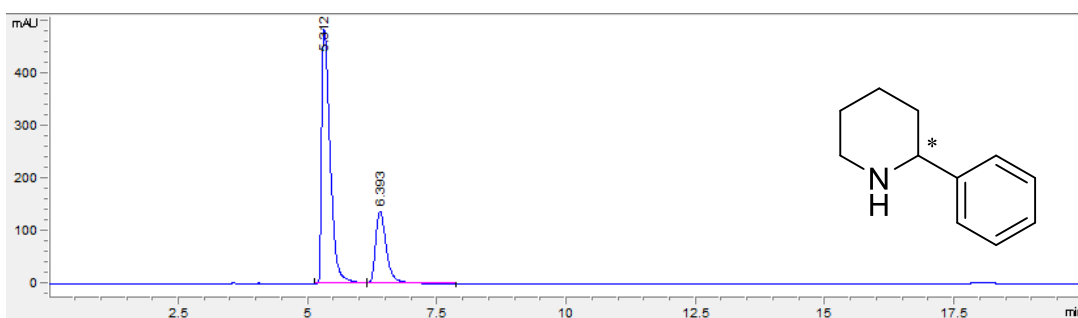

Figure 120: HPLC chromatogram of chemical standard rac-8

Figure 121: HPLC chromatogram of chemical standard (R)-8

*Figure 122: HPLC chromatogram of biotransformation of compound **8** with AdWT*

*Figure 123: HPLC chromatogram of biotransformation of compound **8** with AdN94A*

*Figure 124: HPLC chromatogram of biotransformation of compound **8** with AdY177F*

*Figure 125: HPLC chromatogram of biotransformation of compound **8** with AdW208A*

*Figure 126: HPLC chromatogram of biotransformation of compound **8** with AdH215A*

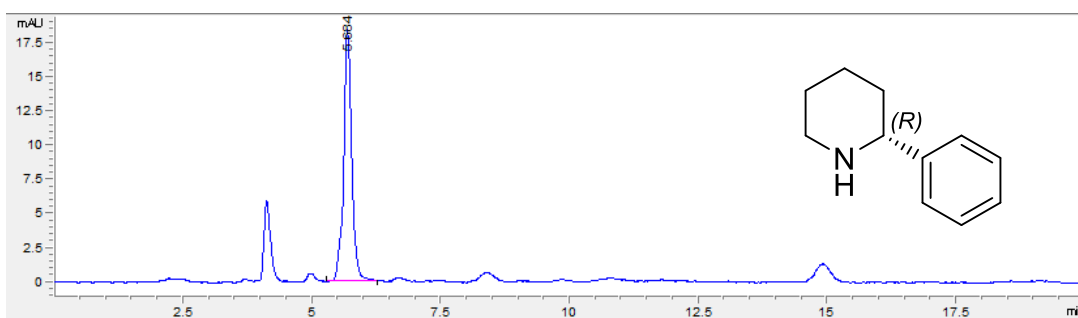*Figure 127: HPLC chromatogram of biotransformation of compound **8** with AdM237A*
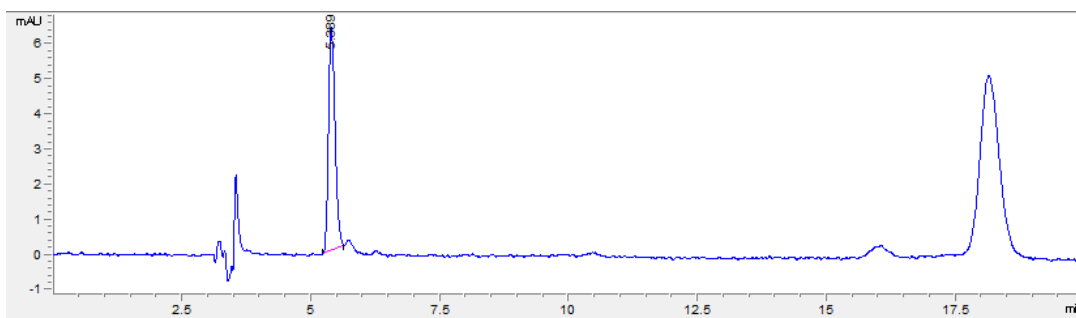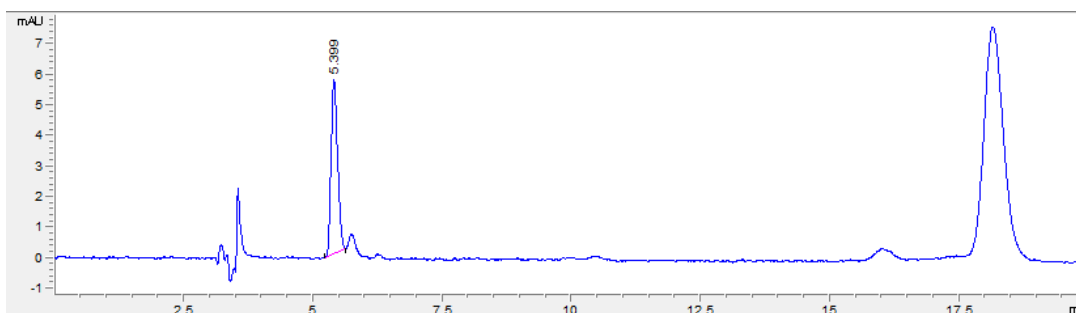

*Figure 128: HPLC chromatogram of biotransformation of compound **8** with AdQ238A*

*Figure 129: HPLC chromatogram of biotransformation of compound **8** with AdM237G*
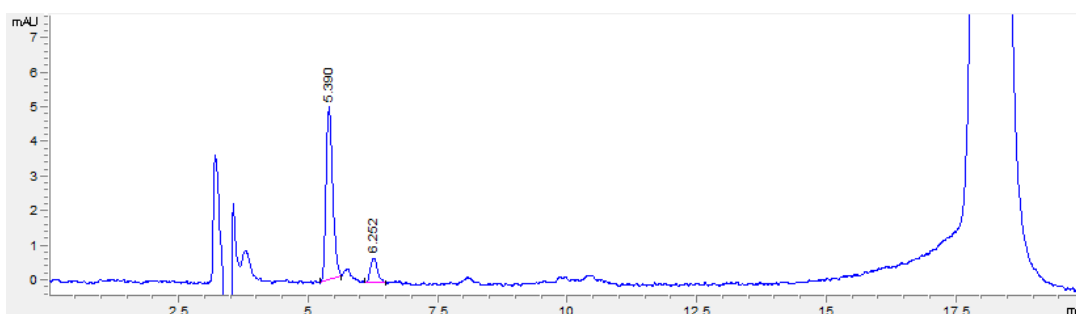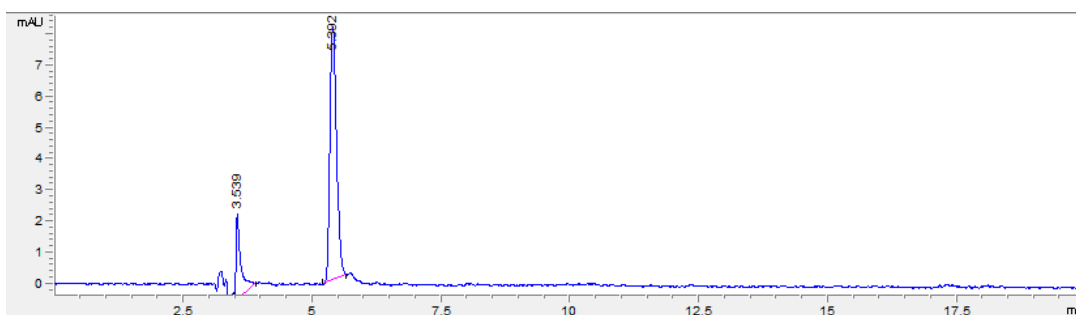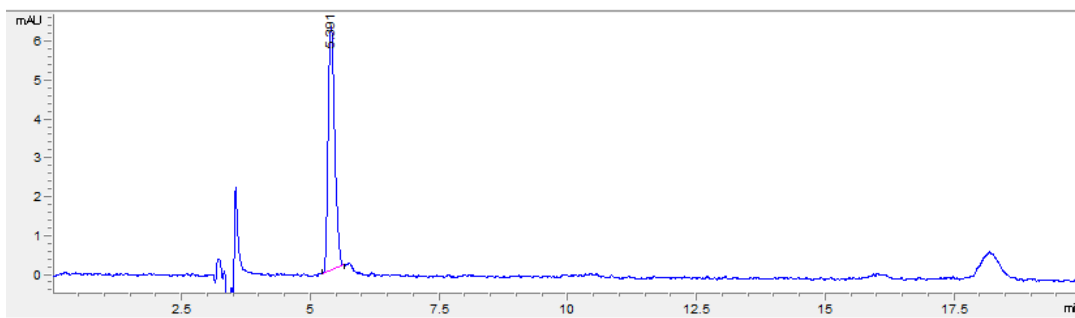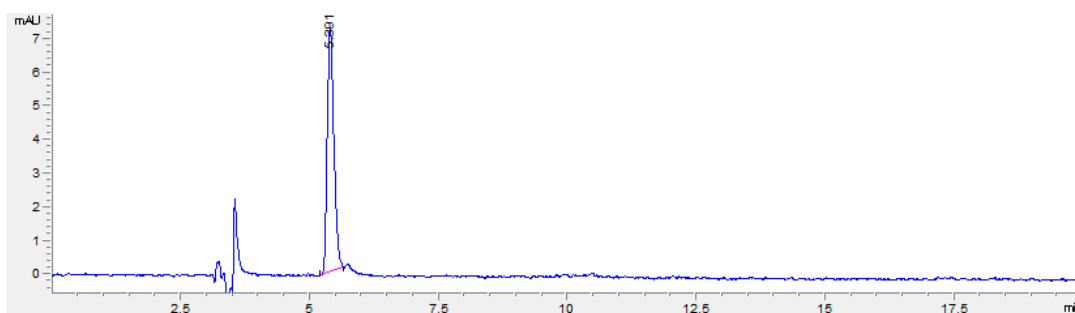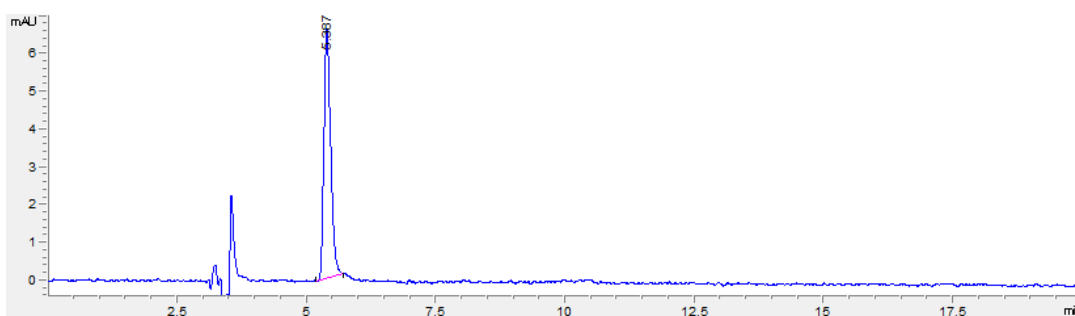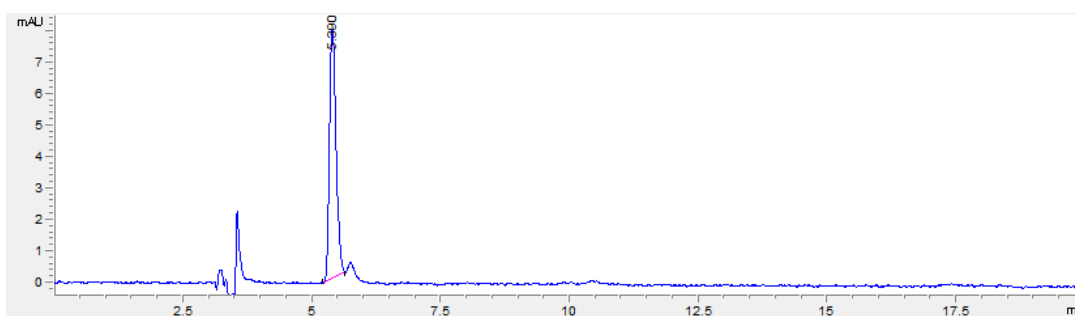
5.8.7 NADPH Assays

5.8.7.1 Depletion assay

The E. coliBL21 (DE3) colonies obtained after transformation of the NNK codon into AdWT were picked using sterile pipette tips and transferred into 96-deep

well plates (containing 300 μL LB with 50 μg/mL kanamycin in each well), and incubated overnight at 37°C and 250 rpm. 50 μL culture from each well was transferred into a corresponding well in a second 96-deep well plate (containing 400 μL LB with 50 μg/mL kanamycin in each well), and the second 96-deep well plates were incubated at 37°C and 250 rpm for 3–4 h. Afterwards, 50 μL LB containing 2 mM β-D-1-thiogalactopyranoside (IPTG) was added into each well to induce protein expression and the plates were then incubated at 20°C and 250 rpm for another 16–18 h. The cells were harvested in the 96-deep well plates via centrifugation. After centrifugation, 200 μL of Tris-HCl buffer (5 mM, pH 8.0),containing 0.75 mg/mL lysozyme and 2 U/mL DNase I ,was added into each well of the 96-deep well plates, and the plates were incubated at 37°C for 1 h. Subsequently, each well was supplemented with 200 μL of Tris-HCl buffer (5 mM, pH 8.0) and the supernatant in each well was used for high throughput activity screening. The imine reduction activity towards 2-phenylpyrroline of each well was assayed at 25°C, by measuring the initial rate of change in absorbance at 340 nm (corresponding to the amount of NADPH (ε = 6220 M^{-1} cm^{-1}) using a microplate reader. An assay reaction mixture (200 μL) contained 16 μL lysate, 5 mM 2-phenylpyrroline, 0.2 mM NADPH, and 100 mM phosphate buffer (pH 7.0). The rates of depletion where all compared with respect to the rate of depletion for AdWT (H11) and are displayed in the table below. A9 showed the greatest rate of depletion compared to AdWT and was sent for sequencing and corresponded to M237G.

	1	2	3	4	5	6	7	8	9	10	11	12
A	-0.41	4.28	2.09	2.64	1.69	0.51	1.00	-3.66	13.28	0.96	-3.29	-16.73
B	0.20	0.64	-0.16	3.06	-1.14	1.93	0.47	2.43	-4.11	2.58	-1.64	-13.62
C	2.24	1.80	-1.32	3.04	0.34	-1.06	2.17	-15.13	3.11	-21.88	1.19	-11.90
D	-0.22	-3.43	4.13	-0.88	1.82	-1.71	2.99	-9.30	4.05	0.86	-39.35	1.04
E	0.46	2.42	2.98	4.01	3.58	1.17	2.20	-3.05	3.65	2.46	0.72	-0.05
F	2.46	0.48	2.41	2.70	0.78	-0.04	1.93	1.46	4.65	1.92	1.94	0.32
G	-1.27	0.52	0.75	3.63	1.40	1.34	0.97	-1.28	1.63	2.40	-3.60	-0.89
H	0.73	-1.40	0.29	1.03	0.00	0.75	0.91	0.56	1.01	2.74	1.00	0.00

5.8.7.2   Kinetic Studies

Initial rates for NADP(H)-dependent *Ad*RedAm activities were measured for the imine reduction of 2-phenypyrroline at concentrations of 0.45, 0.90, 2.25, 4.5, 9.0, 18, 36, and 54 mM. Depletion of NADPH was monitored over 10 minutes using a TECAN Plate Reader at an absorbance of 540 nm. Reactions were carried out in a 96-well plate with a reaction volume of 200 µL and 0.5 mM NADPH and 0.1 mg mL^{-1} purified reductive aminase

Figure 130: Michaelis-Menten plot for the kinetic study carried out with AdWT

Figure 131: Michaelis-Menten plot for the kinetic study carried out with AdN94A

Figure 132: Michaelis-Menten plot for the kinetic study carried out with AdY177F

Figure 133: Michaelis-Menten plot for the kinetic study carried out with AdW208A

Figure 134: Michaelis-Menten plot for the kinetic study carried out with AdH215A

Figure 135: Michaelis-Menten plot for the kinetic study carried out with AdM237A
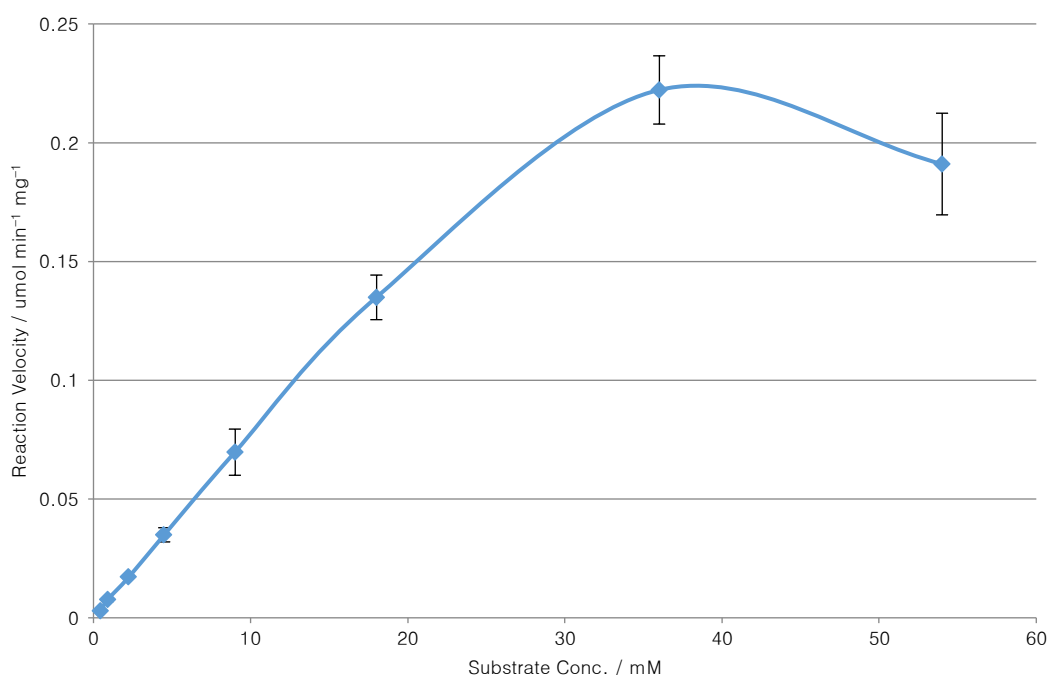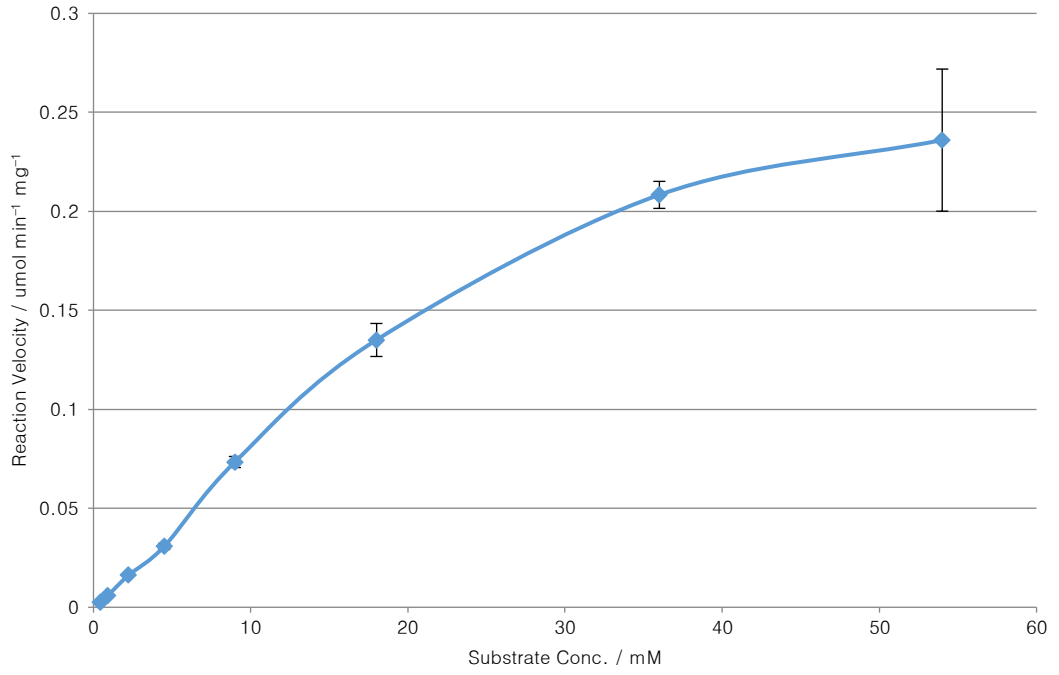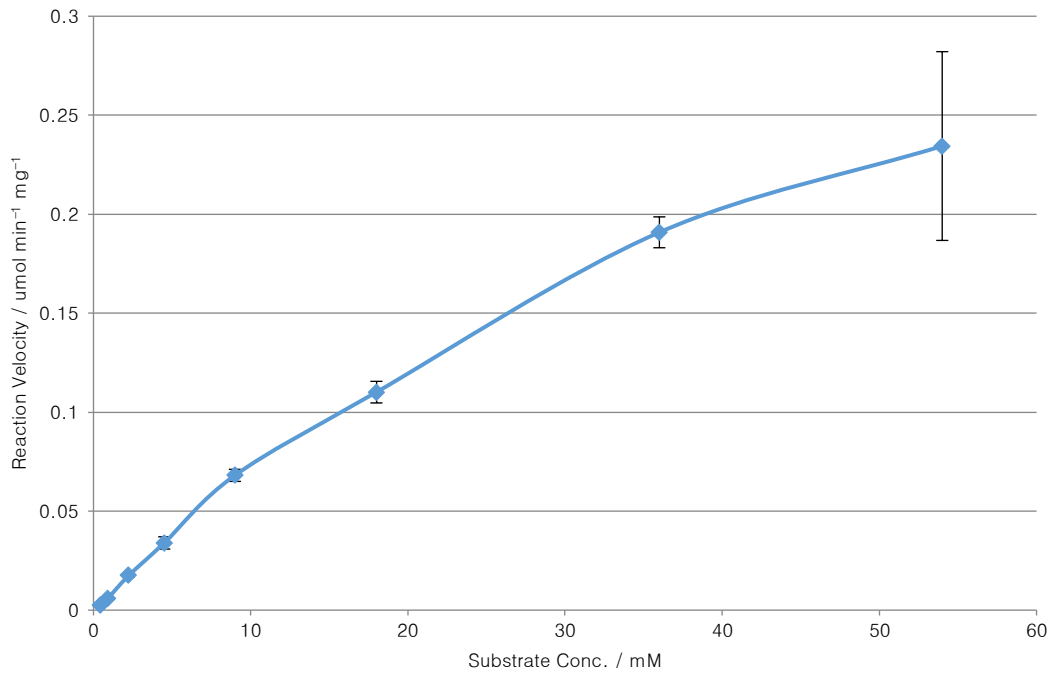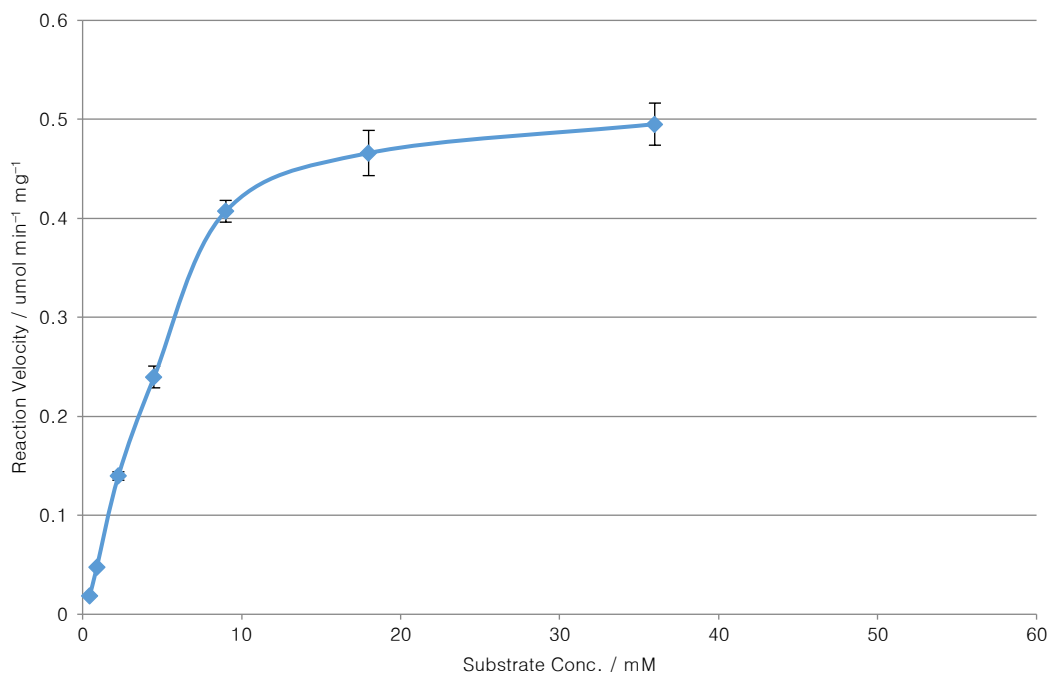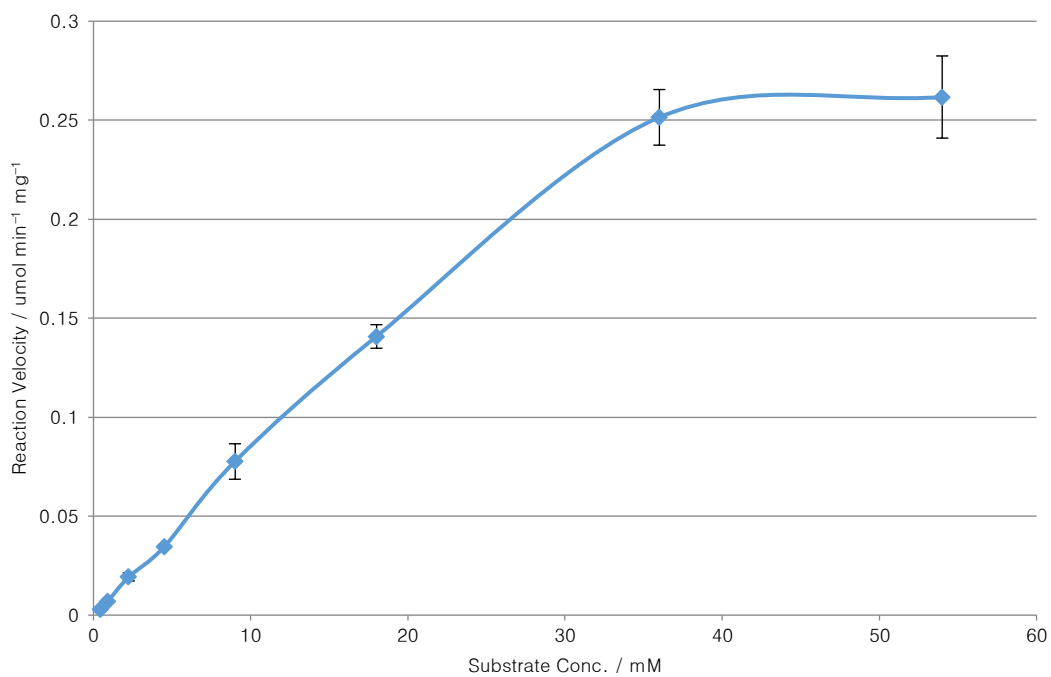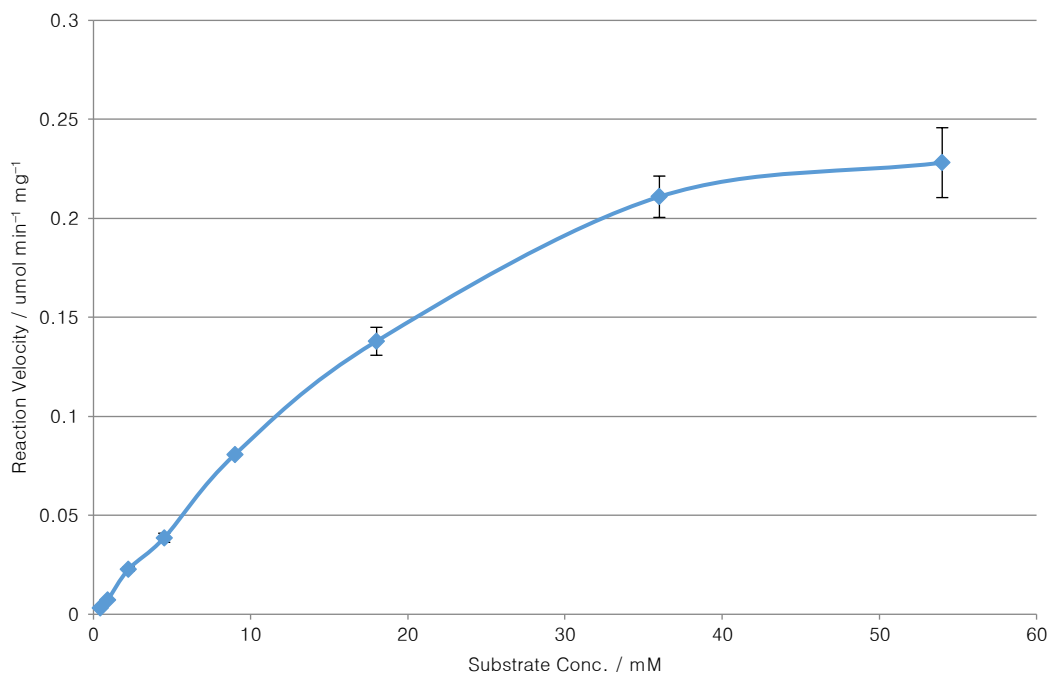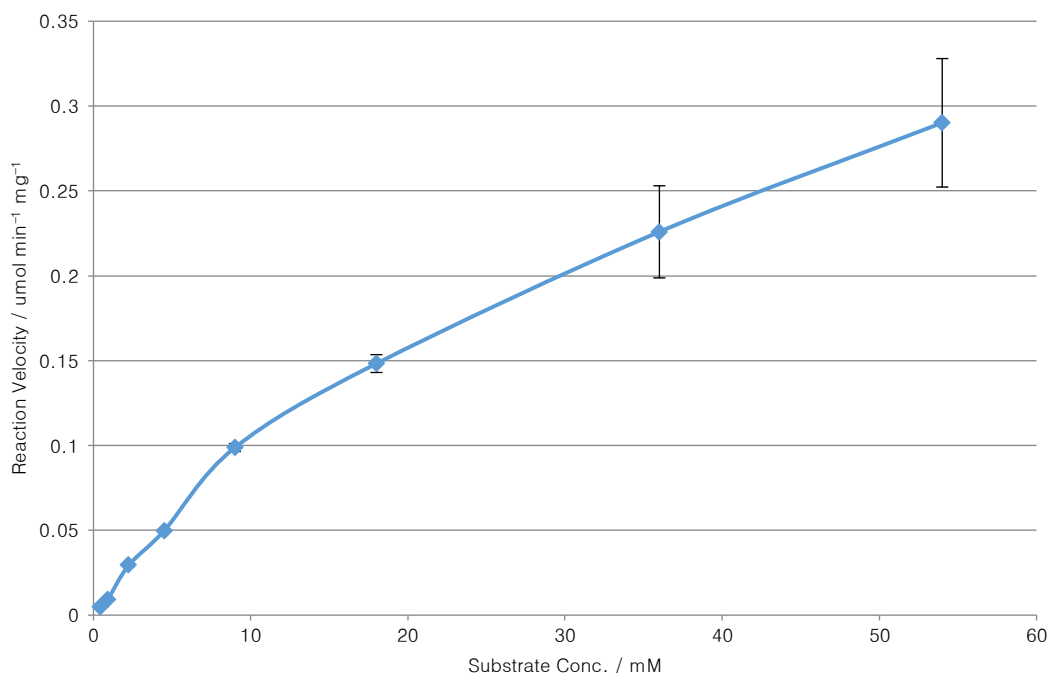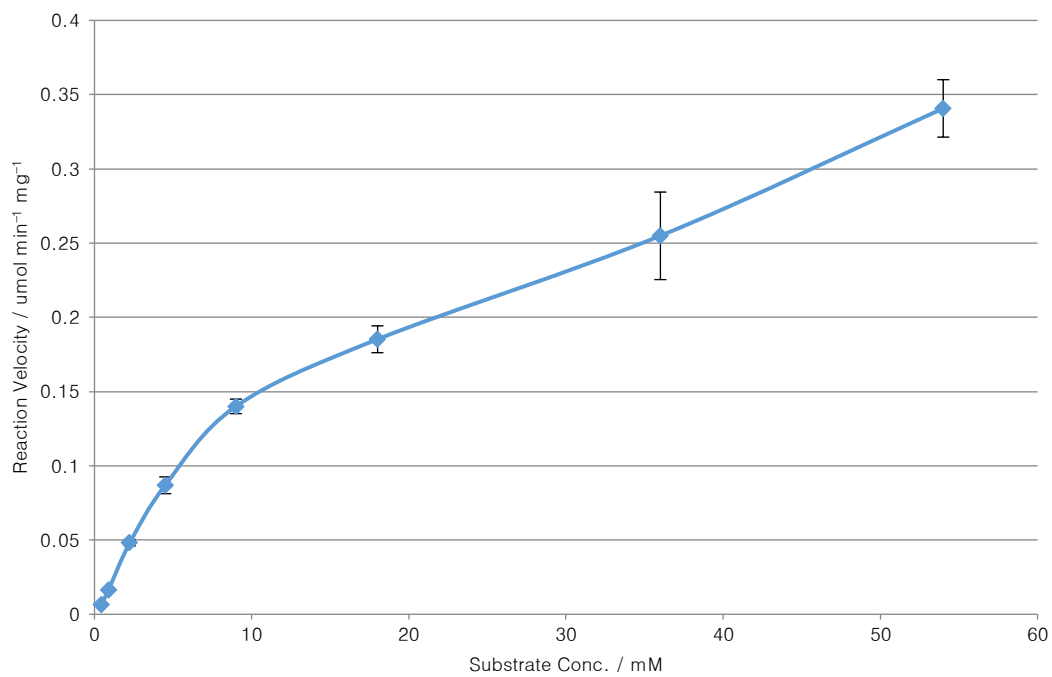

Figure 136: Michaelis-Menten plot for the kinetic study carried out with AdQ238A

Figure 137: Michaelis-Menten plot for the kinetic study carried out with AdM237G

Chapter 6: Extending the Substrate Scope of *Ad*RedAm Beyond its Wild-Type Capabilities

6.1 Foreword

Compound numbering for this chapter correspond to compounds in this chapter only.

6.2 Introduction

In the last chapter, it was shown that the activity of the reductive aminase could be drastically improved from just a single point mutation. The W208A variant showed an 82 fold increase in ToF and so makes a sensible variant to test on other substrates that have typically been difficult for reductive amination.

Aniline is one such amine donor that has been notoriously difficult to get to work for bioreductive amination reactions. The delocalisation of the nitrogen lone pair on the ring results in aniline being a poorer nucleophile than most other amine donors. Although some effort has been exerted to screen and identify IREDs, with some success achieved in reductive aminations with carbonyls, no success had been achieved using the reductive aminases from *Aspergillus oryzae*, *Ajellomyces dermatitidis*, or *Ajellomyces terreus*. [77,78,81]

Recently, unrelated work[110] focused on the structure-activity relationships of imine reductases and reductive aminases and highlighted position 210 in *Asp*RedAm as a potential site for engineering to improve activity towards aniline. This position corresponds to 208 in *Ad*RedAm and therefore W208A has promise for success with aniline as an amine donor.[82]

6.3 Screening of Carbonyls with Aniline

Initial screening was carried out using cyclohexanone and aniline at stoichiometric ratio with 10 mM substrate and *Ad*RedAm wild type and all the variants. These initial biotransformations were analysed by GC-MS for identification and only W208A showed any conversion to the reductive amination product. It was then decided to take W208A and screen reductive aminations of a selection of carbonyls with aniline at stoichiometric ratios.

The first three carbonyls tested were the cyclic ketones cyclohexanone, cycloheptanone, and cyclopentanone. It had already been shown by GC-MS that cyclohexanone and aniline worked for reductive amination, and when ran on GC-FID were shown to produce the amine product in 56% conversion. This value dropped when the ring size was change from six: the 5-membered cyclopentanone showed a drop to 16% for the reductive amination and the 7-membered cycloheptanone showed an even poorer conversion of 3.6%, Figure 138. This decrease in activity between cyclohexanone and cyclopentanone has been seen before, where it was reported by Aleku *et al*. that to achieve good conversions between cyclopentanone and methylamine, a higher amino ratio was required than when used with cyclohexanone.[103] This was however not the case when the acyclic carbonyls heptan-2-one, hexan-2-one, and pentan-2-one were tested. The enzyme appears to prefer the longer chain acyclic ketones with conversions for heptan-2-one, hexan-2-one, and pentan-2-one with aniline being 16%, 8%, and 4% respectively.

The next ketone tested for reductive amination with aniline was methoxyacetone due to it being a precursor to Metolachlor, a herbicide that is estimated to have a usage of 60 – 65 million pounds per year in the United States.[107] Although a desired compound, this ketone proved to be unsuccessful for reductive amination with aniline using W208A. Alternatively, benzaldehyde proved to be the best carbonyl tested with a conversion of >90% with aniline. The stabilisation of the imine intermediate over the benzene ring aids in driving the equilibrium towards the product.
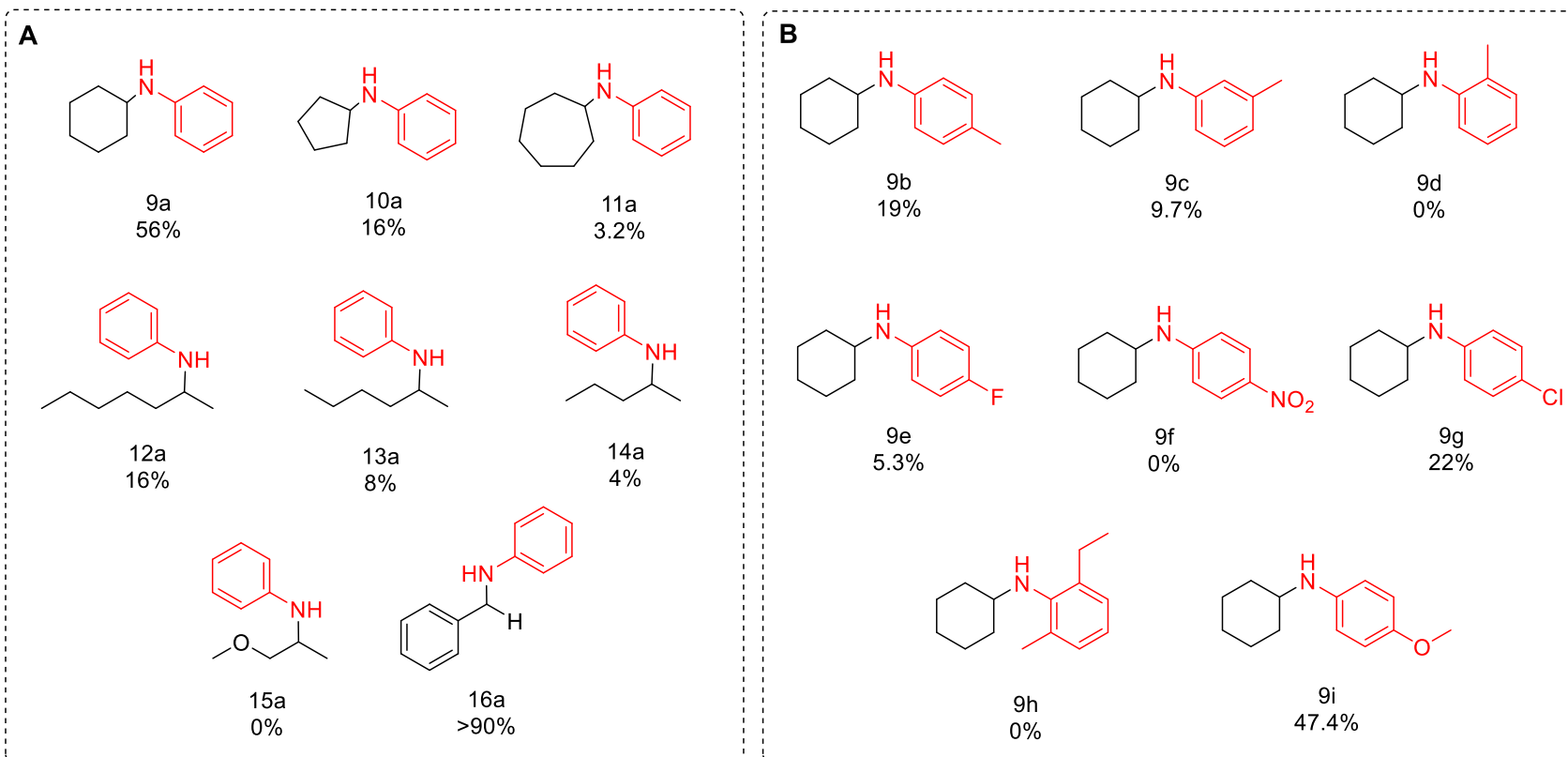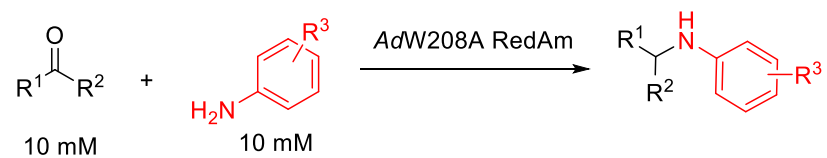
Figure 138: Investigation into aniline and substituted anilines as a successful amine donor for reductive amination.

6.4 Screening of Anilines with Cyclohexanone

In order to investigate the effect of substituents on the aniline ring, reductive aminations were carried out using cyclohexanone as the carbonyl of choice. This was chosen over benzaldehyde due to not achieving full conversion with aniline, thus allowing for the effect of the substituents to be observed.

The steric effect of substituents on aniline was investigated using *p*-methylaniline, *m*-methylaniline, and *o*-methylaniline. *p*-methylaniline was the most active amine of the three with a conversion of 19%. As the methyl group approached closer to the nitrogen of aniline, the conversion dropped to 9.7% for *m*-methylaniline and 0% for *o*-methylaniline. Increasing the steric bulk around the reaction centre results in a decrease in activity. This was also observed with 2-ethyl-6-methylaniline which was also tested since it's a precursor to Metolachlor. Unsurprisingly, this also did not work just like *o*-methylaniline.

Investigation of electronic effects of substituents was investigated with different groups at the *para*-position of aniline. A *para*-fluorine group showed a major decrease in conversion than cyclohexanone and aniline with 5.3% conversion compared to 56%. When the substituent was changed to chlorine, an increase in conversion is observed, although still less than aniline at 22%. Halogens are highly electron withdrawing with a strong negative inductive effect. This draws electron density away from the nitrogen resulting in an even poorer nucleophile. Chlorine is less electron withdrawing than fluorine and thus results in less of a decrease in conversion when compared to aniline. This can be investigated further by testing a more electron withdrawing and a more electron donating group in the *para*-position.
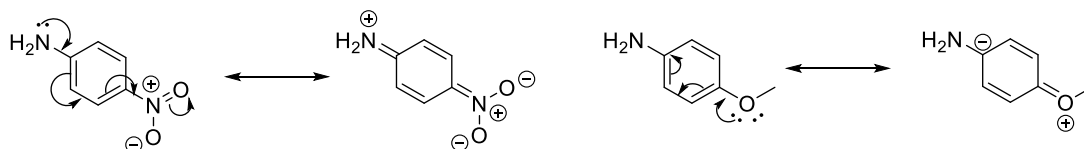

Figure 139: Electron delocalisation of p-nitroaniline and p-methoxyaniline

One substituent, which is more electron withdrawing than fluorine, is the nitro group (Figure 139). With a nitro group in the *para*-position instead of fluorine, the conversion for reductive amination with cyclohexanone drops further and no

157

conversion is observed. When the substituent is changed to one that is more electron donating than chlorine, such as a methoxy group (Figure 138), an increase in conversion is observed to 47%. Although the conversion has increased from using *p*-chloroaniline, the conversion is still lower than when aniline is used. *p*-methoxyaniline is a bulkier amine than *p*-methylaniline due to the oxygen group, however the drop in conversion observed from the reductive amination of cyclohexanone and aniline is much lower.

6.5 Conclusions and Outlook

Reductive aminations with aniline as an amine donor have been notoriously difficult due to the poor nucleophilicity of the nitrogen. Although some work has been done to identify enzymes capable of catalysing these reductive aminations, which has found some IREDs capable, the reductive aminases have never been shown to be successful. Through engineering of the reductive aminase from *Ajellomyces dermatitidis*, an active variant has been engineered that was capable of catalysing the reductive amination between cyclohexanone and aniline where the wild type was incapable.

Despite the improvement in reductive amination with aniline, not all tested substrates were as successful as cyclohexanone and aniline. Different ring sized cyclic ketones outside of cyclohexanone were not as successful. Pentan-2-one and hexan-2-one were shown to be less active than their cyclic counterparts were however heptan-2-one resulted in a higher conversion than cycloheptanone. The low conversions may also be a result of high K_M values of either starting material and so kinetic studies into the Michaelis-Menten concentration would highlight if the reactions were operating at the right substrate concentrations. Therefore, these reactions may benefit from running the biotransformations at higher substrate loading or even at higher amine loadings.

6.6 Experimental and Methods

6.6.1 General

Solvents used were of HPLC grade and when necessary solvents were further dried over molecular sieves. Spectra from ^{1}H and ^{13}C NMR runs were recorded on a Bruker

Avance 400 instrument (400 MHz for ^{1}H and 100 MHz for ^{13}C) in CDCl$_3$, (CD$_3$)$_2$SO, or CD$_3$OD using residual protic solvent as an internal standard. Reported chemical shifts (δ) (in parts per million (ppm)) are relative to the residual protic solvent signal (CHCl$_3$ in CDCl$_3$, ^{1}H = 7.26; ^{13}C = 77.0; (CHD$_2$)(CD$_3$)SO in (CD$_3$)$_2$SO, ^{1}H = 2.50; ^{13}C = 39.52; CHD$_2$OD in CD$_3$OD, ^{1}H = 3.31; ^{13}C = 49.0).

Chiral normal phase HPLC was performed on an Agilent system (Santa Clara, CA, USA) equipped with a G1379A degasser, G1312A binary pump, a G1367A well plate autosampler unit, a G1316A temperature controlled column compartment and a G1315C diode array detector.CHIRALPAK®IC Analytical (all Daicel (Osaka, Japan), 250 mm length, 4.6 mm diameter, 5 µm particle size) as well as CHIRALCEL®OD-H Analytical (Daicel (Osaka, Japan), 250 mm length, 4.6 mm diameter, 5 µm particle size) columns were used. The typical injection volume was 10 µl and chromatograms were monitored at 265 nm. All solvent mixtures are given in (v/v) ratios.

GC analysis was performed on an Agilent 6850 GC (Agilent, Santa Clara, CA, USA) with a flame ionization detector (FID) and autosampler using an HP-1 column with 0.32 mm inner diameter and 0.25 µm film thickness (Agilent, 6 Santa Clara, CA, USA).

6.6.2 Chemicals

HPLC solvents were obtained from Sigma-Aldrich (Poole, Dorset, UK) or Honeywell (Seelze, Lower Saxony, Germany) and solvent additive diethylamine was obtained from Sigma-Aldrich (Poole, Dorset, UK). GC gases were obtained from BOC gases (Guildford, Surrey, UK). Carbonyls cyclohexanone, cyclopentanone, cycloheptanone, 2-pentanone, and benzaldehyde and amines aniline, *p*-toluidine, *m*-toluidine, *o*-toluidine, 4-fluoroaniline, 4-nitroaniline, 4-chloroaniline, 2-ethyl-6-methylaniline, and *p*-anisidine were all purchased from Sigma-Aldrich (UK) and used without further purification. 2-heptanone and methoxyacetone were purchased from Fluorochem (Hadfield, UK) and 2-heptanone was purchased from Alfa Aesar (UK) and all were used without further purification.

Cyclohexylamine, cyclopentylamine, 2-hexylamine, 2-pentylamine, iodobenzene, 4-iodotoluene, 3-iodotoluene, 2-iodotoluene, 1-fluoro-4-iodobenzene, 1-chloro-4-iodobenzene, 1-iodo-4-nitrobenzene, and 4-iodoanisole were all purchased from

Fluorochem (Hadfield, UK). Cyclohexylamine, benzylamine, and 2-ethyl-6-methyliodobenzene were all purchased from Alfa Aesar (UK). 2-heptylamine was purchased from Acros Organics (UK) and 1-methoxy-2-propylamine was purchased from Sigma-Aldrich (UK). All chemicals were used without further purification.

### 6.6.3 Synthesis of Aniline Product Standards
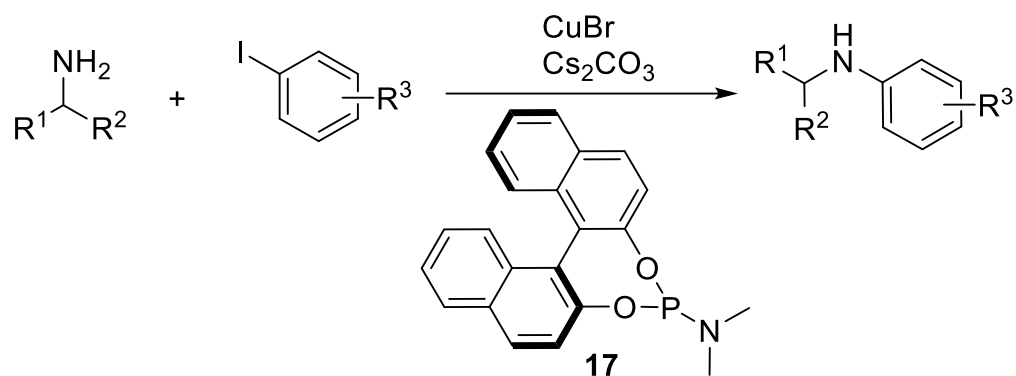
Copper bromide (5.0 mg, 0.035 mmol), caesium carbonate (977.5 mg, 3 mmol), **17** (18 mg, 0.05 mmol, and amine (1.5 mmol) (if solid)) were added to a screw-capped vial. The vial was then evacuated and backfilled with nitrogen (5 cycles). DMF (1 mL), amine (1.5 mmol) (if liquid), and aryl iodide (1 mmol) were added by syringe at room temperature. The vial was again evacuated and backfilled with nitrogen (3 cycles). The reaction mixture was heated at 90 °C under stirring for 24 h. After cooling to room temperature, the resulting mixture was added with 10 mL of ethyl acetate and 10 mL of water. The organic layer was separated and the aqueous layer was further extracted with ethyl acetate (3 x 10 mL). The combined organic phase was washed with brine. The organic phase was then acidified to pH 1 using HCl (10 mL, 9 M), the aqueous layer separated and the organic phase was further extracted with 9 M HCl (2 x 10 mL). The combined aqueous phase was then basified to pH 14 using NaOH and extracted with ethyl acetate (4 x 15 mL). The combined organic phase was dried over $MgSO_4$ and the solvent removed in vacuo to yield the desired product.
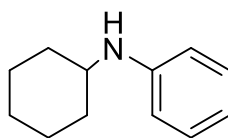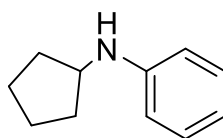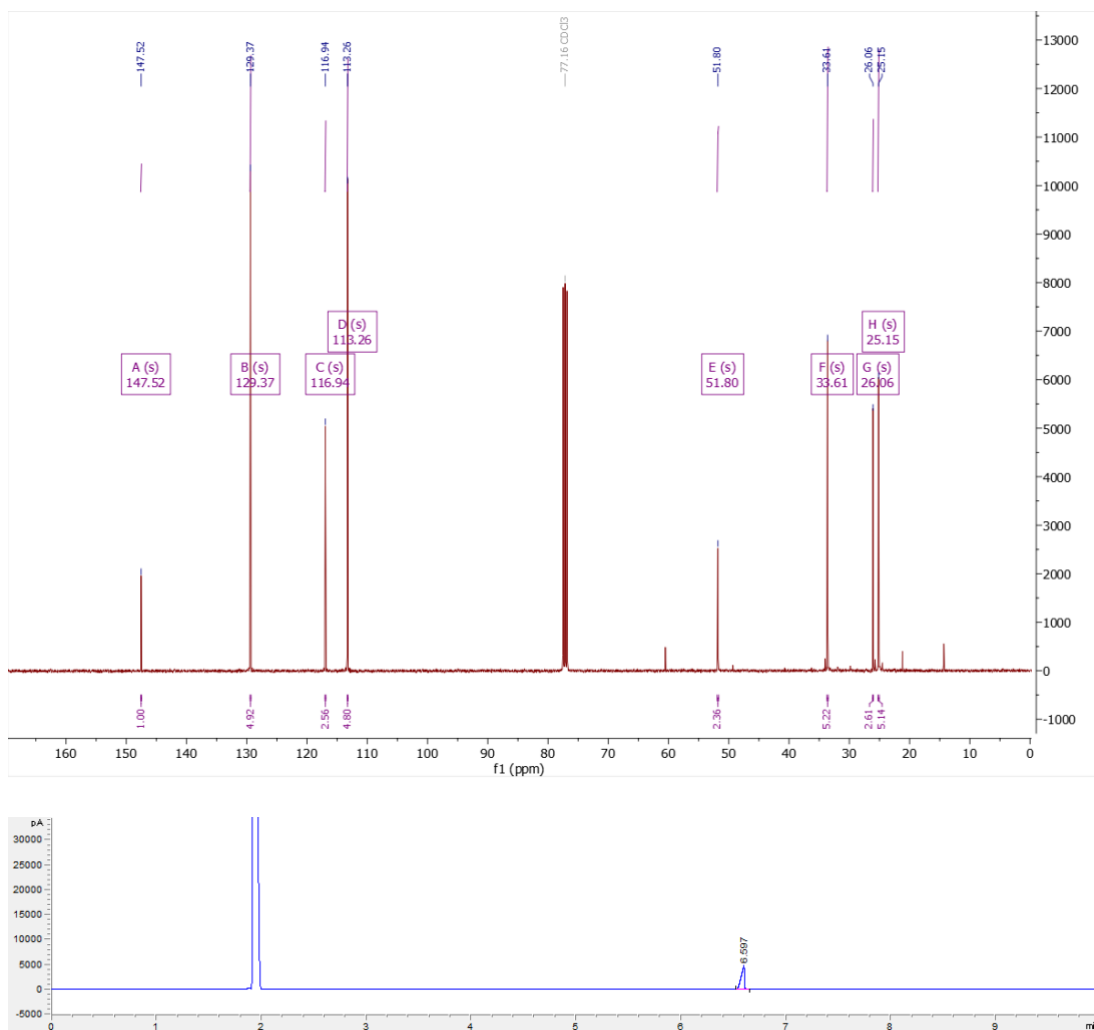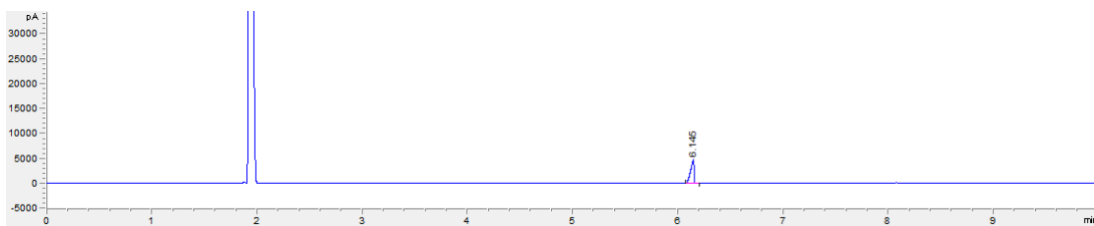
9a

N-cyclohexylamine, **9a** (Isolated yield, 85.7 mg, 49%, Brown Oil): ^{1}H NMR (400 MHz, CDCl$_3$) δ 7.20 – 7.13 (m, 2H), 6.67 (tt, J = 7.4, 1.1 Hz, 1H), 6.63 – 6.57 (m, 2H), 3.27 (tt, J = 10.2, 3.8 Hz, 1H), 2.12 – 2.01 (m, 3H), 1.83 – 1.72 (m, 2H), 1.72 – 1.61 (m, 1H), 1.46 – 1.32 (m, 2H), 1.31 – 1.07 (m, 4H). ^{13}C NMR (101 MHz, CDCl$_3$) δ 147.52, 129.37, 116.94, 113.26, 51.80, 33.61, 26.06, 25.15. HRMS calculated for C$_{12}$H$_{18}$N$^+$ 176.1434 [M+H], found 176.1433.
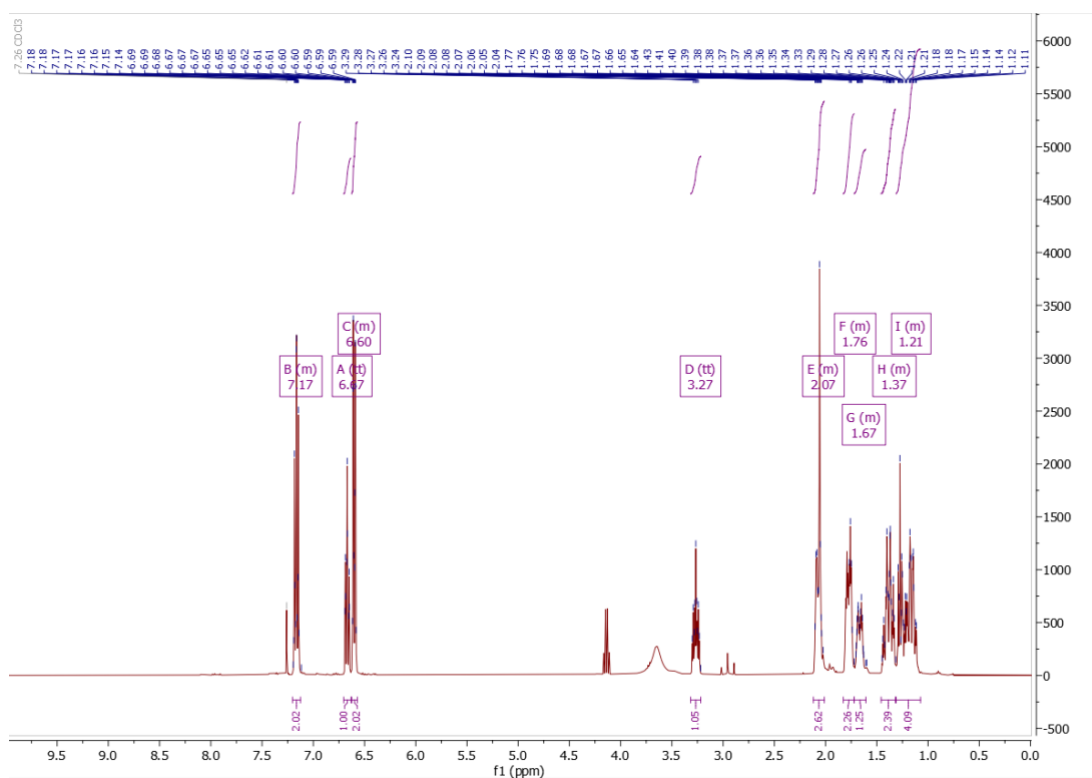
10a

N-cyclopentylaniline, 10a (Isolated yield, 76.6 mg, 48%, Brown Oil): ^{1}H NMR (400 MHz, CDCl$_3$) δ 7.22 − 7.13 (m, 2H), 6.70 (tt, J = 7.3, 1.2 Hz, 1H), 6.65 − 6.60 (m, 2H), 3.80 (ddd, J = 12.3, 6.8, 5.5 Hz, 1H), 2.11 − 1.92 (m, 2H), 1.74 (dtd, J = 10.1, 7.6, 4.4 Hz, 2H), 1.68 − 1.57 (m, 2H), 1.55 − 1.42 (m, 2H). ^{13}C NMR (101 MHz, CDCl$_3$) δ 148.01, 129.30, 117.15, 54.89, 33.67, 24.19. HRMS calculated for C$_{11}$H$_{16}$N$^+$ 162.1277 [M+H], found 162.1273.

11a

***N*-cycloheptylaniline, 11a** (Isolated yield, 112 mg, 59%, Brown Oil)**:** ^{1}H NMR (400 MHz, CDCl$_3$) δ 7.21 – 7.13 (m, 2H), 6.71 – 6.64 (m, 1H), 6.59 – 6.54 (m, 2H), 3.46 (dp, J = 8.2, 4.0 Hz, 1H), 2.02 (dtd, J = 13.2, 6.7, 2.5 Hz, 2H), 1.74 – 1.42 (m, 10H). ^{13}C NMR (101 MHz, CDCl$_3$) δ 147.30, 129.40, 117.05, 113.50, 53.93, 34.93, 28.48, 24.54. HRMS calculated for C$_{13}$H$_{20}$N$^+$ 190.1590 [M+H], found 190.1594.
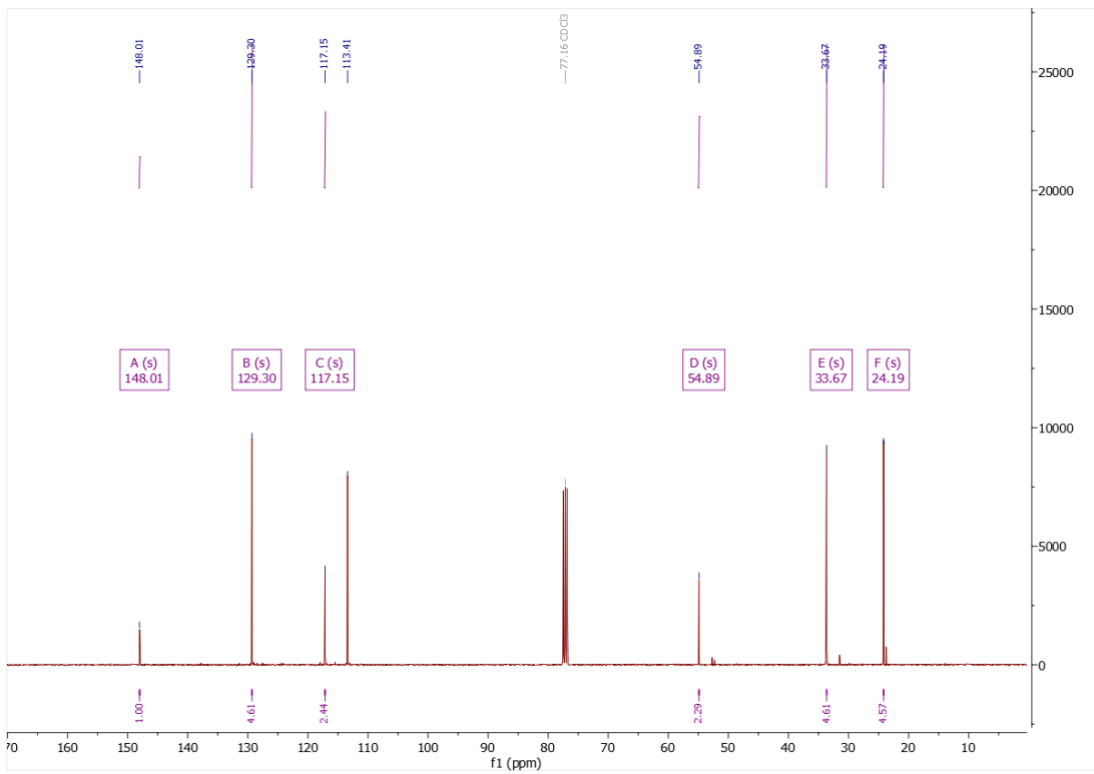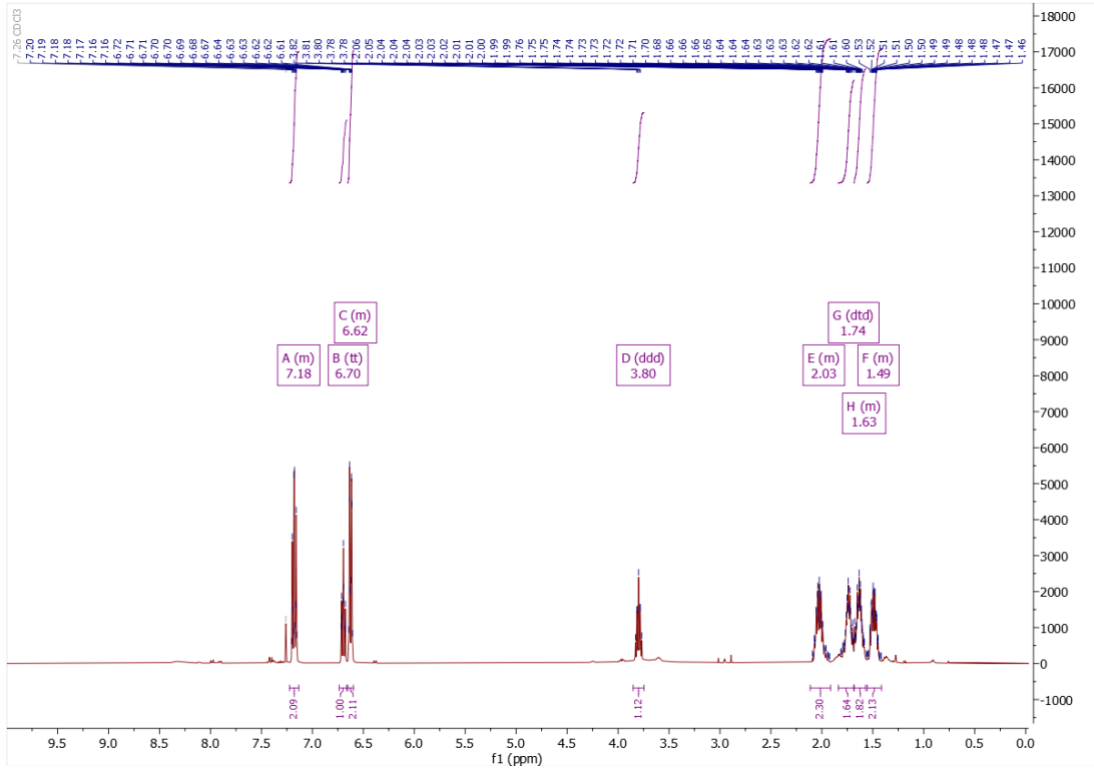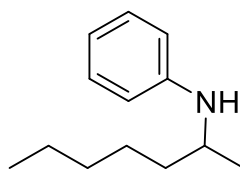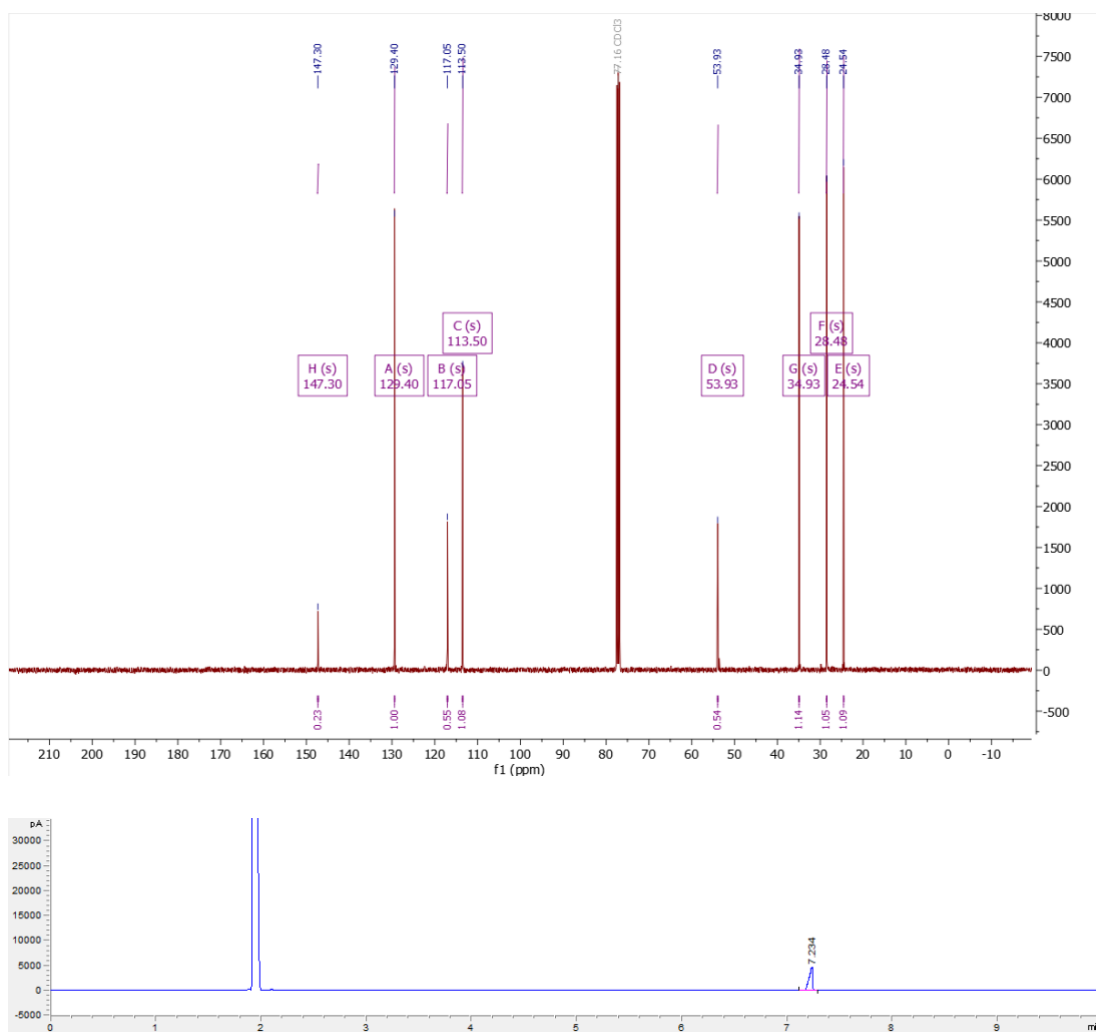
12a

***N*-(heptan-2-yl)aniline, 12a** (Isolated yield, 59.7 mg, 31%, Brown Oil): ^{1}H NMR (400 MHz, CDCl$_3$) δ 7.21 – 7.11 (m, 2H), 6.66 (tt, J = 7.3, 1.1 Hz, 1H), 6.61 – 6.55 (m, 2H), 3.45 (p, J = 6.2 Hz, 1H), 1.57 (dp, J = 8.5, 4.1 Hz, 1H), 1.46 – 1.24 (m, 7H), 1.18 (d, J = 6.3 Hz, 3H), 0.94 – 0.86 (m, 3H). ^{13}C NMR (101 MHz, CDCl$_3$) δ 147.74, 129.28, 116.76, 113.09, 48.49, 37.22, 31.92, 25.87, 22.68, 20.80, 14.07. HRMS calculated for C$_{13}$H$_{22}$N$^+$ 192.1747 [M+H], found 192.1754.
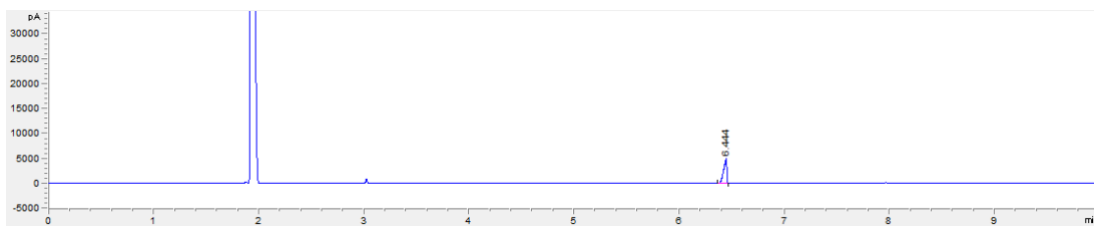
13a

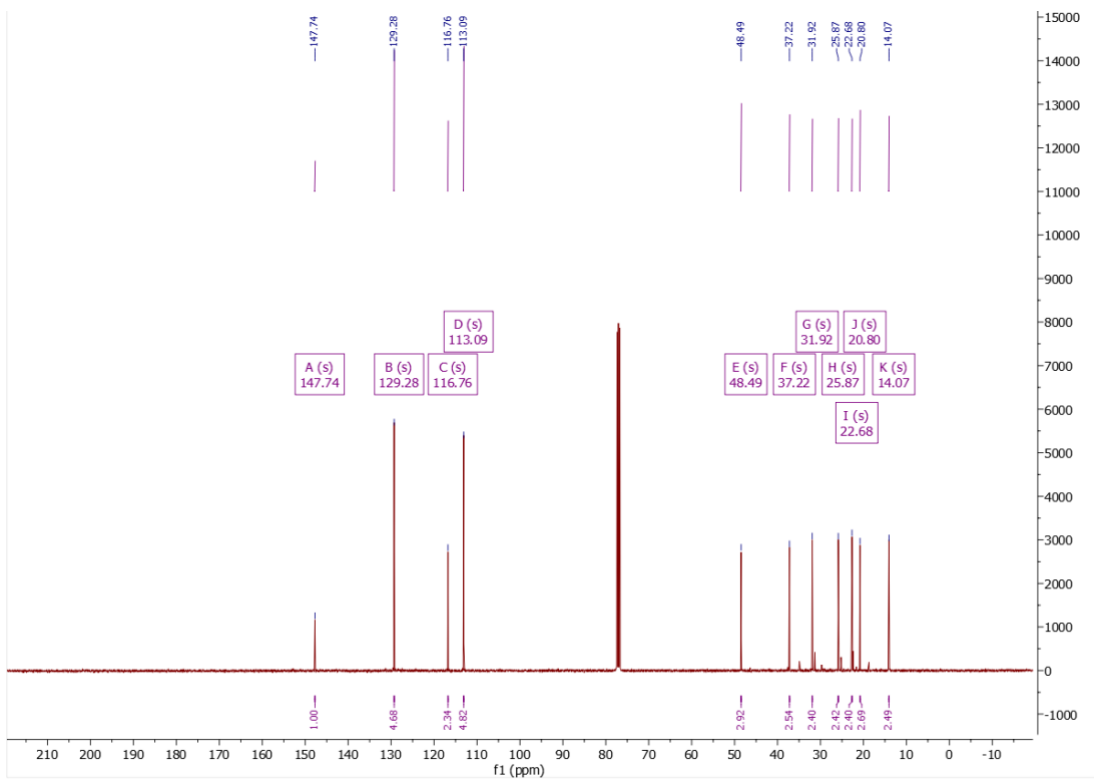**N-(hexan-2-yl)aniline, 13a** (Isolated yield 46.8 mg, 27%, Brown Oil)**:** ^{1}H NMR (400 MHz, CDCl$_3$) δ 7.21 – 7.11 (m, 2H), 6.66 (tt, J = 7.3, 1.1 Hz, 1H), 6.62 – 6.54 (m, 2H), 3.45 (h, J = 6.2 Hz, 1H), 1.64 – 1.51 (m, 1H), 1.37 (ddd, J = 13.5, 6.9, 4.3 Hz, 5H), 1.18 (d, J = 6.3 Hz, 3H), 0.91 (t, J = 7.0 Hz, 3H). ^{13}C NMR (101 MHz, CDCl$_3$) δ 147.85, 129.40, 116.88, 113.21, 48.58, 37.07, 28.50, 22.90, 20.93, 13.96. HRMS calculated for C$_{12}$H$_{20}$N$^+$ 178.1590 [M+H], found 178.1582.
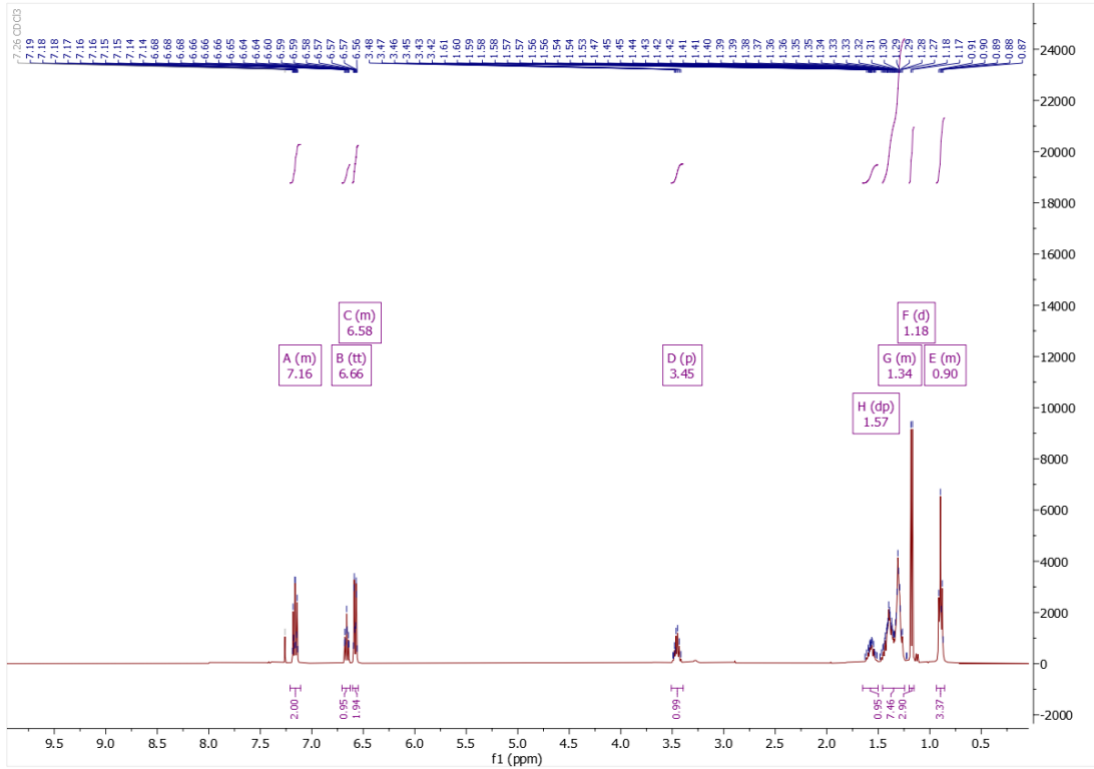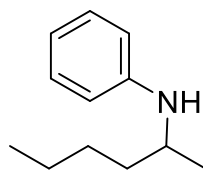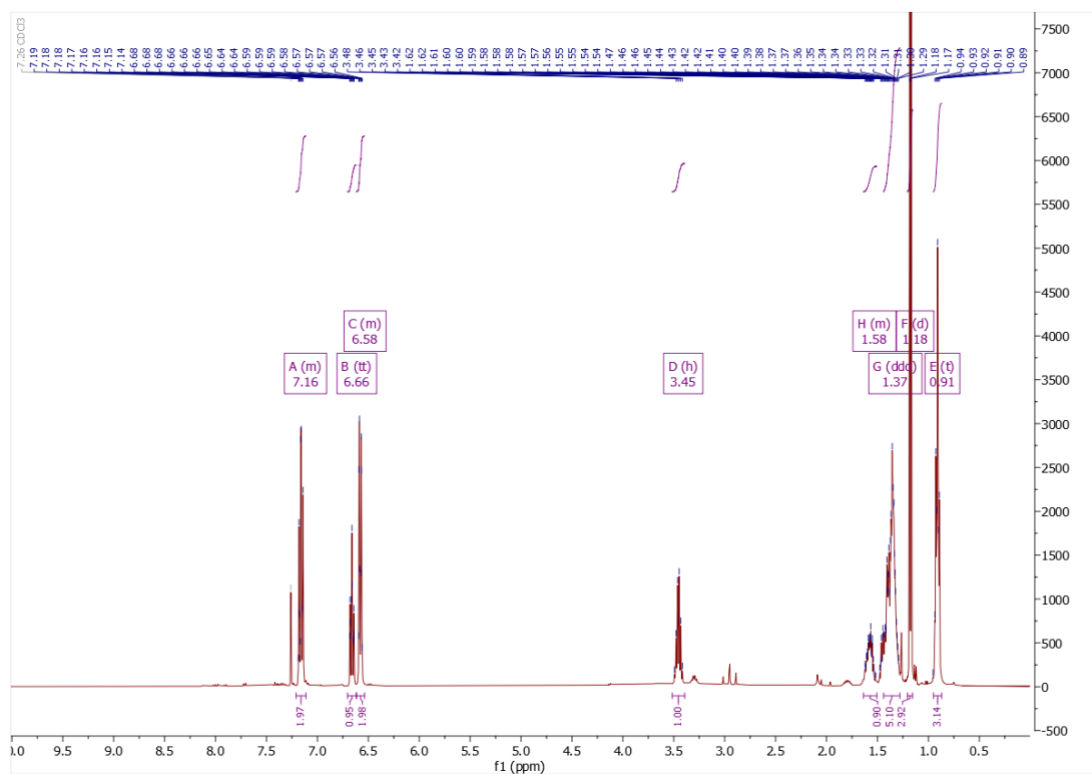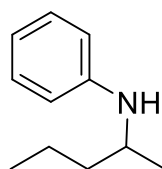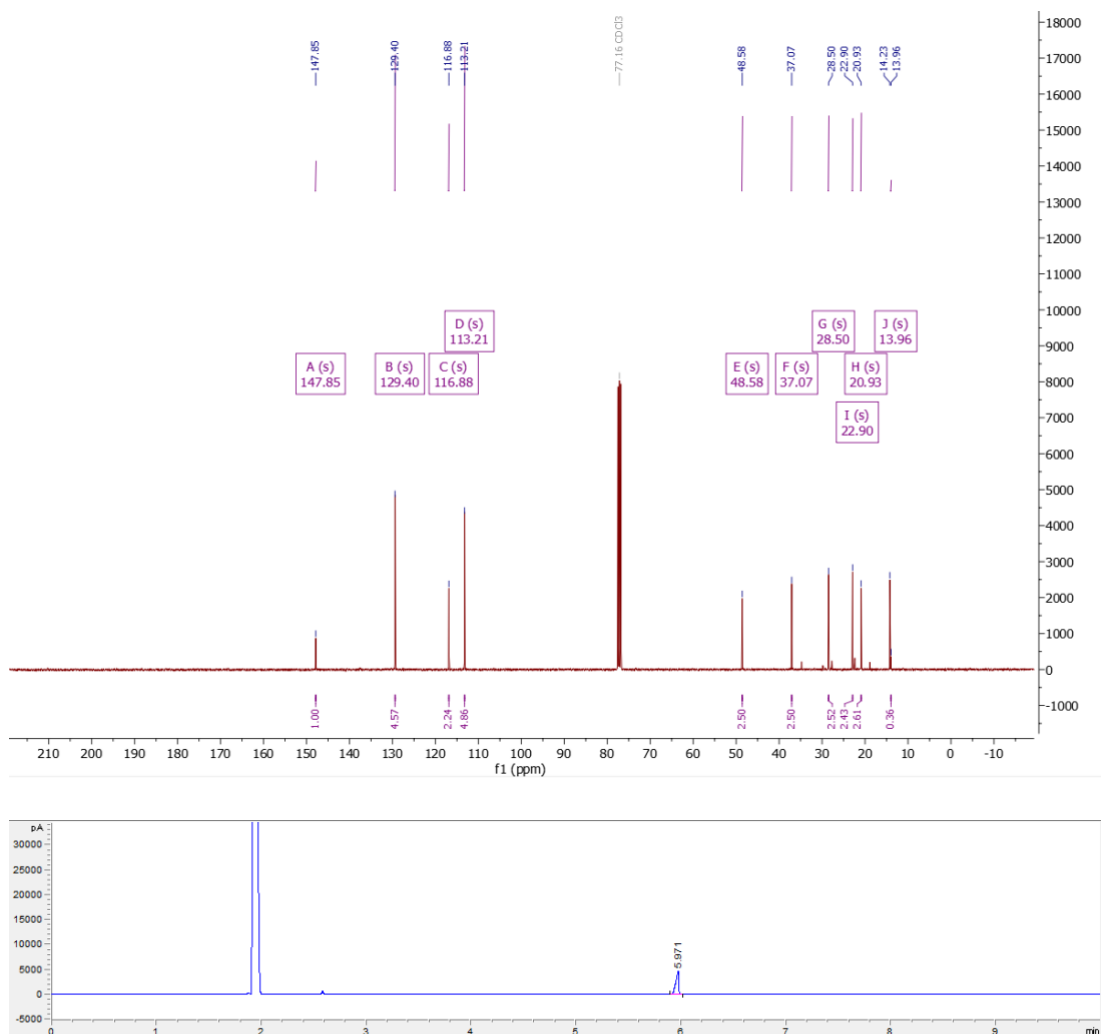
14a

N-(pentan-2-yl)aniline, 14a (Isolated yield 98.4 mg, 60%, Brown Oil)**:** ^{1}H NMR (400 MHz, CDCl$_3$) δ 7.21 − 7.11 (m, 2H), 6.66 (tt, J = 7.2, 1.1 Hz, 1H), 6.62 − 6.54 (m, 2H), 3.47 (h, J = 6.2 Hz, 1H), 1.56 (qdd, J = 11.7, 6.2, 2.4 Hz, 1H), 1.49 − 1.35 (m, 3H), 1.18 (d, J = 6.3 Hz, 3H), 0.94 (t, J = 7.1 Hz, 3H). ^{13}C NMR (101 MHz, CDCl$_3$) δ 147.79, 129.36, 116.86, 113.19, 48.30, 39.53, 20.85, 19.42, 14.22. HRMS calculated for C$_{11}$H$_{18}$N$^+$ 164.1434 [M+H], found 164.1434.
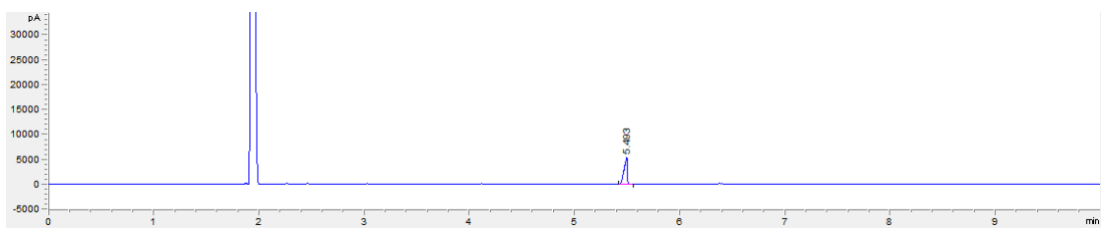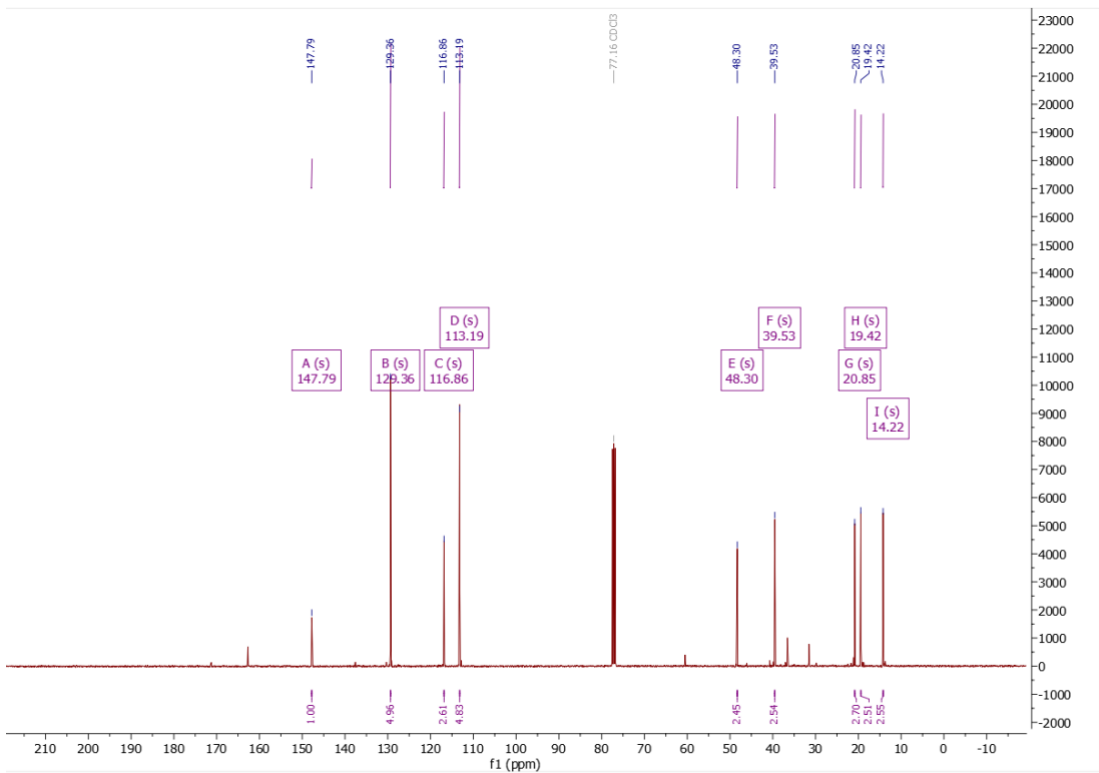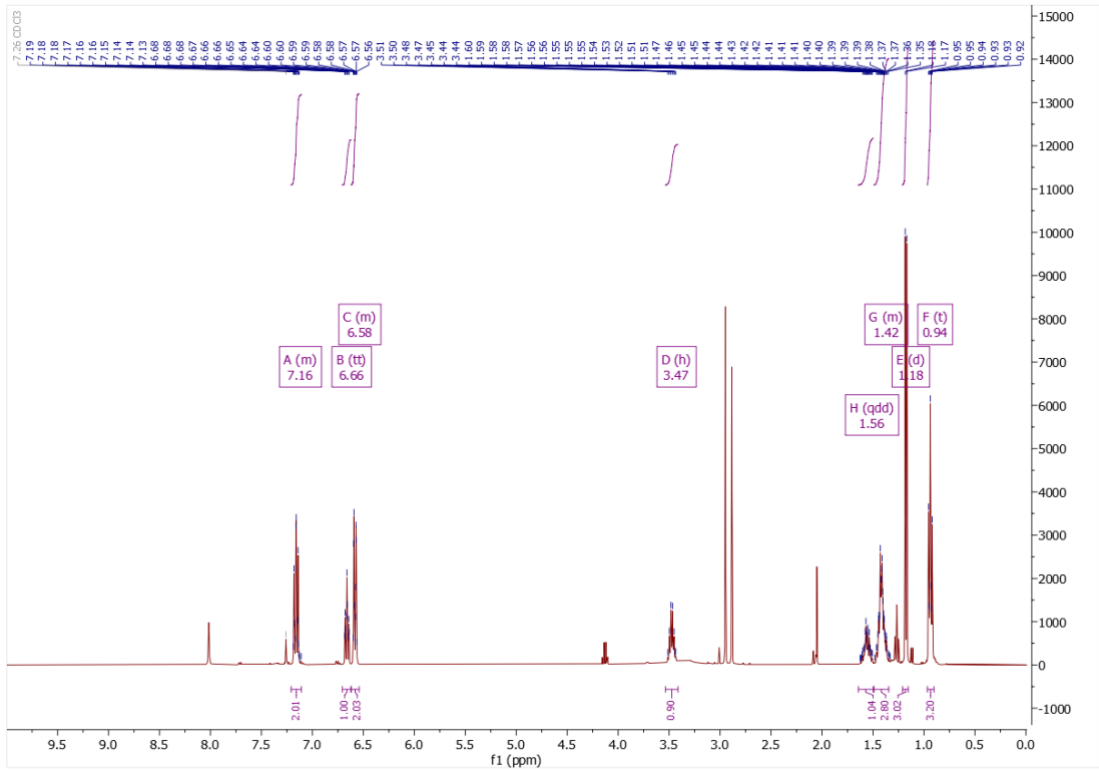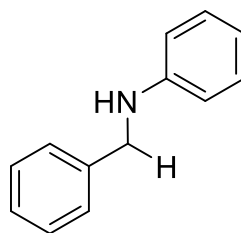
16a

N-benzylaniline, 16a (Isolated yield 149.3 mg, 82%, Brown Oil)**:** ^{1}H NMR (400 MHz, CDCl$_3$) δ 7.45 – 7.36 (m, 4H), 7.36 – 7.29 (m, 1H), 7.25 – 7.18 (m, 2H), 6.81 – 6.75 (m, 1H), 6.73 – 6.63 (m, 2H), 4.37 (s, 2H). ^{13}C NMR (101 MHz, CDCl$_3$) δ 148.24, 139.54, 129.34, 128.71, 127.58, 127.30, 117.62, 112.92, 48.37. HRMS calculated for C$_{13}$H$_{14}$N$^+$ 184.1121 [M+H], found 184.1116.
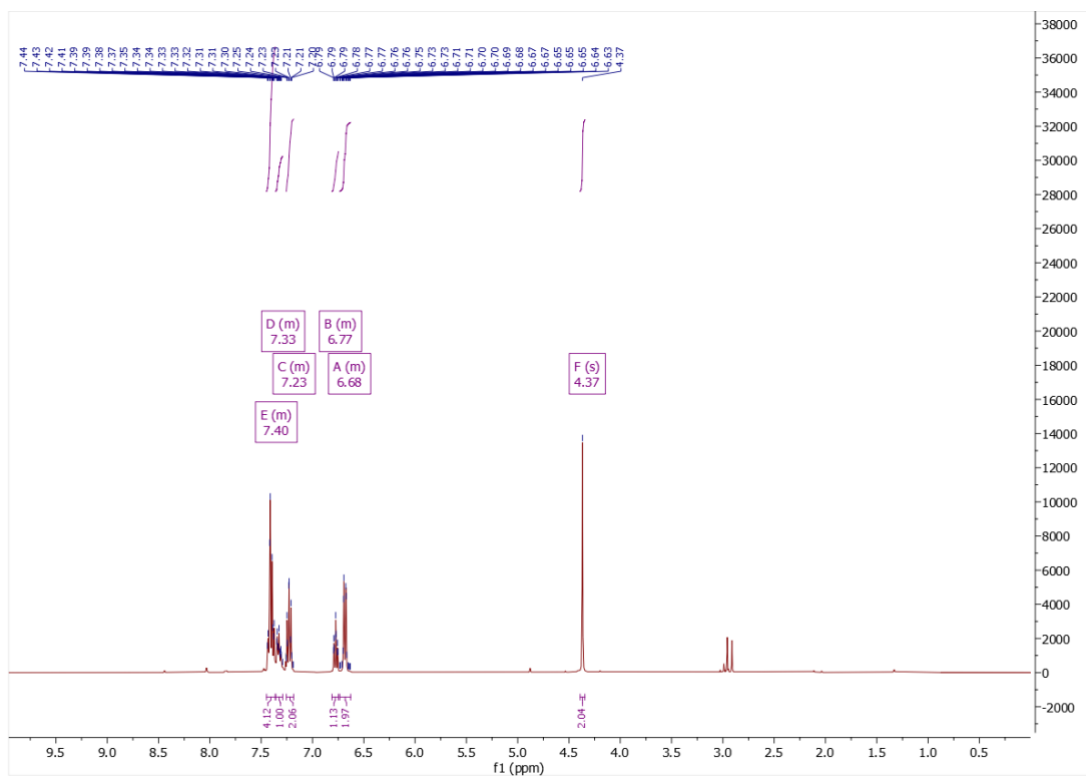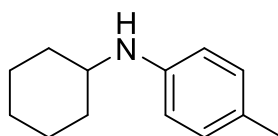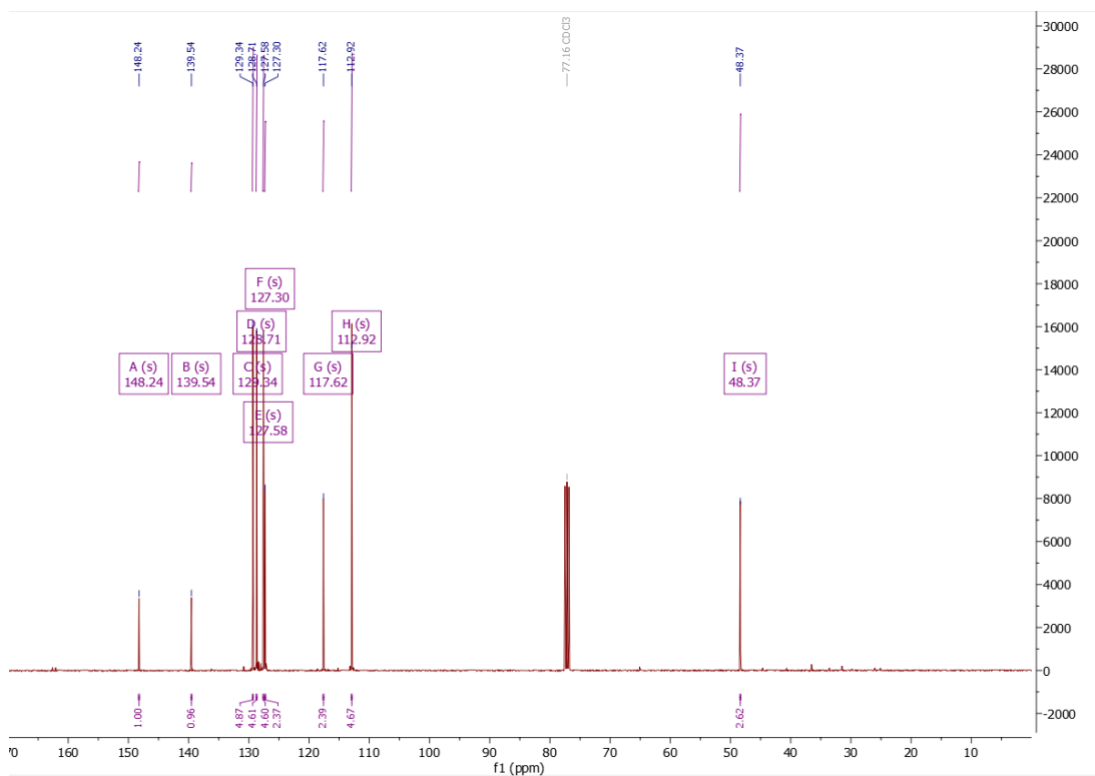
N-cyclohexyl-4-methylaniline, 9b (Isolated yield 92.5 mg, 49%, Brown Oil)**:** ^{1}H NMR (400 MHz, CDCl$_3$) δ 7.03 − 6.94 (m, 2H), 6.58 − 6.49 (m, 2H), 3.23 (tt, J = 10.1, 3.7 Hz, 1H), 2.24 (s, 3H), 2.07 (dt, J = 12.8, 3.8 Hz, 2H), 1.81 − 1.60 (m, 3H), 1.44 − 1.31 (m, 2H), 1.29 − 1.09 (m, 3H). ^{13}C NMR (101 MHz, CDCl$_3$) δ 145.09, 129.76, 126.17, 113.55, 52.10, 33.56, 26.01, 25.08, 20.39. HRMS calculated for C$_{13}$H$_{20}$N$^+$ 190.1590 [M+H], found 190.1576.
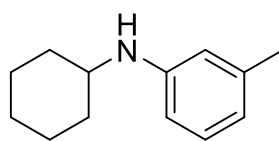
9c

N-cyclohexyl-3-methylaniline, 9c (Isolated yield 93.7 mg, 50%, Brown Oil): ^{1}H NMR (400 MHz, CDCl$_3$) δ 7.10 – 6.99 (m, 1H), 6.50 (d, J = 7.4 Hz, 1H), 6.45 – 6.38 (m, 2H), 3.26 (tt, J = 10.2, 3.7 Hz, 1H), 2.28 (s, 3H), 2.11 – 2.02 (m, 2H), 1.77 (dp, J = 11.8, 3.9 Hz, 2H), 1.71 – 1.62 (m, 1H), 1.45 – 1.32 (m, 2H), 1.30 – 1.09 (m, 3H). ^{13}C NMR (101 MHz, CDCl$_3$) δ 147.54, 139.10, 129.24, 117.89, 114.03, 110.39, 51.75, 33.65, 26.07, 25.15, 21.76. HRMS calculated for C$_{13}$H$_{20}$N$^+$ 190.1590 [M+H], found 190.1594
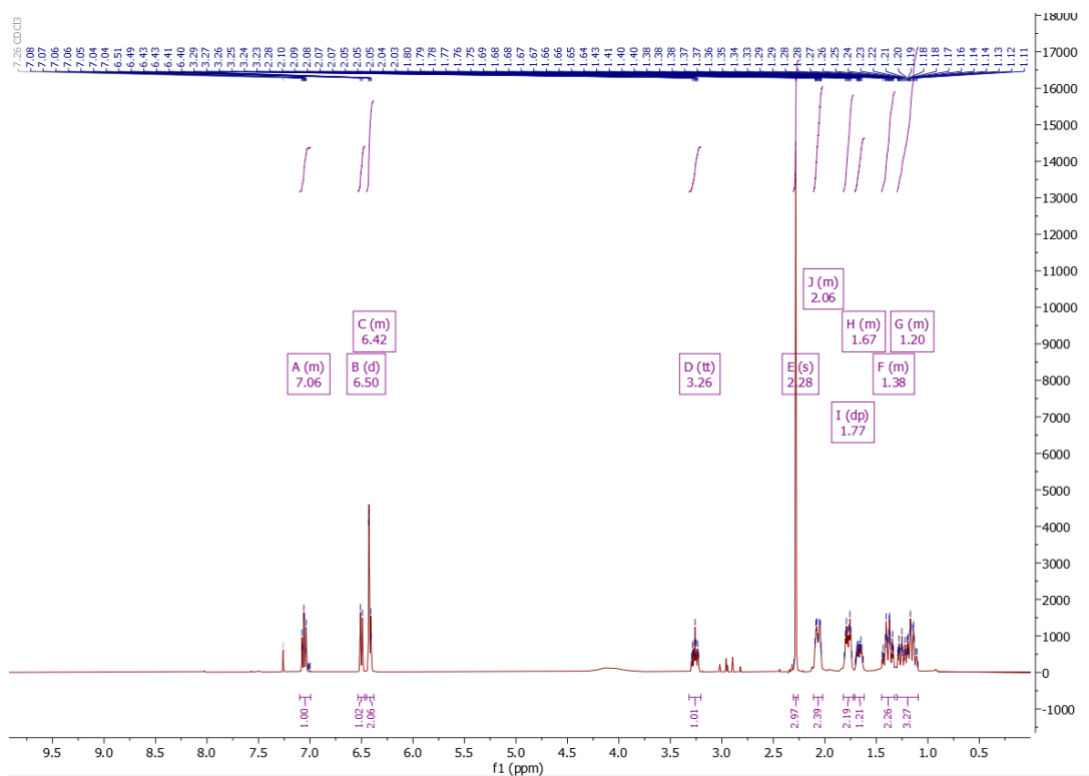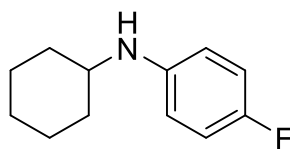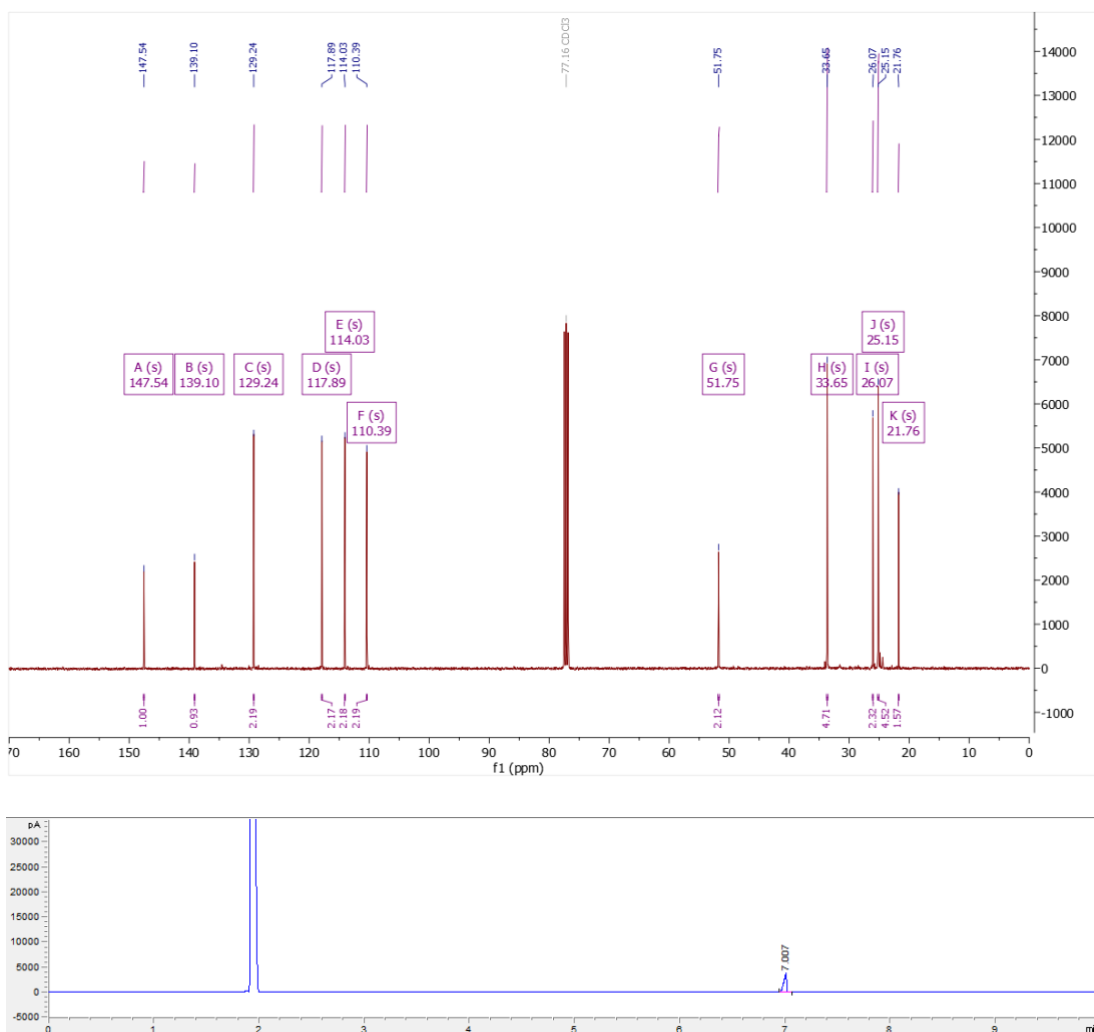
N-cyclohexyl-4-fluoroaniline, 9e (Isolated yield 61 mg, 32%, Brown Oil): ^{1}H NMR (400 MHz, CDCl$_3$) δ 6.91 – 6.81 (m, 2H), 6.57 – 6.47 (m, 2H), 3.17 (tt, J = 10.2, 3.7 Hz, 1H), 2.10 – 1.98 (m, 2H), 1.76 (dt, J = 13.2, 3.9 Hz, 2H), 1.70 – 1.60 (m, 1H), 1.42 – 1.29 (m, 2H), 1.24 (tdt, J = 11.8, 7.5, 3.2 Hz, 1H), 1.12 (tdd, J = 12.6, 10.3, 3.5 Hz, 2H). ^{13}C NMR (101 MHz, CDCl$_3$) δ 155.65 (d, J = 234.4 Hz), 143.83 (d, J = 1.9 Hz), 115.74 (d, J = 22.3 Hz), 114.23 (d, J = 7.3 Hz), 52.60, 33.58, 26.05, 25.14. HRMS calculated for C$_{12}$H$_{17}$FN$^+$ 194.1340 [M+H], found 194.1331.
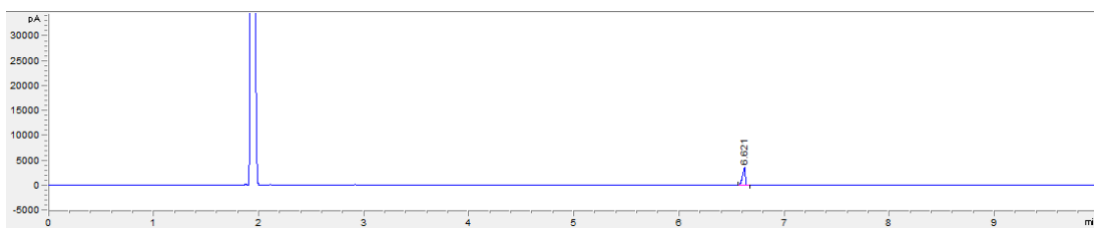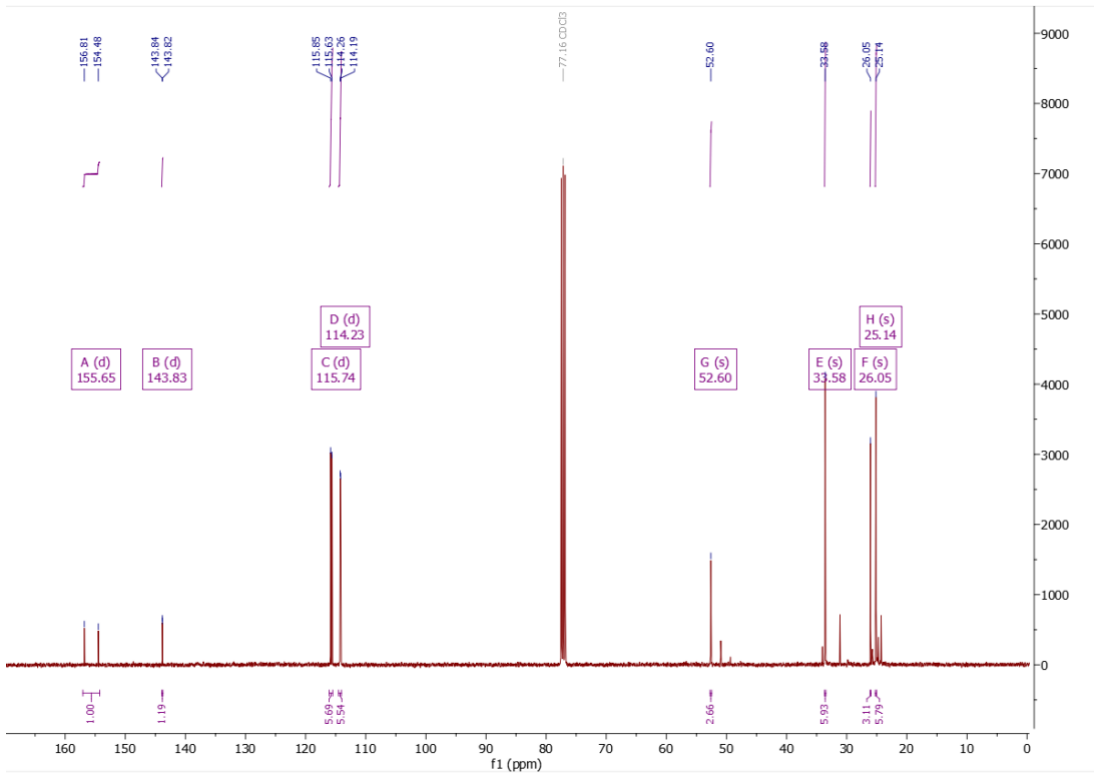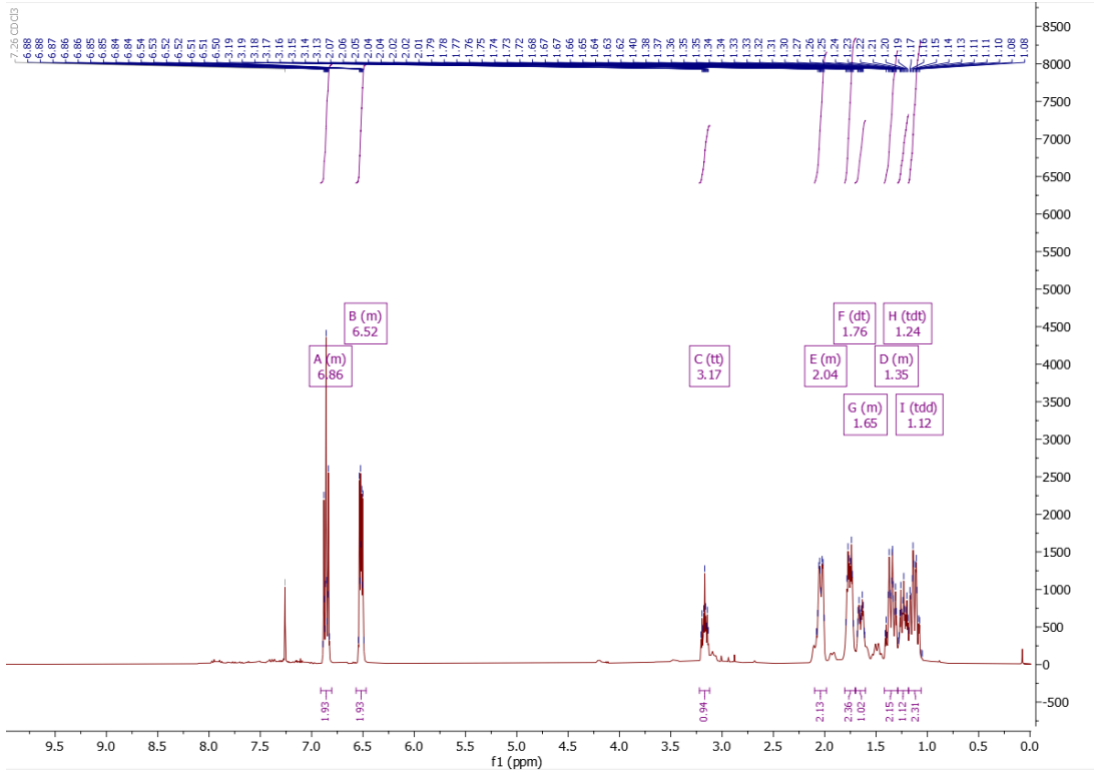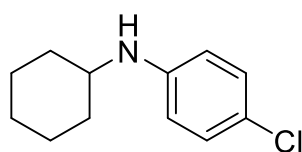
9g

N-cyclohexyl-4-chloroaniline, 9g (Isolated yield 147.9 mg, 70%, Brown Oil): ^{1}H NMR (400 MHz, CDCl$_3$) δ 7.15 – 7.05 (m, 2H), 6.55 – 6.46 (m, 2H), 3.20 (tt, J = 10.2, 3.8 Hz, 1H), 2.11 – 1.98 (m, 2H), 1.77 (dp, J = 11.6, 3.9 Hz, 2H), 1.66 (dq, J = 12.8, 3.4 Hz, 1H), 1.44 – 1.31 (m, 2H), 1.24 (tt, J = 11.9, 3.3 Hz, 1H), 1.14 (tdd, J = 12.5, 10.4, 3.6 Hz, 2H). ^{13}C NMR (101 MHz, CDCl$_3$) δ 145.93, 129.07, 121.25, 114.23, 51.90, 33.31, 25.89, 24.99. HRMS calculated for C$_{12}$H$_{17}$ClN$^+$ 210.1044 [M+H], found 210.1041.
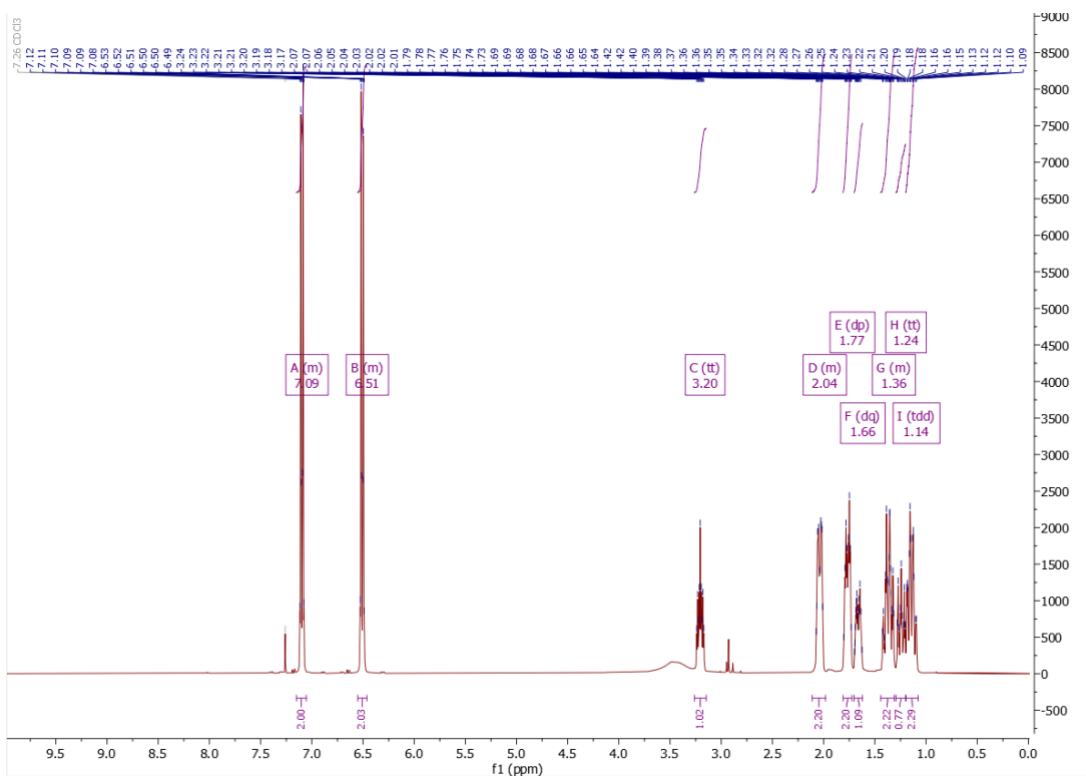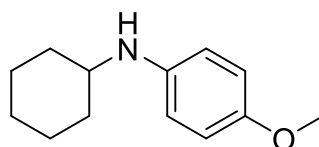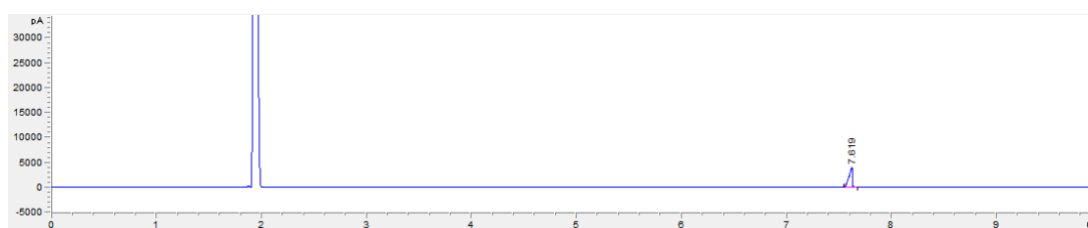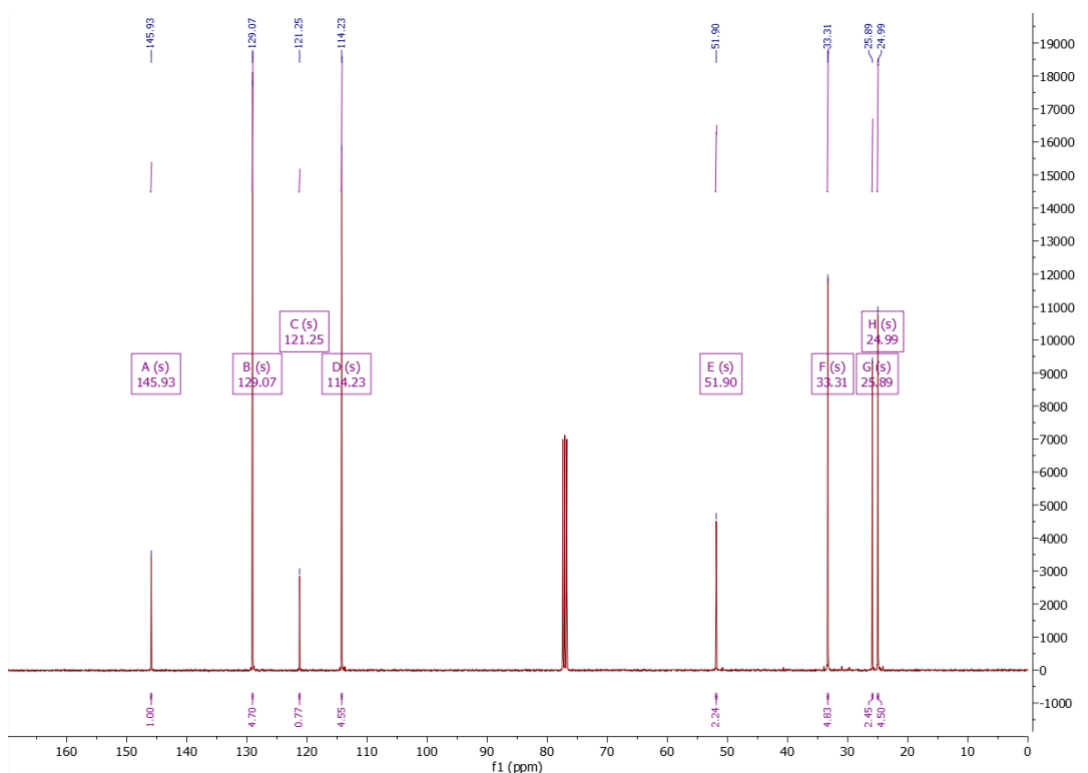
9i

N-cyclohexyl-4-methoxyaniline, 9i (Isolated yield 118.8 mg, 58%, Brown Oil): ^{1}H NMR (400 MHz, CDCl$_3$) δ 6.81 – 6.71 (m, 2H), 6.59 (dd, J = 9.4, 2.7 Hz, 2H), 3.74 (s, 3H), 3.16 (tt, J = 10.3, 3.8 Hz, 1H), 2.11 – 1.99 (m, 2H), 1.75 (dp, J = 11.5, 3.9 Hz, 2H), 1.70 – 1.58 (m, 1H), 1.41 – 1.29 (m, 2H), 1.27 – 1.18 (m, 1H), 1.18 – 1.06 (m, 2H). ^{13}C NMR (101 MHz, CDCl$_3$) δ 152.03, 141.36, 115.07, 114.93, 55.84, 52.99, 33.58, 25.99, 25.08. HRMS calculated for C$_{13}$H$_{20}$NO$^+$ 206.1539 [M+H], found 206.1531.
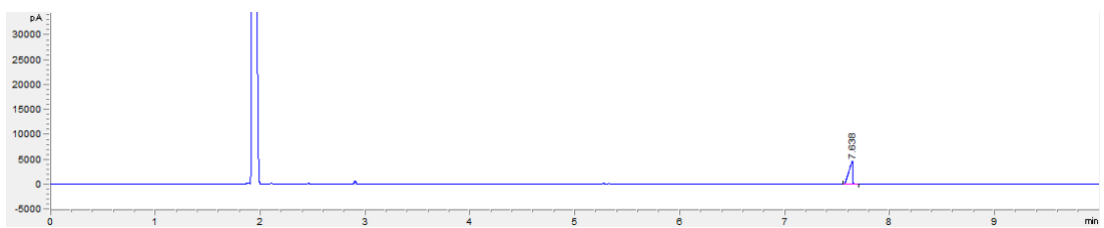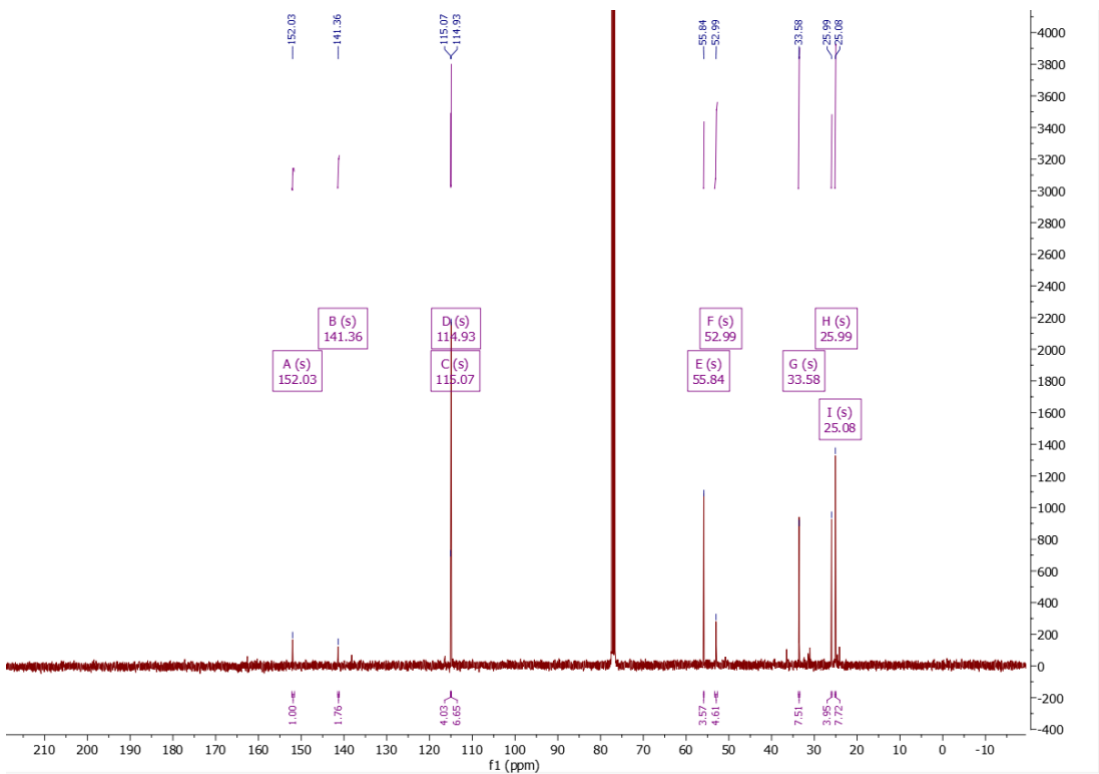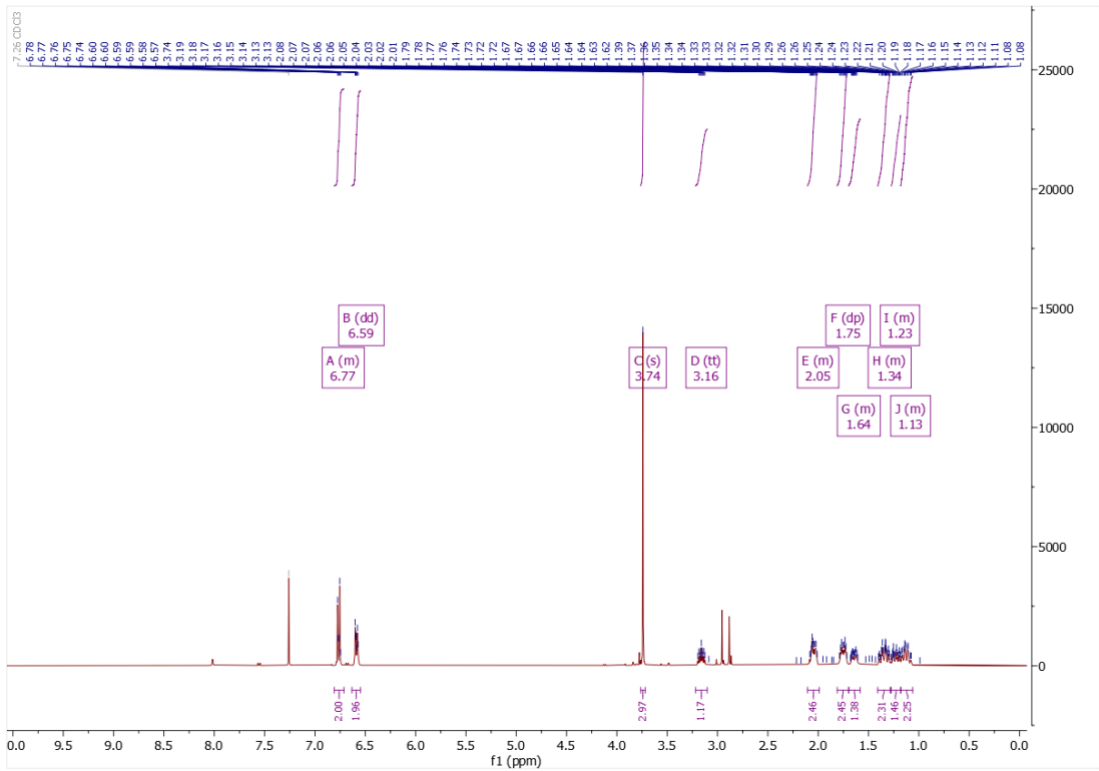
6.6.4 Biotransformation Protocol

A 500 μL reaction contained 20 mM D-glucose, 0.1 mg mL-1 GDH (Codexis, CDX GDH-901), 0.5 mM NADP$^+$, 1 mg mL^{-1} purified RedAm, 10 mM ketone, 10 mM amine donor, and 10% v/v DMSO in 100 mM phosphate buffer pH 7. Reactions were incubated at 30 °C with 250 r.p.m. shaking for 18 h to 24 h, after which they were quenched by the addition of 100 μL 5M NaOH and extracted twice with 500 μL diethyl ether. The organic fractions where combined, dried over MgSO$_4$ and analysed by GC-FID.

6.6.5 GC-FID Analysis Conditions

Samples were analysed using a HP-1 column, injector temperature of 200°C, a helium flow rate of 1.3 mL min^{-1}, oven temperature 50 °C – 300 °C with a ramp of 25 °C min^{-1}, and a detector temperature of 250 °C.

6.6.6 GC-FID Chromatograms of Biotransformations
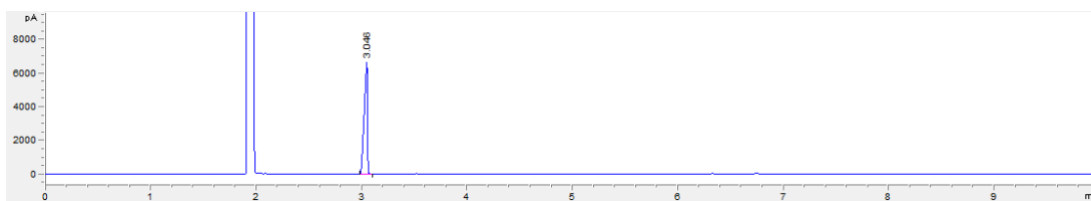
Figure 140: GC-FID chromatogram of cyclohexanone
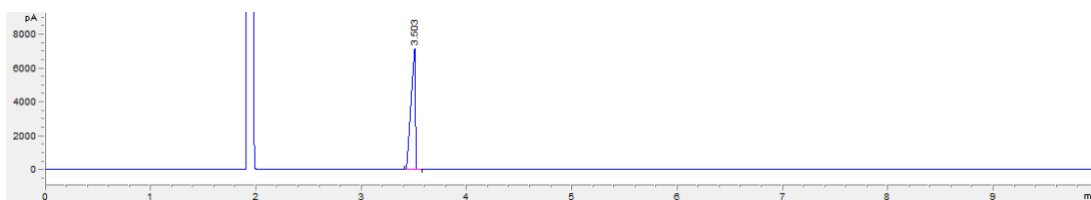
Figure 141: GC-FID chromatogram of aniline
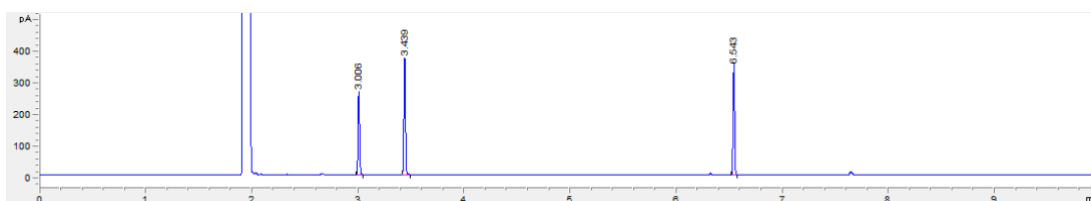
Figure 142: GC-FID chromatogram for the biotransformation of the reductive amination between cyclohexanone and aniline
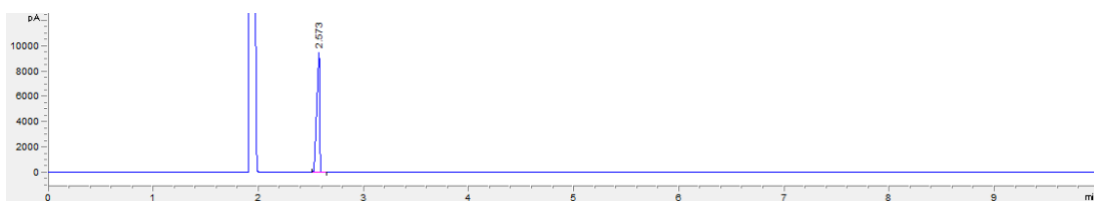
Figure 143: GC-FID chromatogram of cyclopentanone

Figure 144: GC-FID chromatogram for the biotransformation of the reductive amination between cyclopentanone and aniline
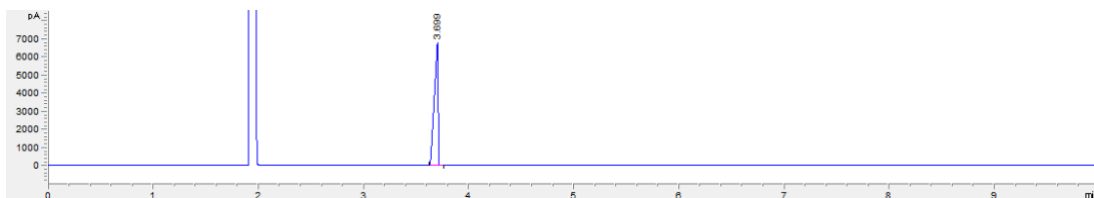
Figure 145: GC-FID chromatogram of cycloheptanone
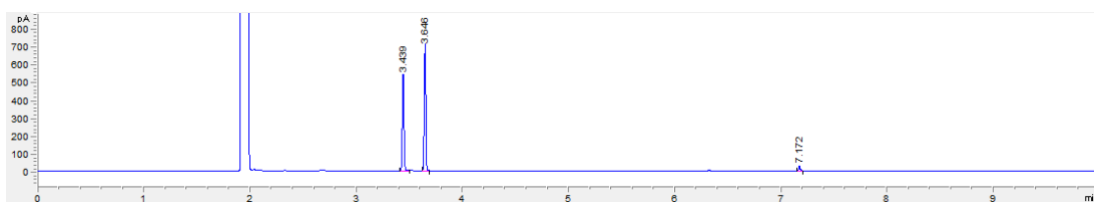
Figure 146: GC-FID chromatogram for the biotransformation of the reductive amination between cycloheptanone and aniline

Figure 147: GC-FID chromatogram of 2-heptanone
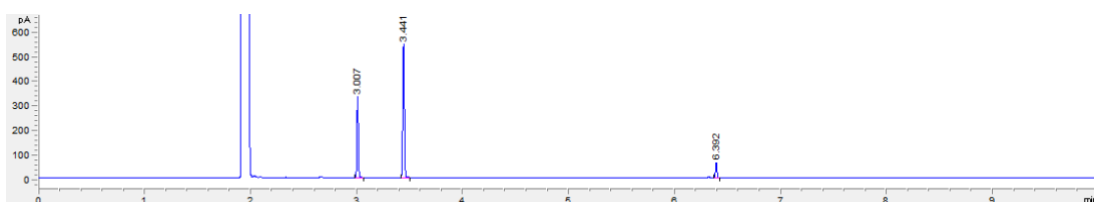
Figure 148: GC-FID chromatogram for the biotransformation of the reductive amination between 2-heptanone and aniline
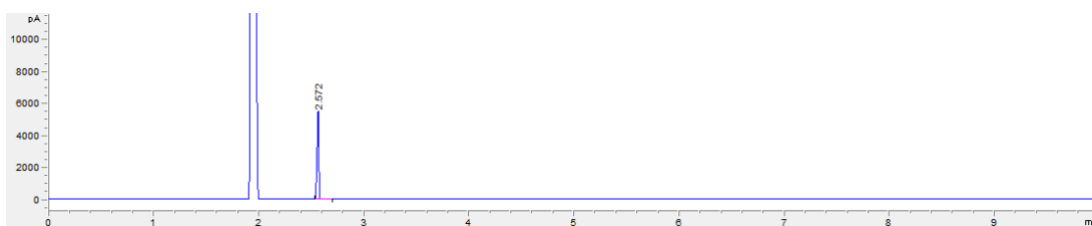
Figure 149: GC-FID chromatogram of 2-hexanone
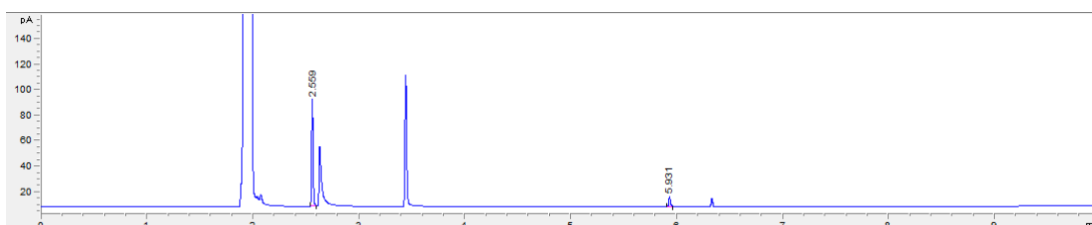
Figure 150: GC-FID chromatogram for the biotransformation of the reductive amination between 2-hexanone and aniline
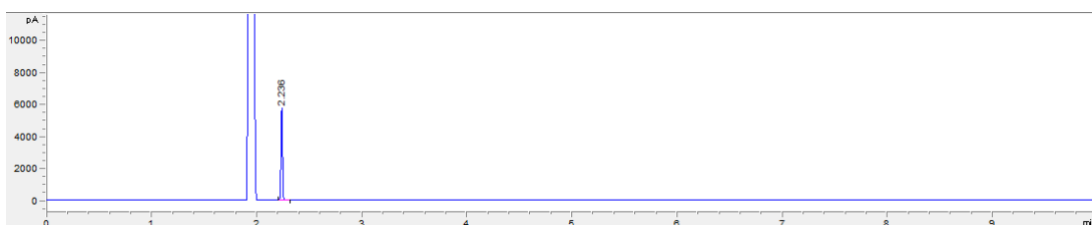
Figure 151: GC-FID chromatogram of 2-pentanone
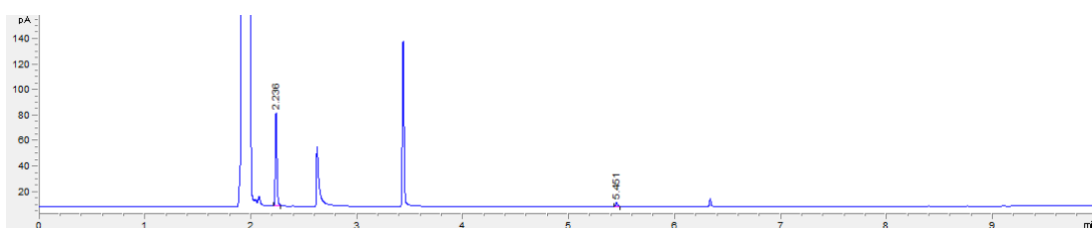
Figure 152: GC-FID chromatogram for the biotransformation of the reductive amination between 2-pentanone and aniline
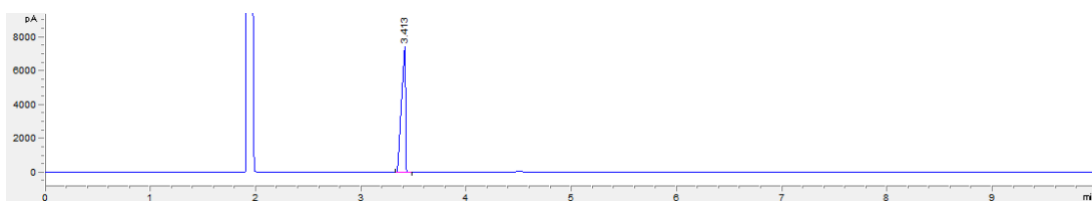
Figure 153: GC-FID chromatogram of benzaldehyde
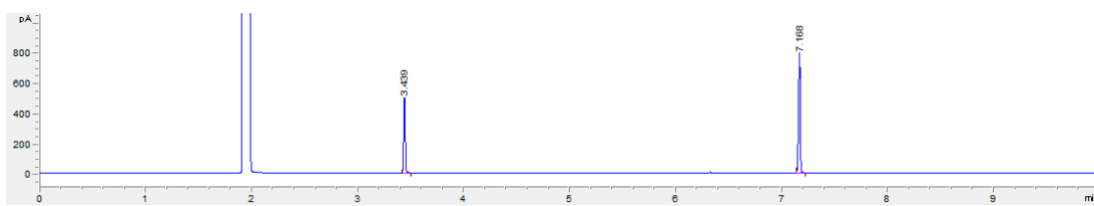
Figure 154: GC-FID chromatogram for the biotransformation of the reductive amination between benzaldehyde and aniline
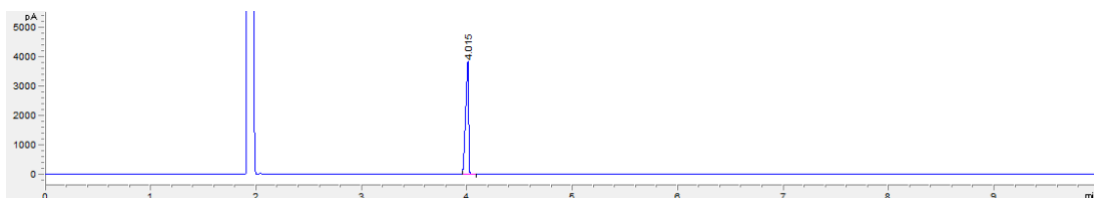
Figure 155: GC-FID chromatogram of p-toluidine
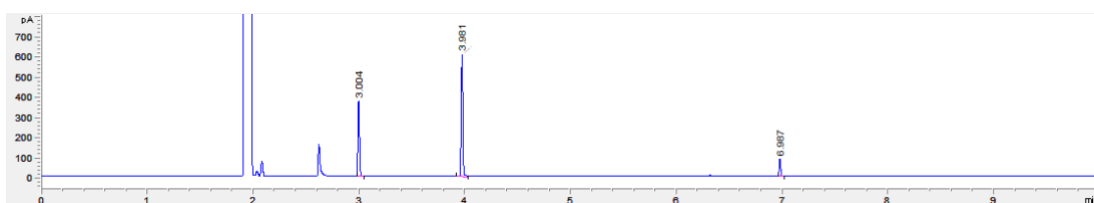
Figure 156: GC-FID chromatogram for the biotransformation of the reductive amination between cyclohexanone and p-toluidine
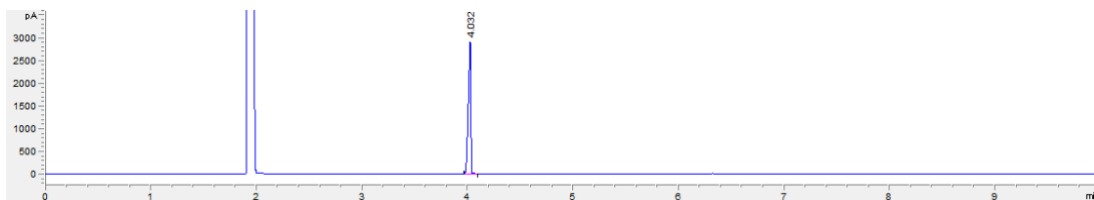
Figure 157: GC-FID chromatogram of m-toluidine
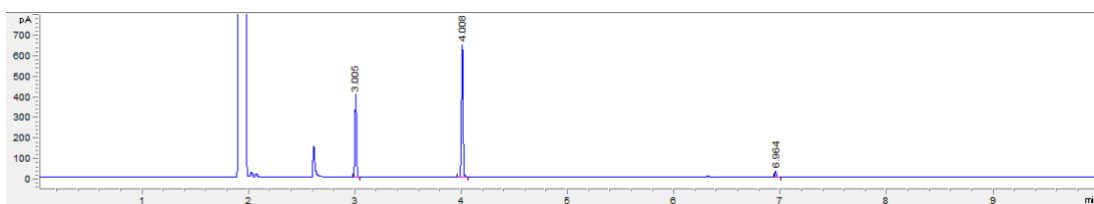
Figure 158: GC-FID chromatogram for the biotransformation of the reductive amination between cyclohexanone and m-toluidine
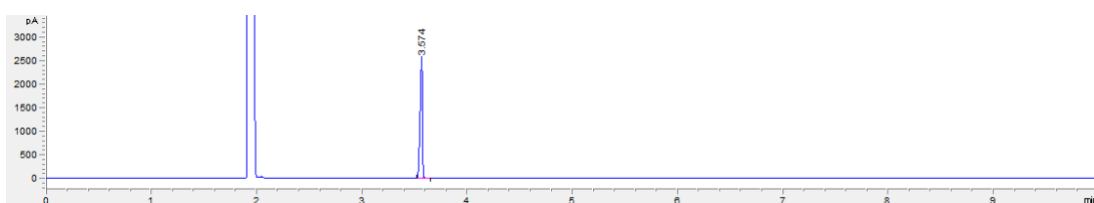
Figure 159: GC-FID chromatogram of 4-fluoroaniline
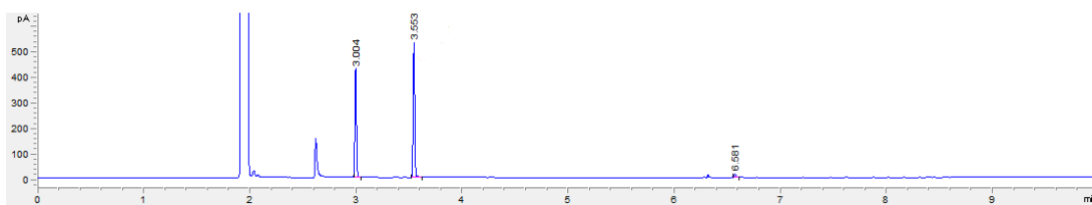
Figure 160: GC-FID chromatogram for the biotransformation of the reductive amination between cyclohexanone and 4-fluoroaniline
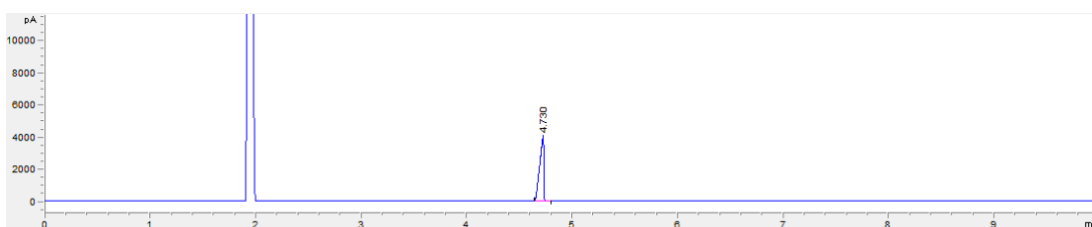
Figure 161: GC-FID chromatogram of 4-chloroaniline
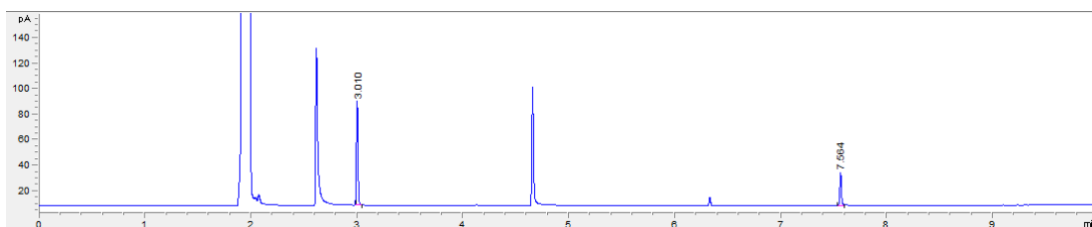
Figure 162: GC-FID chromatogram for the biotransformation of the reductive amination between cyclohexanone and 4-chloroaniline
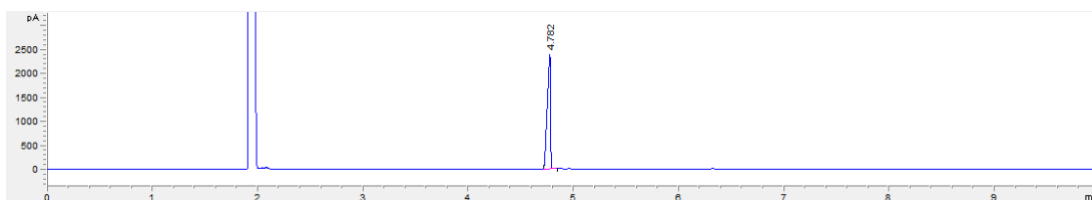
Figure 163: GC-FID chromatogram of p-anisidine
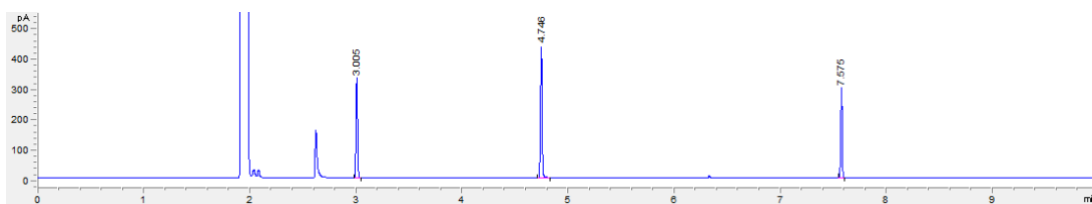
Figure 164: GC-FID Chromatogram for the Biotransformation of the Reductive Amination between Cyclohexanone and p-Anisidine

6.6.7 Calibration Curve of the Product for the Reductive Amination between Benzaldehyde and Aniline

Due to the overlap of benzaldehyde and aniline in the GC-FID chromatograms, a calibration curve of the synthesised product was produced to calculate the conversion. The area from the GC trace was calculated and the concentration value output from the calibration curve was then doubled to account for the dilution factor on extraction from the biotransformation.

Plot: GC-FID Peak Area vs Concentration / mM

$y = 286.9x - 27.689$
$R^2 = 0.9988$
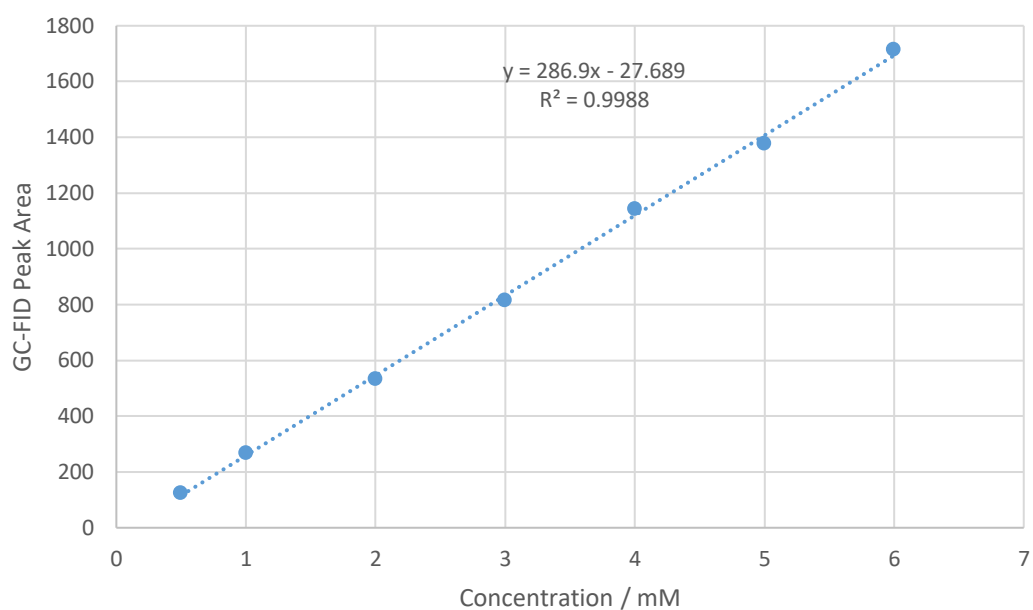
Chapter 7: Conclusions and Outlooks

Imine reductase and reductases aminases have both been well researched since their discoveries in 2010 and 2017 respectively. IREDs have shown great improvement from their initial capabilities on the selective reduction of 2-phenylpyrroline. Through concentrated efforts carried out both by academic groups and industry, the panel of accessible IREDs has been greatly increased to show activity towards a large panel of cyclic and acyclic imines.[50–52,60,62,84–88]

Imine reductases have also been well explored for the use in reductive amination reactions, however these typically require the use of an excess of amine to drive the equilibrium of the reaction and preform the imine *in situ*. The discovery of the reductive aminase in 2017 aided in the capability to carry out bioreductive aminations.[103] Unlike the imine reductases, the RedAms were shown to be capable of carrying out reductive aminations at stoichiometric ratios of carbonyls and amines. The RedAms were also shown to be capable of accessing reductive aminations with a wider substrate scope of carbonyls and amines that had been previously shown with IREDs.[52,81,103,108]

Despite this, the activity of both IREDs and RedAms has been shown to be highly substrate dependent. Addition of substituents (even small ones) can result in large decreases (or increases) in activity and can even have an effect on stereoselectivity, by either resulting in a decrease in ee values, or inverting stereoselectivity. Enzyme engineering of these enzymes is one route in overcoming these selectivity issues by designing and evolving the enzymes towards a targeted synthesis. Both GSK[80] and Pfizer[101] have showed this for the engineering of an IRED and a RedAm respectively towards the large-scale reductive amination between a specific carbonyl and a specific amine.

The mechanism for the reductive aminase was determined by Sharma *et al.*[91] highlighting the catalytically important active site residues. However, outside these three residues, the roles of other active site residues was not determined. In this report, an investigation into a selection of the active site residues of the RedAm from

Ajellomyces dermatitdis has been investigated through mutagenesis of the residues to alanine.

It was shown that through single point mutations that the stereoselectivity and activity of *Ad*RedAm towards the reduction of cyclic imines can be controlled. Variants W208A and M237G were stand out mutations from the panel tested. W208A showed an improvement on wild type activity and selectivity towards the reduction of 5-membered cyclic imines, retaining (*S*)-selectivity across the panel of substrates and showing activity towards 2-(4-methoxyphenyl)pyrroline where the wild type did not. M237G showed an inversion in stereoselectivity compared to the wild type for the reduction of 2-phenylpyrroline which was conserved against all active substrates. Despite observing no different in the stereoselectivity across the panel of enzymes for the reduction of the 6-membered cyclic imine, the activity was improved on with half of the variants reaching full conversion (with the wild type only reaching 30%).

The activity of W208A was then tested further and shown to be active for the reductive amination reactions containing aniline (and aniline derivatives) as the amine donor. This reductive amination was a great improvement on the wild type which showed no activity towards the reductive amination of cyclohexanone and aniline, but W208A showed a conversion of 56%.

To conclude, the possibility of improving the reductive aminase from *Ajellomyces dermatitdis* in terms of activity, stereoselectivity, and substrate scope through active site engineering has been shown. Six positions were investigated within the active site with two positions (208 and 237) showing the best results. There is still space to gain a further understanding of these residues and for development of the active site through further mutagenesis to improve the capabilities of these enzymes. It has been seen that from the substrate scope tested with the *Ad*RedAm variants, that there is still a dependency on the substrate when it comes to activity and stereoselectivity.

The future of this work lies in further exploring the residues of the active site. Two other residues have been identified from computational studies as potential

engineering positions; leucine at 170 and leucine at 173. Incorporating these two positions with the six already tested and carrying out site-saturation mutagenesis would allow for the exploration of other residues at each position. For example, whereas alanine at position 208 allows for the reductive amination with aniline when tryptophan does not, alanine may not be the optimal residue in that position with other amine donors.

Combinations of mutations is also a potential route to explore. As seen with the in-silico modelling in section 5.5, positions 239 and 240 have both moved in space when compared to the wild type. Combining mutations at both these positions may result in different changes in activity and stereoselectivity, as well as could be a way to alter the substrate scope of these enzymes further.

Improvement of the activity of the reductive aminase also provides potential to access the reductive amination products using the carbonyls mentioned in Chapter 4. It has been shown that activity can be created towards more complicated substrates such as aniline where the wild type shows no initial activity. Most of the carbonyls tested in Chapter 4 were unsuccessful candidates for reductive amination however, potentially through engineering, it could be possible to revisit these substrates.

Although IREDs and RedAms have been well established as valuable tools for accessing primary, secondary, and tertiary amines, there implementation into industrial processes has been slow. The examples shown by Pfizer and GSK, although impressive, required extensive engineering to make the enzymes suitable for the substrates in mind and the desired process conditions by each company. Hopefully with recent advances in computational tools such as AlphaFold[109], the process of developing engineered enzymes can be sped up to allow for improved implementation into industrial processes.

Chapter 8: References

1   R. A. Sheldon, D. Brady and M. L. Bode, *Chem. Sci.*, 2020, **11**, 2587-2605.

2   C. M. Clouthier and J. N. Pelletier, *Chem. Soc. Rev.*, 2012, **41**, 1585–1605.

3   G. W. Huisman and S. J. Collier, *Curr. Opin. Chem. Biol.*, 2013, **17**, 284–292.

4   M. Sharma, J. Mangas-Sanchez, N. J. Turner and G. Grogan, *Adv. Synth. Catal.*, 2017, **359**, 2011–2025.

5   G. W. Zheng and J. H. Xu, *Curr. Opin. Biotechnol.*, 2011, **22**, 784–792.

6   S. Wu, R. Snajdrova, J. C. Moore, K. Baldenius and U. T. Bornscheuer, *Angew. Chemie - Int. Ed.*, 2021, **60**, 88–119.

7   J. Chapman, A. E. Ismail and C. Z. Dinu, *Catalysts*, 2018, **8(6)**, 239-264.

8   F. H. Arnold, *Acc. Chem. Res.*, 1998, **31**, 125–131.

9   O. Kuchner and F. H. Arnold, *Trends Biotechnol.*, 1997, **15**, 523–530.

10   F. H. Arnold and A. A. Volkov, *Curr. Opin. Chem. Biol.*, 1999, **3**, 54–59.

11   R. O. M. A. de Souza, L. S. M. Miranda and U. T. Bornscheuer, *Chem. - A Eur. J.*, 2017, **23**, 12040–12063.

12   D. Ghislieri and N. J. Turner, *Top. Catal.*, 2014, **57**, 284–300.

13   J. H. Schrittwieser, S. Velikogne and W. Kroutil, *Adv. Synth. Catal.*, 2015, **357**, 1655–1685.

14   M. Höhne, *Nat. Cat.*, 2019, **2**, 841-842.

15   C. A. Willoughby and S. L. Buchwald, *J. Am. Chem. Soc.*, 1992, **114**, 19, 7562–7564.

16   C. A. Willoughby and S. L. Buchwald, *J. Am. Chem. Soc.*, 1994, **116**, 11703–11714.

17   O. Vassylyev, A. Panarello and J. G. Khinast, *Molecules*, 2005, **10**, 587-619

18   S. ¯ Kobayashi and H. Ishitani, *Chem. Rev.*, 1999, **99**, 1069–1094

19 M. J. Burk, Y. M. Wang and J. R. Lee, *J. Am. Chem. Soc.*, 1996, **118**, 5142–5143.

20 F. Y. Zhang, C. C. Pai and A. S. C. Chan, *J. Am. Chem. Soc.*, 1998, **120**, 5808–5809.

21 A. A. Boezio, J. Pytkowicz, A. Côté and A. B. Charette, *J. Am. Chem. Soc.*, 2003, **125**, 14260–14261.

22 Y. Zhang, D. Kong, R. Wang and G. Hou, *Org. Biomol. Chem.*, 2017, **15**, 3006-3012.

23 Z. Zhang, J. Mao, D. Zhu, F. Wu, H. Chen and B. Wan, *Catal. Commun.*, 2005, **6**, 785-787

24 T. Yasukawa, R. Masuda and S. Kobayashi, *Nat. Catal.*, 2019, **2**, 1088-1092

25 L. Rios-Solis, B. Mothia, S. Yi, Y. Zhou, M. Micheletti and G. J. Lye, *J. Mol. Catal. B Enzym.*, 2015, **120**, 100–110.

26 V. F. Batista, J. L. Galman, D. C. G. A. Pinto, A. M. S. Silva and N. J. Turner, *ACS Catal.*, 2018, **8**, 11889-11907

27 D. Ghislieri, A. P. Green, M. Pontini, S. C. Willies, I. Rowles, A. Frank, G. Grogan and N. J. Turner, *J. Am. Chem. Soc.*, 2013, **135**, 10863–10869.

28 K. E. Atkin, R. Reiss, V. Koehler, K. R. Bailey, S. Hart, J. P. Turkenburg, N. J. Turner, A. Marek Brzozowski and G. Grogan, *J. Mol. Biol.*, 2008, **384**, 1218-1231.

29 D. Ghislieri, D. Houghton, A. P. Green, S. C. Willies and N. J. Turner, *ACS Catal.*, 2013, **3**, 2869–2872.

30 S. Herter, F. Medina, S. Wagschal, C. Benhaïm, F. Leipold and N. J. Turner, *Bioorganic Med. Chem.*, 2018, **26**, 1338–1346.

31 O. Mayol, S. David, E. Darii, A. Debard, A. Mariage, V. Pellouin, J.-L. Petit, M. Salanoubat, V. de Berardinis, A. Zaparucha and C. Vergne-Vaxelaire, *Catal. Sci. Technol.*, 2016, **6**, 7421–7428.

32 M. J. Abrahamson, E. Vázquez-Figueroa, N. B. Woodall, J. C. Moore and A. S.

Bommarius, *Angew. Chemie - Int. Ed.*, 2012, **51**, 3969–3972.

33   N. Itoh, C. Yachi and T. Kudome, *J. Mol. Catal. B Enzym.*, 2000, **10**, 281–290.

34   M. D. Patil, S. Yoon, H. Jeon, T. P. Khobragade, S. Sarak, A. D. Pagar, Y. Won and H. Yun, *Catalysts*, 2019, **9(7)**, 600-613.

35   M. J. Abrahamson, J. W. Wong and A. S. Bommarius, *Adv. Synth. Catal.*, 2013, **355**, 1780–1786.

36   A. Pushpanath, E. Siirola, A. Bornadel, D. Woodlock and U. Schell, *ACS Catal.*, 2017, **7**, 3204–3209.

37   S. K. Au, B. R. Bommarius and A. S. Bommarius, *ACS Catal.*, 2014, **4**, 4021–4026.

38   O. Mayol, K. Bastard, L. Beloti, A. Frese, J. P. Turkenburg, J.-L. Petit, A. Mariage, A. Debard, V. Pellouin, A. Perret, V. Berardinis, A. Zaparucha, G. Grogan and C. Vergne-Vaxelaire, *Nat. Catal.*, 2019, **2**, 324-333

39   S. T. Ahmed, F. Parmeggiani, N. J. Weise, S. L. Flitsch and N. J. Turner, *ACS Catal.*, 2015, **5**, 5410-5413.

40   F. Parmeggiani, S. L. Lovelock, N. J. Weise, S. T. Ahmed and N. J. Turner, *Angew. Chemie - Int. Ed.*, 2015, **54**, 4608–4611.

41   F. Parmeggiani, N. J. Weise, S. T. Ahmed and N. J. Turner, *Chem. Rev.*, 2018, **118**, 73-118.

42   S. Mathew and H. Yun, *ACS Catal.*, 2012, **2**, 993-1001.

43   D. Koszelewski, I. Lavandera, D. Clay, D. Rozzell and W. Kroutil, *Adv. Synth. Catal.*, 2008, **350**, 2761–2766.

44   C. K. Savile, J. M. Janey, E. C. Mundorff, J. C. Moore, S. Tam, W. R. Jarvis, J. C. Colbeck, A. Krebber, F. J. Fleitz, J. Brands, P. N. Devine, G. W. Huisman and G. J. Hughes, *Science (80-.).*, 2010, **329**, 305–309.

45   A. Gomm and E. O. Reilly, *Curr. Opin. Chem. Biol.*, 2018, **43**, 106–112.

46   S. E. Payer, J. H. Schrittwieser and W. Kroutil, 2017, 2553–2559.

47   K. Mitsukura, M. Suzuki, K. Tada, T. Yoshida and T. Nagasawa, *Org. Biomol. Chem.*, 2010, **8**, 4533–4535.

48   K. Mitsukura, M. Suzuki, S. Shinoda, T. Kuramoto, T. Yoshida and T. Nagasawa, *Biosci. Biotechnol. Biochem.*, 2011, **75**, 1778-1782.

49   K. Mitsukura, T. Kuramoto, T. Yoshida, N. Kimoto, H. Yamamoto and T. Nagasawa, *Appl. Microbiol. Biotechnol.*, 2013, **97**, 8079-8086

50   F. Leipold, S. Hussain, D. Ghislieri and N. J. Turner, *ChemCatChem*, 2013, **5**, 3505–3508.

51   S. Hussain, F. Leipold, H. Man, E. Wells, S. P. France, K. R. Mulholland, G. Grogan and N. J. Turner, *ChemCatChem*, 2015, *7*, 579–583.

52   G. Grogan and N. J. Turner, *Chem. - A Eur. J.*, 2016, **22**, 1900–1907.

53   T. Huber, L. Schneider, A. Präg, S. Gerhardt, O. Einsle and M. Müller, *ChemCatChem*, 2014, **6**, 2248–2252.

54   M. Rodríguez-Mata, A. Frank, E. Wells, F. Leipold, N. J. Turner, S. Hart, J. P. Turkenburg and G. Grogan, *ChemBioChem*, 2013, **14**, 1372–1379.

55   P. N. Scheller, S. Fademrecht, S. Hofelzer, J. Pleiss, F. Leipold, N. J. Turner, B. M. Nestl and B. Hauer, *ChemBioChem*, 2014, **15**, 2201–2204.

56   M. Gand, H. Müller, R. Wardenga and M. Höhne, *J. Mol. Catal. B Enzym.*, 2014, **110**, 126–132.

57   H. Li, Z. J. Luan, G. W. Zheng and J. H. Xu, *Adv. Synth. Catal.*, 2015, **357**, 1692–1696.

58   H. Li, G. X. Zhang, L. M. Li, Y. S. Ou, M. Y. Wang, C. X. Li, G. W. Zheng and J. H. Xu, *ChemCatChem*, 2016, **8**, 724–727.

59   H. Li, P. Tian, J.-H. Xu and G.-W. Zheng, *Org. Lett.*, 2017, **19**, 3151–3154.

60   P. Yao, Z. Xu, S. Yu, Q. Wu and D. Zhu, *Adv. Synth. Catal.*, 2019, **361**, 556–561.

61   Y. Zhang, F. Chen, B. Li, X. Zhou, Q. Chen, J. Xu and G. Zheng, *Org. Lett.*, 2020,

22, 3367-3372

62   P. Matzel, M. Gand and M. Höhne, *Green Chem.*, 2017, **19**, 385–389.

63   N. Zumbrägel, K. Wagner, N. Weißing and H. Gröger, *J. Heterocycl. Chem.*, 2019, **56**, 788–794.

64   N. Zumbrägel and H. Gröger, *J. Biotechnol.*, 2019, **291**, 35–40.

65   N. Zumbrägel, C. Merten, S. M. Huber and H. Gröger, *Nat. Commun.*, 2018, **9**, 60–69.

66   N. Zumbrägel, P. Machui, J. Nonnhoff and H. Gröger, *J. Org. Chem.*, 2019, **84**, 1440–1447.

67   P. N. Scheller, M. Lenz, S. C. Hammer, B. Hauer and B. M. Nestl, *ChemCatChem*, 2015, **7**, 3239–3242.

68   N. Borlinghaus, S. Gergel and B. M. Nestl, *ACS Catal.*, 2018, **8**, 3727–3732.

69   Z. Xu, P. Yao, X. Sheng, J. Li, J. Li, S. Yu, J. Feng, Q. Wu and D. Zhu, *ACS Catal.*, 2020, **10**, 8780-8787

70   D. G. Gourley, A. W. Schüttelkopf, G. A. Leonard, J. Luba, L. W. Hardy, S. M. Beverley and W. N. Hunter, *Nat. Struct. Biol.*, 2001, **8**, 521-525.

71   H. Man, E. Wells, S. Hussain, F. Leipold, S. Hart, J. P. Turkenburg, N. J. Turner and G. Grogan, *ChemBioChem*, 2015, **16**, 1052–1059.

72   S. Velikogne, V. Resch, C. Dertnig, J. H. Schrittwieser and W. Kroutil, *ChemCatChem*, 2018, **10**, 3236–3246.

73   G. A. Aleku, H. Man, S. P. France, F. Leipold, S. Hussain, L. Toca-Gonzalez, R. Marchington, S. Hart, J. P. Turkenburg, G. Grogan and N. J. Turner, *ACS Catal.*, 2016, **6**, 3880–3889.

74   S. Eddy, *Nat. Biotechnol.*, 2004, **10**, 1315-1316.

75   D. Wetzl, M. Berrera, N. Sandon, D. Fishlock, M. Ebeling, M. Müller, S. Hanlon, B. Wirz and H. Iding, *ChemBioChem*, 2015, **16**, 1749–1756.

76   D. Wetzl, M. Gand, A. Ross, H. Müller, P. Matzel, S. P. Hanlon, M. Müller, B. Wirz, M. Höhne and H. Iding, *ChemCatChem*, 2016, **8**, 2023–2026.

77   G.-D. Roiban, M. Kern, Z. Liu, J. Hyslop, P. L. Tey, M. S. Levine, L. S. Jordan, K. K. Brown, T. Hadi, L. A. F. Ihnken and M. J. B. Brown, *ChemCatChem*, 2017, **9**, 4475–4479.

78   S. P. France, R. M. Howard, J. Steflik, N. J. Weise, J. Mangas-Sanchez, S. L. Montgomery, R. Crook, R. Kumar and N. J. Turner, *ChemCatChem*, 2018, **10**, 510–514.

79   A. Bornadel, S. Bisagni, A. Pushpanath, S. L. Montgomery, N. J. Turner and B. Dominguez, *Org. Process Res. Dev*, 2019, **23**, 1262-1268.

80   M. Schober, C. MacDermaid, A. A. Ollis, S. Chang, D. Khan, J. Hosford, J. Latham, L. A. F. Ihnken, M. J. B. Brown, D. Fuerst, M. J. Sanganee and G. D. Roiban, *Nat. Catal.*, 2019, **2**, 909–915.

81   S. L. Montgomery, A. Pushpanath, R. S. Heath, J. R. Marshall, U. Klemstein, J. L. Galman, D. Woodlock, S. Bisagni, C. J. Taylor, J. Mangas-Sanchez, J. I. Ramsden, B. Dominguez and N. J. Turner, *Sci. Adv.*, 2020, **6**, 9320-9331.

82   J. R. Marshall, P. Yao, S. L. Montgomery, J. D. Finnigan, T. W. Thorpe, R. B. Palmer, J. Mangas-Sanchez, R. A. M. Duncan, R. S. Heath, K. M. Graham, D. J. Cook, S. J. Charnock and N. J. Turner, *Nat. Chem.*, 2020, **13**, 140-148.

83   R. S. Heath, M. Pontini, S. Hussain and N. J. Turner, *ChemCatChem*, 2016, **8**, 117–120.

84   S. P. France, S. Hussain, A. M. Hill, L. J. Hepworth, R. M. Howard, K. R. Mulholland, S. L. Flitsch and N. J. Turner, *ACS Catal.*, 2016, **6**, 3753–3759.

85   A. Al-Shameri, N. Borlinghaus, L. Weinmann, P. N. Scheller, B. M. Nestl and L. Lauterbach, *Green Chem.*, 2019, **21**, 1396–1400.

86   N. Borlinghaus, L. Weinmann, F. Krimpzer, P. N. Scheller, A. Al-Shameri, L. Lauterbach, A. Coquel, C. Lattemann, B. Hauer and B. M. Nestl, *ChemCatChem*, 2019, **11**, 5738–5742.

87   G. J. Ford, N. Kress, A. P. Mattey, L. J. Hepworth, C. R. Baldwin, J. R. Marshall, L. S. Seibt, M. Huang, W. R. Birmingham, N. J. Turner and S. L. Flitsch, *Chem. Commun*, 2020, **56**, 7949.-7952

88   T. W. Thorpe, S. P. France, S. Hussain, J. R. Marshall, W. Zawodny, J. Mangas-Sanchez, S. L. Montgomery, R. M. Howard, D. S. B. Daniels, R. Kumar, F. Parmeggiani and N. J. Turner, *J. Am. Chem. Soc.*, 2019, **141**, 19208-19213.

89   W. Zawodny, S. L. Montgomery, J. R. Marshall, J. D. Finnigan, N. J. Turner and J. Clayden, *J. Am. Chem. Soc.*, 2018, **140**, 17872–17877.

90   G. A. Aleku, S. P. France, H. Man, J. Mangas-Sanchez, S. L. Montgomery, M. Sharma, F. Leipold, S. Hussain, G. Grogan and N. J. Turner, *Nat. Chem.*, 2017, **9**, 961–969.

91   M. Sharma, J. Mangas-Sanchez, S. P. France, G. A. Aleku, S. L. Montgomery, J. I. Ramsden, N. J. Turner and G. Grogan, *ACS Catal.*, 2018, **8**, 11534–11541.

92   S. L. Montgomery, J. Mangas-Sanchez, M. P. Thompson, G. A. Aleku, B. Dominguez and N. J. Turner, *Angew. Chemie*, 2017, **129**, 10627–10630.

93   M. Tavanti, J. Mangas-Sanchez, S. L. Montgomery, M. P. Thompson and N. J. Turner, *Org. Biomol. Chem*, 2017, **15**, 9790-9793

94   G. A. Aleku, J. Mangas-Sanchez, J. Citoler, S. P. France, S. L. Montgomery, R. S. Heath, M. P. Thompson and N. J. Turner, *ChemCatChem*, 2018, **10**, 515–519.

95   S. P. France, G. A. Aleku, M. Sharma, J. Mangas-Sanchez, R. M. Howard, J. Steflik, R. Kumar, R. W. Adams, I. Slabu, R. Crook, G. Grogan, T. W. Wallace and N. J. Turner, *Angew. Chemie - Int. Ed.*, 2017, **56**, 15589–15593.

96   B. Z. Costa, J. L. Galman, I. Slabu, S. P. France, A. J. Marsaioli and N. J. Turner, *ChemCatChem*, 2018, **10**, 4733–4738.

97   J. I. Ramsden, R. S. Heath, S. R. Derrington, S. L. Montgomery, J. Mangas-Sanchez, K. R. Mulholland and N. J. Turner, *J. Am. Chem. Soc.*, 2019, **141**, 1201–1206.

98   M. Lenz, J. Meisner, L. Quertinmont, S. Lutz, J. Kästner and B. M. Nestl,

ChemBioChem, 2017, **18**, 253–256.

99   D. González-Martínez, A. Cuetos, M. Sharma, M. García-Ramos, I. Lavandera, V. Gotor-Fernández and G. Grogan, *ChemCatChem*, 2020, **12**, 2421–2425.

100   J. Mangas-Sanchez, M. Sharma, S. C. Cosgrove, J. I. Ramsden, J. R. Marshall, T. W. Thorpe, R. B. Palmer, G. Grogan and N. J. Turner, *Chem. Sci.*, 2020, **11**, 5052-5057

101   R. Kumar, M. J. Karmilowicz, D. Burke, M. P. Burns, L. A. Clark, C. G. Connor, E. Cordi, N. M. Do, K. M. Doyle, S. Hoagland, C. A. Lewis, D. Mangan, C. A. Martinez, E. L. Mcinturff, K. Meldrum, R. Pearson, J. Steflik, A. Rane and J. Weaver, *Nat. Cat.*, 2021, **4**, 775-782

102   S. Duan, D. W. Widlicka, M. P. Burns, R. Kumar, I. Hotham, J.-N. Desrosiers, P. Bowles, K. N. Jones, L. D. Nicholson, M. T. Buetti-Weekly, L. Han, J. Steflik, E. Hansen, C. M. Hayward, H. Strohmeyer, S. Monfette, S. C. Sutton and C. Morris, *Org. Process Res. Dev.*, 2022, **26**, 879-890

103   G. A. Aleku, S. P. France, H. Man, J. Mangas-Sanchez, S. L. Montgomery, M. Sharma, F. Leipold, S. Hussain, G. Grogan and N. J. Turner, *Nat. Chem.*, 2017, **9**, 961–969.

104   E. T. Farinas, T. Bulter and F. H. Arnold, *Curr. Opin. Biotechnol.*, 2001, **12**, 545–551.

105   N. J. Turner, *Nat. Chem. Biol.*, 2009, **5**, 567–573.

106   A. Currin, N. Swainston, P. J. Day and D. B. Kell, *Chem. Soc. Rev.*, 2015, **44**, 1172–1239.

107   P. E. Rosenfeld and L. G. H. Feng, in *Risks of Hazardous Waste*, Elsevier, United Kingdom, First Edition,. 2011, Chapter 11, 127-154.

108   J. Mangas-Sanchez, S. P. France, S. L. Montgomery, G. A. Aleku, H. Man, M. Sharma, J. I. Ramsden, G. Grogan and N. J. Turner, *Curr. Opin. Chem. 127Biol.*, 2017, **37**, 19–25.

109   J. Jumper, R. Evans, A. Pritzel, T. Green, M. Figurnov, O. Ronneberger, K.

Tunyasuvunakool, R. Bates, A. Žídek, A. Potapenko, A. Bridgland, C. Meyer, S. A. A Kohl, A. J. Ballard, A. Cowie, B. Romera-Paredes, S. Nikolov, R. Jain, J. Adler, T. Back, S. Petersen, D. Reiman, E. Clancy and M. Zielinski, *Nature*, 2021, **596**, 583-589

110   S. L. Montgomery, A. Pushpanath, R. S. Heath, J. R. Marshall, U. Klemstein, J. L. Galman, D. Woodlock, S. Bisagni, C. J. Taylor, J. Mangas-Sanchez, J. I. Ramsden, B. Dominguez, N. J. Turner, *Sci. Adv.*, 2020, **6**,

111   C. M. Heckmann, F. Paradisi, *ChemCatChem*, 2020, **24**, 6082-6102

112   J. Tryggvi, *J. Chem. Ed.*, 2010, **87**, 1348

113   Meyers, Robert A., ed. *Molecular Biology and Biotechnology: A Comprehensive Desk Reference*. Wiley-VCH, New York, p. 296

Appendix

Asymmetric synthesis of primary amines catalyzed by thermotolerant fungal reductive aminases

Juan Mangas-Sanchesz, Mahima Sharma, Sebastian C. Cosgrove, Jeremy I. Ramsden, James R. Marshall, Thomas W. Thorpe, Ryan B. Palmer, Gideon Grogan, Nicholas J. Turner

Abstract

Chiral primary amines are important intermediates in the synthesis of pharmaceutical compounds. Fungal reductive aminases (RedAms) are NADPH-dependent dehydrogenases that catalyse reductive amination of a range of ketones with short-chain primary amines supplied in an equimolar ratio to give corresponding secondary amines. Herein we describe structural and biochemical characterisation as well as synthetic applications of two RedAms from Neosartorya spp. (*Nf*RedAm and *Nfis*RedAm) that display a distinctive activity amongst fungal RedAms, namely a superior ability to use ammonia as the amine partner. Using these enzymes, we demonstrate the synthesis of a broad range of primary amines, with conversions up to >97% and excellent enantiomeric excess. Temperature dependent studies showed that these homologues also possess greater thermal stability compared to other enzymes within this family. Their synthetic applicability is further demonstrated by the production of several primary and secondary amines with turnover numbers (TN) up to 14 000 as well as continous flow reactions, obtaining chiral amines such as (R)-2-aminohexane in space time yields up to 8.1 g L^{-1} h^{-1}. The remarkable features of *Nf*RedAm and *Nfis*RedAm highlight their potential for wider synthetic application as well as expanding the biocatalytic toolbox available for chiral amine synthesis.

Screening and characterization of a diverse panel of metagenomic imine reductases for biocatalytic reductive amination

James R. Marshall, Peiyuan Yao, Sarah L. Montgomery, James D. Finnigan, Thomas W. Thorpe, Ryan B. Palmer, Juan Mangas-Sanchez, Richard A. M. Duncan, Rachel S. Heath, Kirsty M. Graham, Darren J. Cook, Simon J. Charnock, and Nicholas J. Turner

Abstract

Finding faster and simpler ways to screen protein sequence space to enable the identification of new biocatalysts for asymmetric synthesis remains both a challenge and a rate-limiting step in enzyme discovery. Biocatalytic strategies for the synthesis of chiral amines are increasingly attractive and include enzymatic asymmetric reductive amination, which offers an efficient route to many of these high-value compounds. Here we report the discovery of over 300 new imine reductases and the production of a large (384 enzymes) and sequence-diverse panel of imine reductases available for screening. We also report the development of a facile high-throughput screen to interrogate their activity. Through this approach we identified imine reductase biocatalysts capable of accepting structurally demanding ketones and amines, which include the preparative synthesis of N-substituted β-amino ester derivatives via a dynamic kinetic resolution process, with excellent yields and stereochemical purities.

Development of Continuous Flow Systems to Access Secondary Amines Through Previously Incompatible Biocatalytic Cascades

Ashley P. Mattey, Grayson J. Ford, Joan Citoler, Christopher Baldwin, James R. Marshall, Ryan B. Palmer, Matthew Thompson, Nicholas J. Turner, Sebastian C. Cosgrove, and Sabine L. Flitsch

Abstract

A key aim of biocatalysis is to mimic the ability of eukaryotic cells to carry out multistep cascades in a controlled and selective way. As biocatalytic cascades get more complex, reactions become unattainable under typical batch conditions. Here a number of continuous flow systems were used to overcome batch incompatibility, thus allowing for successful biocatalytic cascades. As proof-of-principle, reactive carbonyl intermediates were generated in situ using alcohol oxidases, then passed directly to a series of packed-bed modules containing different aminating biocatalysts which accordingly produced a range of structurally distinct amines. The method was expanded to employ a batch incompatible sequential amination cascade via an oxidase/transaminase/imine reductase sequence, introducing different amine reagents at each step without cross-reactivity. The combined approaches allowed for the biocatalytic synthesis of the natural product 4O-methylnorbelladine.